

Production and Modeling of Recombinant Protein.

by

Jason Yaeck

A thesis
presented to the University of Waterloo
in fulfillment of the
thesis requirement for the degree of
Master of Applied Science
in
Chemical Engineering

Waterloo, Ontario, Canada, 2006

©Jason Yaeck 2006

AUTHOR'S DECLARATION

I hereby declare that I am the sole author of this thesis. This is a true copy of the thesis, including any required final revisions, as accepted by my examiners.

I understand that my thesis may be made electronically available to the public.

Jason Yaeck

Abstract

Computational models of recombinant production of tissue-type Plasminogen Activator (tPA) were created, studied and compared for two hosts, Chinese Hamster Ovary (CHO) cells and *Escherichia coli* (*E. coli*), using SuperPro® Designer. In addition, several fermentations were run using enhanced Yellow Fluorescent Protein (eYFP) in *E. coli* to provide knowledge for the SuperPro model and to explore the effect of temperature when used to maintain dissolved oxygen in a high density fed-batch fermentation.

The models show that production of tPA is feasible using either host, but under the current basecase CHO holds the economic advantage despite the initial higher capital costs. In order to become more competitive with CHO, production using *E. coli* must become higher on a cell specific level and the potential of refolding insoluble protein in inclusion bodies should be explored. Since *E. coli*'s growth rate allows for higher plant throughput in a given production year, if this was combined with strains which produce higher titers of protein than those available in literature, it would allow *E. coli* to become competitive with CHO for the production of recombinant tPA.

Experiments demonstrate that temperature control can be used to slow the metabolic rate of *E. coli*, allowing aerobic conditions to be maintained in the high density fermentations. Although temperature reduction has also been used to increase the yield of soluble protein, it is likely this occurs with reduced protein production. Temperature control was initiated using five minute moving averages to monitor overall oxygen and stirrer speed trends. Temperature was dropped 5 °C when averaged oxygen content fell below 18% and averaged stirrer speeds were greater than 1000 rpm. Temperature controlled runs for *E. coli* BL21DE3 producing eYFP appeared to allow the cultures to maintain better aerobic conditions. It is known that eYFP was produced since homogenized cell paste fluoresced yellow under UV light. However, protein analysis was hampered due to low protein production even after induction.

Purifications involving large amounts of cell paste (50 g or more) were difficult to perform and all purifications resulted in contamination by other proteins.

Several recommendations can be made. The modeling would be greatly facilitated by additional information such as equipment specifications at large-scale production. The work with eYFP containing *E. coli* would be greatly enhanced by better strain selection. Choosing strains which over-express the protein of interest on the small scale would lead to better results in the fermentor. A densitometric analysis of the SDS PAGE gels run would allow a better understanding of general proteomic response to temperature control. When combined with mass spectrometry this may lead to different approaches in reducing temperature. Temperature control is often thought to increase soluble protein. From the densitometric SDS PAGE analysis of both the supernatant and pellet after homogenization it would be interesting to examine the partitioning of recombinant protein into soluble and insoluble forms in future experiments.

Acknowledgements

I would like to express my sincerest gratitude to:

- My supervisors Professor W. Anderson, Professor E. Jervis and Professor P. Douglas for the financial assistance, opportunities, encouragement, and assistance throughout the project.
- Special Thanks are due to Dr. Anderson, Dr. Jervis and his lab, for their encouragement and for allowing me to expand my horizons.
- Heather who trained an engineer to be a little less of a “menace to microbiology.” Charlie, for his time and assistance during my fermentation runs and agreeing to forgo sleep for a night to help me in my experiments.
- Dr. Palmer for the use of his equipment for use in downstream processing and fluorescence analysis.
- Dr. Guy Guillemette and his entire lab for their indefatigable patience in answering my many questions, sometimes the same one several times.
- Don and Jillian Spratt, Genevieve Labbé and Andrea Dupont for their encouragement, friendship and humour. Maja Stressman, who always seem to catch the biggest, and sometimes the only, fish. Matt and Helen Fagan for their enduring friendship, the many plays in Stratford, and the time spent throwing 6 wt fishing line around. My friends in Engineering.
- My parents Don and Judy Yaeck and my sister Angela who provided the bedrock to begin my journeys and who offered sanctuary when I needed a safe harbour.
- Elita Chan, my fiancée, whose dedication and love made the long days and nights bearable.

Table of Contents

AUTHOR'S DECLARATION	ii
Abstract.....	iii
Acknowledgements.....	v
Table of Contents.....	vi
List of Figures.....	ix
List of Tables	xviii
Chapter 1 Introduction	1
1.1 Scope of Work.....	1
1.2 Modeling of Large Scale Recombinant Protein Production.....	1
1.3 Protein Functionality and Fermentations	2
1.4 Contributions to Research.....	4
Chapter 2 Literature Review for CHO and <i>E. coli</i> Modeling.....	5
2.1 Introduction.....	5
2.2 Process Synthesis	5
2.3 Process Flowsheeting.....	7
2.4 Process Design	8
2.5 Equipment Selection	10
2.5.1 Preinoculation and Fermentation.....	10
2.5.2 Development of Downstream Processing Steps.....	11
2.6 Unit Operations Common in Basecases: General overview	16
2.6.1 Homogenization.....	16
2.6.2 Primary Recovery and Clarification.....	18
2.6.3 Purification: Chromatography	20
2.7 Plasminogen Activator variants, functionalities and production	21
2.8 Chinese Hamster Ovary Cell Properties.....	24
2.9 Escherichia coli Properties.....	27
2.9.1 Production of tissue-type plasminogen activator and variants in <i>E. coli</i>	30
Chapter 3 SuperPro® Designer Modeling.....	36

3.1 Introduction to CHO and <i>E. coli</i> Basecases	36
3.2 CHO Basecase.....	36
3.2.1 CHO Basecase Unit Model and Data	37
3.3 <i>E. coli</i> Basecases	40
3.3.1 Introduction	40
3.3.2 Biomass and Protein Yield Prediction.....	41
3.3.3 200 hr <i>E. coli</i> Basecase with Centrifuge Initial Clarification Step.....	41
3.3.4 <i>E. coli</i> Basecase Unit Model and Data	43
3.3.5 200 hr <i>E. coli</i> Basecase with Microfiltration initial clarification step.....	46
3.3.6 200 hr <i>E. coli</i> Basecase with Microfiltration as Initial Clarification: Unit Model and Data.....	47
3.3.7 Need for Additional Microfiltration Step.....	48
3.3.8 200 hr <i>E. coli</i> Basecase with extra Microfiltration Step.....	49
3.3.9 Effect of lower production time on <i>E. coli</i> Basecase	52
3.3.10 <i>E. coli</i> 36 Hr Basecase modified to match CHO yearly tPA output.....	52
3.4 Basecase Comparisons	54
3.5 Discussion and Recommendations.....	59
Chapter 4 Fermentations and Purifications.....	62
4.1 Green Fluorescent Protein (GFP) and Variants.....	62
4.1.1 Fluorescence Biology and Characteristics of GFP and Variants.....	63
4.1.2 Construction of eYFP	65
4.2 Objectives of Fermentations.....	71
4.3 Fermentation and Temperature Control Literature Review	72
4.3.1 Strategies for High Density Fermentations	72
4.3.2 Temperature Control in Fermentations.....	75
4.4 Expected Protein Transcription and Gene Responses to Temperature Control.....	77
4.5 Production and Purification Schemes for GFP and variants.	80
4.6 Fermentation Protocols	85
4.7 Temperature - Dissolved Oxygen Controller	88

Chapter 5 Temperature Control Experiments.....	90
5.1 Introduction.....	90
5.2 Shake Flask Run.....	90
5.2.1 Introduction.....	90
5.2.2 Growth for Shake Flask Runs.....	93
5.2.3 Final Weights and Protein Production.....	101
5.2.4 Shake Flask SDS PAGE Gels.....	103
5.3 Initial Bioreactor Temperature Control Runs.....	108
5.3.1 Inoculum.....	108
5.3.2 Growth.....	109
5.3.3 Protein.....	112
5.4 Temperature Control Experiments.....	116
5.4.1 Inocula.....	116
5.4.2 Growth.....	117
5.4.3 Protein Production Information.....	137
5.5 Purifications.....	141
5.5.1 Introduction.....	141
5.5.2 Ni ²⁺ Purification.....	141
5.5.3 Denature-Renature Experiments.....	146
5.5.4 Fluorescence Spectra Inconsistencies.....	150
5.6 Conclusions.....	158
5.7 Recommendations.....	159
5.7.1 Strain Selection and Initial Inoculation.....	159
5.7.2 Protein Density Calculation from SDS PAGE Gels.....	160
5.7.3 Inclusion Body Formation and Protein Partitioning.....	160
Appendix A Basecase Stream Reports.....	162
Appendix B Fermentator Supplementary Material.....	216

List of Figures

Figure 2.1: Prediction of Centrifugation data using SuperPro® Designer (Shanklin et al. 2001). This shows that predictive results are possible using SuperPro®.	7
Figure 2.2: Simulation results versus manufacturing scale results using SuperPro® Designer (Shanklin et al. 2001).	8
Figure 2.3: Simplified bioprocess layout. Depending on the host homogenization may be required if the protein is not normally secreted. The initial clarification removes cell debris and whole cells and concentrates the protein solution. The protein solution is purified by several steps until the desired purity is reached. Volumes decrease during the fermentation while purity increases.	9
Figure 2.4: Flowsheet for Fermentation Scale Up. These are the typical steps in terms of increasing scales (number of liters produced) of production. Each step requires optimization. It may be necessary to revise the process at each step as units may not behave in similar characteristics at differing scales.	10
Figure 2.5: Protein purity required as a function of end use (human Erythropoietin (EPO), Super Oxide Dismutase (SOD)) (Wheelwright 1989). This gives an example of how the closer to in-vivo use the final product comes the higher the purity demanded.	12
Figure 2.6: Techniques for Large Scale Disruption of Microorganisms (Middelburg 1995). Several of these choices are infeasible for large scale production such as decompression. In large scale purifications enzymatic choices are usually eliminated due to the cost. ..	17
Figure 2.7: tPA full domain amino acid representation (Rouf et al. 1996). The tPA has four main domains: Kringle 1, Kringle 2, Serine Protease, and a fibrin binding domain. The tPA protein has 527 amino acids and a molecular weight of 70 kDa.	23
Figure 3.1: CHO Basecase Unit Model. The CHO Basecase model was taken from previous work by Rouf (1999). The storage devices between each unit are used to store processed proteins after each step. The clarification section involves a microfilter and ultrafilter. The downstream purification involves two passes on an affinity column with an ultrafiltration step in-between to reduce volumes. The final purification uses gel filtration.	37

Figure 3.2: 200 hr <i>E. coli</i> Basecase Unit Model with centrifuge unit for initial clarification. Centrifugation was chosen as the initial clarification method. High pressure homogenization was chosen as the cell disruption method. The downstream process remains the same as the CHO Basecase.	43
Figure 3.3: Water consumption for <i>E. coli</i> Basecase with centrifuge.	44
Figure 3.4: 200 hr <i>E. coli</i> Basecase with initial microfiltration unit added to avoid water consumption problems. Problems were discovered downstream of the homogenization step shortly after the water consumption problem was solved.	47
Figure 3.5: 200 hr <i>E. coli</i> Basecase with extra microfilter after homogenizer. The relative cost of the microfiltration step is minimal and avoids loading cell debris or whole cells onto the first affinity chromatography step.....	49
Figure 4.1: Maturation steps of GFP with kinetic data. The rate limiting step in this is the formation of the chromophore (Reid and Flynn 1997).....	64
Figure 4.2: Modified GFP Chromophore formation with an intermediate mechanism as prolines switch to opposing configuration in-vivo (Rosenow et al. 2004).....	64
Figure 4.3: Base pair substitutions required to create eYFP from wild type GFP (wt GFP). In order to create GFP variant it is required to switch the chromophore amino acids (65-67) and certain amino acids which end up close to the chromophore (Clontech 2001).	65
Figure 4.4: Typical Emission and Excitation Spectra for GFP and variants. eYFP has emission at 528 nm and excitation at 518 nm (Heim et al. 1994).	66
Figure 4.5: Plasmid map for eYFP vector (Clontech 1999). BAMH1 and ECOR1 were used to cut the plasmid and clone the protein cDNA into the plasmid.	68
Figure 4.6: Vector map for pRSET _B plasmid (Invitrogen 2001).....	69
Figure 4.7: DNA Gel of plasmid cut with BAMHI and EcoRI. Plasmid size is approximately 2950 bp with the protein DNA size of approximately 250 bp (there remains some uncut plasmid around 3700 bp).	69
Figure 4.8: Gene from <i>Aequorea victoria</i> for GFP. Underlined sequences are silent or are introns (Prasher et al. 1992).....	71
Figure 4.9: Genetic glucose utilization pathways in <i>E. coli</i> (Phue et al. 2005).	74

Figure 5.1: Data from previous inoculum cultures used to determine timing for shake flask experiment. Average growth rate was 0.69 hr^{-1} and maximum OD_{600} of 1.35 was achieved in 7 -9 hours. 92

Figure 5.2: 50 mL inoculum culture for 1.25L shake flask culture. Cell growth rate was 0.45 min^{-1} which is lower than the expected growth rate of 0.69 min^{-1} . The growth profiles, however, were similar. 93

Figure 5.3: Growth for Large 1.25L Shake Flask. Growth rate, 0.18hr^{-1} , was lower than the 50mL inoculum likely due to dilution effects. Inoculum reached 0.436 OD_{600} at 275 minutes. 94

Figure 5.4: Growth for All Shake Flasks during the 240 minute growth trial. Growth rates varied from 0.29 to 0.40 hr^{-1} but all growth appeared to reach near the maximum growth of 1.3 OD_{600} achieved in 50 mL shake flasks. 95

Figure 5.5: Growth Rate as a function of time at 22 C. The pattern appears to follow a concave curve with a maximum at 60 min. This may be a function of the cultures ability to adapt. Cultures at the beginning were given temperature shocks quicker and this may indicate a need for time to adapt. Cultures after 60 min may have adapted to the lower temperatures but the growth rates were affected and could not recover during the experiment run time. 97

Figure 5.6: Time of cultures to reach O.D. of 1 when subject to a temperature change for a given time. The length of time at a lower temperature corresponds well to the amount of time required to reach 1 O.D. compared to the $37 \text{ }^{\circ}\text{C}$ control cultures. It is interesting to note that this graph may indicate that there are certain critical times after which the culture has adapted well enough. 98

Figure 5.7: Standard Deviation for $22 \text{ }^{\circ}\text{C}$ and $37 \text{ }^{\circ}\text{C}$ Control. Standard Deviation for the $22 \text{ }^{\circ}\text{C}$ shake flasks were much better than the $37 \text{ }^{\circ}\text{C}$ shake flasks. This may indicate that any potential differences in inoculation density are not favoured too heavily and growth rates (0.29 versus 0.35 hr^{-1}) are slow enough not to select for higher inoculums. This may be supported by the higher growth rate, 0.35 hr^{-1} , compared to $22 \text{ }^{\circ}\text{C}$, 0.29 hr^{-1} . 100

Figure 5.8: Final Weights for all 50mL shake flasks at 240 minutes. The cultures show minor weight variances with the lowest weight, 8B, being 0.06g and the highest being, 7B, at 0.13g. This may be a result of $Y_{x/s}$ not being affected by temperature at this volume. 101

Figure 5.9: Correlation plot for final weight and OD_{600} . This indicates that $Y_{x/s}$ may not be affected by temperature at this volume. 102

Figure 5.10: SDS PAGE Gel 1 104

Figure 5.11: SDS PAGE Gel 2 104

Figure 5.12: SDS PAGE Gel 3 104

Figure 5.13: SDS PAGE Gel 4 104

Figure 5.14: SDS PAGE Gel 5 104

Figure 5.15: SDS PAGE Gel 6 104

Figure 5.16: SDS PAGE Gel 7A..... 104

Figure 5.17: SDS PAGE Gel 7B..... 104

Figure 5.18: SDS PAGE Gel 8A..... 104

Figure 5.19: SDS PAGE Gel 8B..... 105

Figure 5.20: SDS PAGE Gel 9A..... 105

Figure 5.21: SDS PAGE Gel 9B..... 105

Figure 5.22: SDS PAGE Gel 22A..... 105

Figure 5.23: SDS PAGE Gel 22B..... 105

Figure 5.24: SDS PAGE Gel 22C..... 105

Figure 5.25: SDS PAGE Gel 22D..... 105

Figure 5.26: SDS PAGE Gel 37A..... 106

Figure 5.27: SDS PAGE Gel 37B..... 106

Figure 5.28: SDS PAGE Gel 37C..... 106

Figure 5.29: SDS PAGE Gel 37D..... 106

Figure 5.30: Inoculum growth profile for Run without Temperature Control. The growth rate was 0.307. The inoculum density for the no temperature control run was 0.771 OD_{600} compared to 0.730 OD_{600} for the temperature control run. The two inoculums had differing growth rates, 0.307 versus 0.637 for no temperature control and temperature

control inoculums respectively. Each inoculum reached the seeding density in approximately the same amount of time.....	108
Figure 5.31: Optical Density versus glucose fed for no temperature control run. This run began the Fed-batch feeding phase 2 hours earlier than the temperature control run. The glucose fed was much higher during the exponential feeding phase of the run and growth noticeably deviated from the glucose fed profile 5 hours before the end of the end. There is increased pH control indicate more glucose being converted to acetate.	109
Figure 5.32: Optical density versus glucose fed for temperature control run. The run began Fed-batch feeding phase 2 hours later than the non-temperature controlled run. The glucose fed was much lower than the non-temperature controlled run and the optical density followed the glucose fed profile very closely.	110
Figure 5.33: No Temperature Control 10% SDS PAGE. Samples 1-7 shown.....	113
Figure 5.34: No Temperature Control 10% SDS PAGE. Samples 8-12 shown. The sample beside lane 12 is overflow from lane 12.	113
Figure 5.35: Temperature Control 10% SDS PAGE. Samples 1-9 shown.....	113
Figure 5.36: Temperature Control 10% SDS PAGE. Samples 10-17 shown.....	113
Figure 5.37: Fluorescence Readings from SDS Pellet Samples. There is no clear pattern suggested in the No Temperature Control Samples. The temperature control samples may show a slightly exponential pattern but this is uncertain. Excitation of 515 nm, emission of 535 nm and a cut-off of 530 nm.	115
Figure 5.38: Inocula Growths for Temperature Control Experiments. The average optical density before seeding into the bioreactor was 0.95 with a variance of 0.1. The first 2 runs took 5.5 hours to reach seeding density and the last 2 runs took 7 hours.	117
Figure 5.39: Run A Biocontroller data. A, shows oxygen limitation during the exponential growth phase. The wider oxygen spikes after 8 hours show the beginning of 30% oxygen supplementation. Figure B, shows the increasing fluctuations in pH indicating excessive metabolic formation of acetate. The stirrer speed increased and then rapidly decreased during the initial oxygen supplementation period. Once growth related	

oxygen demand reached oxygen transfer capacity the stirrer speed quickly reached a maximum value of 1224 rpm.....	119
Figure 5.40: Run B Biocontroller Data. Oxygen supplementation, started at 9.6 hours, ranged from 0-100%. Pure oxygen supplementation increases variance in dissolved oxygen. Figure B, shows the increasing fluctuations in pH indicating excessive metabolic formation of acetate.	120
Figure 5.41: Run C Biocontroller Data. Both oxygen supplementation and temperature control were used in this run. Dissolved oxygen concentration was maintained around 30% although short periods of limitation occurred. pH fluctuated much less compared to non-temperature controlled runs. Temperature control was continued past the low set point of 22°C to explore temperature effects and system capacities for low temperatures.	121
Figure 5.42: Run D Biocontroller Data. This run simulated a 45 minute oxygen supplementation failure. Temperature control was reset afterwards. Temperature came down to 22°C in three steps over a 10 hour period. pH fluctuated much less than non-temperature controlled runs and seemed to slow as the temperature decreased below 27°C.	122
Figure 5.43: Antifoam and NH ₄ SO ₄ addition effects during culture runs on D.O. and Temperature.	123
Figure 5.44: 0.5°C temperature spike caused by NH ₄ SO ₄ addition. Moving averages was used in the temperature control programming to avoid temperature fluctuations like those caused by pH additions.....	124
Figure 5.45: Run A glucose fed versus optical density. Y _{x/s} was 1.60 for this run the highest for all the runs. The ability to provide oxygen supplementation on demand allows for higher growth at 37°C. Optical density and glucose fed deviate at 14 hours at approximately 75 O.D. but keep similar rates compared to runs with the 30% maximum oxygen supplementation.	125
Figure 5.46: Semi-log plot of glucose fed and optical density versus temperature for Run A. During the initial Fed-batch phase the growth was almost linear. After 80 O.D. growth	

appeared to slow and eventually reached a maxima at 107 O.D. There appears to be a switch in growth rate around 12 hours. This is likely caused by metabolic by-product build up and depletion of media components. 126

Figure 5.47: Run B glucose versus optical density. $Y_{x/s}$ for this run was 0.97 wet weight. Glucose deviated significantly at 13.5 hrs at approximately 55 O.D. after which the glucose feed rate proceeded exponentially. Optical density tapered off around 19 hours. Again there appears to be two growth rates during the culture with the switch in rate occurring at 15 hours. 127

Figure 5.48: Semi-log plot of glucose fed and optical density versus temperature for Run B. Growth during the initial Fed-batch phase was higher than glucose fed rate. Near 12 hours when growth appeared to exceed glucose fed then fell and thereafter followed a more exponential rate. 128

Figure 5.49: Run C glucose versus optical density. This run's $Y_{x/s}$ was 1.48 (wet weight). Interestingly, the glucose and optical density deviated around 12.5 hours at approximately 55 to 60 O.D. There was a rate change in glucose feeding between 14 and 15 hours around the time that the culture reached 22°C. 129

Figure 5.50: Semi-log plot of glucose fed and optical density versus temperature for Run C. Optical Density appeared to decrease at each temperature decrease but was greatest during the first temperature change. With each change in temperature there appears to be a decrease in the growth rate. 130

Figure 5.51: Run D glucose versus optical density. $Y_{x/s}$ is unknown since final cell weights were unknown. Glucose fed rates and optical density rates appeared to be fairly similar and follow the same course until 15 hours. Even after this the optical density rate and glucose rate appear fairly similar. 131

Figure 5.52: Semi-log plot of glucose fed and optical density versus temperature for Run D. Glucose fed and optical density were exponential with the rates decreasing after the simulated oxygen failure and temperature decreases. 132

Figure 5.53: Events for Run A. At approximately 16 hours it was necessary to clear the sparger using 10% HCl. IPTG was induced at 75 O.D. and 150 O.D. During the culture it was necessary to change the glucose bottle at 18 hrs.	134
Figure 5.54: Events for Run B. Run B was relatively uneventful. Once oxygen supplementation began antifoam was added at regular intervals during the culture. The culture was inoculated at 55 O.D. due to worries about the culture's apparent lag in reaching 75 O.D. As per procedure the culture was induced a second time at 80 O.D.	135
Figure 5.55: Events for Run C. Antifoam was added to the culture three times in order control foam. Antifoams additions were minimized to avoid lowering dissolved oxygen in the culture. IPTG was added at 75 and 125 O.D.'s according to set procedures. A slight delay in optical density can be observed during the glucose bottle change.....	136
Figure 5.56: Events for Run D. Four antifoam additons were made during the run. Oxygen supplementation was started around 12 hrs. The simulated failure occurred around 13.5 hours and lasted 45 minutes.....	137
Figure 5.57: Gel 1 Run A.....	138
Figure 5.58: Gel 2 Run A.....	138
Figure 5.59: Gel 1 from Run B.....	138
Figure 5.60: Gel 2 from Run B.....	138
Figure 5.61: Gel 1 Run C.....	139
Figure 5.62: Gel 2 Run C.....	139
Figure 5.63: Gel 3 Run C.....	139
Figure 5.64: Gel 1 Run D.....	140
Figure 5.65: Gel 2 Run D.....	140
Figure 5.66: Gel 3 Run D.....	140
Figure 5.67: Protein Concentrations for 28 Aug 06 Purifications	143
Figure 5.68: Purification Gel from 28 Aug 06 Ni ²⁺ Affinity Purification (5 uL loadings) ..	144
Figure 5.69: Fluorescence measurements using microwell plate reader. No linear range was found between 1250 and 12000. This was further evidence that problems existed with the eYFP expression.	146

Figure 5.70: SDS PAGE gel for Denature Renature Experiment.....	147
Figure 5.71 Fluorescence and protein concentrations for supernatant dilutions from Denature- Renature Experiment. The dilutions appeared to follow an exponential decrease in protein concentration but an increase in Fluorescence.	149
Figure 5.72: Excitation and Emission Spectra for protein produced in July 15 th run Chemistry fluorescence spectrometer in 100mM Tris-HCl, 100mM NaCl (pH 7.0). The emission maxima was 520nm and the excitation maxima was 466 nm.....	151
Figure 5.73: 3D Plot of Fluorescence emission for produced protein. There are several emission peaks but the maximum occurs at nearly 448 nm excitation and 524 nm emission. 100mM Tris-HCl, 100mM NaCl (pH 7.0).....	152
Figure 5.74: 3D Emission and Excitation Profile for Produced Protein from Engineering Fluorescence Spectrometer. 100mM Tris-HCl, 100mM NaCl (pH 7.0).	153
Figure 5.75: Fluorescence of supernatant for homogenized final cell pellet samples from temperature control runs. These plots do not follow the linear correlation expected when plotted on a log-log scale.	154
Figure 5.76: Fluorescence scan at typical eYFP values for all Temperature Control runs and one Initial Temperature Control run for eYFP and peak emission found in scan.	155
Figure 5.77: Excitation absorbance peaks for 520 nm Emission for BL21 DE3. Several peaks are observed with similarity to shake flask protein peaks. Maximum was at 468 and 448.	156
Figure 5.78: Excitation scan for fluorescence for shake flask samples. Several peaks are observed for the excitation scan with the biggest at 468 nm with a smaller peak at 448 nm.	157
Figure 5.79: Fluorescence spectra for peak excitation value for BL21 DE3 with No Plasmid. Peaks at 520nm were observed for excitations of 448 nm and 466 nm.....	157
Figure 5.80: Fluorescence spectra for peak excitation value for shake flask samples. A peak at 520 nm were observed for both the 448 and 468 nm excitation values. A excitation peak at 520 nm was suggested for the 372 nm emission.	158
Figure 5.81: eYFP Plates imaged using UV imager.....	160

List of Tables

Table 2.1: Heuristic classifications used to determine downstream processes (Wheelwright 1989). Differing heuristic types are utilized to reach an optimized process. Understanding the application of each method aids in optimization.....	14
Table 2.2: A list of rules of thumb for each type heuristic (Wheelwright 1989). Using these rules-of-thumb makes process selection easier eliminating certain initial choices and making downstream process choices easier to reach.....	15
Table 2.3: Comparison of design heuristics (Wheelwright 1989). Additional rules of thumb for downstream processes used to eliminate certain option early on and make downstream unit selection easier.	16
Table 2.4: Production of recombinant tPA in CHO. The sizes of fermentation vary but the time of fermentations is always measured in days for CHO culture.	26
Table 2.5: Techniques for high density cell culture with <i>E. coli</i> (Shiloach and Fass 2005). These techniques are also applicable to other hosts.....	28
Table 2.6: Production of recombinant tPA and tPA variants in <i>E. coli</i> and other selected proteins. The production scales vary by paper but the fermentation times are much quicker than CHO, measured in hours instead of days. The cell yields, when reported, are typically higher than CHO cultures but the specific productivity is lower than most CHO cases.....	31
Table 2.7: Purification of tPA from <i>E. coli</i> . Purification schemes follow much the same pattern as with CHO with affinity chromatography usually the first or second step.....	33
Table 3.1: SuperPro® Designer default costs used in modeling.	36
Table 3.2: Equipment sizing and costs for CHO Basecase.....	39
Table 3.3: Economics for CHO Basecase.....	40
Table 3.4: Biomass Yields from Literature Review and value used in Basecases.	41
Table 3.5: Equipment sizing and costs for Centrifuge Initial Clarification <i>E. coli</i> Basecases.	45
Table 3.6: Predicted Removal Efficiencies for clarification section of 200 hr <i>E. coli</i> Basecase in Figure 3.4.....	48

Table 3.7: Predicted Removal Efficiencies for clarification section of 200 hr <i>E. coli</i> Basecase with extra Microfiltration unit shown in Figure 3.5.	50
Table 3.8: Equipment sizing and costs for 200 hr and 36 hr <i>E. coli</i> Basecases.....	51
Table 3.9: Equipment sizing and costs for <i>E. coli</i> Basecase with 36 hour fermentation time and 14.48 kg tPA production.	53
Table 3.10: Key for numbered references for Basecases.....	54
Table 3.11: Product Yield from Biomass in Basecases. Initial product yield represents initial amounts of tPA after fermentation or homogenization. Final product yields represent yields at the end of the purification streams.	54
Table 3.12: Summary of materials used and produced for all Basecases.....	55
Table 3.13: All Basecase economic data.	57
Table 3.14: Equipment costs presented as a part of capital costs.	57
Table 3.15: Consumables for Basecases.....	58
Table 4.1: Characteristics of Yellow Fluorescent Protein and Produced Protein. The produced protein has a lower pI at pH 7. This means using a stronger anion exchange column and potentially keeping the flow through instead of protein that binds to the column. The His ₆ tag and amino acids left on the N-terminus from cloning into the plasmid add 1.4 kDa to the protein.....	67
Table 4.2 : Inhibitory concentrations of <i>E. coli</i> media components. Avoiding concentrations greater than these are necessary in order to ensure the long term health of the culture. The health of the culture has effects on the protein production and overall growth parameters (Shiloach and Fass 2005)	72
Table 4.3: Production of GFP and variants in <i>E. coli</i> in selected literature. Several different plasmids, medias and induction strategies were employed.	80
Table 4.4: Literature Review of Purification Schemes for GFP and variants produced using <i>E. coli</i> . pRSET _B containing cells have a His ₆ tag and will use Ni-NTA affinity chromatography as a first step in purification. Several papers discussed resolublizing insoluble proteins and those strategies are presented herein.	81
Table 5.1: Schedule for Shake Flask Experiment.....	91

Table 5.2: Estimated growth rates for 50mL shake flasks taken from 22 °C to 37 °C at various times.	96
Table 5.3: Key for SDS PAGE figures for Shake Flask Runs.....	107
Table 5.4: Summary for initial bioreactor temperature control runs. Final O.D. for the temperature control run was higher than the non-temperature control run, 152 versus 120 O.D. Biomass measured by wet weight differed by 30 g (265g versus 235g).	112
Table 5.5: Key for SDS PAGE figures for Temperature Control Run.....	113
Table 5.6: Parameters for Temperature Control Experiments.....	116
Table 5.7: Final Values for Temperature Control Experiments.	133
Table 5.8: Key for SDS PAGE figures for Temperature Control Run.....	141
Table 5.9: Key for 28 Aug 06 Ni ²⁺ Affinity Purification Gel.....	145
Table 5.10: Key for Renature-Denature SDS PAGE.....	147
Table 5.11: Fluorescence and protein concentration of renatured protein versus homogenized protein. The homogenization pellet showed much higher fluorescence than the renatured protein indicating some fluorescence losses during renaturation. The renatured protein was more concentrated than the homogenized pellet by 300 µg/ml.	148

Chapter 1

Introduction

Recombinant protein production can be a challenging undertaking and there are many decisions to make such as the initial host choices, genetic engineering and production mode. In choosing between different hosts it is important to be familiar with the state-of-the-art regarding the genetic engineering possibilities, as well as the physical limitations of each host and the effects it will have on the protein of interest.

1.1 Scope of Work

This work focuses on comparing and contrasting production of recombinant proteins in CHO and *Escherichia coli* (*E. coli*) with emphasis on production of the biopharmaceutical Tissue-type Plasminogen Activator (tPA) in both hosts. As well, this work explores the effect of temperature as a tool to improve *E. coli* cell culture health by slowing growth to decrease oxygen demand and the maintenance of required dissolved oxygen thresholds in fed-batch *E. coli* fermentations. The latter work also serves as a basis for flowsheet models developed using SuperPro® Designer (Intelligen, Scotch Plains, NJ) and contributes to areas where information is unavailable in literature.

This thesis is divided into two parts each with two chapters:

1. Modeling of Large Scale Recombinant Protein Production using CHO and *E. coli* as hosts.
2. Temperature control to maintain dissolved oxygen concentration in *E. coli* fed-batch fermentations and its effect on growth and protein production.

1.2 Modeling of Large Scale Recombinant Protein Production

Two main types of modeling are favored: mathematical models for which successful implementation depends on the detail and level (single cell versus full process) being observed and heuristic models (known also as expert models) which depend on the skill and knowledge of the person choosing each step in the processes. Each of these modeling

styles are subject to competing objectives (Zhou and Titchener-Hooker 1999a; Zhou and Titchener-Hooker 1999b). An example of a competing set of objectives is the need for high production rates, minimum cost and high purity. Purity is usually the most important objective in a recombinant fermentation for a therapeutic protein.

Production efficiency, expenses and regulatory approval for the process become more important as competitors begin to enter the market (Mustafa et al. 2004). Predictive modeling of large scale industrial production of recombinant proteins is difficult due to the large number of choices for each step, competing objectives such as overall production and purity, inherent non-linearity and downstream unit operations interactions to the product unit operations upstream to them (Zhou and Titchener-Hooker 1999a; Zhou and Titchener-Hooker 1999b).

Before unit processes are chosen, it is necessary to select a host and the genetic engineering techniques which will be used to maximize cell specific productivity. Several options exist in terms of host, and it is necessary to balance the host's traits carefully with the conditions specific to production and use of each protein. For instance, one would not choose *E. coli* as a host in producing a therapeutic glyco-protein which absolutely requires the sugar structures for biological activity (Qiu et al. 1998). However for proteins which do not require glycosylation and are relatively simple, *E. coli* may be an excellent choice of host since it is capable of producing large quantities of protein per cell (Baneyx and Mujacic 2004). Much work has gone into the genetic engineering of each host.

1.3 Protein Functionality and Fermentations

It is also possible to engineer a recombinant protein to have certain features which benefit the end user by making the protein easier to purify, improving its therapeutic function, or inserting different properties from the original protein, such as different chromophores in fluorescent proteins (Hedhammar et al. 2005; Nagai et al. 1999; Rosenow et al. 2004). Protein production on larger scales is dependant upon proper engineering and the stability of protein production on a cellular level.

Most proteins chosen for recombinant production have some characteristics which make the time and difficulty of preparing them for over-expression worthwhile. For eYFP and other members of its family, protein stability and ability to fluoresce without the presence of secondary proteins or additional cofactors has made it a workhorse for genomic studies, protein locationization and applications (Rosenow et al. 2004; Zhang et al. 2006).

Normally, tPA is relatively unstable, subject to attack by proteases and sensitive in a number of ways to the choice of host and its production environment (Lin et al. 1993; Qiu et al. 1998; Yun et al. 2001). However, tPA is a highly sought-after therapeutic capable of specifically dissolving clots in a manner which can prevent further injury or even death in the case of ischemic heart attack or stroke (Rouf et al. 1996). Subsequently, in a highly purified and approved form tPA demands a high market price (Rouf et al. 1996). Such therapeutics earn considerable attention from competitors and generic manufacturers. As patent protection expires, new competitors enter the market driving the costs lower and decreasing relative market share (Mustafa et al. 2004; Wheelwright 1989). This may lead to a revision of production practices and an environment in which modeling and optimization of current production is desirable.

Fed-batch fermentation is dependant upon there being only one limiting component, usually the nitrogen, phosphorous, or carbon source, and assumes that stable protein production can be maintained over its longer time course (Shiloach and Fass 2005). The objective of the fermentation runs was to explore the effect of temperature reduction on protein production and growth as a tool to assist in the control of dissolved oxygen (DO) content. Temperature reduction descreases metabolic rate and increases oxygen solubility. We hypothesize that growth, protein production, and fermentor conditions can be influenced positively by reducing temperature at critical time point during the fermentation.

1.4 Contributions to Research

This work expands on previous work on the industrial production of tPA in CHO by comparing it to production using *E. coli* as a host. It provides an overview of the technologies required from the subcellular to full production scale and uses information available in literature and developed during actual bench scale fermentation runs and purifications to provide insight into areas where literature is unavailable.

Additionally this thesis contributes to the literature regarding temperature control as a means to slow oxygen demand, and its effects on growth and basal protein production. A summary of the production and purification of GFP and variants, effects of temperature control in fermentations on protein and gene expression, as well as observed effects in fermentations, is provided as a basis for final evaluation of the efficacy of temperature control in stabilizing fed-batch fermentations.

Chapter 2

Literature Review for CHO and *E. coli* Modeling

2.1 Introduction

This literature review is done in part to indentify the current information regarding the state-of-the-art in production recombinant proteins, specifically tPA, in *E. coli* or CHO hosts. Secondary to this is to provide a background regarding process synthesis, flowsheeting, and modeling specific to SuperPro® Designer and its direct competitors.

2.2 Process Synthesis

Process synthesis can be defined as methods used to determine the best alternatives in order to achieve an optimal production solution. Traditionally process synthesis has been used mostly in the petrochemical and polymer industries, however new methods enabled by increasingly powerful personal computers are rapidly allowing for synthesis methods to be used in the pharmaceutical and bioprocess industry as they began to feel economic margins (Barnicki and Sirrola 2003). The bioprocess industries face unique regulatory pressures, especially where the product is an active pharmaceutical agent or intended for use for human consumption. Companies engaged in this industry face enormous pressure to effectively use operating capital while reducing costs and still meet increasingly stringent regulatory requirements, while manufacturing costs may account for as much as 25% of sales (Mustafa et al. 2004). Additionally, large scale experimentation is often not feasible until a drug is far into clinical trials, increasing the pressure to find a useable process which is cost effective in a minimum of time.

Often optimization of processes is performed on an unit basis and subsequently it is difficult to account for interactions between units, which may affect the quality and performance of unit operations downstream (Groep et al. 2000). Groep et al. (2000) show how unit interactions affect modeling and simulation of performance of interacting biochemical operations. The work focused on the impact of fermentation and

homogenization on downstream processes using sequential quadratic programming and a defined global objective function to guide optimization. Normally optimization would be achieved over the entire set of manipulated variables. Since there are many conflicting requirements such as purity, product yield, overall process cost and time in this study only the effects of two manipulated variables, growth rate and number of passes in the high pressure homogenizer, were shown and compared using revenue as the global objective function.

Another method to meet these requirements is to simulate how the process would work on the large scale by using smaller scale data and extrapolating it to generalize how a larger scale production sequence might work, requiring heuristic or expert knowledge from the designers. Design of bioprocesses is complicated by a mixture of batch, fed-batch and continuous processes, biological variability, interacting unit operations and multiple options regarding subsequent downstream effects (Zhou and Titchener-Hooker 1999b)

Simulation of a full bioprocess up to the initial clarification stage has been performed by Zhou and Titchener-Hooker (1999) for predicting the effect of homogenization on the performance of a downstream disc-stack centrifuge in separating protein and cell debris from a fed-batch *Saccaromyces cerevisiae* fermentation producing alcohol dehydrogenase (ADH) using Labview™. The simulation was visualized using the “Windows of Operation” technique described in another paper (Zhou and Titchener-Hooker 1999b). The Windows of Operation technique is effective in that it allows the user to visualize the impact of variations in the upstream processes on the subsequent unit operations. In the later paper, the impacts of variances in the fermentation on downstream processes were shown in a graphical manner allowing for easier selection between competing criteria.

Bioprocess simulation done by Greop et al. (2000) using MATLAB demonstrated the effect of a 250 hour continuous fermentation and 1000L fed batch fermentation and homogenization conditions on downstream processes in a *Saccaromyces cerevisiae* strain

producing ADH with an additional step of fractional precipitation allowing for the separation of soluble protein based on sedimentation.

2.3 Process Flowsheeting

Process flowsheeting software provides an easy to implement alternative to creating physical models within MATLAB, Labview or another software packages such as Aspen Batch Plus. Two available software packages are SuperPro® Designer (Intellegen, NJ) and Aspen Batch Plus (Aspentech, MA). Both software packages have been compared in literature and are used in industry (Shanklin et al. 2001). However Aspen Batch Plus, although offered by Aspentech, is not the main focus of the company’s product offerings to their industrial clients and instead they are focused on offering more complete company-spanning solutions. By contrast SuperPro® Designer is now in its sixth version and focuses solely on process and environmental simulation and scheduling (Intelligen 2006). This is an advantage to our current studies since it gives assurance that new models are likely to be incorporated as they are developed.

Predictive results are possible using SuperPro® Designer as shown in Figure 2.1 for centrifugation models.

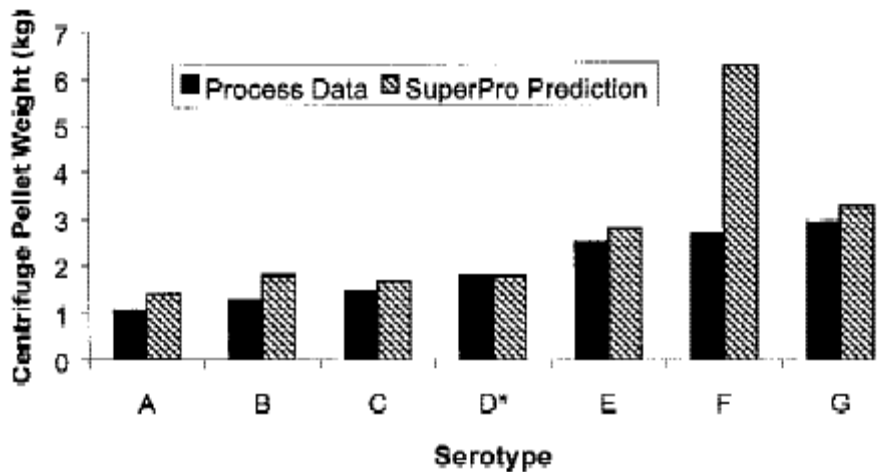


Figure 2.1: Prediction of Centrifugation data using SuperPro® Designer (Shanklin et al. 2001). This shows that predictive results are possible using SuperPro®.

The model fails at times when particle-particle interactions prevent flocculation but is otherwise functional. Some processes such as vapour losses are not included in SuperPro® Designer and subsequently it has limitations, especially in its ability to predict environmental impacts and requirements. Scale up is difficult to predict especially since the simpler processing models are often initialized using pilot or bench scale data and can lead to a over-estimation of yield as shown in Figure 2.2

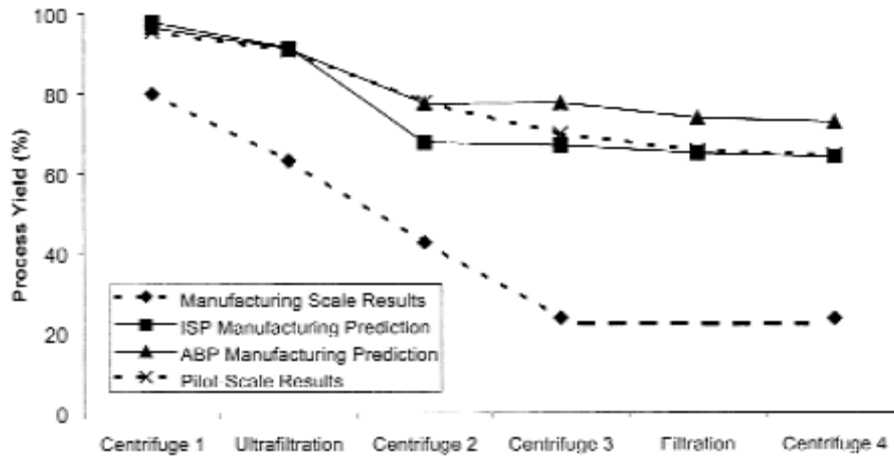


Figure 2.2: Simulation results versus manufacturing scale results using SuperPro® Designer (Shanklin et al. 2001).

2.4 Process Design

After process synthesis, process design involves sizing and choice between different equipment to follow the synthesis steps. Process design is affected by a large number of variables such as host choice and properties, scale and market size of the product, physical properties of the biological product and equipment available to implement the production stream.

Two hosts are being considered: Chinese Hamster Ovary (CHO) cells, a mammalian cell widely used to produce glycoproteins and other therapeutics and *Escherichia coli* (*E. coli*), a prokaryotic host commonly chosen to produce a wide variety of recombinant proteins due its prolific growth and protein production rates and the number of genetic engineered systems available to implement foreign protein production.

Both hosts require differing downstream processing situations due to the way in which they produce the product of interest (in this case a foreign protein such as tissue plasminogen activator) and their genetic properties such as protease production.

There are some common similarities between the equipment and unit processes chosen for differing hosts since similar problems arise, such as solid/liquid separation, and similar goals exist, such as producing large enough amounts of biomass and product to make the process economically feasible.

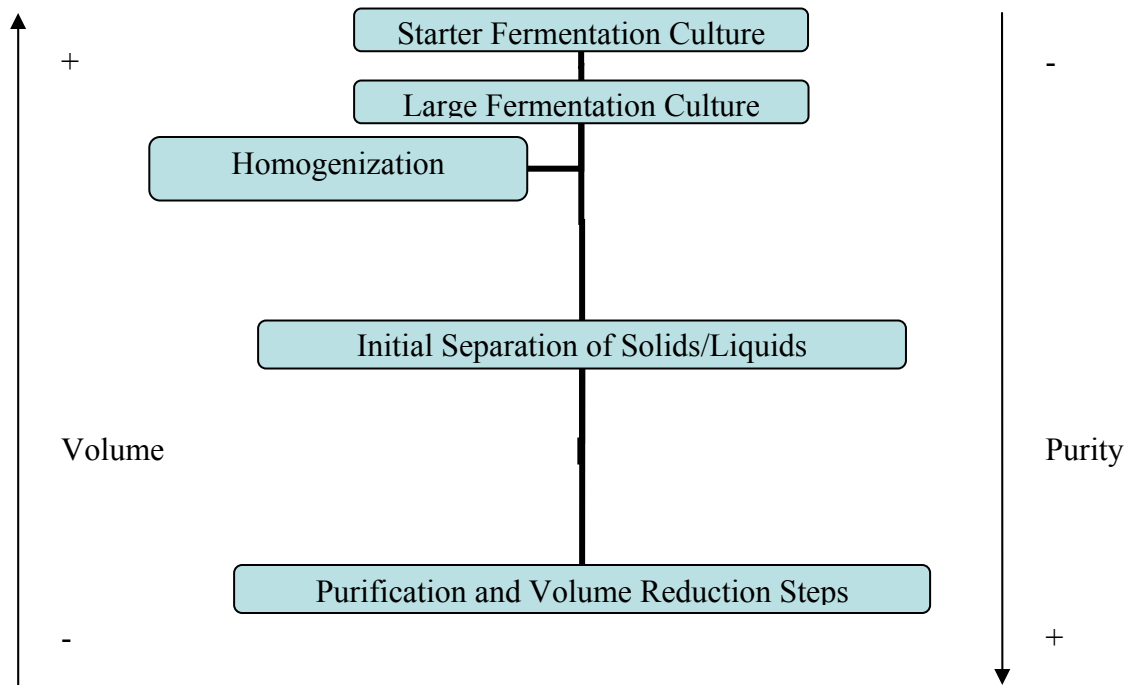


Figure 2.3: Simplified bioprocess layout. Depending on the host homogenization may be required if the protein is not normally secreted. The initial clarification removes cell debris and whole cells and concentrates the protein solution. The protein solution is purified by several steps until the desired purity is reached. Volumes decrease during the fermentation while purity increases.

Figure 2.3 shows a highly simplified bioprocess format typical for recombinant protein production. Throughout the process stream, equipment is selected which reduces volumes and increases purity to produce a highly purified and concentrated product.

2.5 Equipment Selection

2.5.1 Preinoculation and Fermentation

After genetic engineering and introduction of plasmids the typical process is to go to larger and larger scale fermentations until full production is reached, such as shown in Figure 2.4. This may involve several iterations of the small scale fermentation with increasing volumes in order to reach inoculum densities and volumes.

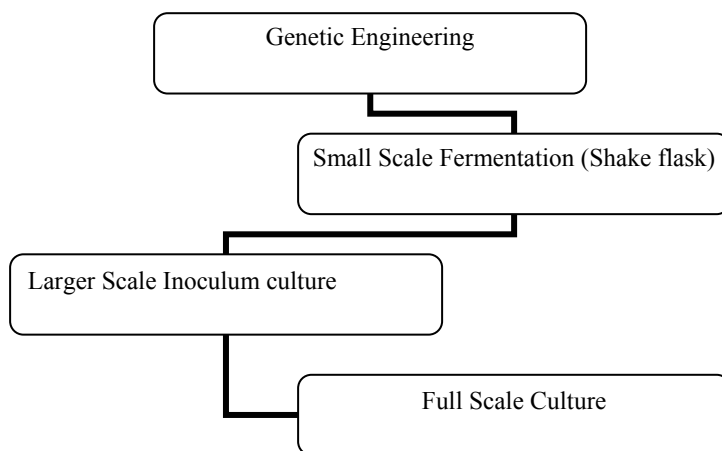


Figure 2.4: Flowsheet for Fermentation Scale Up. These are the typical steps in terms of increasing scales (number of liters produced) of production. Each step requires optimization. It may be necessary to revise the process at each step as units may not behave in similar characteristics at differing scales.

Fermentations are highly species and strain specific with special considerations to media required for each stage and scale of fermentations. Some generalizations are possible however.

There is an increasing focus on using defined media to avoid the costs of commercial media, to control the physical and chemical processes better, aid in understanding of cell requirements, simplify downstream purification and to meet increasingly stringent regulatory requirements.

The most common fermentor process designs are batch, fed-batch, and continuous processes, with batch and fed-batch being the most common process types chosen for use with biopharmaceuticals due to purity and reproducibility issues. The main advantage of fed-batch over batch processes is that the longer run time allows for higher cell and protein concentrations with only moderate additions of media, metabolites and oxygen (Marks 2003).

Much of the control of fermentations on the industrial scale is done heuristically despite sophisticated sensors due to the inherent variability of the system being controlled, inexact data and the lack of deterministic models as a controller basis (Sterbacek and Votruba 1993).

Equipment scale-up and process design at large scales have unique problems and considerations. Reactor designs and sizes determine the size of the downstream processes which can account for as much as 80% of the cost of the overall processes (Rouf et al. 2000).

Scale-down experiments, where a production strain has already been defined and used at large scale but is optimized at the meso-scale in order to meet competitive marketplace needs, is becoming a more common practice as companies attempt to systemize knowledge and decrease process development time (Marks 2003).

2.5.2 Development of Downstream Processing Steps

Downstream processing is the series of steps taken to purify and process the item of interest after production. The design of the process must take into account many conflicting needs such as sterility, safety, consistency of results and economics. While this is not an exhaustive list of requirements it shows some of the areas where trade-offs exist. Wheelwright (1989) defined downstream processing as “a series of steps that, when followed, result in a purified protein product.” The definition of purity is relative to the end use of the product and may be better than 99.9998% for therapeutic products or 95% pure in the case of in-vitro diagnostics (ELISA, etc) with examples given in Figure 2.5 .

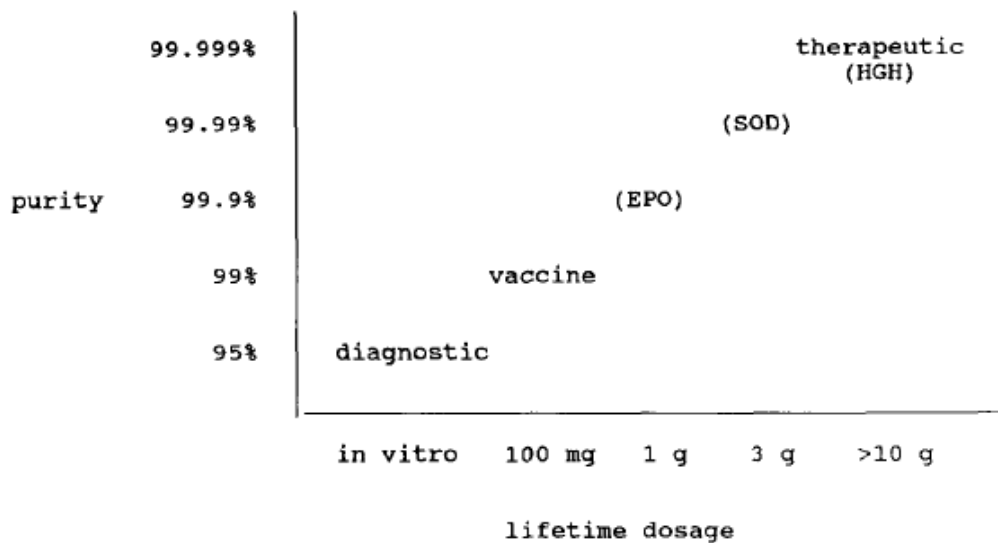


Figure 2.5: Protein purity required as a function of end use (human Erythropoietin (EPO), Super Oxide Dismutase (SOD)) (Wheelwright 1989). This gives an example of how the closer to in-vivo use the final product comes the higher the purity demanded.

In order to meet market demand for new proteins one must have an entire process which can operate on large scales economically. Several downstream processes exist for a variety of commercial and therapeutic protein products and may serve as templates. However the differences between protein, multitude of process options, and development of new process options defies a complete mathematical process by which one can choose the optimal process. The optimal process may be defined as a process which gives the desired quantity of product at the lowest economic cost. The economic costs are not just a function of capital, labour, and manufacturing expenses but also a function of time to market, regulatory, and other considerations which affect the process choices and for which no mathematical models exist.

Economic considerations change also as the product passes from patent protection or as competitors enter the market driving down the products salable value (reducing profit) leading to an increasing focus on manufacturing and economic efficiency. In a highly regulated environment the ability to change the process is reduced since it requires approvals from many different agencies such as the U.S. Food and Drug Administration, Health Canada or European Medicines Evaluation Agency and additional costs.

Industrially, downstream processing begins by considering the likely size of full scale production based on forecasts that indicate the scale of operation. Wheelwright (1989) stated that “the only defensible reason for scale-up studies is a reduction in the possibility of making expensive errors in the design or the operation of commercial size equipment.” While this may be true, another reason to operate small scale equipment is to experiment with new processing options for future consideration in a more economic manner.

In order to meet the design goals of downstream processing it is vital the protein product of interest is fully characterized in terms of size, pH stability, ionic strength, physical make up, folding characteristics and other features which affect the downstream processing. This can be done while the design goals are being assembled since much of the data will have been collected as the protein is screened for potential commercial use.

Choosing the optimal purification process can be done many ways but two of the most commonly used are heuristics, a methodology used to limit the possible alternatives based on experience, and expert systems.

Table 2.1 shows four different methods used in choosing an optimal solution.

Table 2.1: Heuristic classifications used to determine downstream processes (Wheelwright 1989). Differing heuristic types are utilized to reach an optimized process. Understanding the application of each method aids in optimization.

Type	Applications	Example
1. Method heuristics	Specify choice between different unit operations	Describe conditions for preferring ultrafiltration over centrifugation
2. Design heuristics	Specify order or sequence of process steps	Perform low resolution step prior to high resolution step
3. Species heuristics	Specify step based on properties of components	Choose separation method based on greatest difference in properties of product and impurities
4. Composition heuristics	Specify product or feed composition based on separation costs	

The four types of heuristics form an overall picture to allow one to choose a proper order of downstream processes, which will allow for the desired production and quality. The need to emphasize ease of operation and safety is shown in Table 2.2 with each suggested rule which can be applied to systematically limit the number of choices available at each junction.

Table 2.2: A list of rules of thumb for each type heuristic (Wheelwright 1989). Using these rules-of-thumb makes process selection easier eliminating certain initial choices and making downstream process choices easier to reach.

1. Method heuristics

- (a) Favor ordinary distillation.
- (b) Avoid vacuum and refrigeration.
- (c) Remove mass separating agent first.

2. Design heuristics

- (a) Favor smallest product set.
- (b) Use cheapest separator first.
- (c) Favor direct sequence.
- (d) Remove valuable or desired product last.

3. Species heuristics

- (a) Remove corrosive and hazardous components first.
- (b) Perform high-recovery separation last.
- (c) Perform difficult separations last.
- (d) Perform easy separations first.

4. Composition heuristics

- (a) Remove most plentiful component first.
- (b) Favor 50/50 split.

Expanding further on the uses of design heuristics, Table 2.3 gives more rules of thumb on how to choose equipment and processes during the design of downstream processes, with an emphasis on quick completion of purification with the least number of steps.

Table 2.3: Comparison of design heuristics (Wheelwright 1989). Additional rules of thumb for downstream processes used to eliminate certain option early on and make downstream unit selection easier.

1. Choose first step based on:	2. Choose next step based on:	3. Choose last step based on:
Differential solubility (crude adsorption)		Selectivity (high resolution chromatography)
Nonspecific separation	High selectivity	Polishing (i.e., crystallization)
Precipitation	Ion-exchange, affinity chromatography	Gel filtration
Intermediate purification (ion-exchange, adsorption, affinity)	Further (i.e., chromatography)	Gel filtration
Initial (i.e., concentration)	Affinity, ion exchange	Final (i.e., concentration, formulation)
Precipitation		Gel filtration
Largest volume or mass removed		Most expensive (per unit-of-product basis)

2.6 Unit Operations Common in Basecases: General overview

2.6.1 Homogenization

E. coli's unique physiology necessitates the disruption of the cell and the separation of cell debris from the protein of interest. The homogenization of *E. coli* causes potential problems for the separation of solid and liquids in both centrifuges (which follow D'Arcy's Law) and filtration devices (which follow Hagen-Poiseuille flow) by creating fluids which have the potential for high viscosity and small particles.

Cell wall structure has been shown to change throughout the growth cycle and in response to various conditions affecting the degree of difficulty in destroying the

peptidoglycan cross-linked layers providing external cell wall (Middleburg, 1994). Figure 2.6 shows some of the disruption methods which are available to use at the large scale:

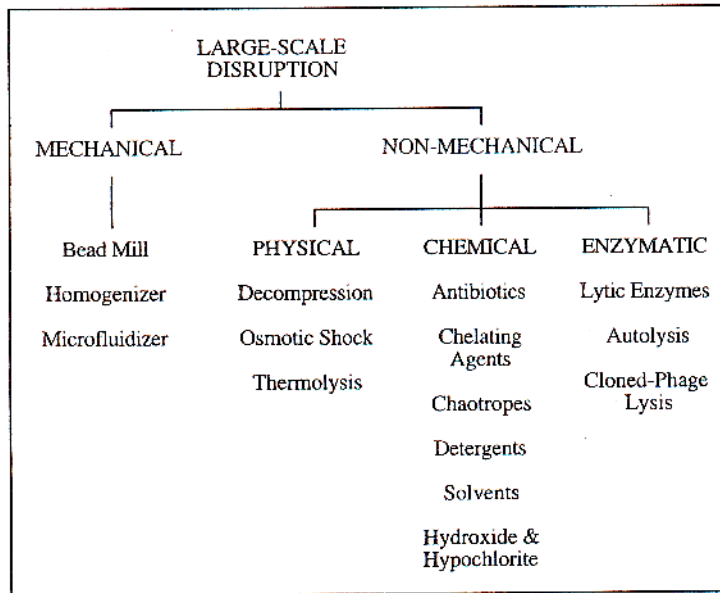


Figure 2.6: Techniques for Large Scale Disruption of Microorganisms (Middelburg 1995). Several of these choices are infeasible for large scale production such as decompression. In large scale purifications enzymatic choices are usually eliminated due to the cost.

2.6.1.1 Bead Mill Homogenization

The mechanism for bead mill homogenization is a combination of liquid shear forces and collisions between dense bodies usually glass beads of less than 1.5 mm in diameter (Middleburg, 1995).

Disruption in a bead mill is a first order function of the mean residence time. The particle size distribution is not influenced by the mean residence time however longer mean residence times have the benefit of lowering the overall viscosity. Increased cell concentrations do not affect the particle size distribution but increases the viscosity (Agerkvist and Enfors 1990)

Ideally the mean residence time should be such that the cell disruption can be modeled closely to a plug flow concept but is also dependent upon the type of agitator due to energy transfer considerations (Middelburg 1995).

2.6.1.2 High Pressure Homogenization

The main mechanism for disintegration in a high pressure homogenizer tends to be the magnitude and velocity of the pressure drop over the value and oscillation from turbulent eddies. *E. coli* homogenates are highly viscous owing to the influence of RNA and DNA with DNA being the major contributor (Agerkvist and Enfors 1990).

The kinetics of homogenization for a high pressure homogenizer is a first order function of the number of passes, with the number of passes determining the relative particle size. The rate of degradative enzyme release relative to protein release is a function of protein location within the cell. As cell concentration and pressure increases in a high pressure homogenizer the efficiency decreases. Temperature has a relatively small effect on the cracking efficiency although lower temperatures seem to be less efficient between 20-60 MPa. *E. coli* which contain inclusion bodies formed from the production of high amounts of recombinant protein are more easily disrupted at higher pressures and pH and storage time appear to have minimal effect on the overall efficiencies. This effect is speculated to be from the metabolic load of overexpression affecting the ability of the *E. coli*'s maintenance and growth ability (Middelburg et al. 1991)

Most *E. coli* and yeast homogenization debris distributions can be described using the Boltzman equation (Ling et al. 1997; Siddiqi et al. 1996).

A rule of thumb is that the more passes through a high pressure homogenizer the wider the debris distribution and the smaller the debris will be. This can lead to difficulty in separating debris from proteins as smaller debris may tend to cause problems with recovery methods involving centrifugation and filtration mediums.

2.6.2 Primary Recovery and Clarification

There are several potential primary recovery steps. The most common are microfiltration usually in a crossflow configuration and centrifugation.

2.6.2.1 Microfiltration

After homogenization it is necessary to separate solids and liquids. Microfiltration units operate by allowing permeates of a certain size to pass through (the filtrate) and keeping larger particles (the retentate) from the permeate stream. Depending on the size of the product this can be used for concentration as well as purification since it provides a means to separate solids from liquids and solids from solids based on size. In cross-flow filtration the flux is washed parallel across the membrane usually resulting in less fouling. Typical membrane sizes are 0.65 μm , 0.45 μm , and 0.22 μm . In literature it has been found that the largest pore size allowed some solids passage into the permeate, the 0.45 μm membrane allowed only 0.01% of packed solids (99.99% retention) through the membrane and although the 0.22 μm membrane allowed no apparent passage of solids the larger membrane size was chosen likely for its better flux capacities (Forman et al. 1990). Forman et al. (1990) also suggest that the presence of inclusion bodies has a strong influence on cake properties, the ability to form high transmembrane pressures (experimental pressures were an order of magnitude lower than experiments without inclusion bodies), and protein concentrations in the flux.

The accumulation of additional solid material creates resistance to flux which can be modeled as a cake resistance. The concentration polarization theory states that there will be a point at which the cake resistance will reduce the flux to the original steady state value. This region of operation is avoided because of the waste of energy for no gain in flux and high soluble protein retention.

2.6.2.2 Diafiltration

In diafiltration a solvent is added to replace permeate and aid in mass transfer during filtration. It is possible to utilize membrane filtration units in a diafiltration configuration when the membrane is only permeable to species collected in the filtrate and for which there exists a means to force mass transfer across the membrane (usually by removing the permeate).Forman et al. (1990) also explored diafiltration as a potential first step to separate soluble proteins from inclusion bodies using a 0.45 μm membrane with low crossflow and flux to maintain a constant TMP.

2.6.2.3 Centrifugation

Centrifugation separates particles based on relative densities through centrifugal force. This can be used effectively for separating components in cell broth such as solids (cell debris, whole cells and insoluble particles) from liquids (supernatant, spent media, and soluble protein) based on Stoke's Law.

Disk stack centrifuges rely on aided sedimentation and utilize several stacked disks with made porous with holes to separate solid and liquids. Basket centrifuges rely on filtration driven by centrifugal force (Miller 1973). Centrifuges are typically avoided due to difficulties associated with sterility, small particle sizes and sizing considerations (van Hee et al. 2006).

2.6.3 Purification: Chromatography

Scale up of chromatography is difficult, and often purification conditions change as the scale is changed (Rouf 1999). Selecting large scale process is usually based on heuristics and selecting the proper sequence of chromatographic steps can be difficult (Vasquez-Alvarez and Pinto 2004).

2.6.3.1 Affinity

Affinity chromatography depends on selectivity of a protein based on a unique characteristic. In the case of tPA affinity, chromatography involves lysine/fibrin or other materials such as lysine derivatives which are selective to the unique binding domains in either the full length or variant types (Rouf 1999; Vlakh et al. 2003). Various binding domains have been genetically engineered in recent years to allow binding to specific affinity columns although the use of these in large scale production is limited by the ability to remove these tags in the final purified product (Hedhammar et al. 2005).

2.6.3.2 Ion Exchange

Ion exchange is based on charge interactions of proteins to a positively (cation) or negatively (anion) charged column. This process is highly dependent upon the pH of the buffers being used and specific column properties (Ghose et al. 2002). As the literature

review in Chapter 2 reveals this is a commonly used type of chromatography since it is widely applicable to many different proteins.

2.6.3.3 Expanded Bed Adsorption

Expanded Bed Adsorption (EBA) is a relatively new technique. Depending on the host and whether it secretes protein the supernatant or homogenized cell lysate is flowed into the column fluidizing the bed allowing small particles to interact with the chromatographic media which binds the protein of interest. After the protein is bound the flow is reversed and the packed bed is then used the same as a regular chromatography column (Cabanne et al. 2004; Johansson et al. 1996). This removes a clarification step before traditional chromatography saving equipment, space and time. This type of chromatography has been reported to be used at the 2000 L scale with good recovery and purity compared to traditional methods, but is sensitive to feed stream characteristics such as viscosity, solid debris density and size, and non specific interactions (Shepard et al. 2001).

2.7 Plasminogen Activator variants, functionalities and production

Plasminogen activators are thrombolytic agents used to break up thrombi which cause heart attacks and strokes by obstructing vascular pathways. Several types of plasminogen activators exist including:

1. Urokinase Plasminogen Activator (uPA)
2. Streptokinase Plasminogen Activator (sPA)
3. Tissue-type Plasminogen Activator (tPA)

Streptokinase derived from prokaryotic sources is not specific to just fibrin-bound plasminogen, leading to increased hemorrhage risks and may result in pyrogenic and immunogenic responses because of its non-human source. Derived from urine, Urokinase is non pyrogenic and non-immunogenic but expensive to produce and supplies are limited. Tissue-type plasminogen activator is specific to fibrin bound plasminogen, more active than urokinase and with a longer half life reported to be 2-6 minutes although half lives of up to 10 minutes have been reported, with a typical therapeutic dose of 60-100 mg (Rouf et al. 1996; Waldenstrom et al. 1991).

Tissue-type plasminogen activator is a 527 amino acid, 70,000 Dalton (of which glycosylation accounts for 7% of the total molecular weight), n-glycosylated protein made up of 5 domains with 17 disulphide bonds and one unpaired cystine residue. Figure 2.7 shows five domains in tPA:

1. A fibrin binding finger near the N-terminus
2. An Epidermal growth like factor domain
3. Two Kringle-like domains caused by disulphide bonds like those found in prothrombin and urokinase
4. A serine protease domain similar to that of urokinase and other serine proteases

The kringle and serine protease domains bind to the fibrin and are essential the activity of tPA. Limited protolytic activity cleaves the bond between arginine 275 and isoleucine 276 leading to a two chain form bound by a single disulphide bond. The one and two chain forms show little difference in their physiological activities. The protein has four potential glycosylation sites at aspargines 117, 184, 218, and 448 however due to folding and sylase activity two glycosylation patterns occur normally (triangles in Figure 2.7 show potential glycosylation sites).

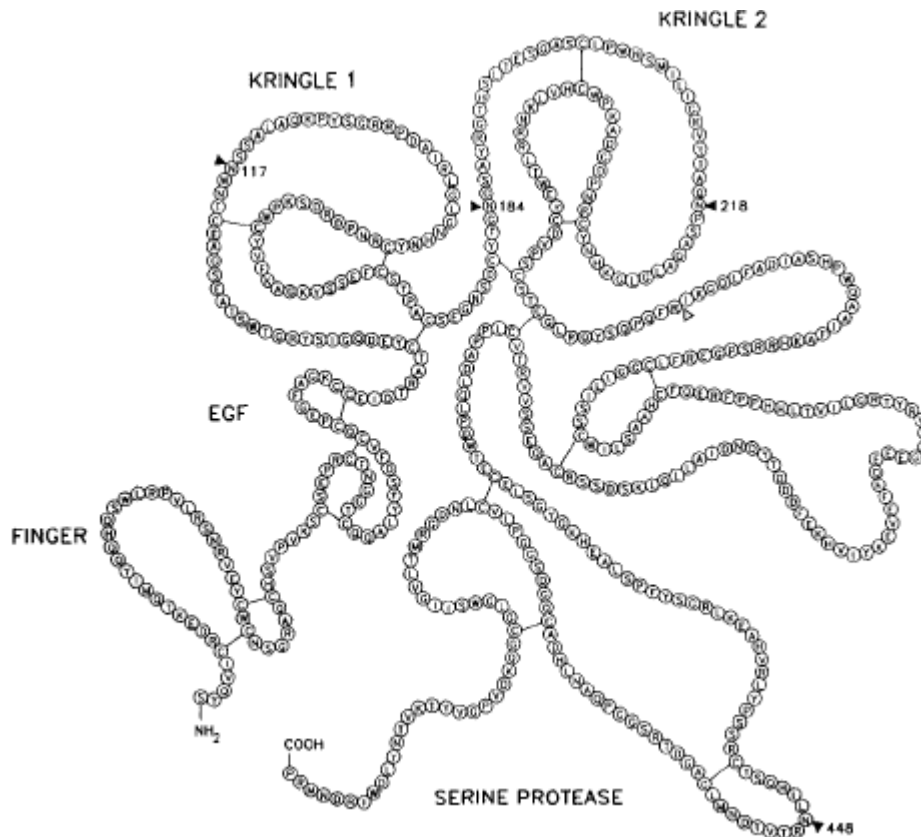


Figure 2.7: tPA full domain amino acid representation (Rouf et al. 1996). The tPA has four main domains: Kringle 1, Kringle 2, Serine Protease, and a fibrin binding domain. The tPA protein has 527 amino acids and a molecular weight of 70 kDa.

Several variants have been made of tissue-type plasminogen activator to allow for production in both eukaryotic and prokaryotic hosts. Of these, the most common are variants with one or both of the kringle domains and the serine protease. Since glycosylation is not essential for tPA functionality, production using prokaryotic hosts can be accomplished and where this has been done longer half lives have been reported (Qiu et al. 1998). Production of tPA and other proteins in CHO and *E. coli* are detailed below.

2.8 Chinese Hamster Ovary Cell Properties

Tissue plasminogen activator was the first recombinant protein produced from Chinese Hamster Ovary (CHO) cells which are now the mammalian cell of choice to produce proteins which have complex folding and glycosylation needs. Much like prokaryotic hosts the host is given genes which encode for the protein of interest as well as a gene which transfers a selective advantage to the cell. Productivity has reportedly increased since the 1980's from 50 mg/L to nearly 4.7 g/L for some proteins (Wurm 2004). DNA is delivered typically as cDNA without introns. It is known however that some introns are needed for proper folding and now most cDNA coding genes come with one intron between the promoter and the coding sequence. One technique to increase productivity is to put the selective gene with a weak promoter. This tends to select for higher producing strains although it gives poorer transfection rates. Other's have attempted to maintain the cell in a specific phase of cell growth (Hendrick et al. 2001; Lee et al. 1998; Lloyd et al. 1998). Unlike prokaryotic hosts gene silencing involving the transfer of the gene from euchromatin to heterochromatin happens and several techniques are available to inhibit this effect (Wurm 2004).

Media that are available via a few manufacturers such as Sigma, are of excellent quality but are generally very expensive. Wurm (2004) suggested that large scale protein manufacturers likely produce their own media and use different media based on what cell cycle the cells are in. Serum free media without bovine serum albumin (BSA) have been developed and been in the market for quite a long time now. This is due to worries over bovine spongiform encephalitis (BSE) or other contaminants and the undefined nature of BSA. Genetic engineering of the cells for superior and stable production as well as longevity is well documented from academic laboratories, but not so from industrial laboratories, likely due to proprietary concerns.

There are several cell culture formats for CHO cells from adherent cells on microcarriers to suspension cultures with free floating cells. The transition between adherent cell culture to suspension culture often requires special media formulations and screenings

called passages. Scale up can be accomplished by 5-20 dilution by prewarmed media that is held in a larger bioreactor. Changing growth and culture characteristics in the fermentation can produce variation in large scale protein production and quality. Subsequently it is necessary to use scale down cultures to optimize production and growth (Wurm 2004). Perfusion technologies are available which allow for the product to be harvested several times over a month at high cell densities and is suitable for large or fragile proteins. Table 2.4 provides a summary of literature on the production of tPA and other selected proteins for comparison in CHO hosts.

Table 2.4: Production of recombinant tPA in CHO. The sizes of fermentation vary but the time of fermentations is always measured in days for CHO culture.

Host	Strain	Induction	Protein Production	Media	Cell production	Type	Vessel Volumes	Aeration	Time	Source
CHO	CL-11G		7823 IU/mL 7358 IU/mL Prurorokinase	DMEM:F12 (1:1)	2.06 e7 cells/mL 1.33 e7 cells/mL	Batch	5 L 20L		43 d 18 d	(Xiao et al. 1999)
CHO	Various	Various	4.70 g/L Type Not Specified	Various	10.0 e7 cells/mL 1.33 e 7 cells/mL	Fed Batch Batch			10-21 d 6-8 d	(Wurm 2004)
CHO	Tf70R	Buytrate	3.65 mg/L tPA	Biopro-1	4.00 e5 cell/mL	Spinner Flask	500 mL 37 °C		168 Hrs	(Hendrick et al. 2001)
CHO	MT2-1-8 (Cytodex)		300 ug/L tPA estimated	DEM:F12 supp w MEM (1:1)	3.30 e6 cells/mL	Batch Perfusion	1 L		<200 Hrs	(Lin et al. 1993)
CHO	ATCC CRL-9606	Methotrexate (MTX)	tPA	IS-CHO V	1.01 E6 cells/mL 9.00 e6 cells/mL	Spinner Flask	1 L 37 °C and 1 L 37 °C -34 °C		≈216 Hrs	(Clark et al. 2004)
CHO	ATCC CRL-9606	Methotrexate (MTX)	5-40 ug/mL tPA	CD-CHO protein free	5.00-35.0 e5 cells/mL	Batch	1 L in 3 L 37 °C	40% DO	280 Hrs	(Senger and Karim 2003)
CHO	ATCC CRL-9606	Methotrexate (MTX)	80-95 mg/L tPA	HAMs F12	15-35 e5 Cells/mL	Spinner Flask	30 mL in 100 mL		11 d	(Takagi et al. 2001a)
CHO	ATCC CRL-9606	Methotrexate (MTX)	8-15 mg/LtPA	HAMS F12	1.50 e6 -3.10 e6 Cells/mL	Spinner Flask	30 mL in 100 mL		4 d	(Takagi et al. 2001b)
CHO	ATCC CRL-9606	Methotrexate (MTX)	0.275-2.017 mg/L tPA	HAMS F12 with 10% NBS	2.00 e5 Cells/mL	Spinner Flask	100 mL		6 d	(Yun et al. 2001)

2.9 Escherichia coli Properties

Escherichia coli (*E. coli*) is a gram negative facultative aerobic bacterium. Several subtle factors influence protein production such as DNA specific issues occurring in promoters and genetic engineering for protein translocation to the outer membrane or periplasm, RNA translation efficiency, protein production, chaperones and folding issues.

Large scale production of proteins from *E. coli* to find the limits in terms of protein production and maximum cell density has been studied since the 1970's resulting in batch, fed-batch and dialysis fermentation methods to achieve high cell titers. Optimized growth media, molecular biology and culture techniques has made it possible to grow cell titers up to 190 g/L dry weight, avoiding media precipitation and acetate accumulation (Shiloach and Fass 2005). For high value products, high production significantly reduces the capital expenditures in expanding fermentations as well as the operational expenses of GMP production facilities. Maximum possible cell density for *E. coli* is estimated to be 200 g/L and fluidity is reportedly lost at titers higher than 220 g/L (Shiloach and Fass 2005). The main idea behind high titer fermentations is that cells will continue to grow provided that there is a constant supply of nutrients, oxygen and no inhibitory byproducts accumulating. Oxygen demand for *E. coli* has been predicted to be close to 1g for every 1.06 g of *E. coli* (Shiloach and Fass 2005). Media conditions are quite demanding for high cell densities and metals required for sustained growth can precipitate in cultures because of improper cation/anion balances which also lead to fluctuating osmotic pressures and conductivities causing cellular stress which slows growth and may stop cellular division. The slow release of phosphate ions has been suggested as a means to control precipitation and cation/anion balance problems. Another common problem is acetate accumulation which when above 2 g/L inhibits growth and protein production (Shiloach and Fass 2005). Fed-batch and dialysis methods for fermentations were developed to avoid these problems and Table 2.5 shows methods used to achieve high level production of proteins.

Table 2.5: Techniques for high density cell culture with *E. coli* (Shiloach and Fass 2005). These techniques are also applicable to other hosts.

Propagation technique	Basic medium	C source	Yield; g dcw/l	Reference
<i>Fed batch</i>				
1. Exponential growth	Semi-defined Medium yeast Extract	Glucose	54	Shiloach and Bauer, 1975
2. Carbon source defended linear growth	Defined Minimal medium	Solid glucose	134	Neidhardt et al., 1974; Matsui et al., 1989
	Defined Minimal medium	Glucose Citric acid	104	Riesenberg et al., 1990
	Defined Minimal medium	Glycerol Glucose	148 128	Korz et al., 1995
	Protein hydrolyzate and yeast extract	Glycerol	84	Macaloney et al., 1996
3. Slow linear growth to keep acetate concentration close to zero	Defined minimal medium	Low glucose Glycerol	145	Horn et al., 1996
<i>Dialysis</i>				
1. Membrane dialysis reactor	Against complete growth medium	Glycerol	174	Märkl et al., 1993
2. "Nutrient-split" feeding	Against basal medium	Glycerol	190	Nakano et al., 1997
	Against buffer salt solution	Separate glycerol feeding	150	Ogbonna and Märkl, 1993

Protein production in the reducing cytoplasm or periplasm in *E. coli* can be as fast as one protein chain in 35 seconds and reach a concentration of 300-400 mg/ml (Baneyx and Mujacic 2004). For single domain small proteins (>100 residues) with fast folding kinetics this host can be extremely effective but for larger proteins with more complicated folding requirements or for proteins with slower folding kinetics folding modulators such as chaperones are often required. Under balanced growth conditions chaperones and other folding modulators are produced constitutively but are quickly outpaced in cases of heat shock or other stressful cellular conditions. Proteins which do not fold quickly usually have one of two fates:

1. Formation of insoluble inclusion bodies
2. Degradation by proteases

Inclusion bodies typically consist of 85-90% of misfolded proteins and are resistant to proteases but are often contaminated with cell debris components from homogenization. This can be exploited to produce proteins which are easily refolded, toxic to the cell, or unstable. As competition intensifies or as products lose patent protection frequently it is necessary to consider refolding proteins to increase overall yields. The costs of traditional refolding is prohibitive however new technologies such as direct chemical extraction, expanded bed absorption, refolding on chromatography columns, or mechanical disruption (Lee et al. 2006b).

In wild type *E. coli* the cytoplasm environment is reducing, making it very difficult to produce proteins with complex tertiary or quaternary structures. In order to deal with this, it is quite common to overexpress foreign chaperones to aid in the folding processes. Another result of this environment is the inability to form complex double disulphide bonds in the cytoplasm, resulting in aggregation of disulphide rich recombinant proteins. Three approaches are available to deal with this. Expression in the oxidizing periplasm using the *sec* pathway, or outer membrane using the proper chaperones can aid in protein folding and formation of disulphide. Another approach is to use a weaker promoter or decreasing the amount of inducer. For *lac*, *tac* or *trc* based promoters (typically IPTG induced) concentrations of IPTG less than 100 μM is recommended. A third strategy is to reduce the temperature below that at which the protein aggregates but the disadvantage is the loss in overall productivity. To overcome this, *cspA* promoters have been developed to operate below a temperature of 15°C (Baneyx and Mujacic 2004).

It has been shown that glucose-limited fed batch cultures of *E. coli* at 37°C produce high amounts of outer membrane components which are endotoxic (Svensson et al. 2005). Utilizing a temperature limited fed batch culture Svensson et al. (2005) was able to reduce the amount of endotoxins while maintaining similar growth and product yields. Although the strain used was *E. coli* W3110 they reported similar results (not shown in the paper) for the strain BL21. The most likely consequence of this is that the

downstream product would need more purification steps in order to remove any endotoxins to meet regulatory requirements.

2.9.1 Production of tissue-type plasminogen activator and variants in *E. coli*

Tissue plasminogen activator (tPA) production in *E. coli* is difficult since the reducing environment in the cytoplasm does not allow for the easy formation of the seventeen natural disulphide bonds in the protein. Qiu, Swartz and Georgiou (1998) targeted protein production in the oxidizing periplasm to allow for proper disulphide folding with coexpression of DsbA and DsbC foldases producing 180 µg/L of soluble full length tPA, 25% of the total tPA production. Schaffner et al. (2001) produced a Kringle 2 and Protease domains variant (K2P variant) with 9 disulphide bonds. After finding that reducing agents in the media aided in disulphide shuffling several additions including glutathione (GSH) and L-arginine were added. Waldenstrom et al. (1990) reported producing an active tPA variant with the K2P domains intact as a fusion protein excreted into the media. Production from media plates as high as 950 µg/mL (Waldenstrom et al. 1991). A KSP variant was produced in shake flasks and ten liter bioreactors with 397 IU/µg activity and half life comparable to Bowes Melanoma standard tPA (Obukowicz et al. 1990). Saito, Ishii et al (1994) created several tPA variants while attempting to find a variant which could be produced reliably in the cytoplasm of *E. coli* by reducing the number of disulphide bonds required. It was found that a K2P variant was the best with a half life superior to the alteplase (full length native tissue plasminogen activator) commercially available. Manosori et al. (2001) developed a K2S domain tPA variant with a specific activity of 236 IU/µg following a different approach than that of Obukowicz et al. (1990). Table 2.6 provides a summary of literature on the production of tPA and selected other proteins.

Since many of the proteins produced in *E. coli* form insoluble inclusion bodies, it is at times advantageous to develop downstream purification processes for the inclusion bodies if they are of sufficient abundance and purity. Table 2.7 outlines the purification methods used in literature to produce tPA.

Table 2.6: Production of recombinant tPA and tPA variants in *E. coli* and other selected proteins. The production scales vary by paper but the fermentation times are much quicker than CHO, measured in hours instead of days. The cell yields, when reported, are typically higher than CHO cultures but the specific productivity is lower than most CHO cases.

Strain	Induction	Protein Production	Media	Cell production	Type	Vessel Volumes	Aeration	Time	Source
SF 110	Pbad induced with Arabinose	25 g/L culture 180 ug/L t-PA	Salt Media		Batch	6.5 L in 15 L Fermentor 37 °C	10 L/min	25 Hrs	(Qiu et al. 1998)
		K1, K2, K1K2, K1K2P,K2P tPA 201 mg K2P	M9 Modified	7.59 kg wet	Fed Batch	100 L 35 °C	300 rpm 70L/min to 400 rpm 140 L/min after 5 hours		(Saito et al. 1994)
XL-1 Blue	IPTG	1.36 ug periplasmic 2.96 ug supernatant K2S tPA variant	Super Broth		Shake Flask	100 mL 37 °C then after induction cultured 30 °C		6 Hrs	(Manosroi et al. 2001)
BL21 and N4830	lac promoter 1mM IPTG	3.978 ng/mL w/ L-arginine addition & DnaJ K2S Variant tPA	LB						(Schaffner et al. 2001)
JM101	tac promoter with IPTG	20 ug/L K2S variant tPA	M9 Modified	1.7 Kg wet	Fed Batch	10L in 15L fermentor, 30 °C			(Obukowicz et al. 1990)
		ZZK2P tPA variant			Culture Plate				(Waldenstrom et al. 1991)
BL21 DE3 pLysS	lac promoter with IPTG	223 mg soluble 279 mg refolded PAI-1	M9 ZB	2.2 g wet	Shake Flask	50 mL, various temperatures			(Lee and Im 2003)

Strain	Induction	Protein Production	Media	Cell production	Type	Vessel Volumes	Aeration	Time	Source
XL-1 Blu	lac promoter IPTG	16.2 ng/mL anti-CD3 scFv			Shake Flask	50 mL in 100 mL shake flasks 37 °C			(Kipriyanov et al. 1997)
BL21	Pzt-1 induced with tetracycline T7 promoter induced with IPTG	16 mg rhEndostatin after refolding			Shake Flask	1 L 16 °C			(Xu et al. 2005)
	Ptac induced with IPTG	20-22 g total 3 g soluble IL-1 receptor antagonist 0.43g active IL-1 receptor antagonist	TB	1.8 kg Paste 36 g/L dry	Batch	50 L in 70 L fermentor 37 °C	70 L/min	19 Hrs	(Zanette et al. 1998)

Table 2.7: Purification of tPA from *E. coli*. Purification schemes follow much the same pattern as with CHO with affinity chromatography usually the first or second step.

Homogenization	Clarification	Purification	Source																		
Sonication	Centrifugation 12,000xg 15min 4°C	<p>L-lysine-Sepharose</p> <table border="1"> <thead> <tr> <th>Equilibrium Buffer</th> <th>Wash Buffer</th> <th>Elution Buffer</th> </tr> </thead> <tbody> <tr> <td>50 mM Tris-HCl, pH 7.5; 5mM EDTA; 0.1% Tween 80</td> <td>8 C.V. 50 mM Tris-HCl, pH 7.5, 5mM EDTA, 0.1% Tween 80</td> <td>50 mM Tris-HCl, pH 7.5; 5mM EDTA; 0.1% Tween 80, 0.5M NaCl, 0.2M Lysine</td> </tr> </tbody> </table> <p><i>E. caffra</i>-Sepharose affinity</p> <table border="1"> <thead> <tr> <th>Equilibrium Buffer</th> <th>Wash Buffer</th> <th>Elution Buffer</th> </tr> </thead> <tbody> <tr> <td></td> <td>4 C.V. 0.5 M NH₄HCO₃, 0.1% Triton X-100 4 C. V. 0.05 M NaH₂PO₄, pH 7.3 4 C. V. 0.05 M NaH₂PO₄, pH 7.3, 0.1M KSCN</td> <td>0.05 M NaH₂PO₄, pH 7.3, 0.9M KSCN</td> </tr> </tbody> </table> <p>Sepharose ZnCl₂ at 4°C for 30 min. Incubation at 4°C for 2 h</p> <table border="1"> <thead> <tr> <th>Equilibrium Buffer</th> <th>Wash Buffer</th> <th>Elution Buffer</th> </tr> </thead> <tbody> <tr> <td></td> <td>0.05 M NaH₂PO₄, 0.5 M NaCl, 0.05% Tween 80 pH 7.3</td> <td>0.05 M NaH₂PO₄, 0.5 M NaCl, 0.05% Tween 80 pH 7.3, 0.05M imidazole</td> </tr> </tbody> </table>	Equilibrium Buffer	Wash Buffer	Elution Buffer	50 mM Tris-HCl, pH 7.5; 5mM EDTA; 0.1% Tween 80	8 C.V. 50 mM Tris-HCl, pH 7.5, 5mM EDTA, 0.1% Tween 80	50 mM Tris-HCl, pH 7.5; 5mM EDTA; 0.1% Tween 80, 0.5M NaCl, 0.2M Lysine	Equilibrium Buffer	Wash Buffer	Elution Buffer		4 C.V. 0.5 M NH ₄ HCO ₃ , 0.1% Triton X-100 4 C. V. 0.05 M NaH ₂ PO ₄ , pH 7.3 4 C. V. 0.05 M NaH ₂ PO ₄ , pH 7.3, 0.1M KSCN	0.05 M NaH ₂ PO ₄ , pH 7.3, 0.9M KSCN	Equilibrium Buffer	Wash Buffer	Elution Buffer		0.05 M NaH ₂ PO ₄ , 0.5 M NaCl, 0.05% Tween 80 pH 7.3	0.05 M NaH ₂ PO ₄ , 0.5 M NaCl, 0.05% Tween 80 pH 7.3, 0.05M imidazole	(Qiu et al. 1998)
Equilibrium Buffer	Wash Buffer	Elution Buffer																			
50 mM Tris-HCl, pH 7.5; 5mM EDTA; 0.1% Tween 80	8 C.V. 50 mM Tris-HCl, pH 7.5, 5mM EDTA, 0.1% Tween 80	50 mM Tris-HCl, pH 7.5; 5mM EDTA; 0.1% Tween 80, 0.5M NaCl, 0.2M Lysine																			
Equilibrium Buffer	Wash Buffer	Elution Buffer																			
	4 C.V. 0.5 M NH ₄ HCO ₃ , 0.1% Triton X-100 4 C. V. 0.05 M NaH ₂ PO ₄ , pH 7.3 4 C. V. 0.05 M NaH ₂ PO ₄ , pH 7.3, 0.1M KSCN	0.05 M NaH ₂ PO ₄ , pH 7.3, 0.9M KSCN																			
Equilibrium Buffer	Wash Buffer	Elution Buffer																			
	0.05 M NaH ₂ PO ₄ , 0.5 M NaCl, 0.05% Tween 80 pH 7.3	0.05 M NaH ₂ PO ₄ , 0.5 M NaCl, 0.05% Tween 80 pH 7.3, 0.05M imidazole																			

Homogenization	Clarification	Purification	Source																		
Biotron Blender with Lysozyme	Centrifugation	<p>Denaturation Buffer 0.4 mM cystine, 0.04 mM cystine, 10 mM NKOAc (pH 9.5), 8 M urea</p> <p>Centrifugation of Denatured Protein Mixture</p> <p>Supernatant Renaturation Dialysis 160 L lo mM NH4OAc (pH 9.51), 0.4 mM cystine, 0.04 mM cystine</p> <p>QAE-Toyopearl column (50 mm x 380 mm, Tosoh)</p> <table border="1" data-bbox="619 576 1522 673"> <thead> <tr> <th data-bbox="619 576 919 609">Equilibrium Buffer</th> <th data-bbox="919 576 1220 609">Wash Buffer</th> <th data-bbox="1220 576 1522 609">Elution Buffer</th> </tr> </thead> <tbody> <tr> <td data-bbox="619 609 919 673">2 M urea in 20 mM Tris-HCl (pH 8.0)</td> <td data-bbox="919 609 1220 673"></td> <td data-bbox="1220 609 1522 673">2 M urea in 20 mM Tris-HCl (pH 8.0) 1 M NaCl</td> </tr> </tbody> </table> <p>Dialysis 40 L of 20 mM Tris-HCl (pH 8.0) at 4 °C for 16 h.</p> <p>QAE-Toyopearl column(16 mm x 80 mm)</p> <table border="1" data-bbox="619 824 1522 954"> <thead> <tr> <th data-bbox="619 824 919 857">Equilibrium Buffer</th> <th data-bbox="919 824 1220 857">Wash Buffer</th> <th data-bbox="1220 824 1522 857">Elution Buffer</th> </tr> </thead> <tbody> <tr> <td data-bbox="619 857 919 954"></td> <td data-bbox="919 857 1220 954"></td> <td data-bbox="1220 857 1522 954">linear gradient 0 to 1 M NaCl in 20 mM Tris-HCl (pH 8.0),2M urea</td> </tr> </tbody> </table> <p>Dialysis 20 L of 20 mM Tris-HCl (pH 8.0)</p> <p>p-aminobenzamidine Sepharose 4B column 16 mm x 25 mm</p> <table border="1" data-bbox="619 1105 1522 1227"> <thead> <tr> <th data-bbox="619 1105 919 1138">Equilibrium Buffer</th> <th data-bbox="919 1105 1220 1138">Wash Buffer</th> <th data-bbox="1220 1105 1522 1138">Elution Buffer</th> </tr> </thead> <tbody> <tr> <td data-bbox="619 1138 919 1227">50 mM Tris-HCl buffer (pH 8.0),1 M NaCl , 0.01% Tween 80</td> <td data-bbox="919 1138 1220 1227"></td> <td data-bbox="1220 1138 1522 1227">50 mM Tris*HCl buffer (pH 8.0), 1 M arginine, 0.01% Tween 80</td> </tr> </tbody> </table>	Equilibrium Buffer	Wash Buffer	Elution Buffer	2 M urea in 20 mM Tris-HCl (pH 8.0)		2 M urea in 20 mM Tris-HCl (pH 8.0) 1 M NaCl	Equilibrium Buffer	Wash Buffer	Elution Buffer			linear gradient 0 to 1 M NaCl in 20 mM Tris-HCl (pH 8.0),2M urea	Equilibrium Buffer	Wash Buffer	Elution Buffer	50 mM Tris-HCl buffer (pH 8.0),1 M NaCl , 0.01% Tween 80		50 mM Tris*HCl buffer (pH 8.0), 1 M arginine, 0.01% Tween 80	(Saito et al. 1994)
Equilibrium Buffer	Wash Buffer	Elution Buffer																			
2 M urea in 20 mM Tris-HCl (pH 8.0)		2 M urea in 20 mM Tris-HCl (pH 8.0) 1 M NaCl																			
Equilibrium Buffer	Wash Buffer	Elution Buffer																			
		linear gradient 0 to 1 M NaCl in 20 mM Tris-HCl (pH 8.0),2M urea																			
Equilibrium Buffer	Wash Buffer	Elution Buffer																			
50 mM Tris-HCl buffer (pH 8.0),1 M NaCl , 0.01% Tween 80		50 mM Tris*HCl buffer (pH 8.0), 1 M arginine, 0.01% Tween 80																			

Homogenization	Clarification	Purification	Source												
High Pressure 4 passes 8000 psi cooled 4 °C	Microfiltration 22 µm spiral cartridge	<p>Lysine affinity (6.2 cm/hr flowrate)</p> <table border="1"> <tr> <td>Equilibrium Buffer</td> <td>Wash Buffer</td> <td>Elution Buffer</td> </tr> <tr> <td>TE Buffer</td> <td></td> <td>TE, NaCl, 0.2M L-lysine</td> </tr> </table> <p><i>E. caffra</i> with 4B sepharose affinity (5 cm/hr flowrate)</p> <table border="1"> <tr> <td>Equilibrium Buffer</td> <td>Wash Buffer</td> <td>Elution Buffer</td> </tr> <tr> <td>0.5M NH₄HCO₃</td> <td></td> <td>.5 M NaCl , 0.2M L-lysine</td> </tr> </table> <p>Amicon ultrafiltration concentration YM5 membrane</p>	Equilibrium Buffer	Wash Buffer	Elution Buffer	TE Buffer		TE, NaCl, 0.2M L-lysine	Equilibrium Buffer	Wash Buffer	Elution Buffer	0.5M NH ₄ HCO ₃		.5 M NaCl , 0.2M L-lysine	(Obukowicz et al. 1990)
Equilibrium Buffer	Wash Buffer	Elution Buffer													
TE Buffer		TE, NaCl, 0.2M L-lysine													
Equilibrium Buffer	Wash Buffer	Elution Buffer													
0.5M NH ₄ HCO ₃		.5 M NaCl , 0.2M L-lysine													
N/A	Centrifugation	<p>2ml IgG Sepharose</p> <table border="1"> <tr> <td>Equilibrium Buffer</td> <td>Wash Buffer</td> <td>Elution Buffer</td> </tr> <tr> <td></td> <td>TST</td> <td>0.2M acetic acid pH 4</td> </tr> </table>	Equilibrium Buffer	Wash Buffer	Elution Buffer		TST	0.2M acetic acid pH 4	(Waldenstrom et al. 1991)						
Equilibrium Buffer	Wash Buffer	Elution Buffer													
	TST	0.2M acetic acid pH 4													
Sonication	Centrifugation	<p>Insoluble Fraction Denatured with 4M GuHCl Refolded with 20mM sodium acetate, 1M NaCl, and 0.01% Tween 80, pH 5.6 diluted with buffer containing no NaCl</p> <p>SP-Sepharose ion-exchange</p> <table border="1"> <tr> <td>Equilibrium Buffer</td> <td>Wash Buffer</td> <td>Elution Buffer</td> </tr> <tr> <td>20mM sodium acetate, 0.5M NaCl, 0.01% Tween 80, pH 5.6</td> <td></td> <td>0.5-1.5M NaCl gradient</td> </tr> </table> <p>Soluble Fraction Ni-NTA Affinity Column</p> <table border="1"> <tr> <td>Equilibrium Buffer</td> <td>Wash Buffer</td> <td>Elution Buffer</td> </tr> <tr> <td>20mM sodium acetate, pH 5.6, 0.5M NaCl, 5mM imidazole, 0.01% Tween 80</td> <td>20mM sodium acetate, 0.5M NaCl, 60mM imidazole, 0.01% Tween 80, pH 5.6</td> <td>60–1000mM imidazole gradient</td> </tr> </table>	Equilibrium Buffer	Wash Buffer	Elution Buffer	20mM sodium acetate, 0.5M NaCl, 0.01% Tween 80, pH 5.6		0.5-1.5M NaCl gradient	Equilibrium Buffer	Wash Buffer	Elution Buffer	20mM sodium acetate, pH 5.6, 0.5M NaCl, 5mM imidazole, 0.01% Tween 80	20mM sodium acetate, 0.5M NaCl, 60mM imidazole, 0.01% Tween 80, pH 5.6	60–1000mM imidazole gradient	(Lee and Im 2003)
Equilibrium Buffer	Wash Buffer	Elution Buffer													
20mM sodium acetate, 0.5M NaCl, 0.01% Tween 80, pH 5.6		0.5-1.5M NaCl gradient													
Equilibrium Buffer	Wash Buffer	Elution Buffer													
20mM sodium acetate, pH 5.6, 0.5M NaCl, 5mM imidazole, 0.01% Tween 80	20mM sodium acetate, 0.5M NaCl, 60mM imidazole, 0.01% Tween 80, pH 5.6	60–1000mM imidazole gradient													

Chapter 3

SuperPro® Designer Modeling

3.1 Introduction to CHO and *E. coli* Basecases

The Basecases presented are in 2005 US dollars. Inoculation fermentors are excluded due to lack of data regarding sequencing and growth for CHO cultures. The soluble protein production from *E. coli* literature is less than that from CHO according to available literature. This is reflected in lower protein yields in *E. coli* cultures. In areas where literature values regarding costs were unavailable, SuperPro® Designer defaults were used (Table 3.1). In both the CHO and *E. coli* Basecases, the purified protein solution would be mixed with stabilizers, lyophilized and packaged after purification. Since no information on these processes is available, they also have been excluded from the models.

Table 3.1: SuperPro® Designer default costs used in modeling.

	Cost (2005 US\$)
Membrane Costs	\$200/m ²
Steam	\$4.20/1000 kg
NaCl Brine	\$0.25/kg
Electricity	\$0.10/kWh
Chromatography Resins	\$200/L
Operator	\$30/hr
Supervisor	\$50/hr

3.2 CHO Basecase

CHO Basecases are based on the work by Rouf (1999) and the literature review performed in Chapter 2. The CHO Basecase is intended to provide a yardstick to measure the models involving *E. coli*. Figure 3.1 shows the fully developed Basecase for CHO. After initial clarification of the spent media, two affinity chromatography steps are used with ultrafiltration before each to concentrate the feedstreams. Gel filtration represents the end of the simulation.

3.2.1 CHO Basecase Unit Model and Data

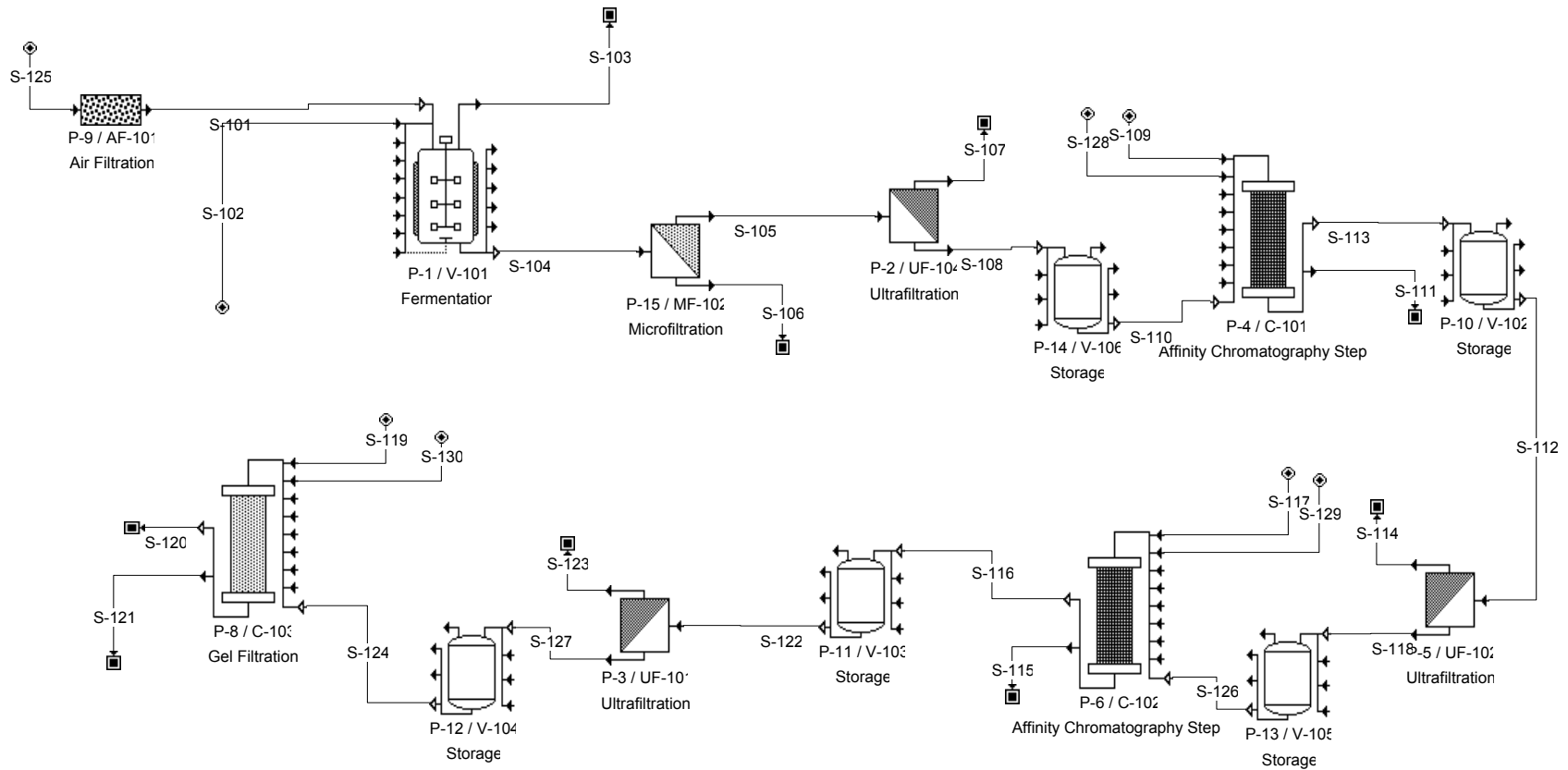


Figure 3.1: CHO Basecase Unit Model. The CHO Basecase model was taken from previous work by Rouf (1999). The storage devices between each unit are used to store processed proteins after each step. The clarification section involves a microfilter and ultrafilter. The downstream purification involves two passes on an affinity column with an ultrafiltration step in-between to reduce volumes. The final purification uses gel filtration.

The expected process time for the CHO Basecase is 241 hrs (10 days) from initial inoculation of the large fermentor to final sterilization of the Gel Filtration column. The batch fermentation process time is modeled to take 200 hrs (8.3 days). A summary of the materials used and produced is given in

Table 3.12. The starting material for the fermentation is media, proteins, L-glutamine, glucose and air. The other raw materials are used in the downstream sections for clarification and purification.

The main products of fermentations involving recombinant proteins are biomass and tPA. Since CHO cells secrete tPA, the microfiltration process is relatively uncomplicated. Table 3.2 presents the unit sizes and costs in the CHO Basecase. The fermentor is the most expensive capital expenditure, \$3.2 million, more than half the capital expense of the project (Table 3.3).

Table 3.2: Equipment sizing and costs for CHO Basecase.

Unit	Description	Volume/Size	Cost (\$US)
P-1/V-101	Fermentor	6800L/1.79m diameter	3,210,000
P-4/C-101	PBA Chromatography Column	1.15m dia/0.5m height	246,000
P-6/C-102	PBA Chromatography Column	0.96m dia/0.5m Height	198,000
P-8/C-103	GFL Chromatography Column	1.05m/0.5m Height	218,000
P-9/AF-101	Air Filter	0.36m ³ /s rated volume	7,000
P-11/V-103	Receiver Vessel	400L/0.55m dia	11,000
P-12/V-104	Receiver Vessel	100L/0.34m dia	11,000
P-13/V-105	Receiver Vessel	280L/.49m dia	11,000
P-14/V-106	Receiver Vessel	50L/0.28m dia	11,000
P-10/V-102	Receiver Vessel	290L/.49m dia	11,000
P-15/MF-102	Microfilter	105 m ²	120,000
P-2/UF-104	Ultrafilter	50 m ²	170,000
P-5/UF-101	Ultrafilter	3.4 m ²	21,000
P-3/UF-102	Ultrafilter	2.7 m ²	21,000

Table 3.3: Economics for CHO Basecase.

Parameter	
Total Capital Investment	\$31,722,000
Operating Cost	\$9,886,000 /year
Production Rate	14.48 kg/year
Unit Production Cost	\$682,784 /kg
Total Revenues	\$173,752,000 /year
Gross Margin	94.31 %
Return on Investment	313.50 %

3.3 *E. coli* Basecases

3.3.1 Introduction

Production of a tPA variant has already been commercially established to compete against full length tPA produced in CHO cells (Chapter 2). Likely this competitor takes advantage of several new developments in recombinant production, such as expanded bed adsorption and improved genetic engineering techniques which allow for better production of proteins requiring disulphide bonds.

Again for areas where information is lacking regarding costs of production, the default costs used in SuperPro® Designer have been used (Table 3.1). In the absence of detailed information on purification, the *E. coli* Basecases use the same downstream processes as the CHO Basecases.

The Basecases present several simulation pathways for comparison of production of tPA from *E. coli*. The initial *E. coli* Basecase is also assumed to have a 200 hour fermentation with initial clarification provided by a centrifuge. When this is found to be unsuitable microfiltration is used for initial clarification. The problems arising from homogenization are

addressed at his juncture with an additional microfiltration step. Since *E. coli* grow at a much faster rate than CHO cells the fermentation time is reduced using the same model with the additional microfiltration step. Once this has been established a model to allow a direct comparison between the CHO and *E. coli* Basecases based on protein production is formed.

3.3.2 Biomass and Protein Yield Prediction

Predicted biomass formed in the fermentation was chosen to be between values reported by Saito et al. (1994 and Obukowicz et al. (1990) (Table 3.4). The value used in this base case is approximately 0.1061 kg wet weight/L favoring the lower end of the reported ranges. Values for wet weight yields will be much higher than the dry weight yield values usually reported. Cell mass yields for cultures grown in rich media will typically be higher than defined salt media cultures and this is reflected in the low and high value yield cases.

Table 3.4: Biomass Yields from Literature Review and value used in Basecases.

	Biomass (Kg wet weight/L)	Glucose Concentration (g/L)	$Y_{x/s}$ g (wet weight)/g
Low Value	0.0759	2.5	30.36
High Value	0.17	0.085 (enriched media)	200
Basecases	0.1061	1	106.1

Protein production is estimated to be 11 $\mu\text{g/L}$ in the Basecases. This is much lower than 180 $\mu\text{g/L}$ tPA reported by Saito et al. (1994) and slightly lower than the 20 $\mu\text{g/L}$ tPA reported by Obukowicz et al. (1990). This is conservative but not unreasonable, considering the values reported in the literature (Chapter 2).

3.3.3 200 hr *E. coli* Basecase with Centrifuge Initial Clarification Step.

In fermentations producing recombinant eYFP (Chapter 4 and Chapter 5) centrifugation was the first and only choice to provide initial clarification of cell broth. Unlike the CHO Basecase, the supernatant is usually discarded in *E. coli* fermentations unless the protein is

presented on the outermembrane where it may potentially defuse into the media and end up in the supernatant.

It has been found desirable to concentrate the cells before homogenization on a small scale to increase homogenization efficiencies and it is assumed that this would follow for large scale cases.

3.3.4 *E. coli* Basecase Unit Model and Data

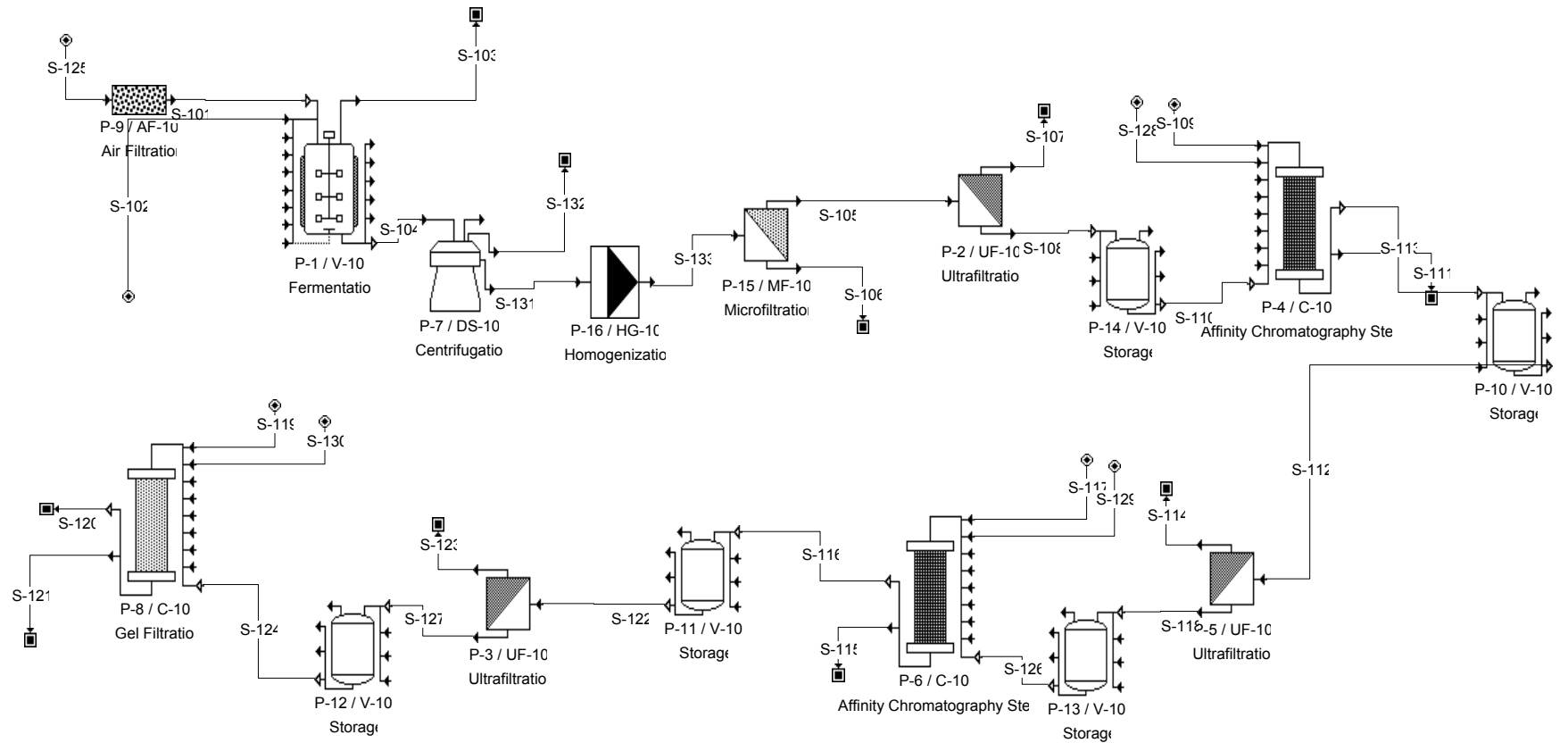


Figure 3.2: 200 hr *E. coli* Basecase Unit Model with centrifuge unit for initial clarification. Centrifugation was chosen as the initial clarification method. High pressure homogenization was chosen as the cell disruption method. The downstream process remains the same as the CHO Basecase.

A preliminary review of the resource consumption charts for this Basecase shows that the predicted volume of water used is approximately 40 million liters, all in an instantaneous load (Figure 3.3). A look at the time demand chart for water reveals that this is associated with the process within the centrifugation unit.

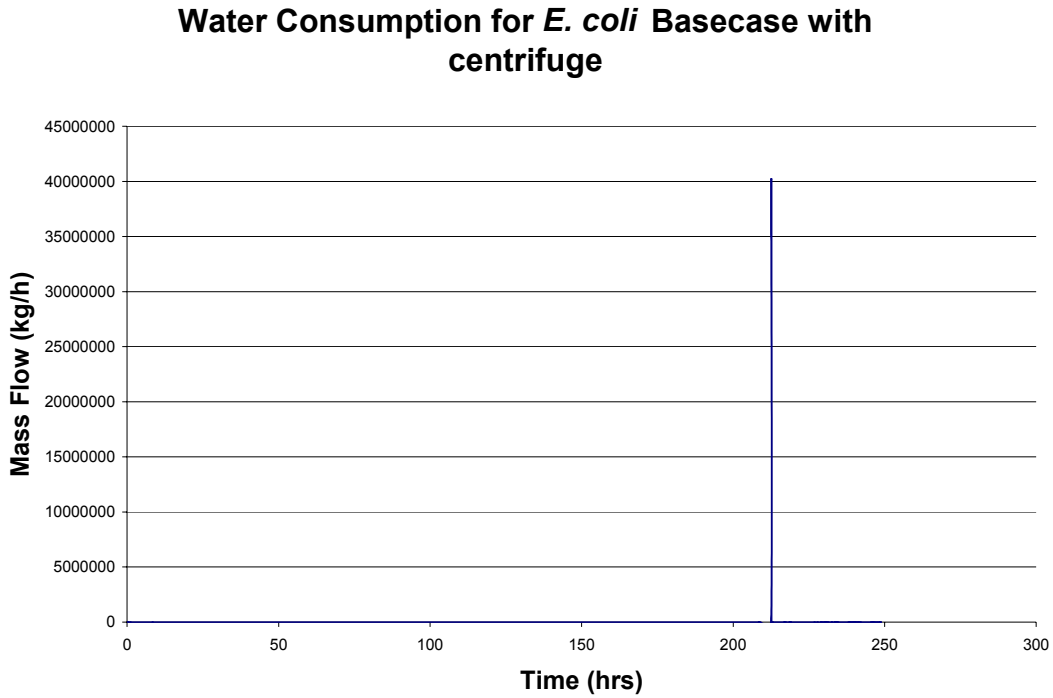


Figure 3.3: Water consumption for *E. coli* Basecase with centrifuge.

Closer inspection reveals that the water consumption is associated with the Clean-In-Place (CIP) operation of the centrifuge and is due to the large predicted size of the centrifuge and large amount of water used per square meter of size (100L/m²).

Table 3.5: Equipment sizing and costs for Centrifuge Initial Clarification *E. coli* Basecases.

Unit	Description	Volume/Size	Cost (\$US)
P-1/V-101	Fermentor	6000L/1.72m diameter	3,150,000
P-4/C-101	PBA Chromatography Column	0.70m dia/0.5m height	162,000
P-6/C-102	PBA Chromatography Column	0.58m dia/0.5m Height	147,000
P-8/C-103	GFL Chromatography Column	0.64/0.5m Height	154,000
P-9/AF-101	Air Filter	0.32m ³ /s rated volume	7,000
P-11/V-103	Receiver Vessel	148L/0.40m diameter	11,000
P-12/V-104	Receiver Vessel	34L/0.24m diameter	11,000
P-13/V-105	Receiver Vessel	18L/0.20m diameter	11,000
P-14/V-106	Receiver Vessel	85L/0.33m diameter	11,000
P-10/V-102	Receiver Vessel	103L/0.35 diameter	11,000
P-17/MF-101	Microfilter	72 m ²	96,000
P-2/UF-104	Ultrafilter	69 m ²	97,000
P-3/UF-101	Ultrafilter	1.27 m ²	21,000
P-5/UF-102	Ultrafilter	1.00 m ²	21,000
P-7/HG-101	Disk-Stack Centrifuge	101,081 m ²	277,000
P-16/HG-101	High Pressure Homogenizer	0.71 m ³ /h	20,000

Clearly, disk stack centrifugation this is not a good choice for initial clarification .This supports the rules of thumb discussed in Chapter 2 for downstream equipment selection; filtration is chosen before centrifugation.

3.3.5 200 hr *E. coli* Basecase with Microfiltration initial clarification step.

Substituting the centrifuge for a Microfilter (Figure 3.4) alleviates the water consumption problem discussed in the previous section. The trade off comes in terms of lower protein production at the end of each fermentation (Table 3.12).

3.3.6 200 hr *E. coli* Basecase with Microfiltration as Initial Clarification: Unit Model and Data

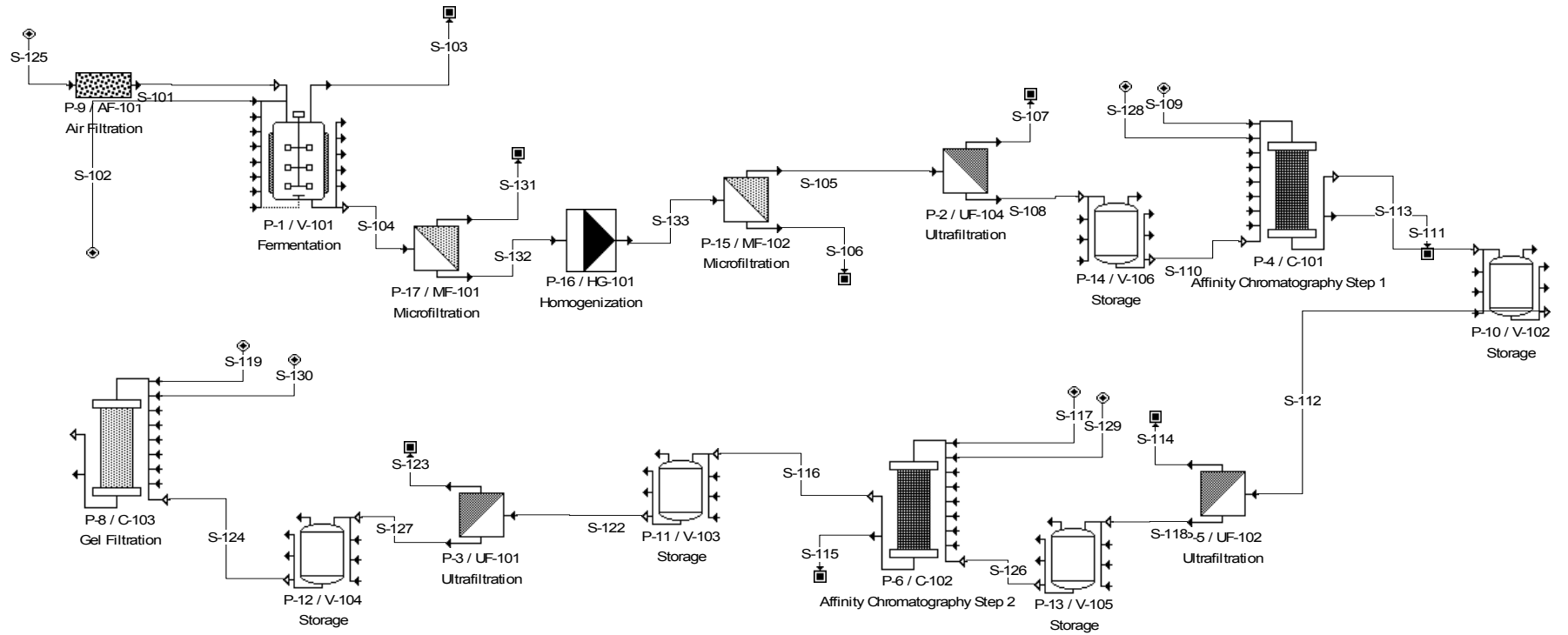


Figure 3.4: 200 hr *E. coli* Basecase with initial microfiltration unit added to avoid water consumption problems. Problems were discovered downstream of the homogenization step shortly after the water consumption problem was solved.

3.3.7 Need for Additional Microfiltration Step

Another problem encountered with the units downstream of the high pressure homogenizer comes from too much debris after homogenization. Some of the left-over biomass is predicted to find its way onto the first affinity chromatography column (Table 3.6), and this will lead to slower flow through the chromatography column, possible plugging and extra cleaning and repacking after each run leading to high process variance, greater labour costs and operation times.

Table 3.6: Predicted Removal Efficiencies for clarification section of 200 hr *E. coli* Basecase in Figure 3.4.

Unit	Initial Cell Debris (kg)	Remaining Cell Debris (kg)	Efficiency (%)	Initial Biomass (kg)	Remaining Biomass (kg)	Efficiency (%)
Microfiltration	385.75	0	100%	46.41	9.92	78.6%
Ultrafiltration	0	0	N/A	9.92	0.46	95.4%

To avoid this, an extra microfiltration unit was added (Figure 3.5). It is unlikely that this would physically represent additional microfilter but would rather represent an additional step or pass.

3.3.8 200 hr *E. coli* Basecase with extra Microfiltration Step

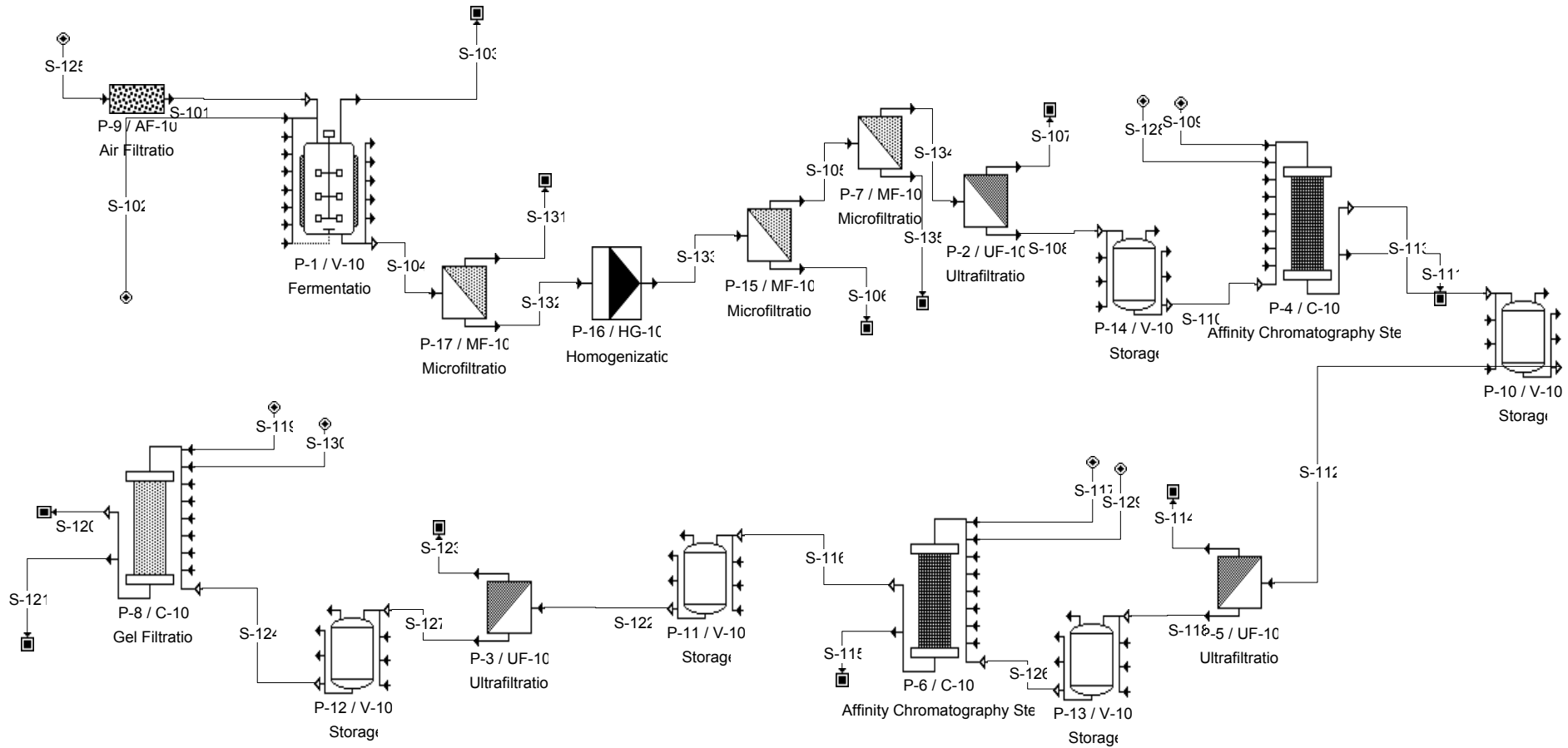


Figure 3.5: 200 hr *E. coli* Basecase with extra microfilter after homogenizer. The relative cost of the microfiltration step is minimal and avoids loading cell debris or whole cells onto the first affinity chromatography step.

The addition of the Microfiltration step resolved the problem of loading cell debris on the first chromatography column (Table 3.7) but leads to greater initial protein losses. The ultrafiltration unit is kept to further concentrate the protein before application to the first chromatography unit minimizing the required size.

Table 3.7: Predicted Removal Efficiencies for clarification section of 200 hr *E. coli* Basecase with extra Microfiltration unit shown in Figure 3.5.

Unit	Initial Cell Debris (kg)	Remaining Cell Debris (kg)	Efficiency (%)	Initial Biomass (kg)	Remaining Biomass (kg)	Efficiency (%)
Microfiltration	385.75	0	100%	46.41	44.41	4.3%
Microfiltration	0	0	N/A	44.41	0	100%
Ultrafiltration	0	0	N/A	0	0	

Equipment sizing and prices are listed in Table 3.8 which are similar in function to the CHO Basecase with the addition of a homogenizer and more microfiltration units. The decreased protein production reported in *E. coli* contributes to decreased costs and equipment sizes downstream of the fermentor.

Table 3.8: Equipment sizing and costs for 200 hr and 36 hr *E. coli* Basecases.

Unit	Description	Volume/Size	Cost (\$US)
P-1/V-101	Fermentor	6000L/1.72m diameter	3,150,000
P-4/C-101	PBA Chromatography Column	0.69m dia/0.5m height	246,000
P-6/C-102	PBA Chromatography Column	0.57m dia/0.5m Height	198,000
P-8/C-103	GFL Chromatography Column	0.63/0.5m Height	218,000
P-9/AF-101	Air Filter	0.36m ³ /s rated volume	7,000
P-11/V-103	Receiver Vessel	142L/0.39m diameter	11,000
P-12/V-104	Receiver Vessel	34L/0.24m diameter	11,000
P-13/V-105	Receiver Vessel	18L/0.20m diameter	11,000
P-14/V-106	Receiver Vessel	85L/0.33m diameter	11,000
P-10/V-102	Receiver Vessel	103L/0.35 diameter	11,000
P-17/MF-101	Microfilter	47 m ²	75,000
P-15/MF-102	Microfilter	35 m ²	62,000
P-7/MF-103	Microfilter	0.45 m ²	0
P-2/UF-104	Ultrafilter	32 m ²	65,000
P-3/UF-101	Ultrafilter	1.22 m ²	21,000
P-5/UF-102	Ultrafilter	0.96 m ²	21,000
P-16/HG-101	High Pressure Homogenizer	0.40 m ³ /h	17,000

3.3.9 Effect of lower production time on E. coli Basecase

The overall economics of the fermentation are in some ways related to time of production since operators are paid per hour. More important, quicker fermentations allow for more campaigns per year increasing plant production capacity. *E. coli* are known for faster growth.

Large scale fermentation of *E. coli* occurs over a shorter period compared to CHO. Typical fermentation times in *E. coli* are closer to 24 to 36 hours for 3 to 50 L fed-batch fermentations (Chapter 5), (Akesson et al. 2001). Another paper using SuperPro® reports using a fermentation time of 12 hours for 1000 L producing 100g dry cell weight (Lee et al. 2006a). The model remains the same as in Figure 3.5 but the fermentation time has been modified to 36 hours.

3.3.10 E. coli 36 Hr Basecase modified to match CHO yearly tPA output

Another method for comparison of *E. coli* and CHO Basecases is to match the production outputs and compare the economics of both Basecases. The Basecase remains the same as Figure 3.5: 200 hr *E. coli* Basecase with extra microfilter after homogenizer. The relative cost of the microfiltration step is minimal and avoids loading cell debris or whole cells onto the first affinity chromatography step. with 36 hour fermentation however the fermentor itself has been modified in size to produce only enough tPA for 14.48 kg/yr to match protein production in the CHO model. The fermentor required to reach similar production as CHO is nearly 1000 L smaller than previous *E. coli* Basecases and 1800 L smaller than the CHO Basecase (Table 3.9).

Table 3.9: Equipment sizing and costs for *E. coli* Basecase with 36 hour fermentation time and 14.48 kg tPA production.

Unit	Description	Volume/Size	Cost (\$US)
P-1/V-101	Fermentor	5011 L/1.72 m diameter	3,150,000
P-4/C-101	PBA Chromatography Column	0.63 m dia/0.5 m height	153,000
P-6/C-102	PBA Chromatography Column	0.52 m dia/0.5m Height	139,000
P-8/C-103	GFL Chromatography Column	0.57 m dia / 0.5 m Height	146,000
P-9/AF-101	Air Filter	0.05 m ³ /s rated volume	5,000
P-11/V-103	Receiver Vessel	118 L /0.37 m diameter	11,000
P-12/V-104	Receiver Vessel	28 L / 0.23 m diameter	11,000
P-13/V-105	Receiver Vessel	15 L / 0.18 m diameter	11,000
P-14/V-106	Receiver Vessel	71 L / 0.31 m diameter	11,000
P-10/V-102	Receiver Vessel	85 L /0.33 m diameter	11,000
P-17/MF-101	Microfilter	40 m ²	67,000
P-15/MF-102	Microfilter	29 m ²	55,000
P-7/MF-103	Microfilter	0.45 m ²	0
P-2/UF-104	Ultrafilter	26 m ²	58,000
P-3/UF-101	Ultrafilter	1.01 m ²	21,000
P-5/UF-102	Ultrafilter	0.80 m ²	21,000
P-16/HG-101	High Pressure Homogenizer	0.33 m ³ /h	17,000

3.4 Basecase Comparisons

For this section the *E. coli* Basecases were numbered (Table 3.10).

Table 3.10: Key for numbered references for Basecases.

Number	<i>E. coli</i> Basecase
1	Centrifuge Clarification
2	Initial Microfiltration Clarification
3	Addition Microfiltration step Clarification
4	36 Hour Fermentation
5	36 Hour Fermentation with final protein production comparable to Basecase 1

The raw materials and products for all Basecases were kept as similar as possible. It was decided to include additional media components including glucose into the overall media components for the *E. coli* Basecases for simplicity (Table 3.12). The higher productivity reported for CHO cultures is shown in the relative amounts of tPA produced despite higher biomass yields for *E. coli*, summarized in Table 3.11.

Table 3.11: Product Yield from Biomass in Basecases. Initial product yield represents initial amounts of tPA after fermentation or homogenization. Final product yields represent yields at the end of the purification streams.

Raw Materials	CHO	1	2	3	4	5
Initial $Y_{p/x}$ (g/g)	2.29 e-2	1.11 e-4	1.11 e-4	1.11 e-4	1.11 e-4	1.11 e-4
Final $Y_{p/x}$ (g/g)	9.38 e-3	4.78 e-5	1.05 e-5	4.53 e-5	4.53 e-5	4.53 e-5

The centrifugation Basecase represents the highest yield for the *E. coli* Basecases. This is likely because less steps are present in this Basecase since addressing the high water consumption issue took precedence over addressing the predicted biomass contamination of the first chromatography step. The higher yields in later Basecases (3-5) occurred because of an optimization step involving the initial microfilter before the homogenizer and the microfiltration units proceeding. It was found that a concentration factor above 2 in the initial

microfiltration unit lead to lower efficiencies in later microfiltration steps. Higher concentration factors where biomass exceeded maximum concentrations lead to the simulation putting all the feedstream in the retentate.

Table 3.12: Summary of materials used and produced for all Basecases.

	kg/Batch					
Raw Materials	CHO	1	2	3	4	5
Affinity Elution						
Buffer	1490	580	130	550	550	460
Affinity Equilibrium						
Buffer	1710	660	145	640	640	530
Gel Filtration Elution						
Buffer	1640	640	140	920	920	760
Water	32600	10,000,000	11,800	16,300	16,300	14,000
Media	5,330	4,800		4,800	4,800	3,990
Proteins	40					
L-glutamine	4.38					
Glucose	5.24					
Air	1530	1,370	1,370	1,370	245	204
Wash Buffer	139	54	12	52	52	43
Products						
Biomass	8.4	640	640	640	640	530
Initial tPA	0.1920	0.0712	0.0712	0.0712	0.0712	0.0712
Final tPA	0.0788	0.0306	0.0067	0.029	0.029	0.024

Capital expenditures include equipment and estimated facility such as instrumentation, installations and other costs incurred in new installations.

Economically the CHO Basecase has the highest capital expenditures and largest equipment costs. Review of equipment costs for all Basecases show that after the cost of the fermentor the main bulk of the cost comes from the downstream processes especially the chromatography units and larger downstream units lead to higher capital costs. The CHO Basecase and *E. coli* Basecase 5 have approximately a \$3.2 million dollar capital cost difference between them. This difference is not as dramatic as it might seem as both Basecases have nearly similar gross margins and revenues would pay for the initial capital expenditures in less than a year for either case.

Table 3.13: All Basecase economic data.

Parameter	CHO	1	2	3	4	5
Total Capital Investment (\$)	31,700,000	31,500,000	2,760,000	29,300,000	29,500,000	28,600,000
Operating Cost (\$/yr)	9,890,000	8,380,000	7,750,000	8,380,000	11,400,000	11,100,000
Production Rate (kg/yr)	14.48	5.41	1.18	5.18	16.55	14.48
Unit Production Cost (\$/kg)	683,000	1,548,000	6,550,000	1,620,000	692,000	767,000
Total Revenues (\$/yr)	174,000,000	64,900,000	14,200,000	62,200,000	199,000,000	174,000,000
Gross Margin (%)	94.31	87.10	45.40	86.53	94.24	93.61
Return on Investment (%)	313.50	80.08	16.86	113.46	193.98	180.55

Table 3.14: Equipment costs presented as a part of capital costs.

Parameter	CHO	1	2	3	4	5
Total Capital Investment (\$)	31,700,000	31,500,000	2,760,000	29,300,000	29,500,000	28,600,000
Equipment Costs (\$)	5,330,000	5,260,000	4,650,000	4,920,000	4,920,000	4,760,000

The 200 hr *E. coli* Basecase with extra microfiltration step has the lowest gross margin compared to the CHO Basecase and a lower internal rate of review (Table 3.13). This is due to the significant losses which occur when the microfiltration steps are not optimized.

Table 3.15: Consumables for Basecases

		Model Costs (\$/yr)					
Unit Operation	Consumable	CHO	1	2	3	4	5
P-17/ MF-101	Membrane	N/A	N/A	16,000	12,000	37,000	31,000
P-15/ MF-102	Membrane	20,000	14,000	88	7,000	21,000	16,000
P-7/ MF-103	Membrane	N/A	N/A	N/A	-	-	-
P-2/ UF-104	Membrane	4,000	4,000	22	2,000	6,000	4,000
P-5/ UF-102	Membrane	270	94	20	90	290	252
P-3/ UF-101	Membrane	354	122	26	116	372	324
P-4/ C-101	Resin	91,500	34,000	7,000	33,000	105,000	91,000
P-6/ C-102	Resin	63,200	24,000	5,000	23,000	72,000	63,000
P-8/ C-103	Resin	152,000	57,000	12,000	54,000	173,000	152,000
Total		331,000	133,000	40,000	131,000	415,000	358,000

In addition to capital costs, which will be amortized over the period of operation there are significant additional costs which come from resins, membrane cloth and other disposables which affect the economic performance of production and add significantly to overhead. Resin costs account for the majority of the consumable costs (Table 3.15).

This highlights that capital costs associated with equipment such as that used in chromatography should also consider the consumable and other operating costs such as maintenance. Operating costs include operator and supervisor hourly rates, consumables, resources, utilities and maintenance. These costs if not monitored can add significantly to economics of production although in this case the predicted gross margins are so large that they can easily accommodate these costs.

The high amounts of cell debris and other solids which must be clarified leads to higher consumables costs. However, costs lower for units downstream of the initial clarification due to smaller protein amounts.

3.5 Discussion and Recommendations

Economically the Basecases predict an excellent return on investment and internal rate of return (Table 3.3). Significant drugs developed by large pharmaceutical companies which at first glance make enormous profits. The costs shown in these models do not costs of marketing, sales or research and development both before and after approval for sale has been granted by the U.S. Food and Drug Administration, Health Canada, European Medicines Evaluation Agency or other similar or government agencies. These costs lead to lower net revenues. Also the price charged to the end user has been marked up to accommodate the overhead involved with hospitals and may not accurately represent the true price realized by the manufacturer. Since Rouf (1999) published, the price of tPA has likely decreased.

It is likely that equipment costs associated with a GMP plant are underestimated in the Basecases. Features inherent with sterility, such as electropolishing the interior surfaces of holding vessels and other considerations cause the prices to be considerably higher for pharmaceutical related equipment. Consumable pricing, which adds significantly to the costs associated with production use the SuperPro® default costs which are unlikely to be completely accurate. However, SuperPro® defaults likely represent a good initial estimation.

Compared with the CHO Basecase the *E. coli* Basecases are not as profitable due to lower productivity although some come extremely close. Refolding protein, if economical, would also increase specific productivity and would push the economics in favour of *E. coli*. Several new downstream technologies such as EBA chromatography, which was not explored here due to lack of data pertaining to EBA chromatography involving tPA, may reduce the capital and consumable costs it replaces the equipment between the homogenizer and second storage unit with a single step. This may be significant, especially if capital and consumable costs are significantly understated in the current models.

The inclusion body production is overstated in the *E. coli* models but was left untouched for later exploration. A recent article by Lee et al. (2006) provides insight into several SuperPro® Designer models of different refolding methods. Combined with a more reasonable approximation of inclusion body formation this may have a significant impact on the bottom lines for *E. coli* production.

It is interesting to note that when a unit is below a certain size it defaults to a base cost set up in the SuperPro® program. Some pieces of equipment may only have a standard size and this necessitate running SuperPro® simulations in a rating mode for these pieces of equipment potentially affecting yield values.

In cases similar to these where the economics of two hosts are close it can be difficult to choose which case is best. One might be tempted to choose the CHO Basecase since there are fewer unit operations. However the *E. coli* operation has a modest specific protein yield and does not take into account the potential economic advantages of new technologies and resolubilization of inclusion bodies. Given the option I would recommend the *E. coli* Basecase since it seems the greatest potential for greater revenues with modest investment.

Lacking data is the biggest problem in modeling. An extensive literature review was conducted there are still gaps in the knowledge surrounding the models. Subsequently it

is important that this taken into account when drawing conclusions from the data presented herein.

Chapter 4

Fermentations and Purifications

4.1 Green Fluorescent Protein (GFP) and Variants

Fluorescent proteins have been used for over a decade to determine protein concentrations and localization within cells. Reid and Flynn (1997) revealed that phycobiliproteins have a very high fluorescence signal but need proper insertion of tetra bilin chromophore into a large apoprotein which is difficult to obtain. In contrast, fluorescent proteins from the jellyfish *Aequorea victoria* form a strong chromophore which appears to need no cofactors or enzymes to form, and is robust *in vivo* (Prasher et al. 1992; Reid and Flynn 1997). The expression of GFP in a wide variety of hosts shows that no specific enzymes are required (Reid and Flynn 1997). Shortly after discovery and sequencing, several groups undertook work to modify the fluorescent signal shifting it to different parts of the spectrum to allow for easier detection and for use in dual labeling, and to increase the relative fluorescence quantum yield of GFP and its variants and make it more stable for use.

Variants of GFP fluorescent spectra are possible by modification of the chromophore (amino acids 65-67) and certain other amino acids. Initial work done by Heim et al. (1994) produced several GFP variants. Nagai et al. (1999) reported producing an eYFP variant with a fast maturation and a resistance to Cl⁻ ions named “Venus”.

Once formed, the chromophore of GFP and its variants is stable. Certain variants of GFP are sensitive to photobleaching, chloride ions, pH changes (Jayaraman et al. 2000). Reid and Flynn (1997) report that 8M Urea and 6M GuHCl along with high temperature, 95°C for 5 min, was required for complete denaturation of GFP.

Complete denaturation of the chromophore has also been reported using guanidine HCl (GuHCl) and extreme pH's. Fluorescence returned upon pH neutralization or dilution of GuHCl (Jayaraman et al. 2000; Rosenow et al. 2004). Although not required, the

chaperones GroEL and GroES speed folding in the presence of adenosine triphosphate (ATP) (Makino et al. 1997). Deliberately producing the protein in a misfolded state via growth at high temperature (37 °C and 42 °C) has facilitated studies of chromophore formation in GFP and variants (Makino et al. 1997; Reid and Flynn 1997; Rosenow et al. 2004).

4.1.1 Fluorescence Biology and Characteristics of GFP and Variants

GFP consists of a β -barrel with distorted α -helix that runs through the center containing the *p*-hydroxybenzylideneimidazolinone chromophore. The chromophore arises from the covalent modification by cyclization and oxidation of amino acids 65-67 (GFP Ser-Try-Gly) (Heim et al. 1994; Reid and Flynn 1997). One problem with the wild type and its variants is the slow rate of maturation; much work has gone into producing variants that mature faster (Nagai et al. 1999; Reid and Flynn 1997; Zhang et al. 2006).

Loss of fluorescence is likely due to quenching in the surrounding aqueous environment as the mature chromophore retains its chemical structure even under denaturing conditions. This suggests that the full tertiary folding of the protein is necessary for fluorescence (Reid and Flynn 1997). In the intermediary stages molecular oxygen is required to allow for complete formation of the chromophore (Heim et al. 1994).

Reid and Flynn (1997) presented a maturation model with two first order stages (Figure 4.1) and suggested that this may be due to the number of prolines in opposing conformation. The fast formation of GFP fluorescence may be due to GFP having proper conformation of prolines while the slower formation occurs as prolines reshuffle to form the tertiary structure. The rate limiting step is chromophore formation and not tertiary structure since refolded mature protein shows fluorescence much faster than protein which must form a mature chromophore (Reid and Flynn 1997; Rosenow et al. 2004).

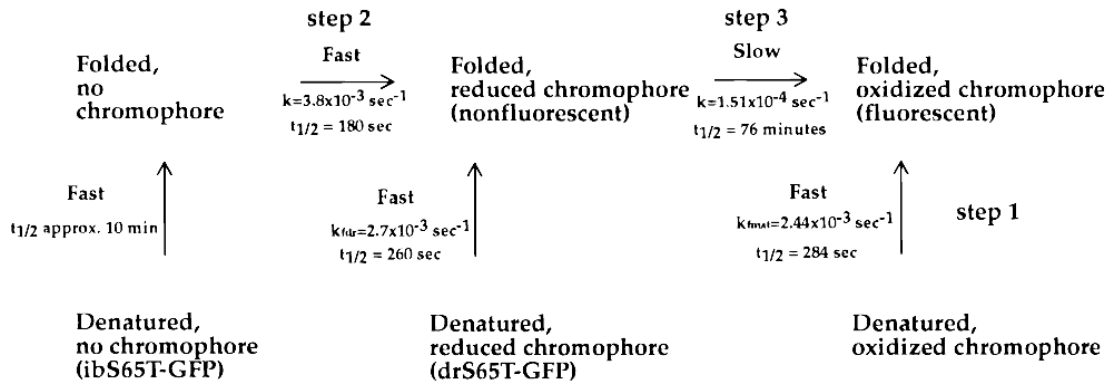
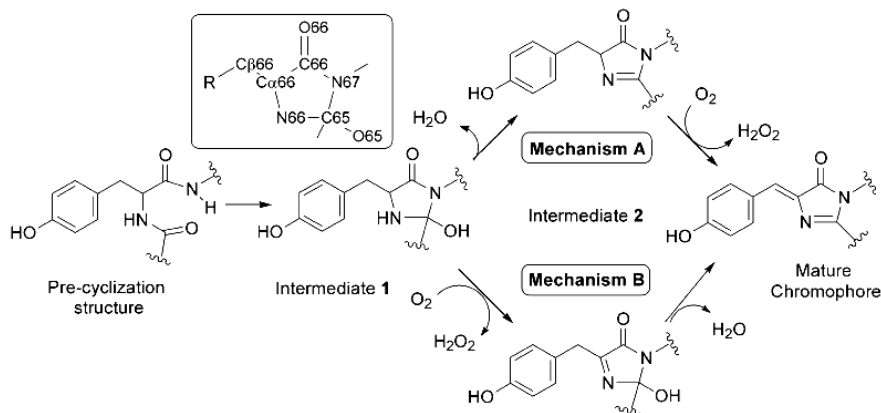


Figure 4.1: Maturation steps of GFP with kinetic data. The rate limiting step in this is the formation of the chromophore (Reid and Flynn 1997).

Rosenow et al. (2000) added to the steps by adding an additional mechanism for folding shown in Figure 4.2.

Scheme 1: Three-Step Mechanism of GFP Chromophore Formation^a



^a (A) Generally accepted mechanism (11) and (B) mechanism proposed in this paper (inset shows atom labels used throughout the text).

Figure 4.2: Modified GFP Chromophore formation with an intermediate mechanism as prolines switch to opposing configuration in-vivo (Rosenow et al. 2004)

Renaturation, and subsequent gain of fluorescence, of misfolded GFP and its variants is estimated to be 80% of soluble protein which has been denatured and refolded (Reid and Flynn 1997). Chromophore formation is a permanent indicator of mature protein and is very resistant to loss of fluorescence and denaturation *in vivo*. Poor fluorescence in culture indicates that a protein was never properly folded and the chromophore was not yet formed.

4.1.2 Construction of eYFP

The DNA encoding for the eYFP used in this study was bought from Clontech Laboratories (Plato Alto, CA) and put into an Invitrogen pRSETB plasmid encoding for ampicillin resistance and inducible by isopropyl-1-thio- β -D-galactopyranoside (IPTG) using a T7-lac promoter (Invitrogen, Carlsbad, CA) by Heather Montgomery for use by Professor E. Jervis's laboratory.

The eYFP protein has base pair substitutions in amino acid position 64 to 66 from wild type GFP and 146, 152 and 162 as shown in Figure 4.3.

wt GFP: Phe⁶⁴ Ser Tyr Gly Val Gln⁶⁹ ... Ser⁷² ... Tyr¹⁴⁵ Asn¹⁴⁶ ... Met¹⁵² ... Val¹⁶² ... Thr²⁰³
EGFP: Leu⁶⁴ Thr Tyr Gly Val Gln⁶⁹
EYFP: Phe⁶⁴ Gly Tyr Gly Leu Gln⁶⁹ ... Ala⁷² Tyr²⁰³
ECFP: Leu⁶⁴ Thr Trp Gly Val Gln⁶⁹ Ile¹⁴⁶ Thr¹⁵² Ala¹⁶²

Figure 4.3: Base pair substitutions required to create eYFP from wild type GFP (wt GFP). In order to create GFP variant it is required to switch the chromophore amino acids (65-67) and certain amino acids which end up close to the chromophore (Clontech 2001).

eYFP has approximately 238 amino acids of which 7-229 are required for fluorescence. The molecular weight is estimated to be 28.7 kDa with a His₆ tag compared to 27 kDa reported for the eGFP. Emission and excitation profiles typical to GFP and its variants are shown in Figure 4.4. eYFP has an excitation peak around 514 nm and an emission peak around 528 nm at pH 7.

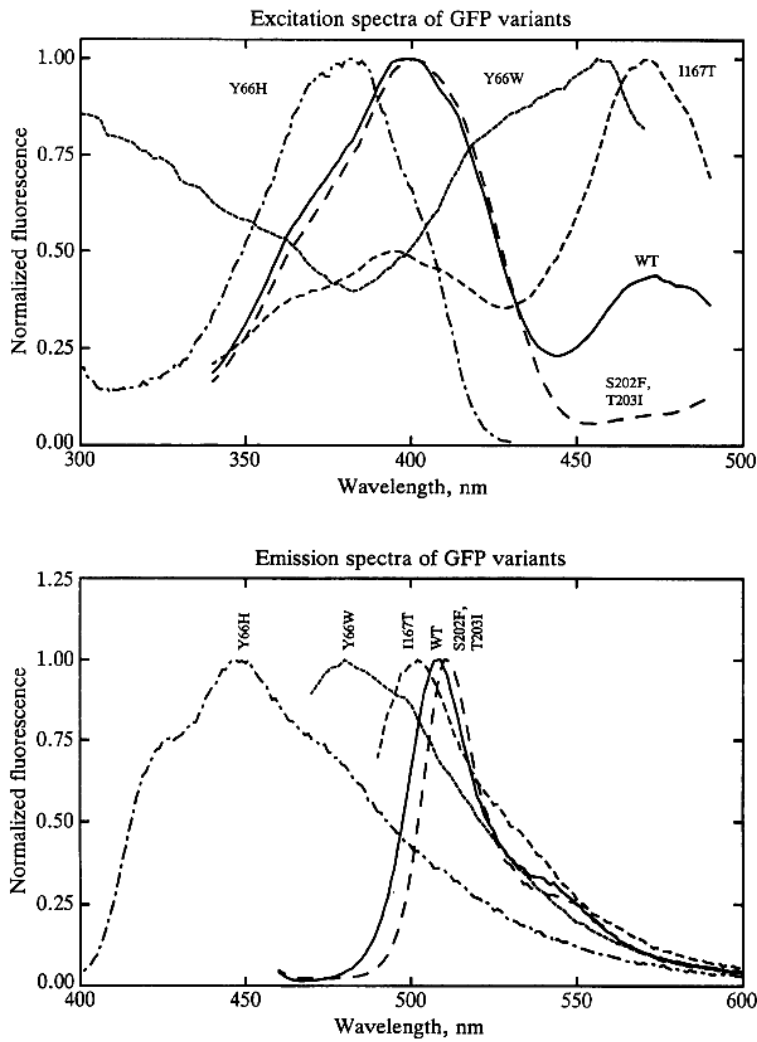


Figure 4.4: Typical Emission and Excitation Spectra for GFP and variants. eYFP has emission at 528 nm and excitation at 518 nm (Heim et al. 1994).

Table 4.1: Characteristics of Yellow Fluorescent Protein and Produced Protein. The produced protein has a lower pI at pH 7. This means using a stronger anion exchange column and potentially keeping the flow through instead of protein that binds to the column. The His₆ tag and amino acids left on the N-terminus from cloning into the plasmid add 1.4 kDa to the protein.

	eYFP	Produced Protein
pI @ pH 7	6.88	6.01
Estimated kDa	28.7	30.1
No. of amino acids	169	
Primary purification	Ni ²⁺ Affinity	Ni ²⁺ Affinity
Secondary purification	Strong Anion Exchange	Strong Anion Exchange
Excitation (nm)	518	448(468)
Emission (nm)	528	520
Copy #	6	
pH range	6-11	
Plasmid		pRSET _B

Table 1 shows typical values for eYFP determined from the Clontech literature and using public domain protein information determination (Putnam 1999) compared with the protein produced in the plasmid used by Professor E. Jervis's Laboratory. The pI for the protein is lower than for eYFP necessitating the use of strong anion exchange chromatography (using Q-sepharose). The His₆ tag and amino acids which were left on the N-terminus of the protein during cloning into the plasmid add 1.4 kDa to the estimated molecular weight. The produced protein does not have the same emission and excitation pair as eYFP for reasons discussed in Chapter 5. eYFP is considered physically similar to eGFP and will lose fluorescence below pH 7.0 and above pH 11.5. eGFP is reported to retain its fluorescence in mild denaturants such as 10 mM DTT and 8M urea and is not sensitive to lower concentrations of salts (Clontech 2001).

The Clontech plasmid is set with several restriction sites shown in Figure 4.5.

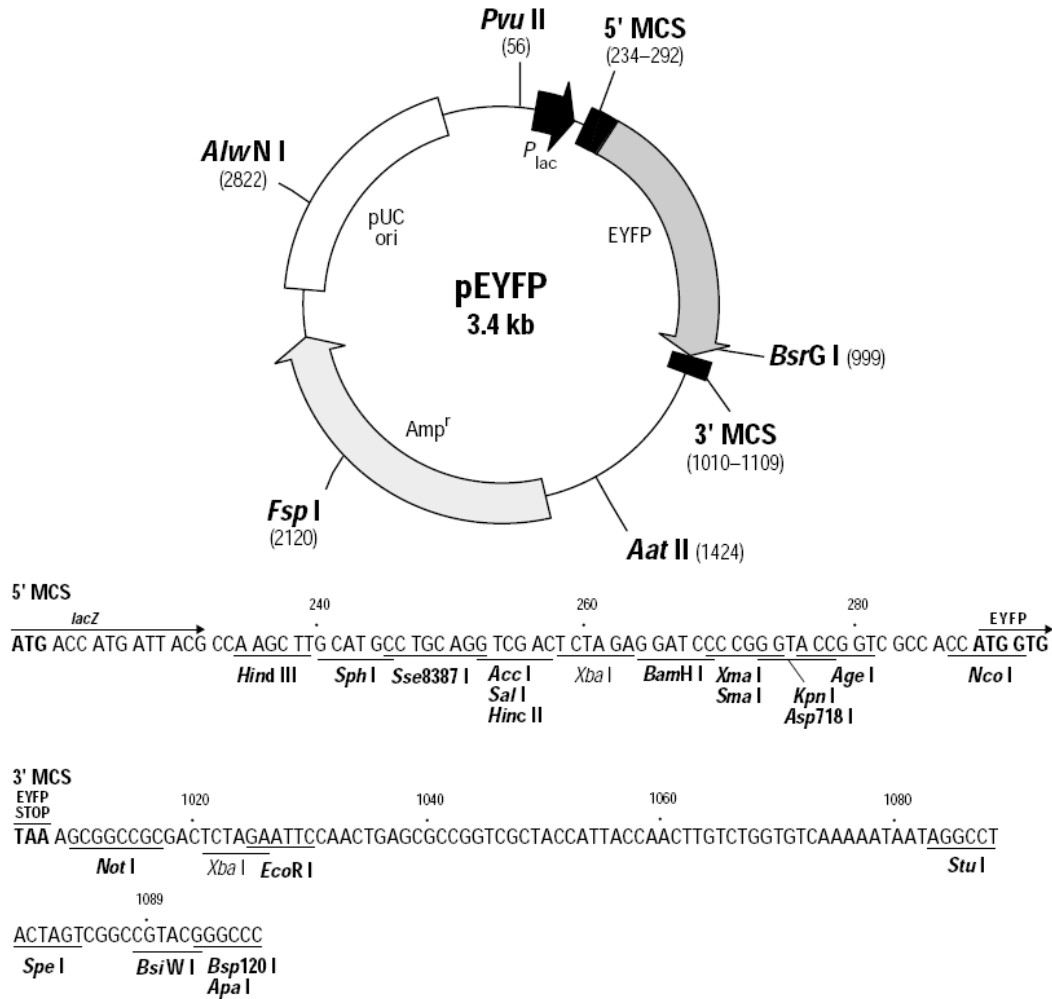


Figure 4.5: Plasmid map for eYFP vector (Clontech 1999). BAMH1 and ECOR1 were used to cut the plasmid and clone the protein cDNA into the plasmid.

The gene for eYFP is set in a pRSET_B plasmid from Invitrogen at the BAM H1 and ECO R1 restriction sites.


```

21  T7 promoter                                     RBS
    AATACGACTC ACTATAGGGA GACCACAACG GTTCCCTCT AGAAATAATT TTGTTAACT TTAAGAAGGA

91  Polyhistidine (6xHis) region
    GATATACAT ATG CGG GGT TCT CAT CAT CAT CAT CAT CAT GGT ATG GCT AGC ATG ACT
    Met Arg Gly Ser His His His His His His Gly Met Ala Ser Met Thr

148 T7 gene 10 leader                               Xpress™ Epitope      BamHI      XhoI SacI
    GGT GGA CAG CAA ATG GGT CGG GAT CTG TAC GAC GAT GAC GAT AAG GAT CCG AGC TCG
    Gly Gly Gln Gln Met Gly Arg Asp Leu Tyr Asp Asp Asp Asp Lys Asp Pro Ser Ser
    EK recognition site      EK cleavage site

205 BglII      PstI PvuII KpnI NcoI EcoRI BstBI HindIII
    AGA TCT GCA GCT GGT ACC ATG GAA TTC GAA GCT TGA TCCGGCTGCT AACAAAGCCC
    Arg Ser Ala Ala Gly Thr Met Glu Phe Glu Ala ***

261 T7 reverse priming site
    GAAAGGAAGC TGAGTTGGCT GCTGCCACCG CTGAGCAATA ACTAGCATAA

```

Figure 4.6: Vector map for pRSET_B plasmid (Invitrogen 2001).

The plasmid when cut using ECORI and BAMHI and run on an agrose gel gave two fragments of approximately the expected size. A plasmid fragment of 2950 bp and a gene fragment of 250 bp which is the expect fragment size of the gene encoding for eYFP (Figure 4.7).

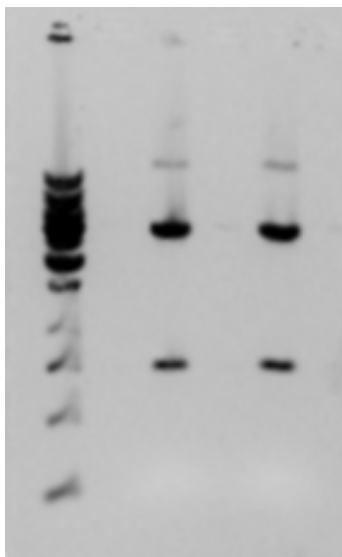


Figure 4.7: DNA Gel of plasmid cut with BAMHI and EcoRI. Plasmid size is approximately 2950 bp with the protein DNA size of approximately 250 bp (there remains some uncut plasmid around 3700 bp).

Sequencing done at Waterloo shows that the plasmid has the DNA sequence:

```
catcatcatcatcatcatggcatggcgagcatgaccggcgccagcagatgggcccgatctgtatgatgatgataaagat
ccgcgctgccggtggcgacctggtgagcaaaggcgaagaactgttaccggcgtggtgccgattctggtggaactggatg
gcgatgtgaacggccataaatttagcgtgagcggcgaaggcgaaggcagatgacacatggcaactgacctgaaattattt
gcaccaccggcaactgccggtgccgtggccgacctggtgaccacctttggctatggcctgcagtgctttgcgcgctatccgg
atcatatgaaacagcatgattttttaaagcgcgatgccggaaggctatgtgcaggaacgcaccattttttaaagatgatggca
actataaaacccgcgcggaagtgaatttgaaggcgataacctggtgaaccgcattgaaactgaaaggcattgattttaaagaaga
tggcaacattctgggccataaactggaataactataacagccataacgttatattatggcggataaacagaaaaacggcatta
aagtgaactttaaattcgccataacattgaagatggcagcgtgcagctggcggatcattatcagcagaacaccccgattggcga
tggcccgtgctgctgccggataaccattatctgagctatcagagcgcgctgagcaaagatccgaacgaaaaacgcgatcatat
ggtgctgctggaatttgtgaccgcggcgggcattaccctgggcatggatgaactgtataaa
```

The amino acid sequence for eYFP from the N to C terminus with His₆ tag within the pRSET_B vector is:

```
HHHHHHGMASMTGGQQMGRDLYDDDDKDPRVPVATMVSKGEELFTGVVP
ILVELDGDVNGHKFSVSGEGEGDATYGKLTCLKFICTTGKLPVPWPTLVTTF
GYGLQCFARYPDHMKQHDFFKSAMPEGYVQERTIFFKDDGNYKTRAEVKF
EGDTLVNRIELKGIDFKEDGNILGHKLEYNYNSHNVYIMADKQKNGIKVNF
KIRHNIEDGSVQLADHYQQNTPIGDGPVLLPDNHLYSYQSALS KDPNEKRDH
MVLLEFVTAAGITLGMDELYK
```

This corresponds to the sequence from Clontech:

```
ADNNFTQETAMTMITPSLHACRSTLEDP RVPVATMVSKGEELFTGVVPILVE
LDGDVNGHKFSVSGEGEGDATYGKLTCLKFICTTGKLPVPWPTLVTTFGYGL
QCFARYPDHMKQHDFFKSAMPEGYVQERTIFFKDDGNYKTRAEVKFE GDT
LVNRIELKGIDFKEDGNILGHKLEYNYNSHNVYIMADKQKNGIKVNF KIRHN
IEDGSVQLADHYQQNTPIGDGPVLLPDNHLYSYQSALS KDPNEKRDH MVLLE
FVTAAGITLGMDELYK
```

```

      ↓
TACACACGAA TAAAGATAA CAAG > ATG AGT AAA GGA GAA GAA CTT TTC ACT GGA GTT GTC CCA ATT CTT GTT GAA TTA GAT GGT 85
M S K G E E L F T G V V P I L V E L D G 20

GAT GTT AAT GGG CAC AAA TTT TCT GTC AGT GGA GAG CGT GAA GGT GAT GCA ACA TAC GGA AAA CTT ACC CTT AAA TTT ATT 166
D V N G H K F S V S G E G E G D A T Y G K L T L K F I 47

TGC ACT ACT GGA AAA CTA CCT GTT CCA TGG CCA ACA CTT GTC ACT ACT TTC TCT TAT GGT GTT CAA TGC TTT TCA AGA TAC 247
C T T G K L P V P W P T L V T T F S Y G V Q C F S R Y 74
      ↓

CCA GAT CAT ATG AAA CAG CAT GAC TTT TTC AAG AGT GCC ATG CCC GAA GGT TAT GTA CAG GAA AGA ACT ATA TTT TTC AAA 328
P D H M K Q H D F F K S A M P E G Y V Q E R T I F F K 101

GAT GAC GGG AAC TAC AAG ACA CGT GCT GAA GTC AAG TTT GAA GGT GAT ACC CTT GTT AAT AGA ATC GAG TTA AAA GGT ATT 409
D D G N Y K T R A E V K F E G D T L V N R I E L K G I 128

GAT TTT AAA GAA GAT GGA AAC ATT CTT GGA CAC AAA TTG GAA TAC AAC TAT AAC TCA CAC AAT GTA TAC ATC ATG GCA GAC 490
D F K E D G N I L G H K L E Y N Y N S H N V Y I M A D 155

AAA CAA AAG AAT GGA ATC AAA GTT AAC TTC AAA ATT AGA CAC AAC ATT GAA GAT GGA AGC GTT CAA CTA GCA GAC CAT TAT 571
K Q K N G I K V N F K I R H W I E D G S V Q L A D H Y 182
      ↓

CAA CAA AAT ACT CCA ATT GGC GAT GGC CCT GTC CTT TTA CCA GAC AAC CAT TAC CTG TCC ACA CAA TCT GCC CTT TCG AAA 652
Q D N T P I G D G P V L L P D N H Y L S T Q S A L S K 209

GAT CCC AAC GAA AAG AGA GAC CAC ATG GTC CTT CTT GAG TTT GTA ACA GCT GCT GGG ATT ACA CAT GCC ATG GAT GAA CTA 733
D P N E K R D H M V L L E F V T A A G I T H G M D E L 236

TAC AAA TAA ATGTCAGAC TTCCAATTGA CACTAAAGTG TCCGAACAAT TACTAAAATC TCAGGGTTCC TGTTAAATT CAGGCTGAGA TATTATTAT 832
Y K . 238

ATATTATAG ATTCATTAAT ATTGTATGAA TAATTTATTG ATGTTATTGA TAGAGGTTAT TTTCTTATTA AACAGGCTAC TTGGAGTGA TTCTTAATTC 932

TATATTAATT ACAATTTGAT TTGACTTGCT CAAA 962

```

Figure 4.8: Gene from *Aequorea victoria* for GFP. Underlined sequences are silent or are introns (Prasher et al. 1992).

Without the introns the sequence for GFP10 reported by Prasher et al. (1992) is:

**MSKGEELFTGVVPIVELDGDVNGHKFSVSGEGEDATYGKLTLSQYGVQC
FSRIELKGIDFKIMQLSTQSALS KDPNEKRDHHVLLFVTAAGITHGHDELY
K**

This corresponds very well with our and Clonetech's sequence except for the reported amino acid substations necessary for eYFP discussed previously.

4.2 Objectives of Fermentations

The objective of the fermentation runs was to explore the effect of temperature reduction on protein production and growth as a tool to assist in the control of dissolved oxygen (DO) content. *E. coli* grow over a temperature range from 42°C to 21°C with an optimum temperature for growth of 37°C (Gadgil, Kapur and Hu, 2005). Temperature reduction decreases metabolic rate and increases oxygen solubility. We hypothesize that growth,

protein production, and fermentor conditions can be influenced positively by reducing temperature at critical time point during the fermentation.

4.3 Fermentation and Temperature Control Literature Review

In both laboratory and industrial settings the objective of the fermentation step is to achieve high volumetric productivity. Cell specific productivity is highly dependant upon upstream genetic engineering and ideally, has previously been optimized in smaller cultures. In bacterial cultures protein production is associated with growth and achieving high cell growth before induction typically allows for the production of larger quantities of recombinant protein or other products.

4.3.1 Strategies for High Density Fermentations

Significant difficulties are encountered at high cell densities with respect to the chemical, environmental and metabolic demands of *E. coli*. Some required media components inhibit growth when present in high concentrations (Table 4.2).

Table 4.2 : Inhibitory concentrations of *E. coli* media components. Avoiding concentrations greater than these are necessary in order to ensure the long term health of the culture. The health of the culture has effects on the protein production and overall growth parameters (Shiloach and Fass 2005) .

Media Component	Inhibitory Concentration (g/L)
Glucose	50
Ammonium	3
Iron	1.15
Magnesium	8.7
Phosphorous	10
Zinc	0.038

Several strategies have been employed to meet the challenges of avoiding inhibitory concentrations of media components or metabolic byproducts and avoid the exhaustion of media components at high densities. Growth will become stalled in batch cultures as media components are exhausted or inhibitory concentrations of metabolic by-products such as acetate are formed.

First, several variations of fermentations have been developed that reduce metabolic waste production, increase the tolerance for inhibitory initial media concentrations and increase the feasible time frame for growth (Akesson et al. 2001; Shiloach and Fass 2005). Second several *E. coli* species have been developed with greater resistance to inhibitory concentrations of media components and metabolic byproducts (Shiloach and Fass 2005). Thus, high density cultures have been facilitated by both upstream and at-stream engineering. Fed-batch and dialysis fermentation strategies are two of the more popular fermentation methods used to reach higher densities of *E. coli*. (Shiloach and Fass 2005)

Dialysis fermentations use the separation effect of semi-permeable membranes to remove metabolic by-products from the fermentation media. Difficulties arise in the fermentor itself since the membranes are sensitive to mechanical damage. Difficulties arise in sterilization and cleaning, and oxygen limitation is common in this type of fermentor (Calik et al. 2004; de Mare et al. 2005; Shiloach and Fass 2005; Sterbacek and Votruba 1993; Zheng et al. 2001).

Fed-batch fermentations in contrast are variations of a typical batch with additional media or other feed components being added to supplement the fermentation later in time (Shiloach and Fass 2005). Fed-batch fermentations usually limit a single component, typically the carbon, phosphorous, or nitrogen source and can feed that component at a preset manner or in response to a measured external variable such as pH or dissolved oxygen (Bezaire 2005; de Mare et al. 2005; Shiloach and Fass 2005). Table 2.2 outlines some of the cell culture densities reported in literature by variations of these two techniques.

Genetic engineering methods to aid in high density fermentations have examined reengineering metabolic pathways involving acetate synthesis and energy pathways as shown in Figure 4.9 (Phue et al. 2005). One method involved enzyme deletion mutants lacking the phosphotransacetylase (pta) and acetate kinase (ack) enzymes important in the acetate formation pathway (*E. coli* W3110). However, acetate pathways play an

important growth function and other pathways may be available in *E. coli* to control excess carbon flow quite often it is difficult to grow these species at high densities (Shiloach and Fass 2005).

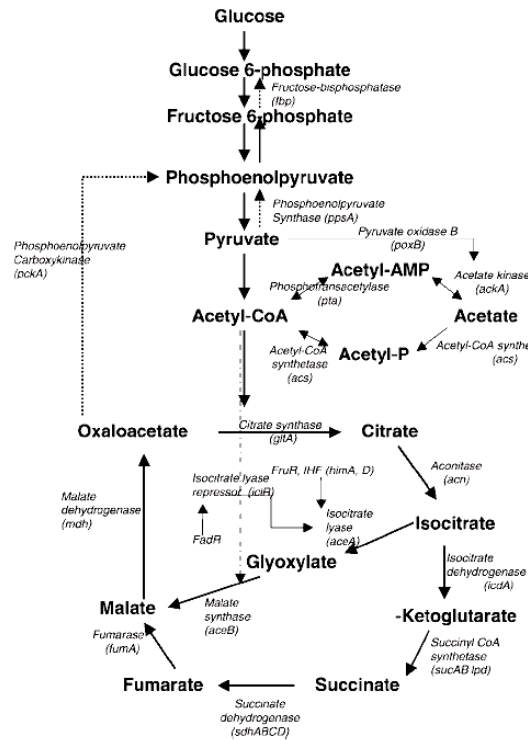


Figure 4.9: Genetic glucose utilization pathways in *E. coli* (Phue et al. 2005).

Another strategy is to increase acetate utilization via the acetyl-CoA, the glyoxylate shunt pathway and TCA cycle. *E. coli* BL21 and its mutants lack the repressors which typically prevent acetate utilization in the presence of glucose taking advantage of increased acetate utilization (Shiloach and Fass 2005). Indeed, the BL21 strain utilize glucose more efficiently than JM109 and produce less acetate making them better for overall growth and protein production (Phue et al. 2005; Shiloach and Fass 2005). Acetate synthesis occurs in *E. coli* JM109 (*E. coli* K) since acetate is produced using pyruvate oxidase (poxB) (utilizing pyruvate) rather than as in *E. coli* BL21 (*E. coli* B) where the Pta-AckA system which utilizes acetyl CoA to produce acetate (Phue et al. 2005). A third strategy used in other hosts is to prevent carbon utilization in pathways other than the glycolysis-TCA pathway. While this approach has been reported, it has not been

determined whether this strategy has led to *E. coli* species appropriate for use in high density fermentations (Shiloach and Fass 2005).

Dissolved oxygen is a key factor in fermentations. Even with sparging pure oxygen into a bioreactor it is necessary to control growth at high cell densities. Media selection and temperature reduction as two methods used in controlling growth (Bezaire 2005; Calik et al. 2004; Chen et al. 1999; de Mare et al. 2005; Hendrick et al. 2001; Shiloach and Fass 2005). Avoiding oxygen limitation has the advantage of limiting stress responses which change the phenotypical and genetic qualities of *E. coli* (Gadgil et al. 2005; Haddadin and Harcum 2005).

Maintenance of aerobic conditions is important to fermentations that take advantage of the *E. coli*'s aerobic metabolic pathways. Anaerobic conditions in some fermentations leads to a shift in metabolic pathways and metabolic fluxes unfavorable to formation of certain recombinant proteins (Calik et al. 2004).

4.3.2 Temperature Control in Fermentations

Much of the control of fermentations on the industrial scale is done heuristically despite the availability of sophisticated at-line sensors. This is due to inherent variability of the system being controlled, inexact data and the lack of deterministic models to base a controller on (Sterbacek and Votruba 1993). Chen et al. (1999) used a multiloop cascade controller to control the growth of mycelia forming *Streptomyces hygroscopicus*, an obligate aerobe, producing rapamycin as a secondary metabolite during suboptimal or stationary growth conditions. The fermentation process was developed to maintain DO at 30% and to induce secondary metabolism using a 130 L fermentor with 100 L working volume. The control loop first lowered pH, then raised pressure, increased agitation speed and finally lowered the fermentation temperature in a single step allowing for better product formation and avoidance of oxygen limitation (Chen et al. 1999).

Temperature control may be advantageous in terms of overall cell yields. de Mare et al. (2005) used a 3 L bioreactor and *E. coli* BL31(DE3) with plasmid pET22b encoding

xylanase to examine the effects of a temperature strategy on glucose consumption. The fermentation utilized a dissolved oxygen based feeding strategy with a 5°C temperature step reduction at maximum oxygen transfer. This avoided a decrease in xylanase activity that was usually observed two hours after induction caused by oxygen limitation and overfeeding. de Mare et al. (2005) reported similar amounts of biomass compared with their modified temperature control strategy with a steady temperature control experiment and was scalable to a 50 L reactor volume using *E. coli* strain W3110.

A common reason to adjust temperature is to enhance protein production. Wei et al. (2003) demonstrated such a strategy using *Candida utilis* at 30°C to optimize cellular growth. Temperature was reduced to 26°C later to optimize production of glutathione.

A piecewise constant temperature strategy was also used for glycerol production in *Candida krusei*. This strategy balanced growth and production. Growth was favoured initially and product formation was favoured towards the end of the fermentation in a 600 mL airloop reactor (Xie et al. 2002).

Calik, Vural and Ozdamur (1997) investigated the effect of decreasing temperature from 31°C to 24°C in fermentations with *Pseudomonas dacunhae* producing L-alanine. They found an optimal temperature around 26°C. During this fermentation it was necessary to maintain an anaerobic environment and the control strategy was optimized to reduce dissolved oxygen content. By switching control parameters one can use a similar strategy for aerobic conditions.

Several batch experiments with *Streptoverticillium mobaraense*, producing microbial transglutaminase, were performed at various constant temperatures to determine optimal protein expression and growth temperatures. The optimum was 30°C at 25.1 g/L dry cell weight and 148 IU/g enzyme activity. A relatively high temperature at the beginning of the fermentation followed by lowering temperature at 18 hours was shown to maximize cell growth, protein production and activity (Zheng et al. 2001).

Rosenow et al. (2004) reduced the temperature of a *E. coli* BL21(DE3) fermentation producing green fluorescent protein (GFP) expressed in a pRSET_B plasmid to 25°C in order to increase protein solubility. Zhang et al. (2006) grew a GFP-trix protein in *E. coli* JM101 at 42°C to produce the protein in inclusion bodies so that it could be later be renatured to elucidate chromophore formation. Deschamp et al. (1995) grew GFP producing *E. coli* CM21 in Luria-Bertani (LB) media at 30°C. A more detailed summary of production of GFP and variants is shown in Table 4.3.

4.4 Expected Protein Transcription and Gene Responses to Temperature Control

The likely cause of increased soluble protein yields at lower temperatures is a reduction in metabolic and growth related protein production. Even a small 4°C change in temperature from 33°C to 29°C resulted in a 9% change in the genome determined through mRNA response (Gadgil et al. 2005). Gadgil et al. (2005) report several responses to temperature change summarized hereafter in this paragraph. The majority of the gene expression changes occurred within the first five to ten minutes after temperature reduction reaching steady state after that. The major reported changes in the genome involve the energy metabolism pathways which preferentially use isozymes but not the glycolysis or pentose phosphate pathway and transport pathways. Four genes of the fourteen in the pathway for the conversion of glucose-6-phosphate to pyruvate (glyceraldehydes-3-phosphate dehydrogenase (*gapA*), phosphoglycerate kinase (*pgk*), phosphoglycerate mutase (*pgmI*) and pyruvate kinase II (*pykA*)) showed a rapid decrease in expression levels indicating a reduced aerobic glucose consumption and glycolysis flux.

Gadgil et al. (2005) also reported that genes utilized in the TCA cycle increase expression and speculated that this indicated reduced activity since oxygen demand is less at lower temperatures. The ability to sense changes in aerobic versus anaerobic conditions (ArcA and ArcB as part of the ArcAB signal transduction system in the electron transport chain) remains unaffected. However, there is a change from the high affinity cytochrome-*o* to the lower affinity cytochrome-*d* system. The genes regulating

acetate production phosphotransacetylase (*pta*) and pyruvate oxidase (*poxB*) are downregulated and acetyl coA synthetase (*acs*) expression is increased indicating that acetate production may be reduced preferentially to produce acetyl coA at lower temperatures. Genes involved in the histidine, arginine and aromatic amino acid production pathways are perturbed but serine, aspartate and pyruvate pathways are less affected.

Protein synthesis and fatty acid metabolism genes are surprisingly unaffected by temperature reduction while heat shock protein genes are expressed to a lesser extent (Gadgill et al. 2005). This would seem to favour *E. coli* K variants for production involving temperature downshifts due to acetate production mechanisms (Shiloach and Fass 2005).

Kim et al. (2000) used two dimensional difference gel electrophoresis (DIGE) and matrix assisted laser desorption/ionization time of flight (MALDI-TOF) mass spectrometry to monitor the proteome response of *E. coli* K12 when temperature was reduced from 37°C to 20°C in mid-exponential phase. They found that 26 proteins significantly increased and 31 proteins were significantly repressed. Cold shock response increased production of several proteins with energy metabolism function such as pyruvate kinase (PykF), isocitrate dehydrogenase (IcD), malate dehydrogenase (Mdh) and Succinyl-CoA synthetase alpha chain (SucD). These are key enzymes in the TCA cycle. This may indicate a response to balance metabolic fluxes. Expression of lysine precursors and enzymes were significantly increased while histidine precursors and enzymes were significantly decreased indicating a proteomic response to an imbalance in the amino acid production after temperature downshift. Proteins and chaperones involved in the proper folding of proteins within the cells (GroEL, Hsp70, and Hsp60) as well as the synthesis of 30S ribosome protein S1 were significantly inhibited. It has been suggested that other proteins take their place and allow the ribosomes to operate with better efficiency in a cold environment. For instance peptidyl-prolyl-cis-trans isomerase (PpiB) is strongly unregulated during cold temperatures and is known to be important to protein folding. This may play an important adaptive role for the *E. coli*.

It is thought that protein misfolding is less likely to occur due to temperature downshift. However, since it is difficult to separate host cell metabolism and recombinant protein production this remains speculative until a more exhaustive study is done (Kim et al. 2005). Previous work has reported an acclimatization or lag phase where various cold shock proteins protecting the cell's protein machinery are produced before growth resumed which would need to be taken into account for this strategy (Phadtare and Inouye 2004).

Several protein production configurations are available and were discussed in detail in Chapter 2. Inclusion body refolding involves cellular disintegration using a high pressure homogenizer or similar method. The insoluble cell pellet is typically washed several times and then denatured with a chaotropic agent such as urea or guanidinium hydrochloride (Reid and Flynn 1997; Rosenow et al. 2004). Subsequent refolding is accomplished by dilution of the denaturant. Refolding proteins on scales larger than those found in the laboratory has been avoided due to the multistep, complicated and costly nature of protein refolding. However, increasingly competitive economic environments have led to the development of new technologies and methodologies on all scales to support protein refolding (Lee et al. 2006b; Middelberg 2002; Rosenow et al. 2004).

Haddadin and Harcum (2005) reported recombinant protein production using IPTG significantly alters the metabolic response of both wild type and plasmid containing *E. coli*. Growth tapered off considerably after the induction of protein synthesis in *E. coli* containing plasmids as a result of energy being redirected towards protein production. Analysis of gene responses indicated an upregulation in TCA and amino acid synthesis related genes but an overall downregulation of energy synthesis genes. This was more evident in log phase growing cultures when compared to stationary phase cultures. The overall upregulation of phage response genes indicate that *E. coli* may see IPTG induction of protein as phage attack and thus downregulate protein machinery to deal with this (Haddadin and Harcum 2005). This suggests that protein synthesis may be best

done at high cell titers during late log phase to ensure that cell growth is optimized before induction slows cell growth.

4.5 Production and Purification Schemes for GFP and variants.

Table 4.3 shows the production of GFP and variants for analysis and study in literature. It should be noted that in none of these cases has the production of GFP or its variants been produced on scale larger than a large shake flask.

Table 4.3: Production of GFP and variants in *E. coli* in selected literature. Several different plasmids, medias and induction strategies were employed.

Strain	Induction	Protein Production	Media	Cell production	Time	Source
JM101	pRSETB IPTG	GFP				(Rosenow et al. 2004)
CM21 (BL21DE3) Variant	pTU58 IPTG	GFP	LB 30°C	0.6 O.D. before induction	4-6 hrs	(Deschamps et al. 1995)
JM101	pQESL75 anhydrotetracycline	GFP	LB 37°C	0.5 O.D. before induction		(Reid and Flynn 1997)
TG1	pQE9 IPTG	CFP/YFP	Tryptone Yeast Media 37°C		16hr Induction	(Felber et al. 2004)
BL21DE3		YFP				(Jayaraman et al. 2000)
BL21(DE3) and JM101(DE3)	pRSETB IPTG	Citrine eYFP				(Griesbeck et al. 2001)
BL21(DE3)	PU 58 0.8mM IPTG	GFP		Middle LOG phase before induction		(Makino et al. 1997)
BL21(DE3)	pET30b	eCFP		0.6 O.D. in Shake Flask		(Wang et al. 2004)
JM101(DE3)	pRSETB IPTG	GFP-trix variant	42°C			(Zhang et al. 2006)

Table 4.4 shows purification schemes used to purify GFP and its variants produced from *E. coli* in literature. It should be noted that cell production using pRSET_B plasmids usually employ Ni-NTA affinity chromatography as first step in purification with further steps added to increase purity as required.

Table 4.4: Literature Review of Purification Schemes for GFP and variants produced using *E. coli*. pRSET_B containing cells have a His₆ tag and will use Ni-NTA affinity chromatography as a first step in purification. Several papers discussed resolubilizing insoluble proteins and those strategies are presented herein.

Homogenization	Clarification	Purification	Source																		
		<p>Soluble Ni-Affinity</p> <table border="1"> <thead> <tr> <th>Equilibrium Buffer</th> <th>Wash Buffer</th> <th>Elution Buffer</th> </tr> </thead> <tbody> <tr> <td></td> <td></td> <td></td> </tr> </tbody> </table> <p>DEAE-Sepharose affinity (His tag cleave with α-chymotrypsin, 4°C, 4Hrs)</p> <table border="1"> <thead> <tr> <th>Equilibrium Buffer</th> <th>Wash Buffer</th> <th>Elution Buffer</th> </tr> </thead> <tbody> <tr> <td>20mM HEPES, 50mM NaCl (pH 7.9)</td> <td>20mM HEPES, 50mM NaCl (pH 7.9)</td> <td>20mM HEPES, 300 mM NaCl (pH 7.9)</td> </tr> </tbody> </table> <p>Insoluble Homogenization Wash Buffer x4 100mM Tris-HCl (pH 7.9), 500mM NaCl, 20mM EDTA, 2% Triton X-100, 5mM DTT</p> <p>Solubilized in 50mM HEPES, 50mM NaCl, 8.0M Urea, 5mM DTT</p> <p>Ni-Affinity</p> <table border="1"> <thead> <tr> <th>Equilibrium Buffer</th> <th>Wash Buffer</th> <th>Elution Buffer</th> </tr> </thead> <tbody> <tr> <td>50mM HEPES, 50mM NaCl, 8M Urea</td> <td>20mM Imidazole</td> <td>100 mM Imidazole</td> </tr> </tbody> </table>	Equilibrium Buffer	Wash Buffer	Elution Buffer				Equilibrium Buffer	Wash Buffer	Elution Buffer	20mM HEPES, 50mM NaCl (pH 7.9)	20mM HEPES, 50mM NaCl (pH 7.9)	20mM HEPES, 300 mM NaCl (pH 7.9)	Equilibrium Buffer	Wash Buffer	Elution Buffer	50mM HEPES, 50mM NaCl, 8M Urea	20mM Imidazole	100 mM Imidazole	(Rosenow et al. 2004)
Equilibrium Buffer	Wash Buffer	Elution Buffer																			
Equilibrium Buffer	Wash Buffer	Elution Buffer																			
20mM HEPES, 50mM NaCl (pH 7.9)	20mM HEPES, 50mM NaCl (pH 7.9)	20mM HEPES, 300 mM NaCl (pH 7.9)																			
Equilibrium Buffer	Wash Buffer	Elution Buffer																			
50mM HEPES, 50mM NaCl, 8M Urea	20mM Imidazole	100 mM Imidazole																			

Homogenization	Clarification	Purification	Source																		
Sonication	Centrifugation	<p>40% Ammonium Sulfate cut GFP in super 70% Ammonium Sulfate cut GFP in Pellet Solublized in 1M Ammonium Sulfate 50mM Tris pH 7.5</p> <p>Fractionation SEC 3000</p> <table border="1" data-bbox="621 456 1623 570"> <thead> <tr> <th data-bbox="621 456 953 500">Equilibrium Buffer</th> <th data-bbox="959 456 1289 500">Wash Buffer</th> <th data-bbox="1295 456 1623 500">Elution Buffer</th> </tr> </thead> <tbody> <tr> <td data-bbox="621 500 953 570">50mM Tris-HCl (pH 7.5), 1.2M Ammonium Sulfate</td> <td data-bbox="959 500 1289 570">50mM Tris-HCl (pH 8), 1.2M Ammonium Sulfate</td> <td data-bbox="1295 500 1623 570"></td> </tr> </tbody> </table> <p>Volume Concentrated to 2mL using Centriprep 10, and then suspended back to 15ml in 5mM EDTA pH 8 x4</p> <p>TSK DEAE 5PW</p> <table border="1" data-bbox="621 724 1623 829"> <thead> <tr> <th data-bbox="621 724 953 768">Equilibrium Buffer</th> <th data-bbox="959 724 1289 768">Wash Buffer</th> <th data-bbox="1295 724 1623 768">Elution Buffer</th> </tr> </thead> <tbody> <tr> <td data-bbox="621 768 953 829">5mM EDTA (pH 8.0)</td> <td data-bbox="959 768 1289 829">5mM EDTA (pH 8.0)</td> <td data-bbox="1295 768 1623 829">5mM EDTA (pH 8.0) 0- 70mM NaCl linear gradient</td> </tr> </tbody> </table> <p>Polishing SEC 3000</p> <table border="1" data-bbox="621 894 1623 997"> <thead> <tr> <th data-bbox="621 894 953 938">Equilibrium Buffer</th> <th data-bbox="959 894 1289 938">Wash Buffer</th> <th data-bbox="1295 894 1623 938">Elution Buffer</th> </tr> </thead> <tbody> <tr> <td data-bbox="621 938 953 997">Low Salt Buffer (50mM Tris)</td> <td data-bbox="959 938 1289 997"></td> <td data-bbox="1295 938 1623 997"></td> </tr> </tbody> </table>	Equilibrium Buffer	Wash Buffer	Elution Buffer	50mM Tris-HCl (pH 7.5), 1.2M Ammonium Sulfate	50mM Tris-HCl (pH 8), 1.2M Ammonium Sulfate		Equilibrium Buffer	Wash Buffer	Elution Buffer	5mM EDTA (pH 8.0)	5mM EDTA (pH 8.0)	5mM EDTA (pH 8.0) 0- 70mM NaCl linear gradient	Equilibrium Buffer	Wash Buffer	Elution Buffer	Low Salt Buffer (50mM Tris)			(Deschamps et al. 1995)
Equilibrium Buffer	Wash Buffer	Elution Buffer																			
50mM Tris-HCl (pH 7.5), 1.2M Ammonium Sulfate	50mM Tris-HCl (pH 8), 1.2M Ammonium Sulfate																				
Equilibrium Buffer	Wash Buffer	Elution Buffer																			
5mM EDTA (pH 8.0)	5mM EDTA (pH 8.0)	5mM EDTA (pH 8.0) 0- 70mM NaCl linear gradient																			
Equilibrium Buffer	Wash Buffer	Elution Buffer																			
Low Salt Buffer (50mM Tris)																					

Homogenization	Clarification	Purification	Source						
French Press	Centrifugation	<p>Soluble Ni-Affinity</p> <table border="1"> <tr> <td>Equilibrium Buffer</td> <td>Wash Buffer</td> <td>Elution Buffer</td> </tr> <tr> <td></td> <td></td> <td></td> </tr> </table> <p>Insoluble Renaturation Buffer 35mM KCl, 2mM MgCl₂ 50mM Tris (pH 7.5), 1mM DTT Denaturation Buffer 8M Urea, 1mM DTT, 5mM Dithionite heated to 95 C, 5 min and cooled to room temp Centrifuged 100 fold dilution in Renaturation buffer</p>	Equilibrium Buffer	Wash Buffer	Elution Buffer				(Reid and Flynn 1997)
Equilibrium Buffer	Wash Buffer	Elution Buffer							
Centrifugation	French Press	<p>Ni-Affinity</p> <table border="1"> <tr> <td>Equilibrium Buffer</td> <td>Wash Buffer</td> <td>Elution Buffer</td> </tr> <tr> <td></td> <td>PBS with 10mM β-mercaptanethanol 20mM Imidazole</td> <td>PBS with 10mM β-mercaptanethanol 150mM Imidazole</td> </tr> </table> <p>Dialysis against 50mM Tris-HCl pH 8.3, 100mM NaCl, 0.05% Triton X-100, 4 °C overnight</p>	Equilibrium Buffer	Wash Buffer	Elution Buffer		PBS with 10mM β-mercaptanethanol 20mM Imidazole	PBS with 10mM β-mercaptanethanol 150mM Imidazole	(Felber et al. 2004)
Equilibrium Buffer	Wash Buffer	Elution Buffer							
	PBS with 10mM β-mercaptanethanol 20mM Imidazole	PBS with 10mM β-mercaptanethanol 150mM Imidazole							
		<p>Ni-Affinity</p> <table border="1"> <tr> <td>Equilibrium Buffer</td> <td>Wash Buffer</td> <td>Elution Buffer</td> </tr> <tr> <td></td> <td></td> <td></td> </tr> </table>	Equilibrium Buffer	Wash Buffer	Elution Buffer				(Jayaraman et al. 2000)
Equilibrium Buffer	Wash Buffer	Elution Buffer							

Homogenization	Clarification	Purification	Source						
Sonication	Centrifugation	<p>Cells Thawed in TE Buffer (25mM Tris-HCl pH 7.5, 1mM EDTA, 1mM DTT with 0.2 mM 4-(2-aminoethyl)-benzenesulfonylfluoride-HCl)</p> <p>Upper brown pellet removed via rinsing. Lower white pellet dissolve in 50mM glycine-SO₄, pH 2.5 with 6M Guanidine HCl, 1mM DTT and 1mM EDTA.</p> <p>Solution was diluted into 200 fold dilution with TE Buffer at 4 C and stirred overnight.</p> <p>Supernatant applied to a 10-30% sucrose density gradient to separate GroEL and GroES.</p> <p>Butyl-Toyopearl column</p> <table border="1"> <tr> <td>Equilibrium Buffer</td> <td>Wash Buffer</td> <td>Elution Buffer</td> </tr> <tr> <td></td> <td></td> <td>20-0% Ammonium Sulphate</td> </tr> </table>	Equilibrium Buffer	Wash Buffer	Elution Buffer			20-0% Ammonium Sulphate	(Makino et al. 1997)
Equilibrium Buffer	Wash Buffer	Elution Buffer							
		20-0% Ammonium Sulphate							
Sonication	Centrifugation	<p>Ni-NTA column</p> <table border="1"> <tr> <td>Equilibrium Buffer</td> <td>Wash Buffer</td> <td>Elution Buffer</td> </tr> <tr> <td>0.1M HEPES (pH 7.7)</td> <td></td> <td>150mM NaCl, 0.5 M Imidazole, 0.1M HEPES (pH 7.7)</td> </tr> </table> <p>Dialysed against phosphate buffered saline (10mM Phosphate buffer pH 7.2, 150mM NaCl)</p>	Equilibrium Buffer	Wash Buffer	Elution Buffer	0.1M HEPES (pH 7.7)		150mM NaCl, 0.5 M Imidazole, 0.1M HEPES (pH 7.7)	(Wang et al. 2004)
Equilibrium Buffer	Wash Buffer	Elution Buffer							
0.1M HEPES (pH 7.7)		150mM NaCl, 0.5 M Imidazole, 0.1M HEPES (pH 7.7)							

4.6 Fermentation Protocols

Fermentations were run in the same media conditions and fermentor controls reported by J. Bezaire (2005) with exceptions reported in Section 4.7. Additional media components were aseptically added to the fermentor through the media port while the fermentor was maintained with a slight overpressure to reduce the chance of outside contamination.

4.6.1.1 Inoculation

The fermentor was inoculated with approximately 45-50 mLs of minimal media inoculation culture (5.7 g $\text{Na}_2\text{HPO}_4 \cdot (7 \text{ H}_2\text{O})$, 1.5 g KH_2PO_4 , 1g NH_4Cl , 0.5 g NaCl in 480 mL of water) at an O.D. of 0.90 which is higher than usual due to an overgrowth of inoculum in the first run and became the standard procedure for the four temperature control experiments to maintain consistency throughout. It was found that the overall growth was not greatly affected by this higher than usual O.D. and that it is likely that the inoculum was still in the late phases of exponential growth. Inoculum was aseptically added through the media port of the vessel at $t=0$.

4.6.1.2 Induction

Protein expression was induced at approximately 75 O.D. with 1 mL 500mM IPTG per liter of media in the reactor. IPTG was added again after 20 to 25 O.D. growth.

4.6.1.3 Acetate Analysis

Following the method of de Mare et al. (2005) cell samples were put into 1.5 mL microcentrifuge tubes (Diamed, Missisauaga Ontario Canada) half filled with 0.132 M ice cold perchloric acid and centrifuged for 1 min at 13,000 rpm in a Biofuge microcentrifuge (Heraeus Instruments, Hanau, Germany) and then neutralized with 3.6 M K_2CO_3 , flash frozen with dry ice and kept at -80°C . Analysis is performed using the same method as J. Bezaire (2005).

4.6.1.4 Time Course Protein Sampling

The fermentor was sampled approximately once per hour after the batch phase (usually after the first seven or eight hours) and following induction at 0.5 hrs, 1 hr and every hour

thereafter. The fermentor was also sampled during any events such as oxygen starvation or glucose feed bottle changes.

Optical Density was determined from initial protein sample collected in an Oakridge tube using a Cary UV-Vis spectrophotometer after being diluted sufficiently to be less than 1 O.D. unit. Three 1 mL samples of this were taken and spun down as in 4.6.1.3 and stored at -20°C until SDS PAGE was run.

Undiluted remaining protein sample was spun down at 20,000 rpm for 10 mins at 4°C in a Beckman JA 25.50 rotor using an Avanti-JE (Beckman Coulter, Missisauaga Ontario Canada) or Avanti-J25 (Beckman, Missisauaga Ontario Canada) centrifuge. Following this the supernatant was separated from the cell pellet. Both supernatant and pellet were stored in separate 15 mL Falcon Tubes (VWR, Missisauaga Ontario Canada), flash frozen with dry ice and stored at -80°C for later analysis.

4.6.1.5 Difference Gel Electrophoresis (DIGE) Sampling

Samples prepared for DIGE were taken from the fermentor at sampling time. Samples were 100 mL and prepared to an O.D. of 0.8. These were then centrifuged at 4°C for 15 min at 15, 000 rpm and resuspended in TE buffer (10 mM Tris-HCl, 1mM EDTA, pH 8.5) three times. The cell pellet after this was flash frozen in dry ice and kept at -80°C for analysis.

4.6.1.6 Temperature Control

Temperature was maintained using house chilled water for non-temperature control experiments and using a 30% ethylene glycol water mixture in an (Beckman-Coutier, Missisauaga Ontario Canada) Pelletier Cell operating at maximum flow set to 4°C for temperature controlled runs. The temperature controller was a BIOCONSOLE and run as per J. Bezaire (2005).

4.6.1.7 Post Fermentation Harvesting

Fermentation media was harvested in 0.5L Nalgene containers (VWR, Missisauaga Ontario Canada) and kept on ice until centrifuged in an Avanti-JE (Beckman Coulter,

Mississauga Ontario Canada) or an Avanti-J25 (Beckman, Mississauga Ontario Canada) centrifuge in a Beckman JA 10.00 rotor at 10,000 rpm for 15 minutes at 4°C. The cells were harvested and weighed in pre-tared 50 mL Falcon Tubes (VWR, Mississauga Ontario Canada), flash frozen in dry ice and placed in a -80°C freezer for later analysis and use.

4.6.1.8 Ni²⁺ Affinity chromatography purifications

Ni²⁺-NTA supplied from EMD Biosciences (formally Novagen distributed through VWR, Mississauga, ON Canada) was used in various quantities (less than 10ml) packed into a small Econo column (Bio-rad Mississauga, ON). Samples were homogenized in either a Emulsi-Flex C5 (Avestin Ottawa, ON) high pressure homogenizer between 10-15 thousand psi, (Autoclave Engineers Erie, PA USA) French press between 15 to 20 thousand psi, or sonicated in lysis buffer (40mM Tris-HCl pH 7.0 or pH 7.5 as specified, 1% glycerol, 100mM NaCl, 1mM PMSF). After lysis, the cells were centrifuged at 20,000 rpm for 25 mins and cell supernatant and pellets were separated. Resin was charged and prepared by first washing with 3 column volumes (C.V.) millipure Water, then 5 C.V. Nickel Sulphate Wash (50mM NiSO₄) and washed with 5 C.V. Pellet Buffer (40mM Tris-HCl pH 7.0 or 7.5, 1% glycerol, 250mM NaCl). The Supernatant was then mixed with Ni²⁺-NTA resin in a 500 mL centrifuge bottle with 1 Roche EDTA-free protease inhibitor tab and mixed for 1 hour. Resin was then centrifuged and spent supernatant poured off and loaded resin was repacked into the chromatography column. The column was then washed with 5 C.V. Pellet Buffer. Loaded protein was further cleaned using 2 C.V. s 50mM Imidazole in Pellet Buffer and eluted using 200mM Imidazole in Pellet Buffer.

4.6.1.9 Ion Exchange chromatography purification

1 and 6mL Resource Q anion or Resource S cation columns (G.E. Healthcare formerly Amersham Biosciences, Piscataway, NJ) were employed for small scale ion exchange purifications. Approximately 100 mL Q-sepharose resin (GE Healthcare formerly Pharmacia Fine Chemicals Piscataway, NJ) was packed into a XL50 column (G.E. Healthcare formerly Amersham Biosciences, Piscataway, NJ). An ACTA FPLC (G.E. Healthcare formerly Amersham Biosciences, Piscataway, NJ) was used to run the column

loading, elution and cleaning procedures. Samples were prepared as for Ni²⁺-NTA chromatography. Columns were equilibrated prior to loading using Pellet Buffer (100mM Tris-HCl pH 7.0 -8.5 depending on run, 100mM NaCl, 1mM PMSF). Samples were loaded using Pellet Buffer, the columns were then washed with Pellet Buffer, and samples eluted using Pellet Buffer with a linear NaCl gradient of 100mM to 1M.

4.6.1.10 Sample collection, fluorescence and protein quantification

Samples were either collected in 15mL 10mm glass tubes (VWR, Missisauaga Ontario Canada) or in Greiner Bio-One microplates (Monroe, NC USA) and read using a Gemini XPS microplate fluorescence spectrophotometer (Molecular Devices Sunnyvale, CA USA). Protein quantification was done using Bio-Rad Protein Assay using a SpectraMax 190 or SpectraMax Plus 334 microplate uv-visible spectrometer (Molecular Devices Sunnyvale, CA USA). Cell samples were also analyzed in Cary Eclipse (Varian Missisauaga, ON or QuantaMaster™ Model QM-4/2005, (Photon Technology International London, ON) fluorescence spectrometers using a Quartz cuvette.

4.6.1.11 SDS PAGE Analysis of Protein Samples

Protein samples taken for SDS PAGE analysis were diluted with 1 mL per O.D. reading (e.g. 0.73 O.D. would be diluted in 730 µl's). Samples were resuspended using a vortex mixer then 4X loading buffer with β-mercaptoethanol was added to a final 1X concentration, vortex mixed again, after which samples were boiled for 2 minutes. 10µl's of sample was loaded into each lane of a 12% SDS PAGE gel unless another concentration is indicated and then run until the front was near the bottom (usually within 1 cm of the bottom). Gels were then stained using Coomassie Brilliant Blue stain.

4.7 Temperature - Dissolved Oxygen Controller

It was chosen to reduce temperature when the D.O. fell below 10% with a moving average over five minutes of less than 18% and a stirrer speed moving average over five minutes above 1000 rpm. Several Labview™ VI's were added to the fermentor control program developed previously (Bezaire 2005). These algorithms control the fermentor temperature and monitored and calculated the moving average estimates.

Since 100% oxygen supplementation at industrial scales is unfeasible due to fire, explosion and health and safety reasons it was decided to limit some of the runs to 30% supplementation by total airflow.

Dissolved oxygen concentrations in the fermentor are function of mass transfer with several variables. The three commonly manipulated variables are:

1. Airflow and Oxygen Supplementation
2. Stirrer speed
3. Pressure

The oxygen transfer can be correlated to the power input and tables for various impeller configurations, reactor designs, and airflows are available. One of the problems encountered in high density fermentations is an inability to maintain growth and meet metabolic demands for oxygen due to limited mass transfer capabilities. This reduces the growth and leads to situations where recombinant protein production is compromised.

Chapter 5

Temperature Control Experiments

5.1 Introduction

In this chapter temperature reduction is explored as a means to maintain sufficient dissolved oxygen concentrations in Fed-batch fermentations under limited pure oxygen supplementation. Temperature reduction on a 50 mL shake flask scale provided information on the time effects of temperature. Two fermentations were run to explore the temperature controller and as a means to determine any problems with the fermentation methodology. Once the methodology had been established four fermentations were run and compared. The effort to quantify the protein production in regards to soluble versus insoluble lead to efforts in protein purification and quantification and some unexpected conclusions.

5.2 Shake Flask Run

5.2.1 Introduction

The protocols were used to determine the effects on growth and protein production of lowering the temperature. A cell culture was grown in minimal media in a 1.25 L flask, inoculated with a 50 mL culture at 0.94 OD to an optical density of close to 0.4 (OD_{600nm}) at 37°C in a Labline Incubator Shaker. The culture was then induced with 1.5 ml of 500 mM IPTG at 0.4333 OD, aseptically separated into 19 50 mL shake flasks, and cooled in a water bath at room temperature (approximately 24°C). The flasks were then placed in an Innova 4330 Refrigerator Incubator Shaker at 22°C and taken out at the scheduled times outlined in Table 5.1.

Table 5.1: Schedule for Shake Flask Experiment

Schedule for Reintroduction to 37°C	
Time (min)	Flask
15	1
30	2
60	3
90	4
120	5
150	6
180	7A,B
210	8A,B
SPARE	9A,B
-	22° C Control (A,B,C,D)
-	37° C Control (A,B,C,D)

To determine the timing for the experiment several inoculum shake flasks were allowed to reach the maximum achievable densities in 50mL shake flasks at 37 °C in the minimal media.

OD for 50 ml inoculum cultures at 37 C in water bath

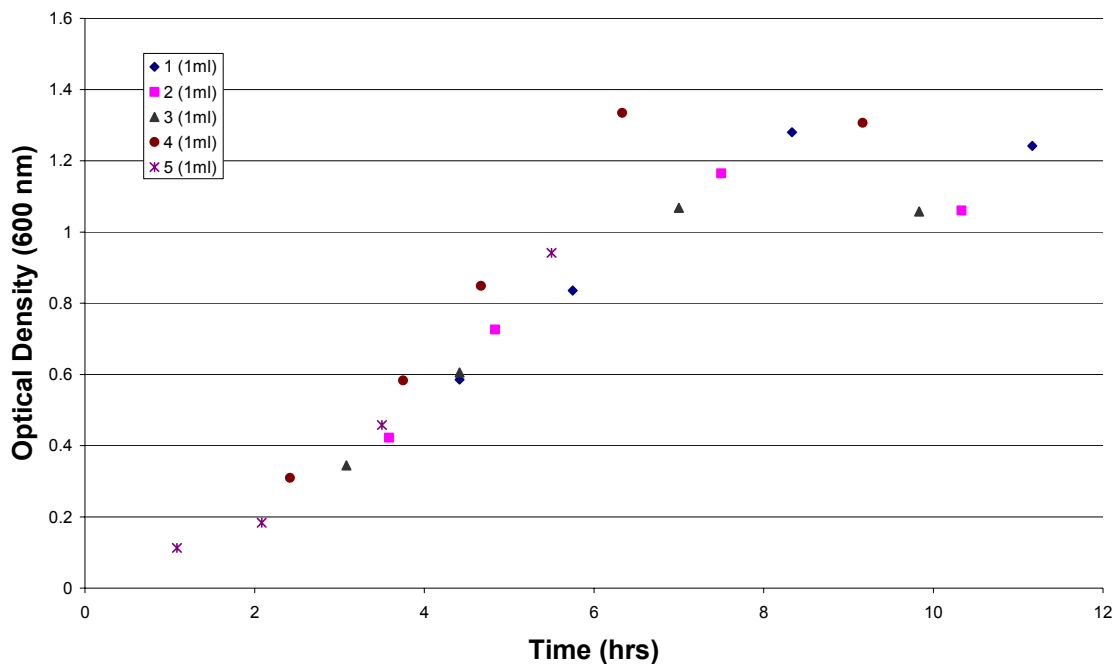


Figure 5.1: Data from previous inoculum cultures used to determine timing for shake flask experiment. Average growth rate was 0.69 hr^{-1} and maximum OD_{600} of 1.35 was achieved in 7-9 hours.

Data from these shake flasks (Figure 5.1) show that the maximal achievable density is approximately 1.35 O.D. at 7 to 9 hours, with an average specific growth rate of 0.69 hr^{-1} . This led to choosing a 4 hour induction period with induction occurring at approximately 0.4 O.D. This was chosen to balance the need for long period of growth after induction and time needed to see a difference in effect by temperature shift.

5.2.2 Growth for Shake Flask Runs

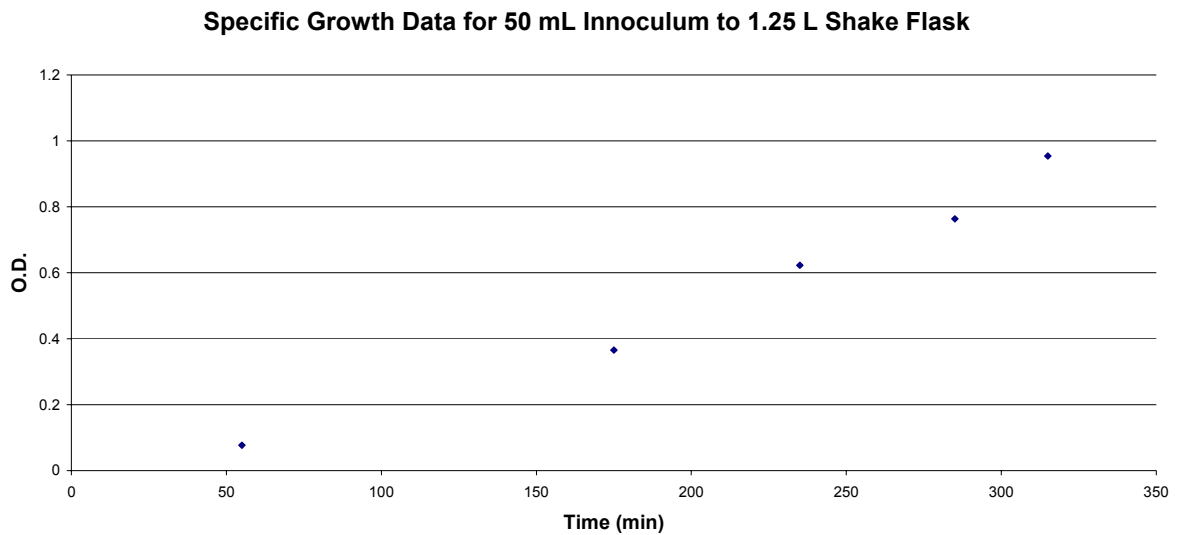


Figure 5.2: 50 mL inoculum culture for 1.25L shake flask culture. Cell growth rate was 0.45 min^{-1} which is lower than the expected growth rate of 0.69 min^{-1} . The growth profiles, however, were similar.

The 50 mL inoculum culture followed the expected growth profile with a specific growth rate of 0.45 min^{-1} . The culture achieved a O.D. of 0.954 at 315 minutes before being diluted into the 1.25 L flask (Figure 5.2). Upon addition of the inoculum the 1.25 L flask O.D. was 0.012 and grew to 0.436 in 275 minutes.

Specific Growth for Large Shake Flask Inoculum

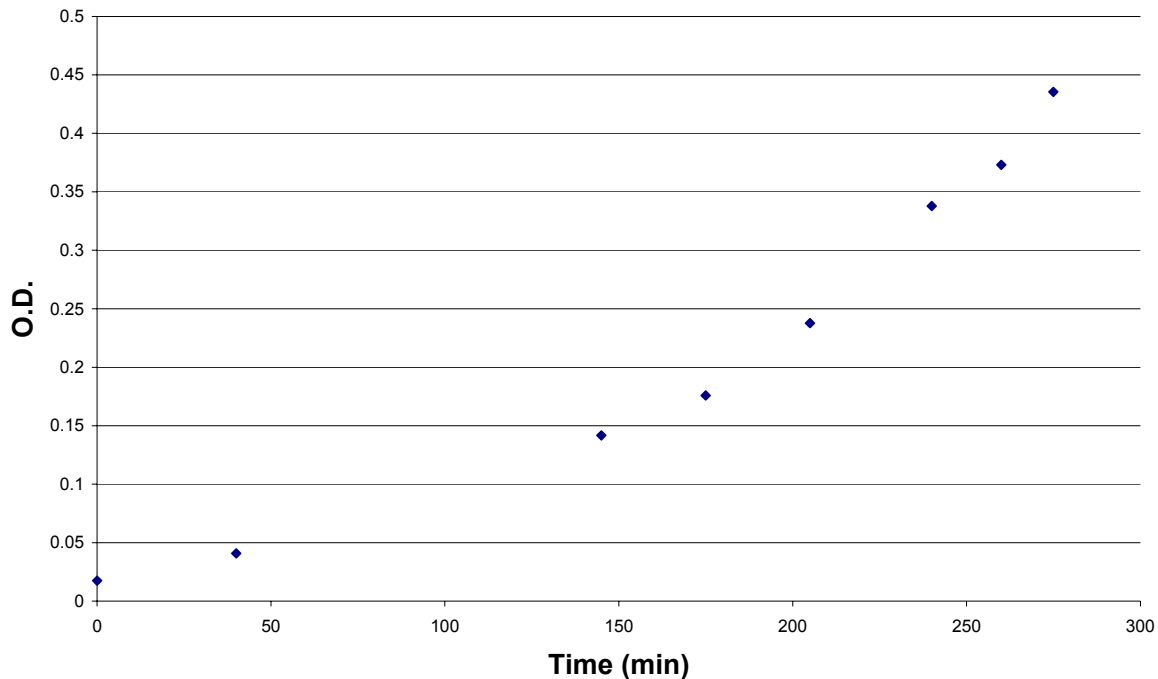


Figure 5.3: Growth for Large 1.25L Shake Flask. Growth rate, 0.18hr^{-1} , was lower than the 50mL inoculum likely due to dilution effects. Inoculum reached 0.436 OD_{600} at 275 minutes.

The growth for the larger shake flask took 90 minutes longer than for the 50 mL cultures but this is not unexpected due to the larger volume and lower seeding density. The specific growth rate was 0.18 hr^{-1} which was, again, lower than the 50 mL shake flasks (Figure 5.3). Induction occurred in the beginning of the exponential phase at an O.D. of 0.436 leaving four hours of growth at 37°C and 22°C to run the experiment in.

Media from the large 1.25 L flask was separated into 19, 50 mL shake flasks using sterile pipettes. With the exception of 37°C control cultures, all shake flasks were immediately placed in a separate incubator set at 22°C . Growth for each shake flask varied. In general growth was slower for cultures which remained at the lower temperature longer. Figure 5.4 summarizes the growth profiles for all growth cultures with the exception of cultures held in reserved (9A, 9B). Control culture averages are shown in this figure. The time courses for

both the 15 and 30 min shake flasks were very similar however there was a large difference between the 30 min and 60 min shake flasks indicating that there is an overall adaptive growth change during this period creating a larger lag time when the culture is reintroduced to 37°C.

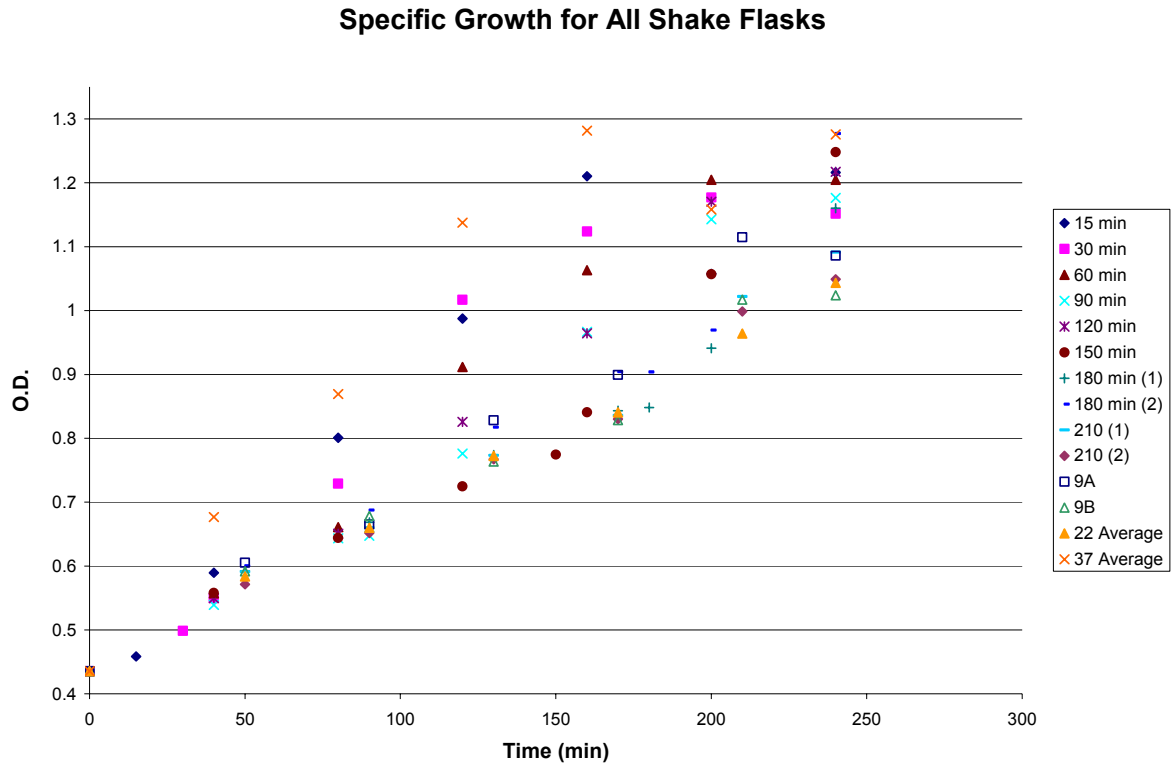


Figure 5.4: Growth for All Shake Flasks during the 240 minute growth trial. Growth rates varied from 0.29 to 0.40 hr⁻¹ but all growth appeared to reach near the maximum growth of 1.3 OD₆₀₀ achieved in 50 mL shake flasks.

Optical density at the end of the 240 minute experiment was close to the maximum predicted growth achieved in 50 mL shake flasks. Growth during the experiments varied and appeared to have a maximum at 60 minutes. This may indicate that the changes in temperatures for cultures before 60 minutes were too rapid and growth suffered. Growth after 60 minutes may be affected by the temperature and after this point growth rate slows and overall growth is affected (Table 5.2).

Table 5.2: Estimated growth rates for 50mL shake flasks taken from 22 °C to 37 °C at various times.

Sample	Estimated Average Specific Growth Rate (μ hr⁻¹)
15	0.29
30	0.36
60	0.40
90	0.39
120	0.39
150	0.35
180A	0.31
180B	0.36
210A	0.34
210B	0.31
22	0.29
37	0.35

Figure 5.5 is the graphical representation of Table 5.2 showing the maxima suggested at 60 minutes.

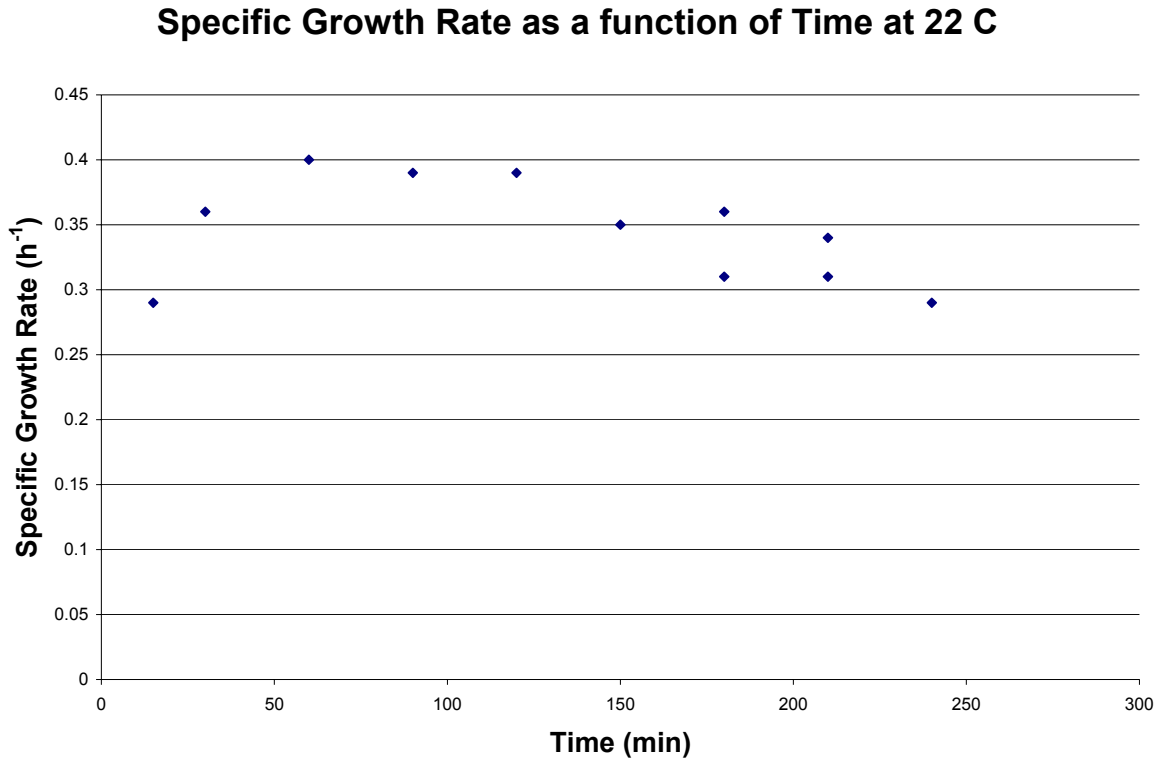


Figure 5.5: Growth Rate as a function of time at 22 C. The pattern appears to follow a concave curve with a maximum at 60 min. This may be a function of the cultures ability to adapt. Cultures at the beginning were given temperature shocks quicker and this may indicate a need for time to adapt. Cultures after 60 min may have adapted to the lower temperatures but the growth rates were affected and could not recover during the experiment run time.

The growth was slowed at the reduced temperature, the 22°C controls lagged 130 minutes behind the 37°C controls and each flask taken out at different times lagged between 45 to 130 minutes measured by the time taken to reach an O.D. of 1 compared with the 37°C controls dependant upon the amount of time at 22°C. Figure 5.6 suggests that despite the maxima at 60 minutes cooling in terms of growth rate, overall growth is temperature affected since later cultures lagged previous cultures. The run is too short to determine whether there is actually

cultures at 210 minutes can recover fully since they are near 1 O.D.₆₀₀ and thus near the maximum expected optical density.

Time to Reach an O.D. of 1 compared to 37 C Controls

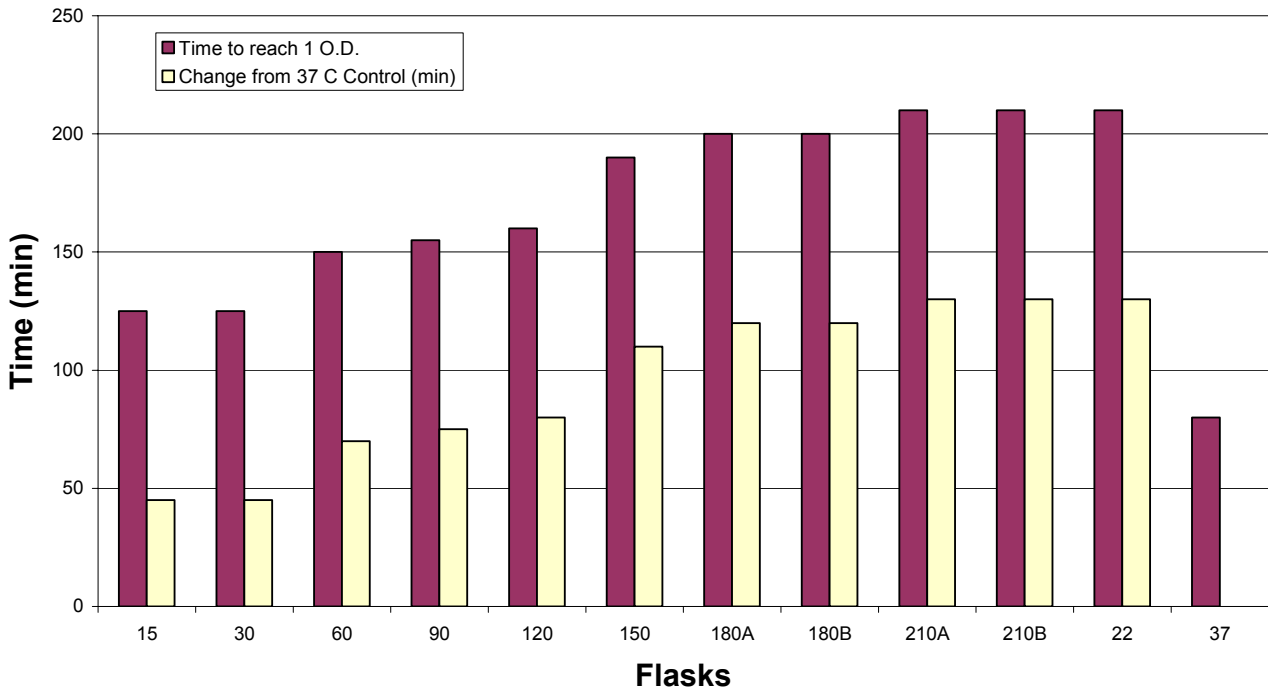


Figure 5.6: Time of cultures to reach O.D. of 1 when subject to a temperature change for a given time. The length of time at a lower temperature corresponds well to the amount of time required to reach 1 O.D. compared to the 37 °C control cultures. It is interesting to note that this graph may indicate that there are certain critical times after which the culture has adapted well enough

The overall growth lag was used to determine the amount of time at 22°C for the simulated oxygen failure run (Section 5.4). Also, the overall growth lag was to estimate the maximum amount of time it was feasible to remain at 22°C in terms of overall protein production.

During the experiment two sets of temperature controls were used at 22°C and 37°C. Overall the 22°C controls show much less deviation and scatter than the 37°C controls. Since the culture to be held at different timings were chosen at random, and cultures were kept well mixed in-between dividing into 50mL cultures, settling is unlikely to have contributed much to the differences between the control cultures. The 22°C control cultures appeared to still be growing near the end of the culture but would have likely reached stationary phase shortly after 240 minutes and had an average final density of 1.043.

Although there is a difference in variances both cultures achieved an O.D. greater than 1 over the 240 minutes of the experiment and the 37°C culture achieved a stationary growth phase at 160 minutes with an average O.D. of 1.29. The variance of the 37°C control cultures was greater than the 22°C control cultures likely due the higher grow rate and differences in inoculum densities in the 37°C control cultures (Figure 5.7).

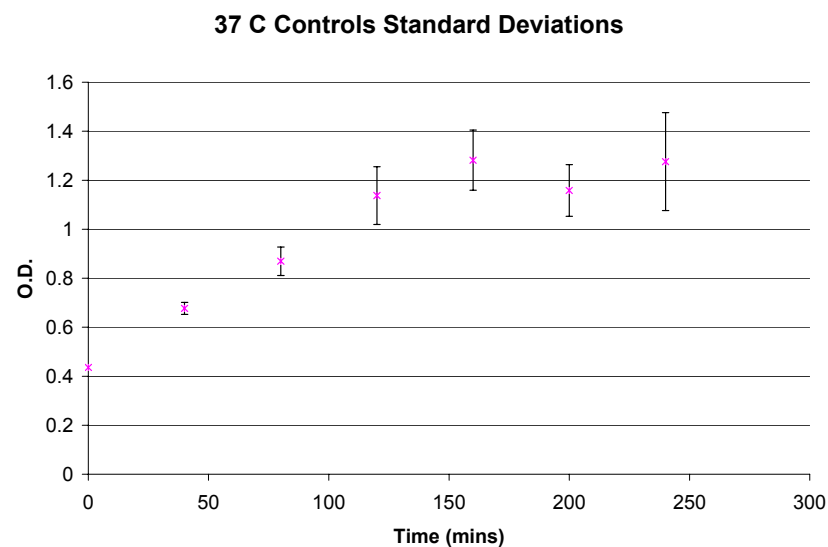
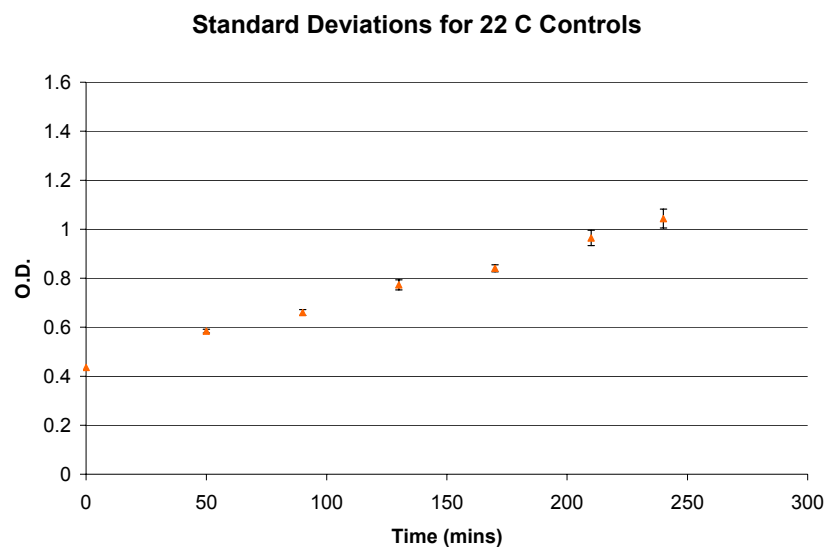


Figure 5.7: Standard Deviation for 22 °C and 37 °C Control. Standard Deviation for the 22 C shake flasks were much better than the 37 C shake flasks. This may indicate that any potential differences in inoculation density are not favoured too heavily and growth rates (0.29 versus 0.35 hr⁻¹) are slow enough not to select for higher inoculums. This may be supported by the higher growth rate, 0.35 hr⁻¹, compared to 22 °C, 0.29 hr⁻¹.

5.2.3 Final Weights and Protein Production

All cultures ended close together in terms of optical density and seemed to be little affected by overall temperature after 240 minutes. A comparison of the standard deviations for the controls shows no significant difference after 240 minutes (Refer to Appendix B).

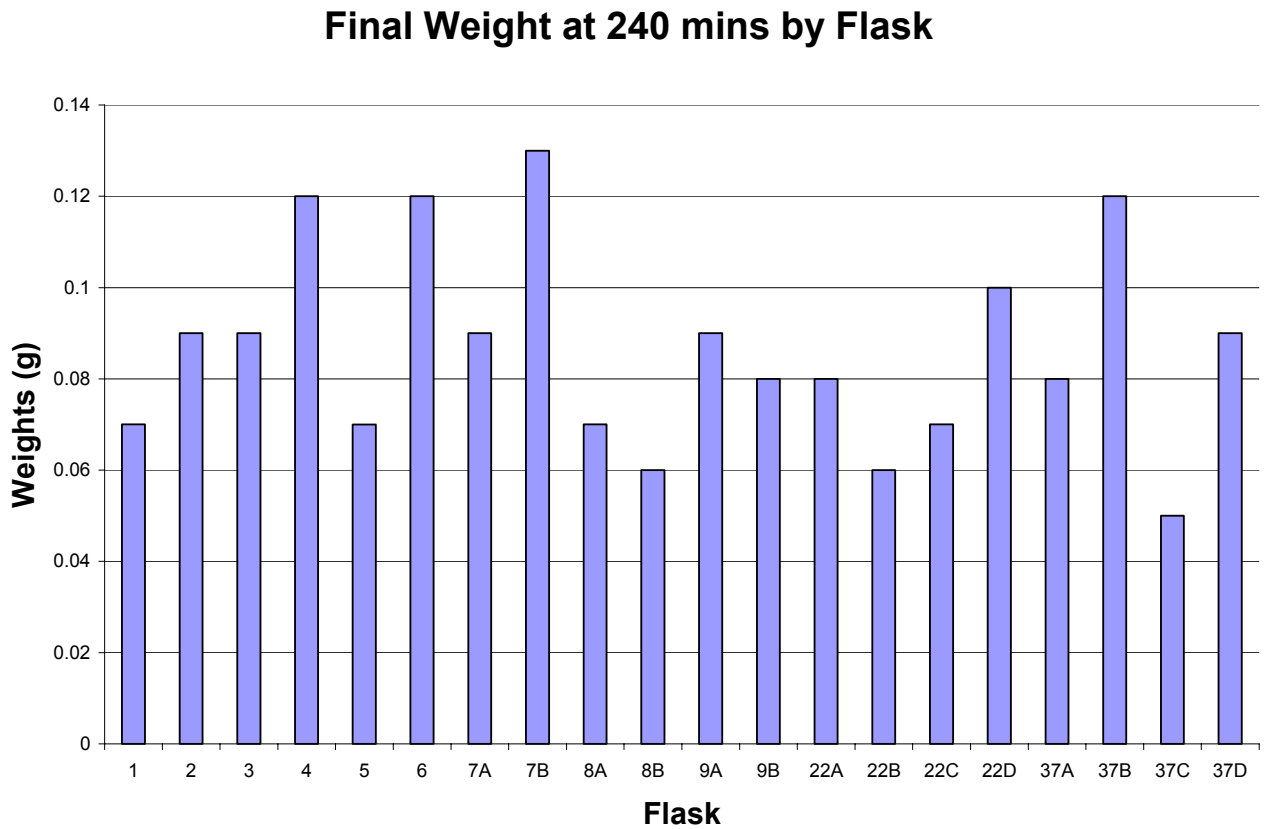


Figure 5.8: Final Weights for all 50mL shake flasks at 240 minutes. The cultures show minor weight variances with the lowest weight, 8B, being 0.06g and the highest being, 7B, at 0.13g. This may be a result of $Y_{x/s}$ not being affected by temperature at this volume.

The differences between the final weights achieved in the standard control cultures at 37°C $0.085g \pm 0.03$ and 27°C 0.078 ± 0.02 , shows no meaningful difference between the two mean weights achieved. It is difficult to tell how much variance in final weight was caused by

temperature versus uncertainty due to the weighing of small masses. The cell mass yields, $Y_{x/s}$, are likely uncoupled from the specific growth rate, μ , at these volumes. A correlation plot of final weights versus final optical densities does not indicate a correlation between these two parameters and this is likely because of magnification of errors due to the small volumes involved.

Weight and Final O.D. Correlation.

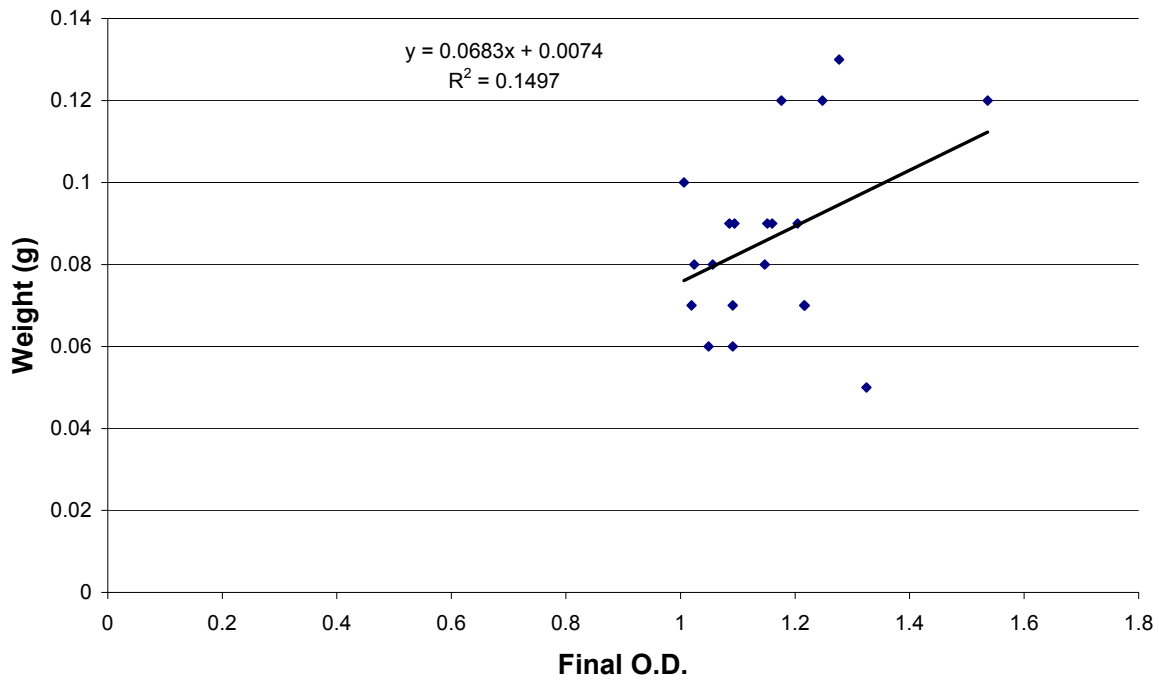


Figure 5.9: Correlation plot for final weight and OD_{600} . This indicates that $Y_{x/s}$ may not be affected by temperature at this volume.

5.2.4 Shake Flask SDS PAGE Gels

Overall induction is not obvious in the SDS PAGE gels (Gels). However Gels 3 (Figure 5.12), 5 (Figure 5.14), 37C (Figure 5.28), and 37D (Figure 5.29) appear to have an increasing band at 30 kDa (the predicted weight of eYFP) with time. All gels show another band between 30 kDa and 45 kDa which is unexplained and may be a protein by-product of induction with IPTG. Given the lack of obvious induction it seems likely that eYFP production was only be at low levels during this experiment.

A comparison of Figure 5.23 and Figure 5.26 provide an excellent basis for comparison between control cultures kept at 22°C and 37°C. Gels from shake flasks which were removed earlier than 150 minutes (Figure 5.10 through Figure 5.15) appear to have less overall proteins than Gels which where left longer (Figure 5.16 through Figure 5.21). This is shown best in a comparison of Figure 5.23 and Figure 5.26. In the range of 66 -97 kDa (the uppermost two standards) several proteins are expressed. In cultures kept longer at 37 °C these band often form what appears a more solid band as they run into each other. For both cultures there is a distinct fading of proteins in-between 20.1 and 30 kDa.

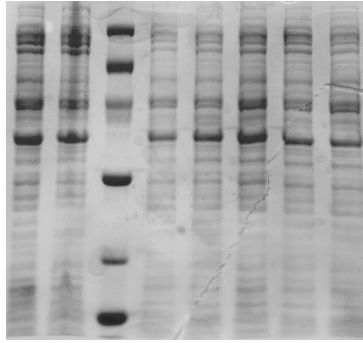


Figure 5.10: SDS PAGE Gel 1

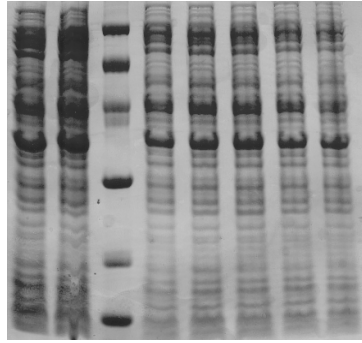


Figure 5.11: SDS PAGE Gel 2

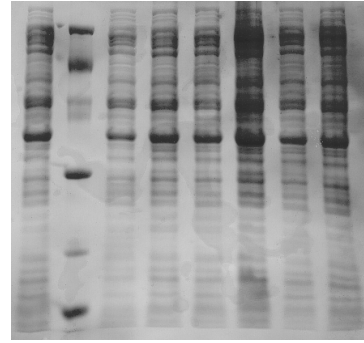


Figure 5.12: SDS PAGE Gel 3

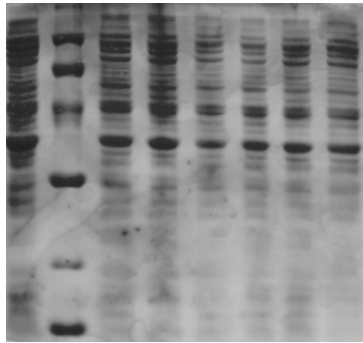


Figure 5.13: SDS PAGE Gel 4

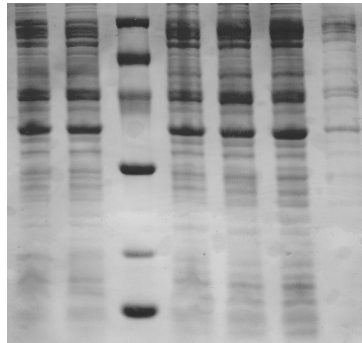


Figure 5.14: SDS PAGE Gel 5

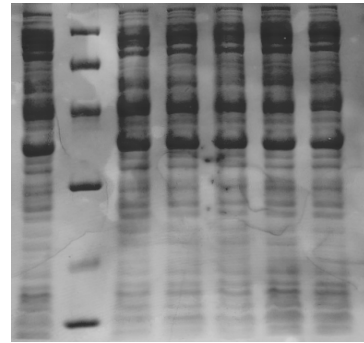


Figure 5.15: SDS PAGE Gel 6

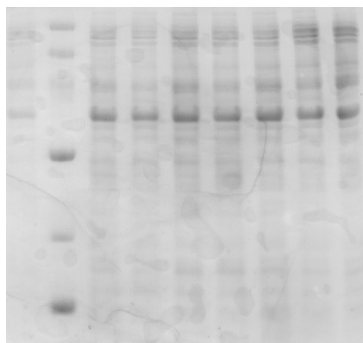


Figure 5.16: SDS PAGE Gel 7A

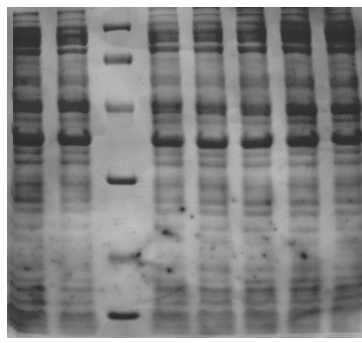


Figure 5.17: SDS PAGE Gel 7B

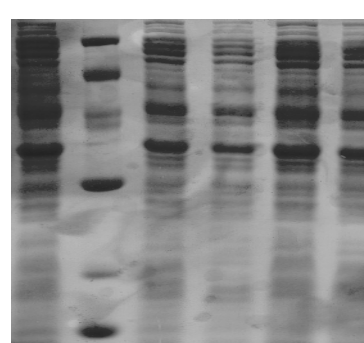


Figure 5.18: SDS PAGE Gel 8A

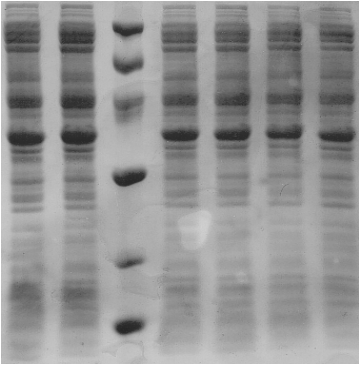


Figure 5.19: SDS PAGE Gel 8B

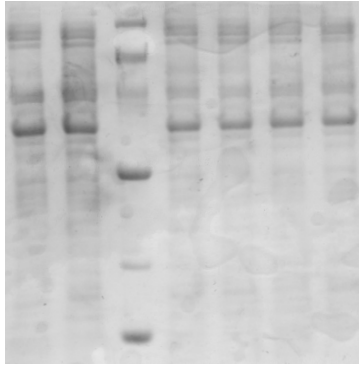


Figure 5.20: SDS PAGE Gel 9A

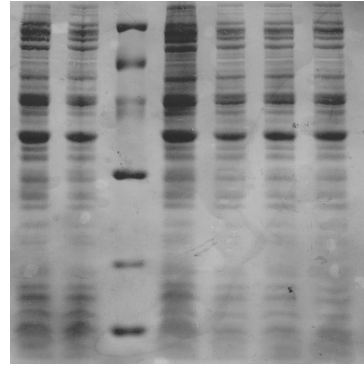


Figure 5.21: SDS PAGE Gel 9B

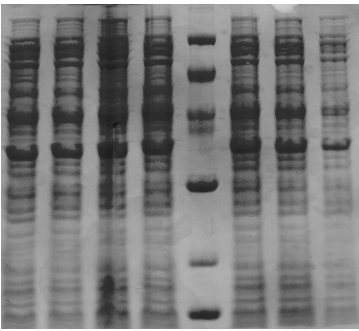


Figure 5.22: SDS PAGE Gel 22A

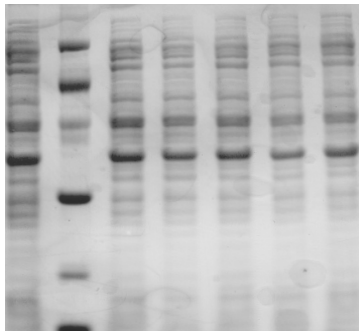


Figure 5.23: SDS PAGE Gel 22B

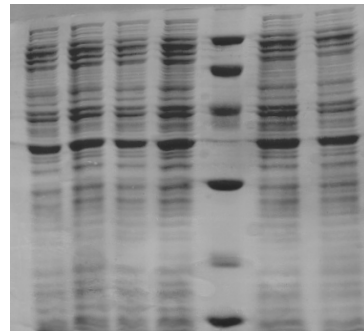


Figure 5.24: SDS PAGE Gel 22C

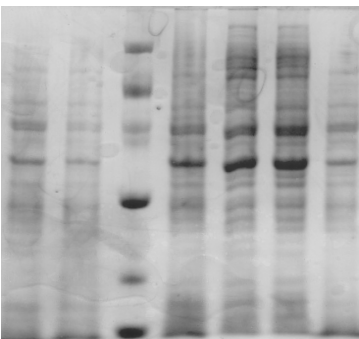


Figure 5.25: SDS PAGE Gel 22D

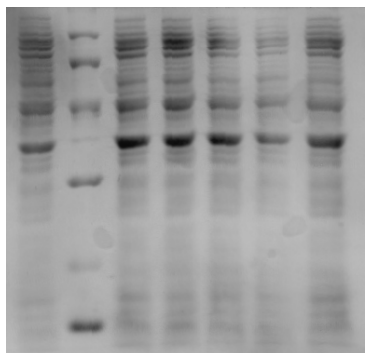


Figure 5.26: SDS PAGE Gel 37A

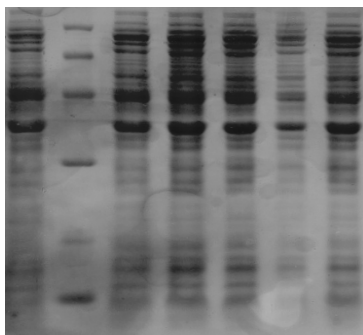


Figure 5.27: SDS PAGE Gel 37B

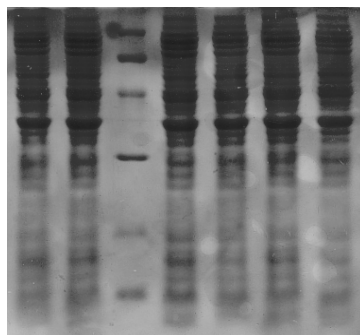


Figure 5.28: SDS PAGE Gel 37C

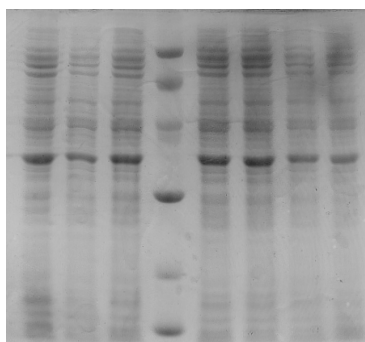


Figure 5.29: SDS PAGE Gel 37D

Table 5.3: Key for SDS PAGE figures for Shake Flask Runs

	Lanes									
GEL	1	2	3	4	5	6	7	8	9	10
1	15	40	STD	80	120	180	200	240	-	-
2	-	30	40	STD	80	120	160	200	240	-
3	40	STD	60	80	120	160	200	240	-	-
4	-	40	STD	80	90	120	160	200	240	-
5	-	40	80	STD	120	160	200	240	-	-
6	-	40	STD	80	120	160	200	-	-	-
7A	-	PreInd	STD	50	90	130	170	180	200	240
7B	-	50	90	STD	130	170	180	200	240	-
8A	-	50	STD	90	170	210	240	-	-	-
8B	-	50	90	STD	130	170	210	240	-	-
9A	-	50	90	STD	130	170	210	240	-	-
9B	-	50	90	STD	130	170	210	240	-	-
22A	-	PreInd	50	90	130	STD	170	210	240	-
22B	-	50	STD	90	130	170	210	240	-	-
22C	-	40	90	130	170	STD	210	240	-	-
22D	-	50	90	STD	130	170	210	240	-	-
37A	-	40	80	STD	120	160	200	240	-	-
37B	-	40	STD	80	120	160	200	240	-	-
37C	-	40	80	STD	120	160	200	240	-	-
37D	-	PreInd	40	80	STD	120	160	200	240	-

***time in minutes**

12% SDS PAGE Gels (Figure 5.10 through Figure 5.29) for the shake flask used low molecular weight standards.

5.3 Initial Bioreactor Temperature Control Runs

5.3.1 Inoculum

Inocula for the temperature control and non-temperature control runs reached seeding densities at 0.730 OD₆₀₀ at 13 hrs and 0.771 O.D. at 12.75 hrs respectively. The specific growth rates however were quite different, 0.637 and 0.307 respectively. This is due to the long initial lag shown in the non-temperature control inoculum. The cause of this is unknown. The inoculum for the temperature controlled run was relatively linear and the inoculum for the non-temperature controlled run was much more exponential in exponential growth phase.

Innoculum for T control Runs

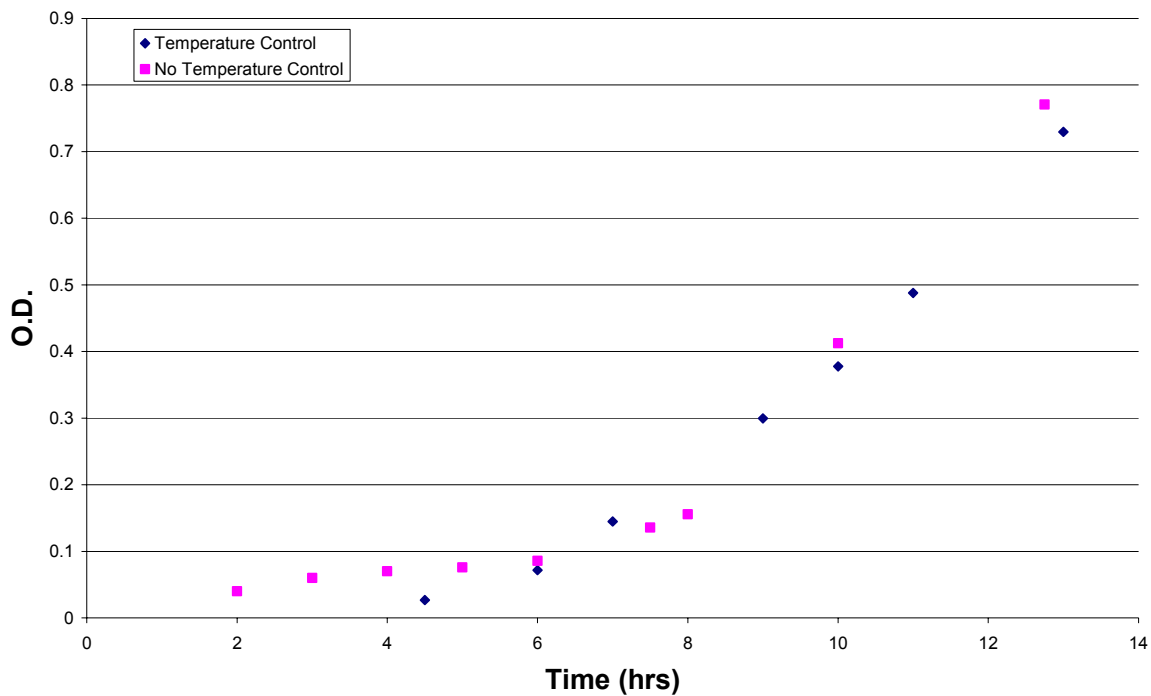


Figure 5.30: Inoculum growth profile for Run without Temperature Control. The growth rate was 0.307. The inoculum density for the no temperature control run was 0.771 OD₆₀₀ compared to 0.730 OD₆₀₀ for the temperature control run. The two inoculums had differing growth rates, 0.307 versus 0.637 for no temperature control and temperature control inoculums respectively. Each inoculum reached the seeding density in approximately the same amount of time.

5.3.2 Growth

The initial lag phase was approximately 2 hours longer in the temperature controlled run (11 hrs versus 9 hrs until first feeding). Compared to the non-temperature controlled run the glucose demand was significantly less over that time frame suggesting somewhat different $Y_{x/s}$. The temperature controlled runs had less pH control than the non-temperature control runs and required much less glucose indicating less acetate formation in the temperature control run.

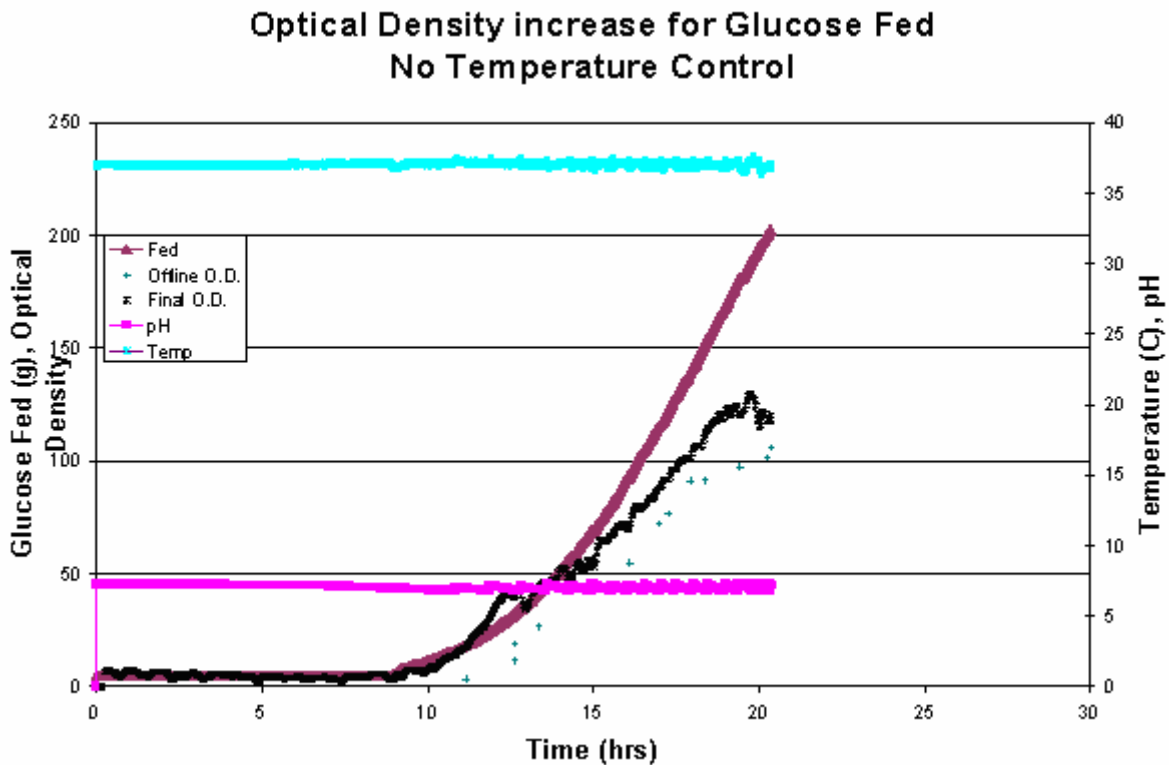


Figure 5.31: Optical Density versus glucose fed for no temperature control run. This run began the Fed-batch feeding phase 2 hours earlier than the temperature control run. The glucose fed was much higher during the exponential feeding phase of the run and growth noticeably

deviated from the glucose fed profile 5 hours before the end of the end. There is increased pH control indicate more glucose being converted to acetate.

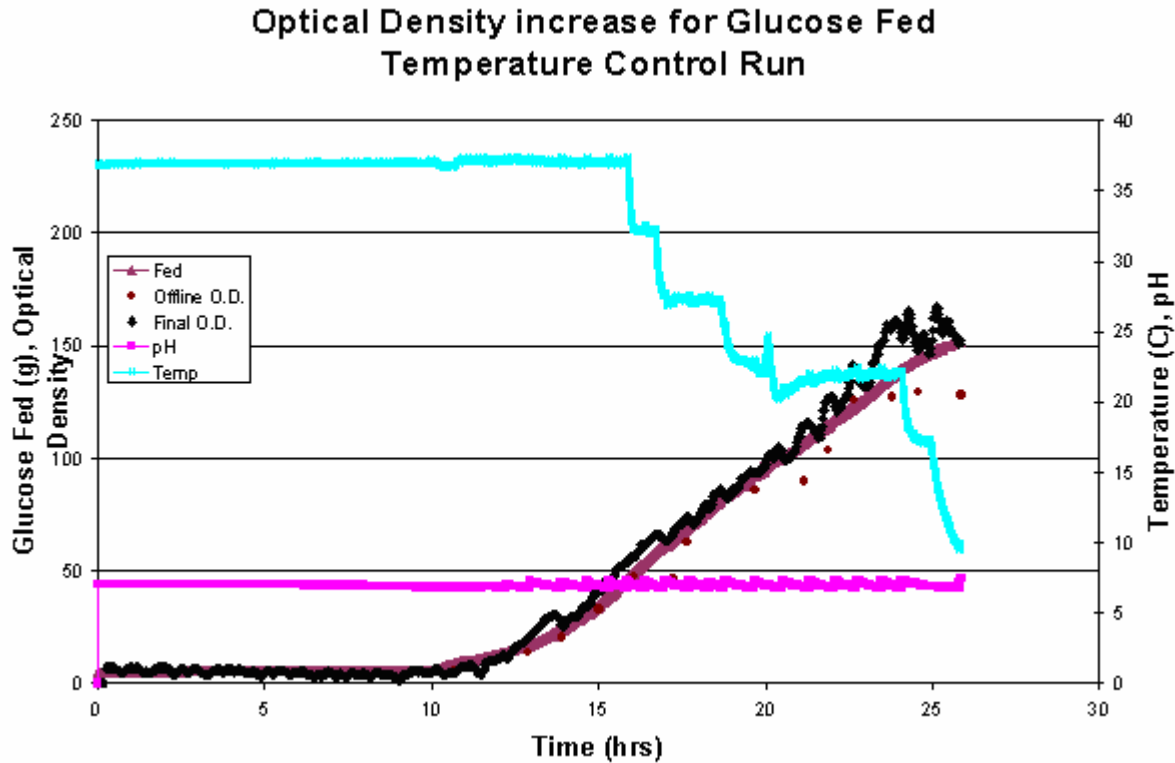


Figure 5.32: Optical density versus glucose fed for temperature control run. The run began Fed-batch feeding phase 2 hours later than the non-temperature controlled run. The glucose fed was much lower than the non-temperature controlled run and the optical density followed the glucose fed profile very closely.

Offline and online optical densities (O.D.) for both runs were within 20 O.D. However, for the temperature controlled run the offline O.D. flattened around 22°C before the offline O.D. peaked at around 170. Online O.D. readings are sensitive to foaming and is indicated by a sudden decrease in the online O.D. in Figure 5.32 at 24.98 hrs.

The temperature controlled run produced a much higher $Y_{x/s}$ (wet cell weight) than the non-temperature controlled run (1.75 versus 1.16 respectively). Table 5.4 summarizes the final

conditions for each run. Optical density and total biomass varied very closely, 32 and 30g respectively.

Table 5.4: Summary for initial bioreactor temperature control runs. Final O.D. for the temperature control run was higher than the non-temperature control run, 152 versus 120 O.D. Biomass measured by wet weight differed by 30 g (265g versus 235g).

	Final O.D.	Glucose Fed (g)	Total Wet Weight Biomass (g)
Non-temperature	120	203	235
Temperature	152	151	265

5.3.3 Protein

As with the SDS PAGE gels for the Shake Flask runs there is no distinct and increasing band at 30 kDa as would be expected from sequencing (Chapter 4). These Gels were run at 10% concentration which is different than discussed in the methods section (Section 4.6). The cell pellets were all diluted in 20 uL of buffer and 15 uL was applied to each of the lanes. Lane to lane comparison is difficult with this method. However, the protein distribution is representative of the proteins expressed at each time point. The high loading of each lane was done to better visualize proteins which were in low abundance. Despite the high loadings and because of the method used it is difficult to determine whether eYFP concentrations within the cells increased with time without densitometric analysis which was not performed.

Gels Figure 5.33 and Figure 5.34 are from the non-temperature control run samples. Gels Figure 5.35 and Figure 5.36 are from the temperature control run samples. In each of the Gels there is a band suggesting overproduced proteins around 36-45 kDa. This does not correspond however with the size of protein suggested in DNA sequencing.

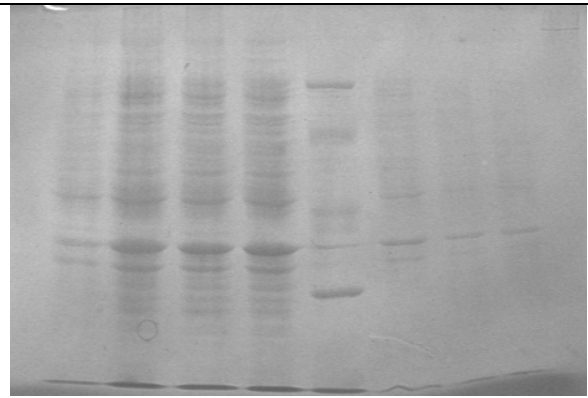


Figure 5.33: No Temperature Control 10% SDS PAGE. Samples 1-7 shown.

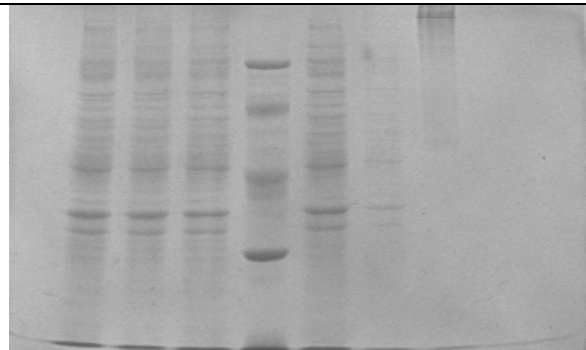


Figure 5.34: No Temperature Control 10% SDS PAGE. Samples 8-12 shown. The sample beside lane 12 is overflow from lane 12.

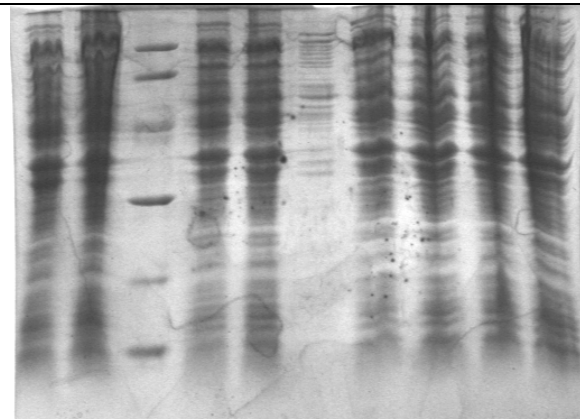


Figure 5.35: Temperature Control 10% SDS PAGE. Samples 1-9 shown.

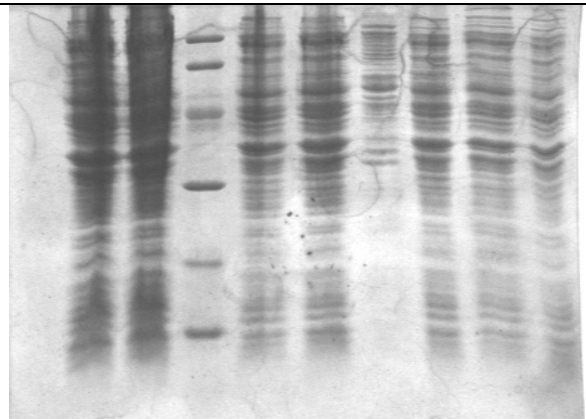


Figure 5.36: Temperature Control 10% SDS PAGE. Samples 10-17 shown.

Table 5.5: Key for SDS PAGE figures for Temperature Control Run

		Lanes									
	GEL	1	2	3	4	5	6	7	8	9	10
Run A	Gel 1	-	9.77	11.16	12.62	13.37	std	15	16.09	16.98	-
	Gel 2	-	17.26	17.91	18.37	std	19.42	20.27	-	-	-
Run B	Gel 1	10.69	12.89	std	13.91	15	16.08	17.23	17.64	18.44	19.69
	Gel 2	-	21.17	21.89	std	22.66	23.78	24.59	25.85	25.85	-

Figure 5.37 suggests an exponential rise, much like cell growth, in eYFP production when measured in a microplate reader with an excitation of 515 nm, emission of 535 nm and a cut-off of 530 nm. The protein fluorescence signal is extremely noisy and this relationship although suggestive, is far from certain.

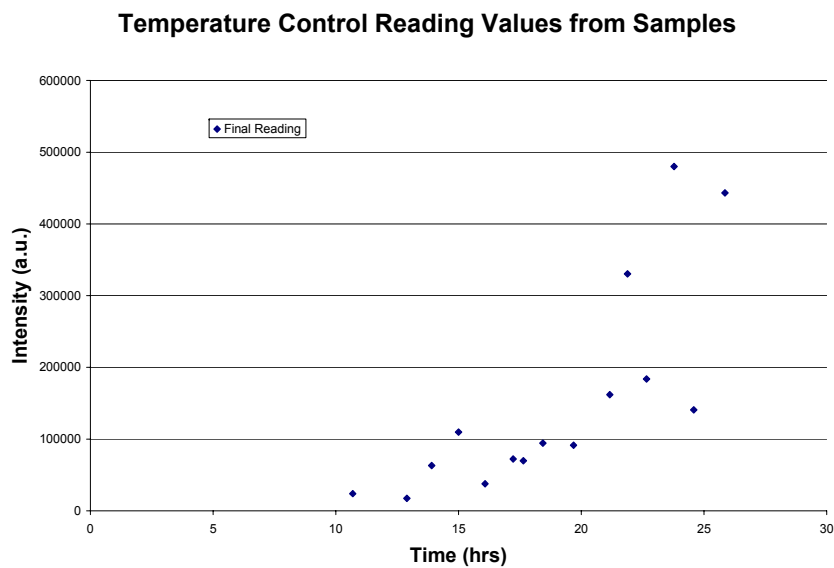
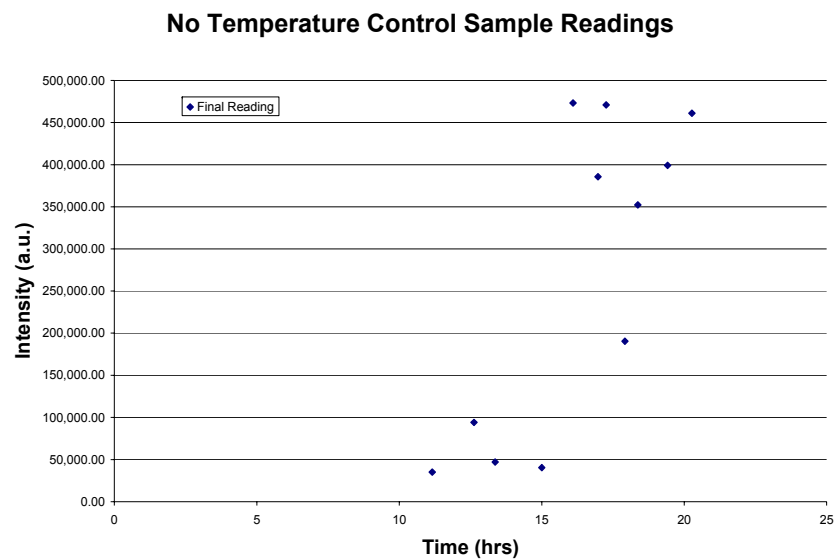


Figure 5.37: Fluorescence Readings from SDS Pellet Samples. There is no clear pattern suggested in the No Temperature Control Samples. The temperature control samples may show a slightly exponential pattern but this is uncertain. Excitation of 515 nm, emission of 535 nm and a cut-off of 530 nm.

5.4 Temperature Control Experiments

Four temperature control experiments were run to determine the effect of temperature on growth and other fermentation parameters. Larger samples were taken to allow for the determination of insoluble versus soluble fractions of proteins. Table 5.6 shows the temperature control and oxygen limitation situations for each experiment. The final experiment, experiment D, is a simulated oxygen failure run done to determine whether the fermentation can survive a low oxygen environment. Pure oxygen was turned off for a period of 30 minutes during this run since it was determined in the shake flask runs to be the longest period before significant lag occurred upon return to favourable growth conditions. In the time between the initial and final temperature control experiments, the online O.D. estimation parameters were adjusted to better fit the new data.

Table 5.6: Parameters for Temperature Control Experiments

Run	Date Performed	Temperature Control	30% Oxygen Limitation
A	8 Jun 06	N	N
B	5 Jun 06	N	Y
C	14 Jun 06	Y	Y
D*	11 July 06	Y	Y

*Interrupted Temperature Control Run

5.4.1 Inocula

The inoculum for each run (Figure 5.38) varied little but reached seeding densities within an hour and a half of each other. The optical density inoculum for this series of experiments averaged 0.95 with a standard deviation of 0.01 O.D., although the first two runs took 5.5 hrs and final two runs took 7 hours to come to seeding densities. This inoculum is significantly higher than previous runs owing to faster than anticipated growth in the initial run. Several possible reasons exist for this including fresher transforms or the plasmid may have been rejected. The later is unlikely since the plasmid must also be present for the cells to survive in

the media. It is also unlikely that the inoculum would have enough β -lactamase to degrade all the ampicillin in the plates, overnight media, inoculum media and the fermentation media. The fermentor was fully prepared at least half an hour before the initial inoculation according to the procedures published in J. Bezaire (2005) with the exception that the inoculum was putting step 11 after 21 (Appendix B).

Inoculum Growth for Temperature Control Runs

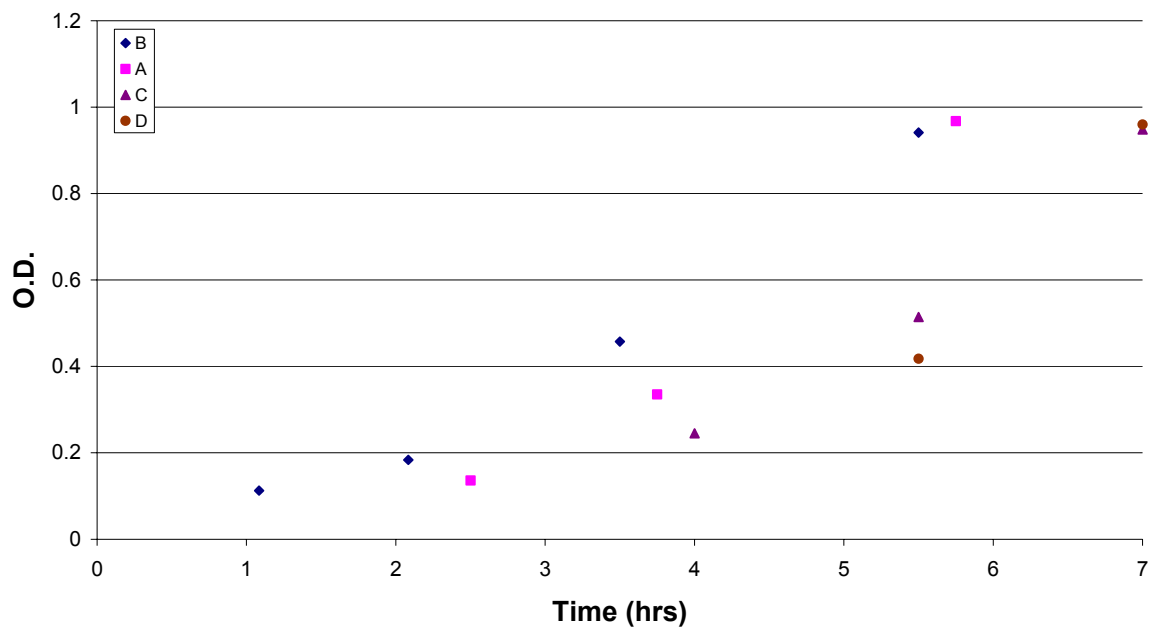


Figure 5.38: Inocula Growths for Temperature Control Experiments. The average optical density before seeding into the bioreactor was 0.95 with a variance of 0.1. The first 2 runs took 5.5 hours to reach seeding density and the last 2 runs took 7 hours.

5.4.2 Growth

Growth varied for each run. Run A's conditions allowed the culture to grow the fastest. Non-temperature controlled runs in general required more pH additions at a higher frequency due to higher acetate productions. These runs also lead to a wider variation between the online and offline growth values indicative of culture problems such as cell lyses and foaming. The cell debris is theorized to have a scattering effect on the probe's functioning leading to an

overestimation of optical density. Run C was kept as long as possible and below the original setpoint value of 22°C to 18°C and then down as low as possible to identify the minimum feasible values possible for the culture and equipment set up. Run C's initial induction occurred at 55 O.D. instead of 75 O.D. due to worries regarding limited growth. Run C and D showed slower acetate metabolism which was especially obvious below 27°C (Figure 5.41B and Figure 5.42B). For brevity, the mas of glucose fed in these experiments is reported as Fed.

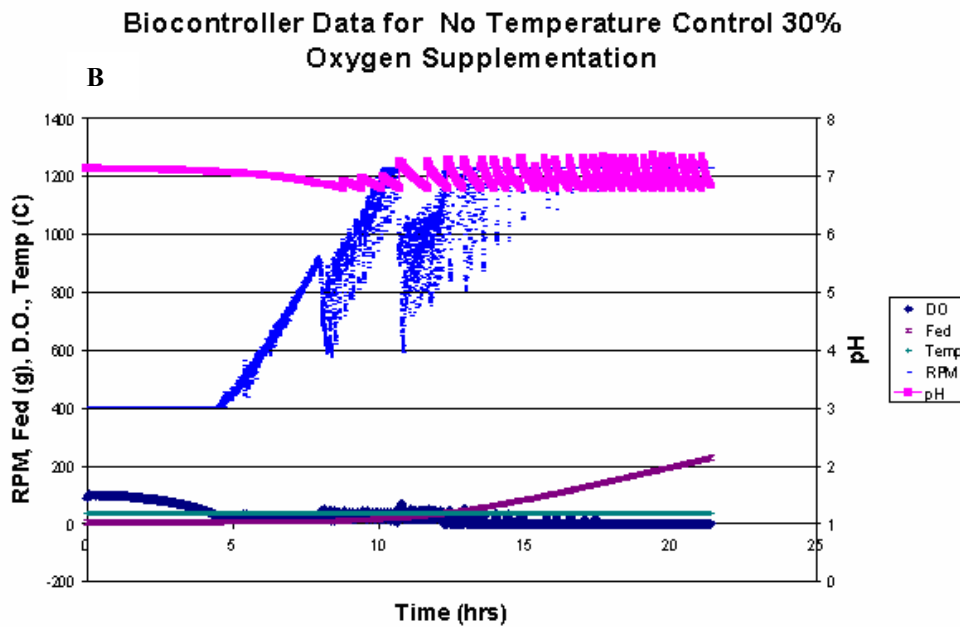
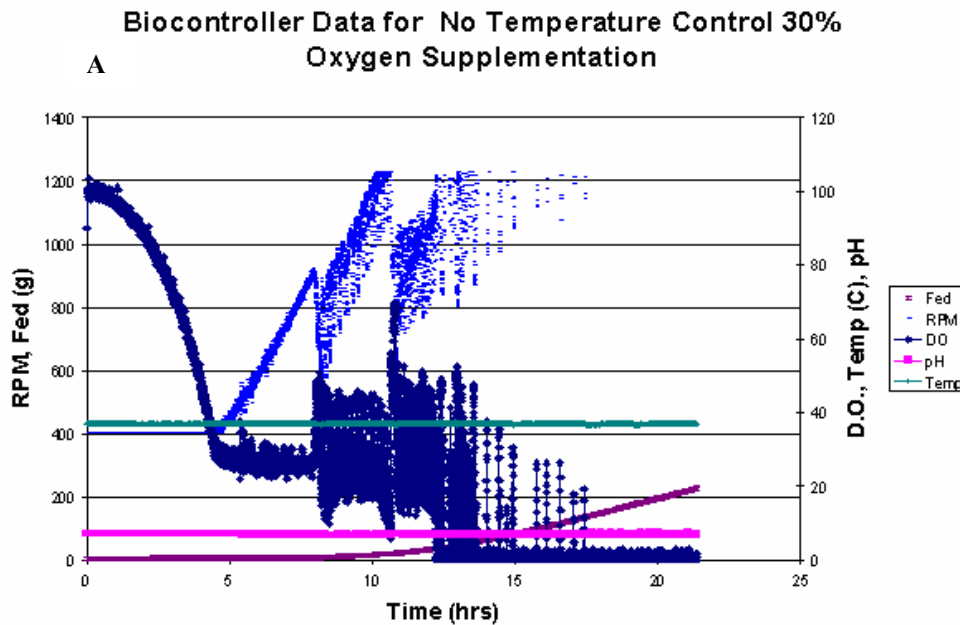


Figure 5.39: Run A Biocontroller data. A, shows oxygen limitation during the exponential growth phase. The wider oxygen spikes after 8 hours show the beginning of 30% oxygen supplementation. Figure B, shows the increasing fluctuations in pH indicating excessive metabolic formation of acetate. The stirrer speed increased and then rapidly decreased during the initial oxygen supplementation period. Once growth related oxygen demand reached oxygen transfer capacity the stirrer speed quickly reached a maximum value of 1224 rpm.

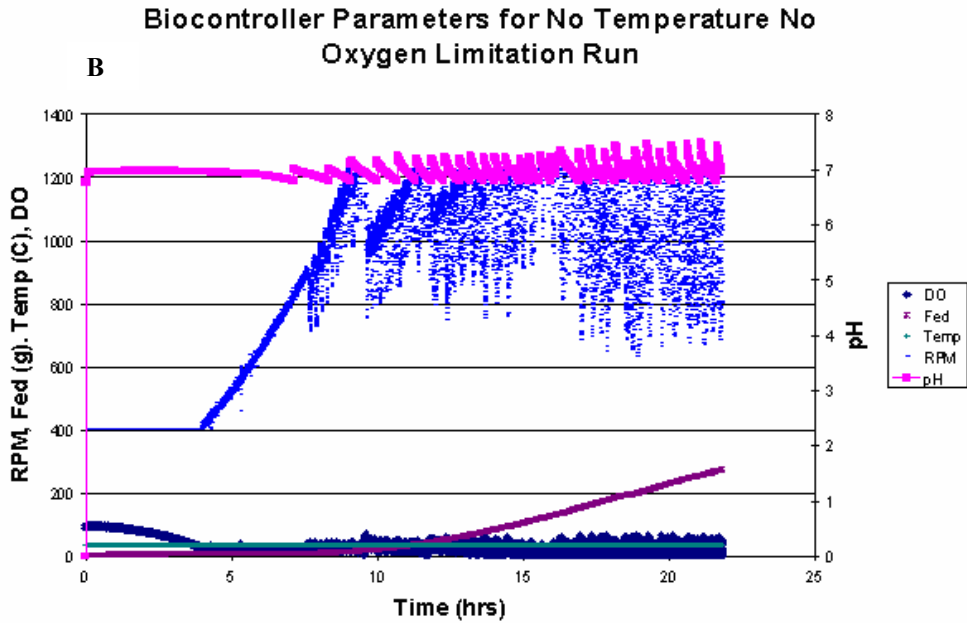
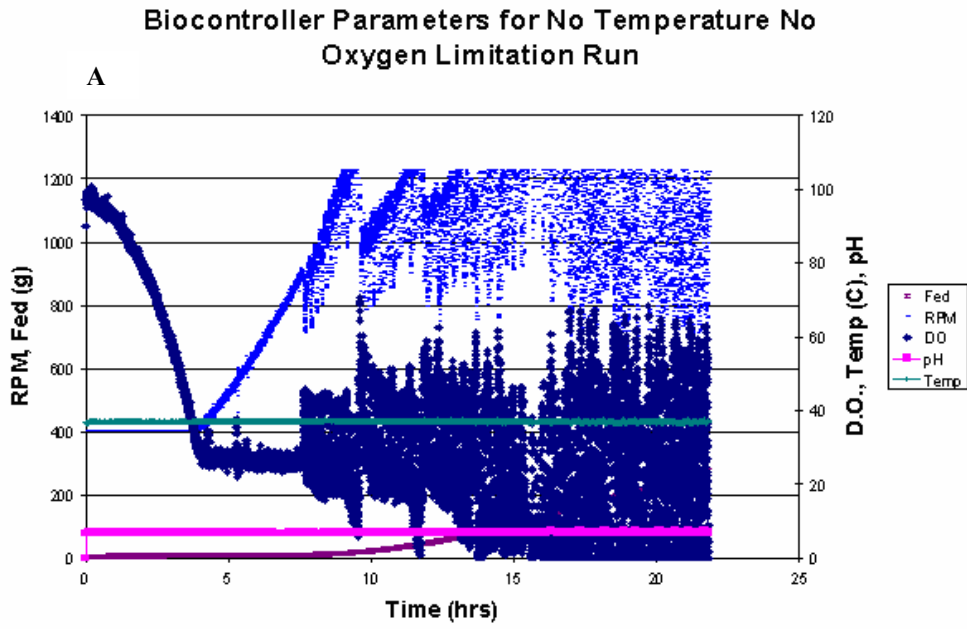


Figure 5.40: Run B Biocontroller Data. Oxygen supplementation, started at 9.6 hours, ranged from 0-100%. Pure oxygen supplementation increases variance in dissolved oxygen. Figure B, shows the increasing fluctuations in pH indicating excessive metabolic formation of acetate.

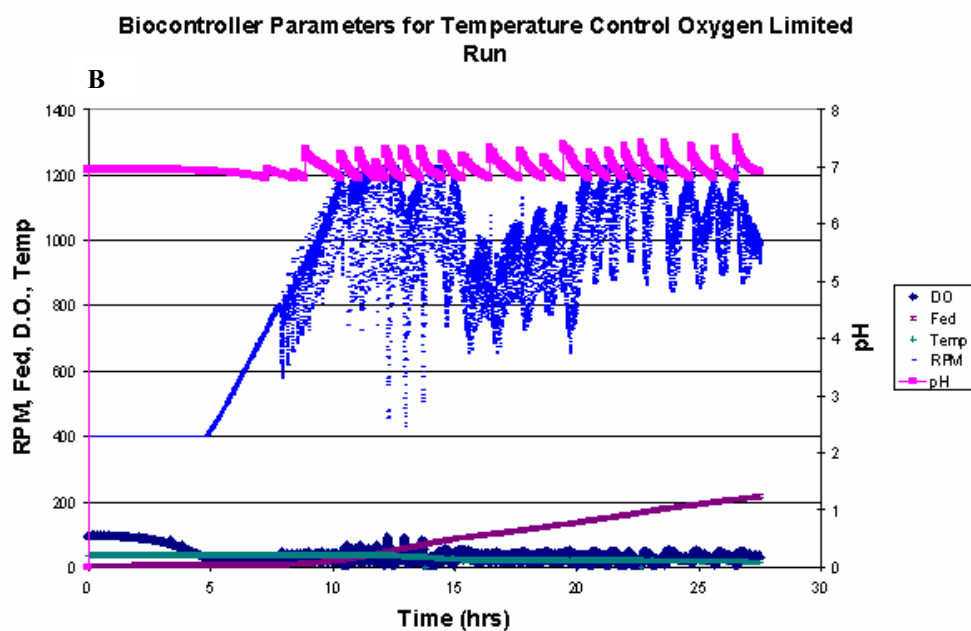
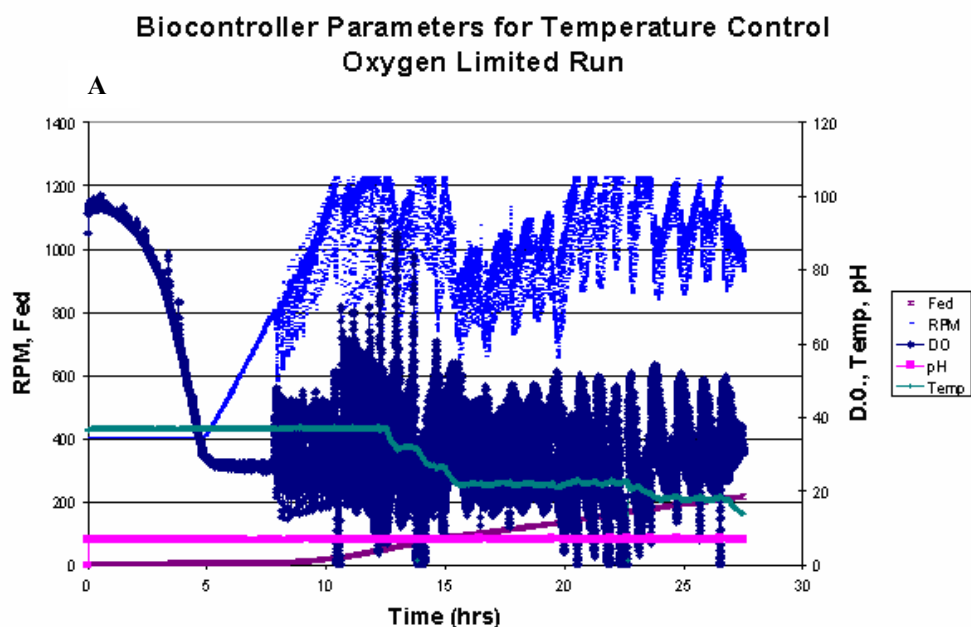


Figure 5.41: Run C Biocontroller Data. Both oxygen supplementation and temperature control were used in this run. Dissolved oxygen concentration was maintained around 30% although short periods of limitation occurred. pH fluctuated much less compared to non-temperature controlled runs. Temperature control was continued past the low set point of 22°C to explore temperature effects and system capacities for low temperatures.

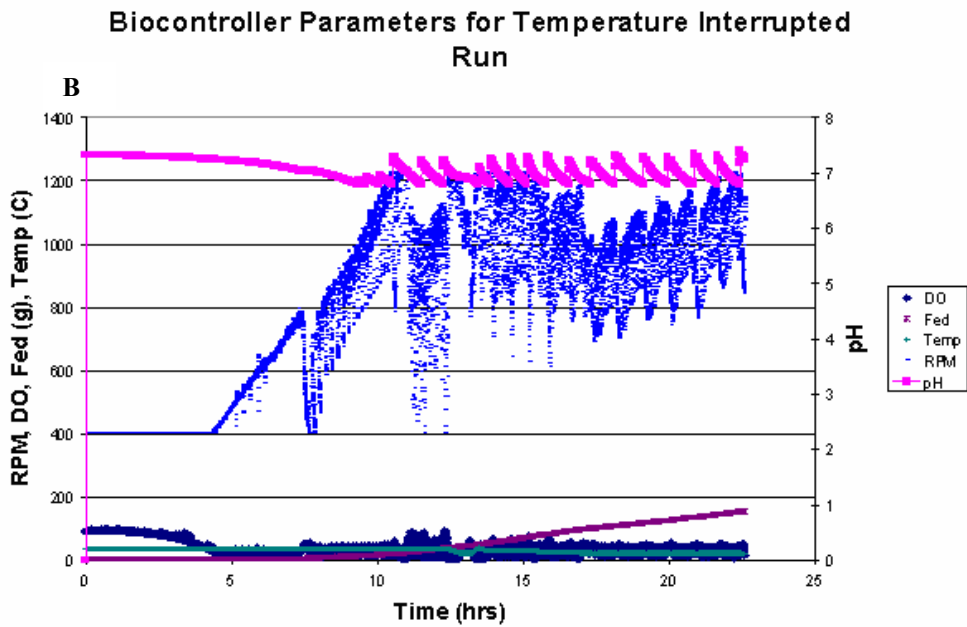
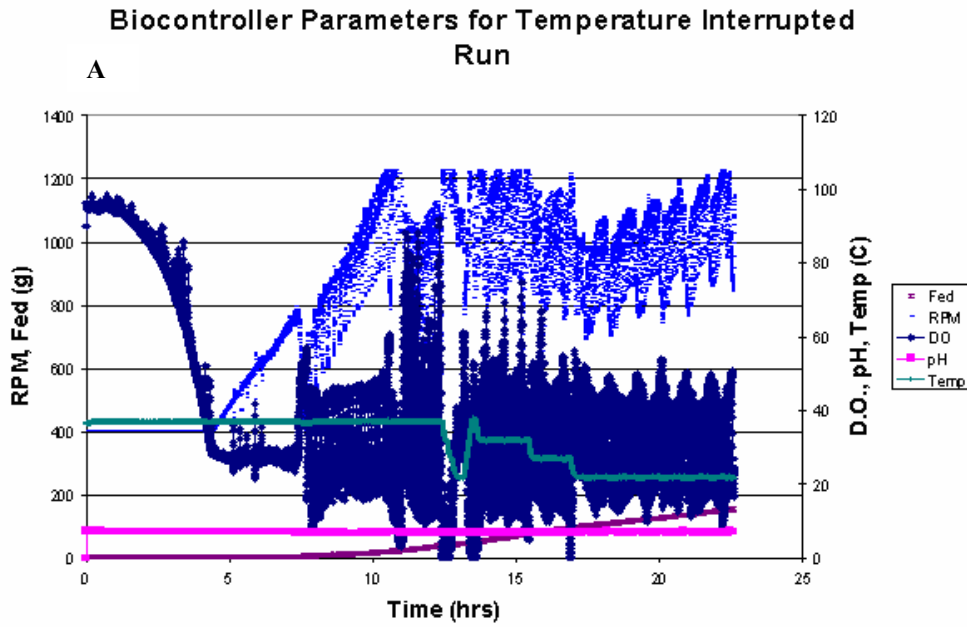


Figure 5.42: Run D Biocontroller Data. This run simulated a 45 minute oxygen supplementation failure. Temperature control was reset afterwards. Temperature came down to 22°C in three steps over a 10 hour period. pH fluctuated much less than non-temperature controlled runs and seemed to slow as the temperature decreased below 27°C.

When antifoam was added there was a direct effect reducing oxygen transfer (Figure 5.43). While this was not unexpected, it adds a complication to foaming control since the objective of most fermentations is to maintain sufficient D.O. while minimizing any potential foaming, goals which are clearly at odds (Akesson et al. 2001). In terms of the effects of both goals, the 30% oxygen limitation represents a worst case scenario since raising oxygen volumetric flowrates to reduce stirrer speeds, decrease foaming and increase oxygen transfer rates is not feasible.

**Typical Effect of Antifoam addition and pH addition.
No Temperature Control, 30% Oxygen Limitation
Experiment**

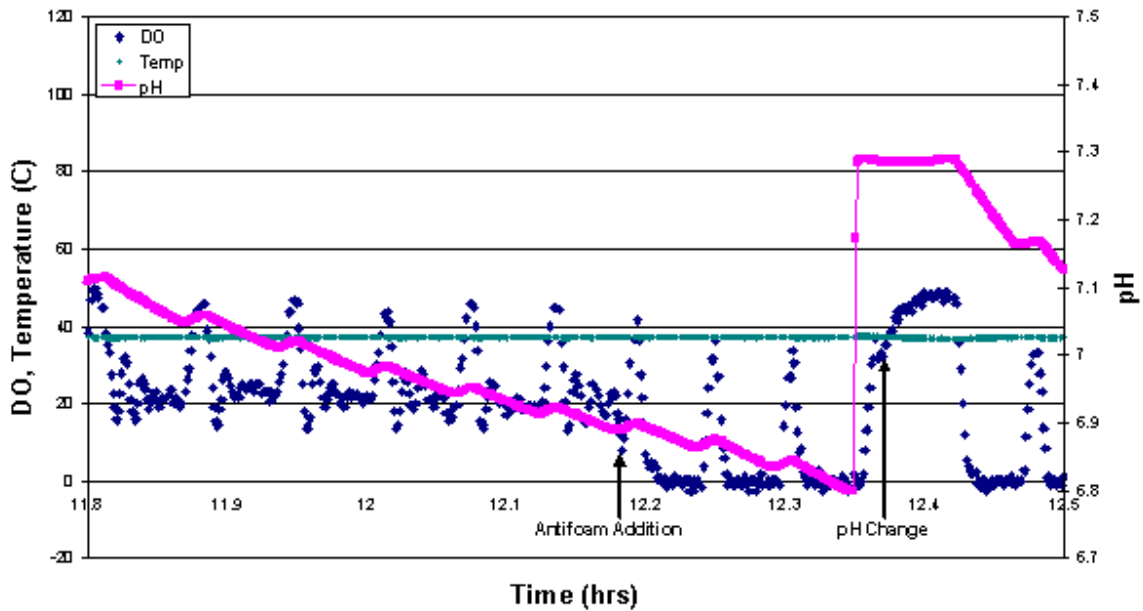


Figure 5.43: Antifoam and NH_4SO_4 addition effects during culture runs on D.O. and Temperature.

Instead foaming agent addition was timed to our advantage to coincide with pH control additions which cause a sharp spike in DO. However, at best this is a temporary benefit since oxygen transfer does not fully recover after. It is interesting to note that there is a 0.5°C change in temperature when NH_4SO_4 was added to reduce acetate and control pH.

Temperature control reduced glucose feeding to fit more closely with overall specific growth. Temperature control is one method suggested in literature to control acetate formation by overfeeding (Akesson et al. 2001). As well it is a method of ensuring aerobic protein production by decreasing growth rate. pH additions are the method used in these fermentations to control acetate formation. The use of glacial NH_4SO_4 causes an exothermic temperature spike. This is shown in Figure 5.44.

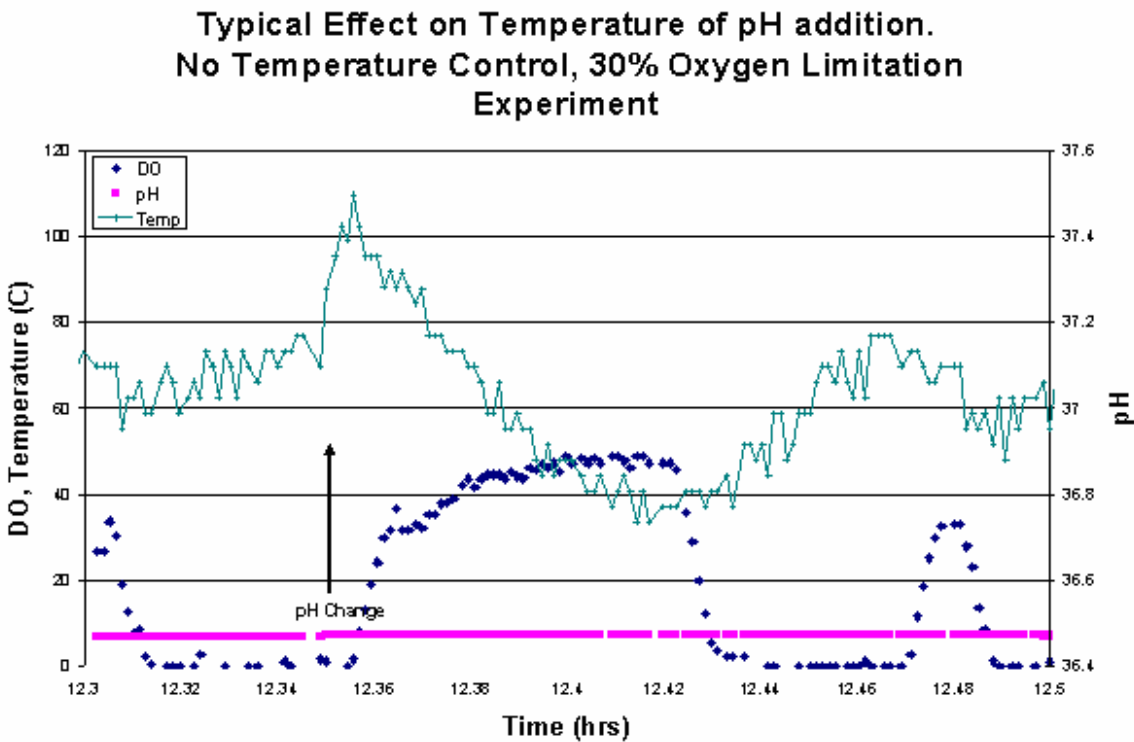


Figure 5.44: 0.5°C temperature spike caused by NH_4SO_4 addition. Moving averages was used in the temperature control programming to avoid temperature fluctuations like those caused by pH additions.

The first two non-temperature controlled runs had exponentially increasing feeding requirements near the ends of their fermentations whereas the temperature controlled runs maintained feeding profiles similar to the online growth profiles. Limited oxygen supplementation exacerbated lower $Y_{x/s}$ and lowered the final O.D.

Overall cell yields are affected by temperature reduction and oxygen limitations. Run A has a $Y_{x/s}$ of 1.60 wet cell weight the highest of all runs. This run was relatively unaffected by oxygen limitation and there was no temperature reduction. As with the shake flask it is expected that growth would be faster at higher temperatures. Optical density and glucose consumption rates shown in Figure 5.45 deviate at 14 hours at approximately 75 O.D.

Glucose Fed compared to Growth for No Temperature No Oxygen Limitation Run

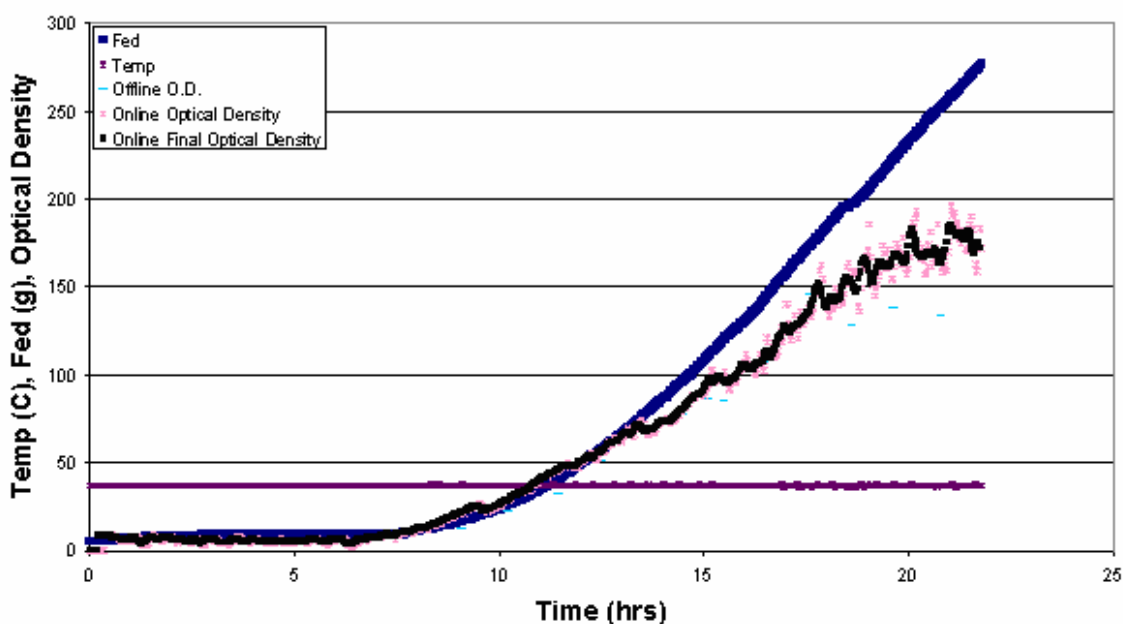


Figure 5.45: Run A glucose fed versus optical density. $Y_{x/s}$ was 1.60 for this run the highest for all the runs. The ability to provide oxygen supplementation on demand allows for higher growth at 37°C. Optical density and glucose fed deviate at 14 hours at approximately 75 O.D. but keep similar rates compared to runs with the 30% maximum oxygen supplementation.

During the initial fed-batch phase growth was near linear but around 80 O.D. growth slowed somewhat and appeared to be reaching a maxima at 107 O.D. There are two clear specific growth rate values in the culture. The early growth rate is visibly higher than the later μ value. The switch between the two values is likely caused by metabolic by-products formation and media component depletion.

Glucose Fed compared to Growth for No Temperature No Oxygen Limitation Run

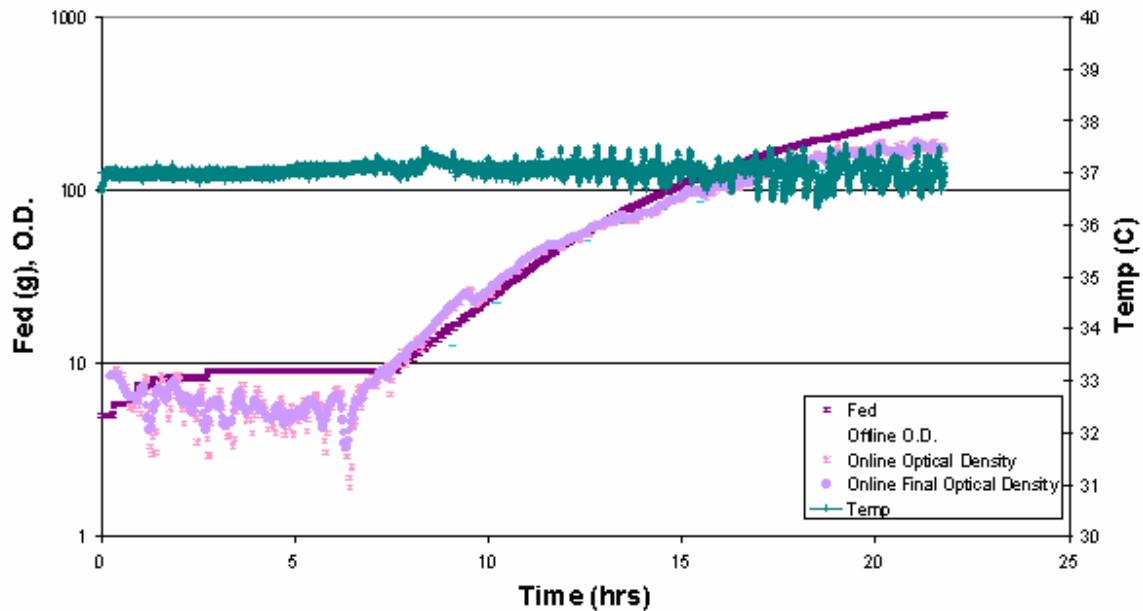


Figure 5.46: Semi-log plot of glucose fed and optical density versus temperature for Run A. During the initial Fed-batch phase the growth was almost linear. After 80 O.D. growth appeared to slow and eventually reached a maxima at 107 O.D. There appears to be a switch in growth rate around 12 hours. This is likely caused by metabolic by-product build up and depletion of media components.

Oxygen limited cultures show a deviation between the glucose feed rate and optical density much earlier in the cultures. For Run B this occurred at 13.5 hours at 55 O.D. (Figure 5.47). Optical density tapered off after 19 hours and the culture was ended. Again there appears to be two growth rates during the culture this time the switch appears to happen at 15 hours.

Glucose Fed versus Growth No Temperature Control 30% Oxygen Supplementation

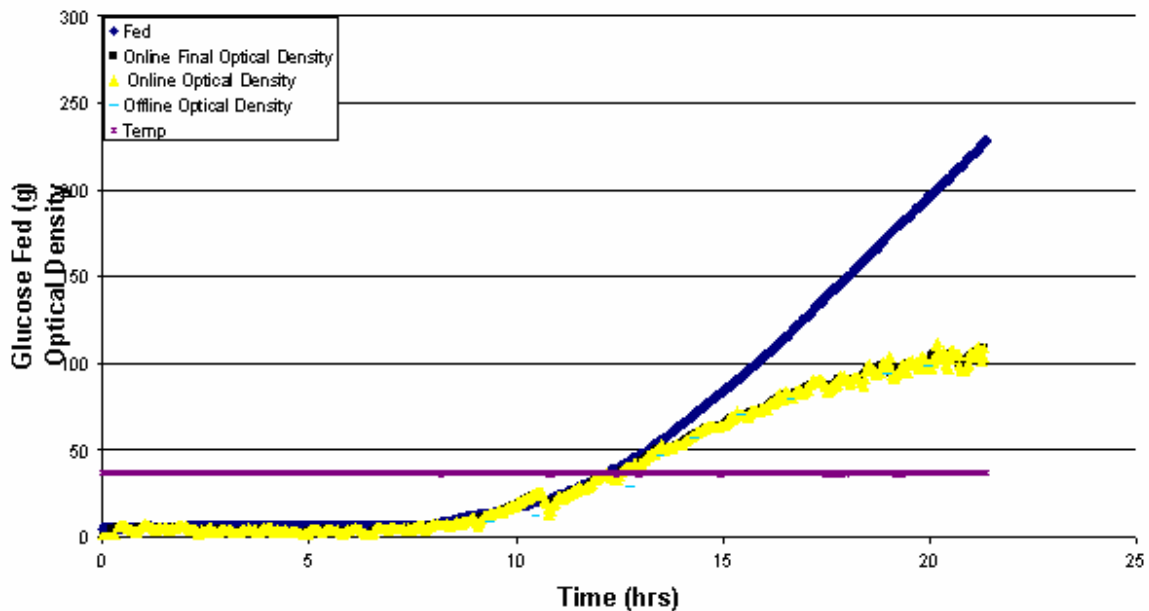


Figure 5.47: Run B glucose versus optical density. $Y_{x/s}$ for this run was 0.97 wet weight. Glucose deviated significantly at 13.5 hrs at approximately 55 O.D. after which the glucose feed rate proceeded exponentially. Optical density tapered off around 19 hours. Again there appears to be two growth rates during the culture with the switch in rate occurring at 15 hours.

Temperature remained between 36.25°C and 37.75°C for Run B (Figure 5.48). Optical density deviated from glucose fed in the early exponential Fed-batch phase of the run. Optical density during the initial Fed-batch appeared almost linear but was corrected near 12 hours after optical density had exceeded glucose fed. After the initial period, optical density followed a more exponential phase slowing near 18 hours until the end of the run.

Temperature Effect on Growth for No Temperature Control, 30% Oxygen Supplementation

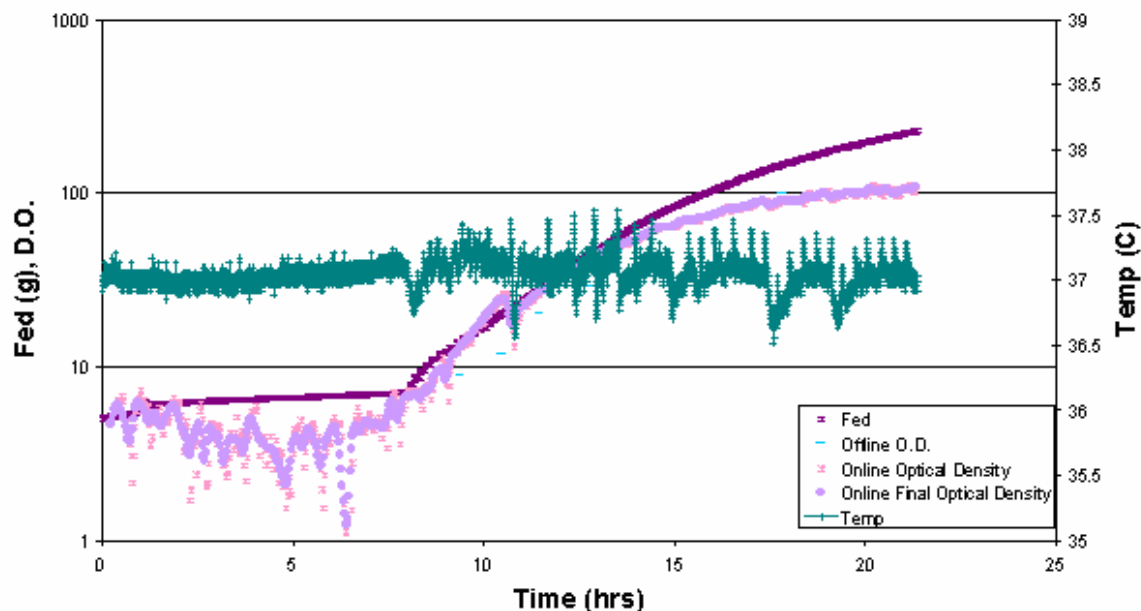


Figure 5.48: Semi-log plot of glucose fed and optical density versus temperature for Run B. Growth during the initial Fed-batch phase was higher than glucose fed rate. Near 12 hours when growth appeared to exceed glucose fed then fell and thereafter followed a more exponential rate.

Temperature control in previous runs has lead to a closer glucose and optical density rate such as those shown in the Initial Bioreactor Temperature Control Runs. Run C's glucose feed rate and optical density did deviate around 12.5 hr at 55 to 60 O.D. The yield from this run ($Y_{x/s}$ 1.48) was lower than Run A but higher than Run B.

Glucose Fed and Growth for Temperature Controlled 30% Oxygen Supplementation

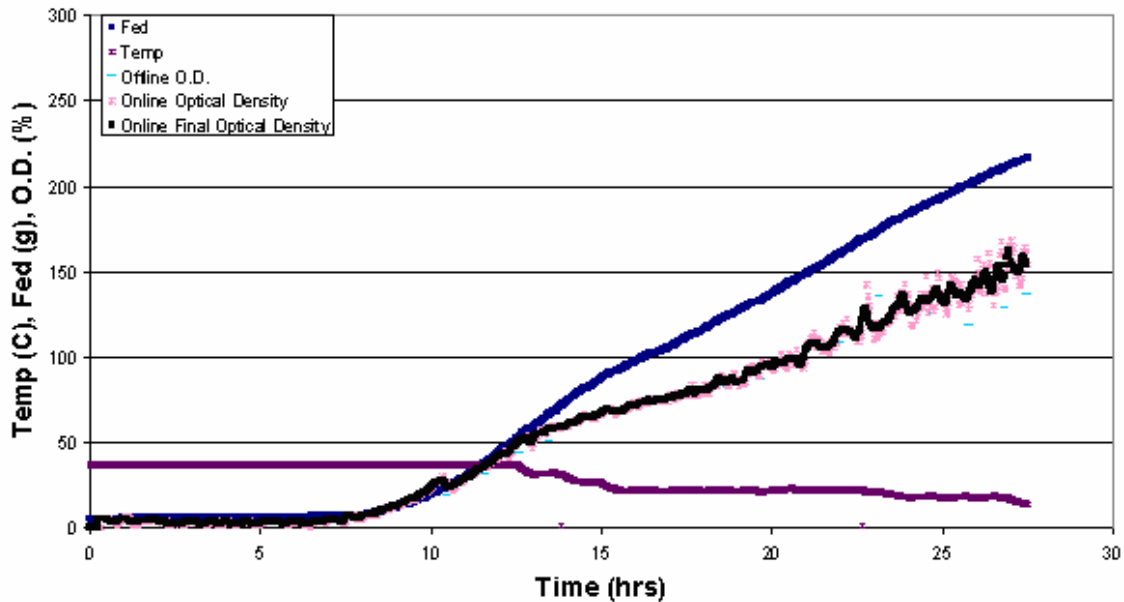


Figure 5.49: Run C glucose versus optical density. This run's $Y_{x/s}$ was 1.48 (wet weight). Interestingly, the glucose and optical density deviated around 12.5 hours at approximately 55 to 60 O.D. There was a rate change in glucose feeding between 14 and 15 hours around the time that the culture reached 22°C.

Optical density plotted on a semi-log plot (Figure 5.50) showed a downward trend quickly in Run C. This to be due to protein production or an adverse response to temperature reduction. Temperature varied near the end as the Pelletier cell had a difficult time maintaining enough flow to allow the temperature to drop. It was necessary to increase the pump speed of the Pelletier cell to maximum in order to achieve the temperatures required. As the temperature decreased there appeared to be a decrease in the growth rate.

**Temperature Effect on Growth and Glucose Fed for
Temperature Control, 30% Oxygen Supplemented**

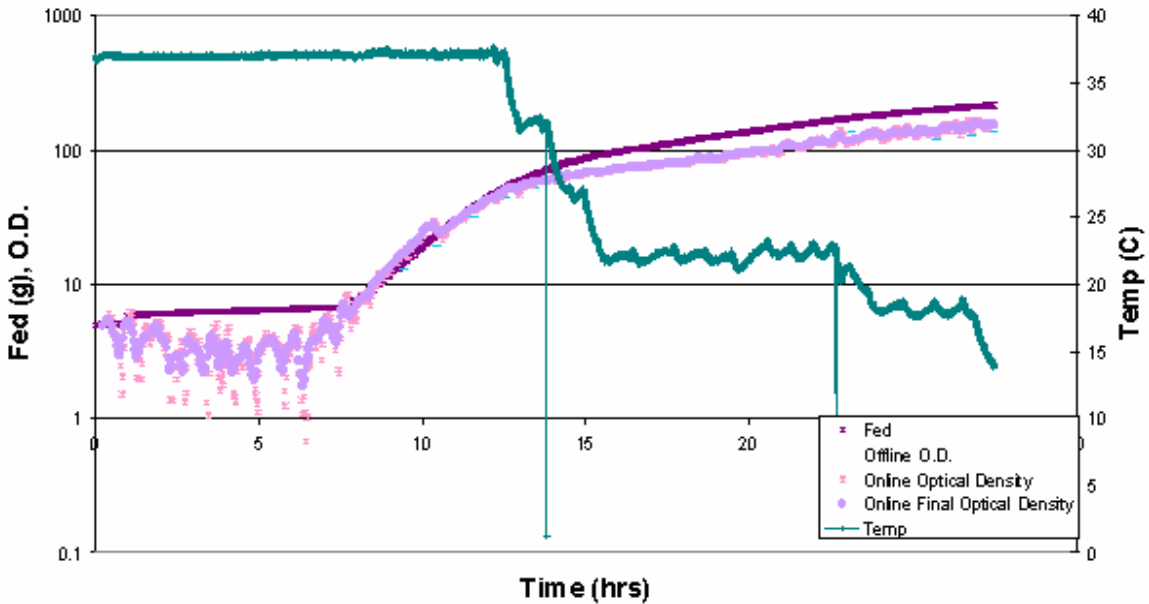


Figure 5.50: Semi-log plot of glucose fed and optical density versus temperature for Run C. Optical Density appeared to decrease at each temperature decrease but was greatest during the first temperature change. With each change in temperature there appears to be a decrease in the growth rate.

For Run D the $Y_{x/s}$ is unknown due to lost data. However, for this run optical density and glucose fed both seem fairly similar although in the later stages of the run at 15 there was a slight deviation (Figure 5.51).

Glucose Fed and Growth for Interrupted Temperature Run

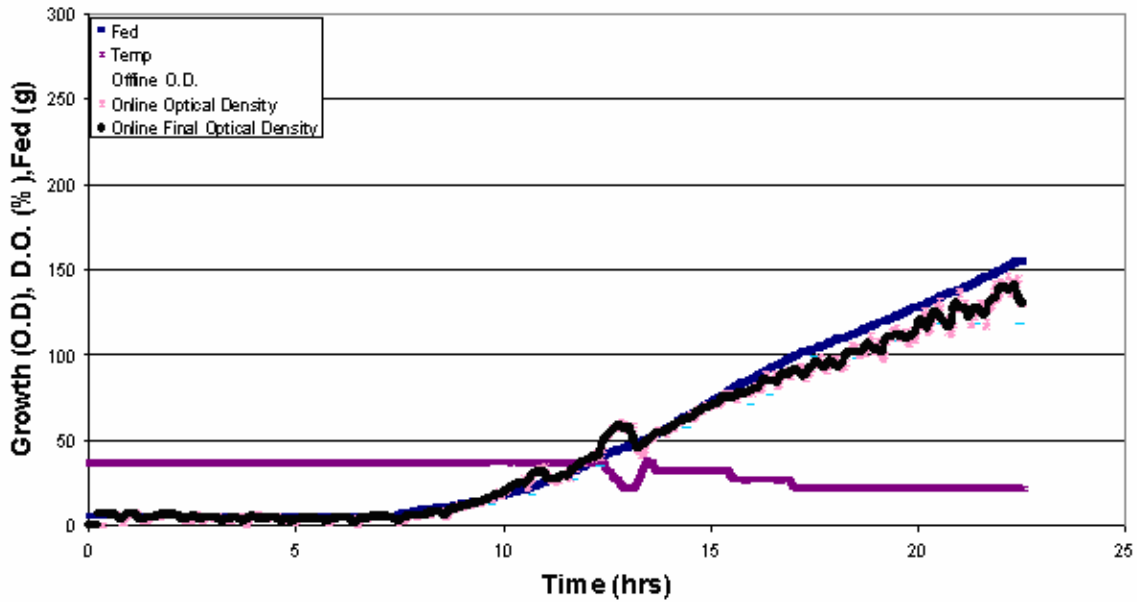


Figure 5.51: Run D glucose versus optical density. $Y_{x/s}$ is unknown since final cell weights were unknown. Glucose fed rates and optical density rates appeared to be fairly similar and follow the same course until 15 hours. Even after this the optical density rate and glucose rate appear fairly similar.

During Run D, the glucose fed and optical density plots were exponential with the rates decreasing after the simulated oxygen supplementation failure. Again temperature appears to be correlated to growth rate.

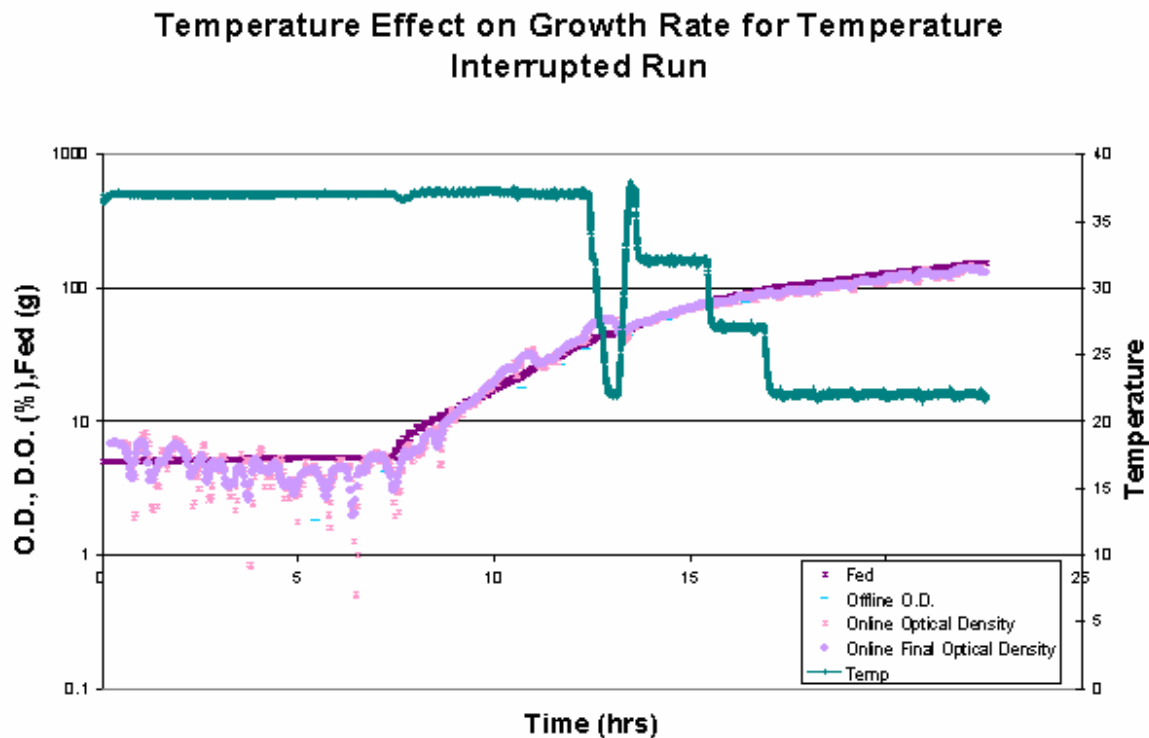


Figure 5.52: Semi-log plot of glucose fed and optical density versus temperature for Run D. Glucose fed and optical density were exponential with the rates decreasing after the simulated oxygen failure and temperature decreases.

The temperature controlled run came to nearly the same final optical density as the no controls run but took approximately 6 hours longer and required nearly 60 grams less glucose. Run D required 122g less glucose and reached 21 O.D. higher than Run B in nearly the same amount of time without the oxygen limitations seen in Run B. Final conditions are summarized in Table 5.7.

Table 5.7: Final Values for Temperature Control Experiments.

	Glucose (g)	Offline O.D.	Online O.D.	Fermentation Time (hrs)	Final Cell Weights (g)	Y_{x/s}
A	228	144	172	21.3	364	1.60
B	277	107	109	21.8	270	0.97
C	217	137	154	27.5	322	1.48
D	155	118	130	22.5	-	-

As the temperature lowered there was a noticeable change in the morphology of the *E. coli*. The *E. coli* was easily initially centrifuged but as temperature dropped became white and fluffy to the eye. The *E. coli* in late temperature controlled cultures was harder to centrifuge.

All the runs had several events in common such as adding antifoam (A.F.), induction (IPTG), glucose bottle changes (Glucose), clearing blocked sparger pores (HCl), and changes to the air and oxygen rotameter settings (air/oxygen).

During Run A, it was necessary to unblock the sparger using 10% HCl in order have uninterrupted airflow. Several times oxygen content was raised until finally at 14.01 hrs pure oxygen was pumped into the vessel at 5L/min.

Culture Events for No Temperature No Oxygen Limitation Run

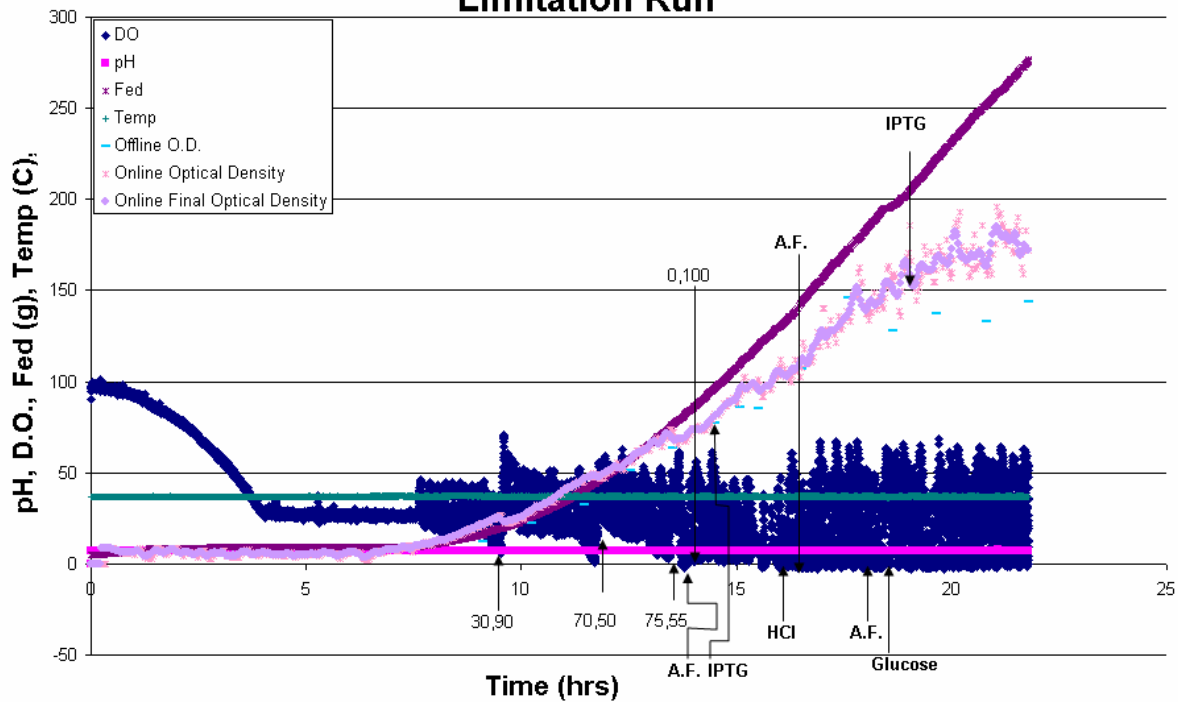


Figure 5.53: Events for Run A. At approximately 16 hours it was necessary to clear the sparger using 10% HCl. IPTG was induced at 75 O.D. and 150 O.D. During the culture it was necessary to change the glucose bottle at 18 hrs.

Run B was relatively uneventful. Antifoam was added four times as necessary. The culture was inoculated sooner than usual because of worries about the significant lag the culture showed compared to Run A.

Culture Events for No Temperature Control 30% Oxygen Supplementation

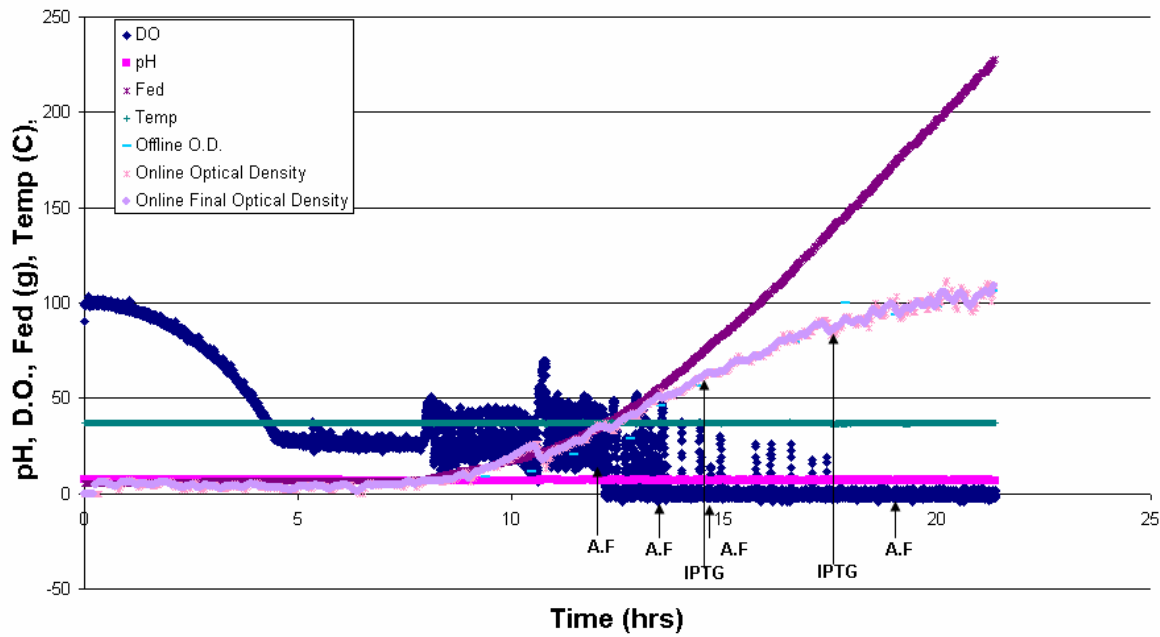


Figure 5.54: Events for Run B. Run B was relatively uneventful. Once oxygen supplementation began antifoam was added at regular intervals during the culture. The culture was inoculated at 55 O.D. due to worries about the culture’s apparent lag in reaching 75 O.D. As per procedure the culture was induced a second time at 80 O.D.

Run C had several additions of antifoam as a preventative measure with consideration of the effect that antifoam has on dissolved oxygen. IPTG was added to the culture at 75 and 125 O.D. It was necessary to change the glucose bottle during the experiment causing a slight delay in the glucose feed and a short period of no change in optical density.

Culture Events for Temperature Control Oxygen Limited Run

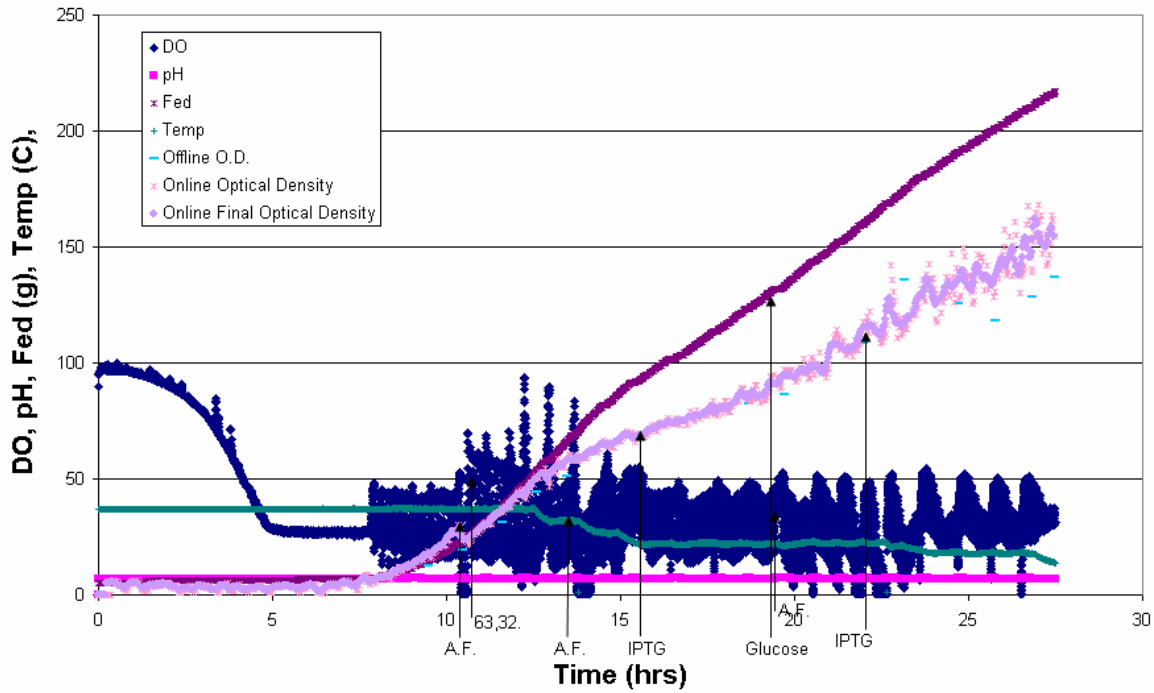


Figure 5.55: Events for Run C. Antifoam was added to the culture three times in order control foam. Antifoams additions were minimized to avoid lowering dissolved oxygen in the culture. IPTG was added at 75 and 125 O.D.'s according to set procedures. A slight delay in optical density can be observed during the glucose bottle change.

Run D's simulated an oxygen failure was chosen to occur at point in the run where oxygen demand did not exceed supply so that the culture could recover after (Figure 5.56). The simulated length of time was approximately 45 minutes as this was found to be a reasonable amount of time in the shake flask runs and did not affect the overall growth endpoints or culture lag time.

Culture Events for Interrupted Temperature Run

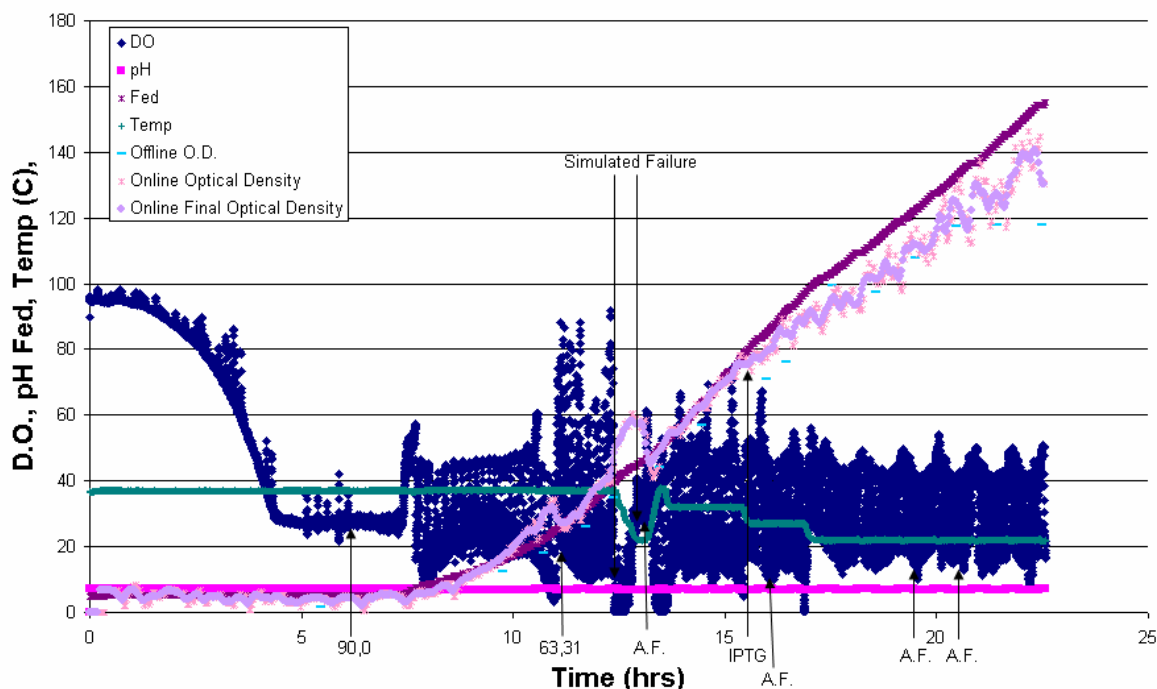


Figure 5.56: Events for Run D. Four antifoam additions were made during the run. Oxygen supplementation was started around 12 hrs. The simulated failure occurred around 13.5 hours and lasted 45 minutes.

5.4.3 Protein Production Information

There is again little evidence that induction increased recombinant production of proteins at the expected 30 kDa band. With the exception of Run B, the bands surrounding the 30 kDa standard do not appear to be affected at all and remain constant during the runs. Run B seems to show an increase in the amount of protein in the 30 kDa range at 10.48 and 11.45 hrs, although this is not entirely clear due to imaging problems. This does not correspond to the induction period at 14.6 hr. Nor does it appear to be increasing from time period to time period. Unfortunately, recombinant protein production during these temperature control run was also very low. Again this is confusing since the vector was present since the cells grew in selective conditions.

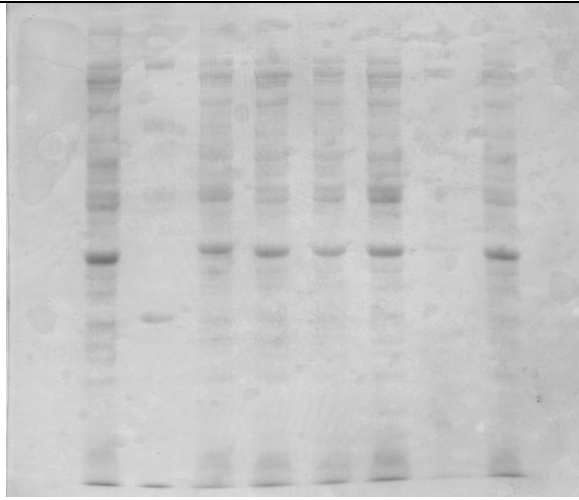


Figure 5.57: Gel 1 Run A

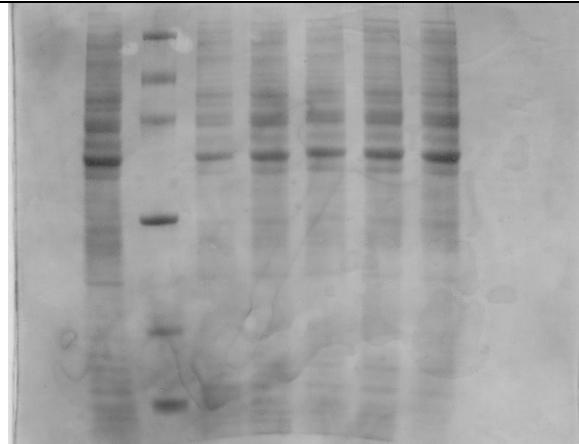


Figure 5.58: Gel 2 Run A

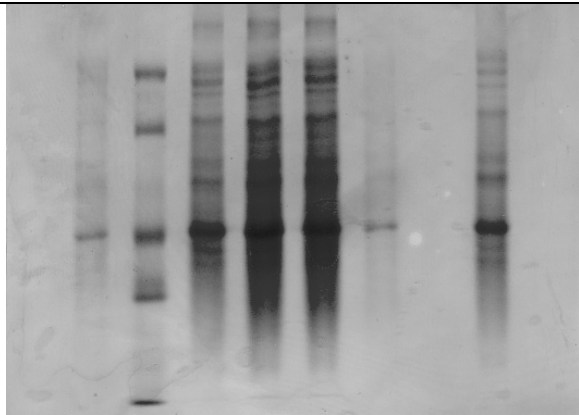


Figure 5.59: Gel 1 from Run B

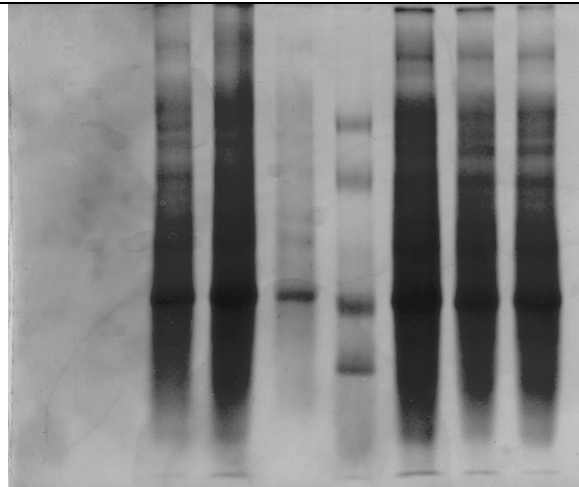


Figure 5.60: Gel 2 from Run B

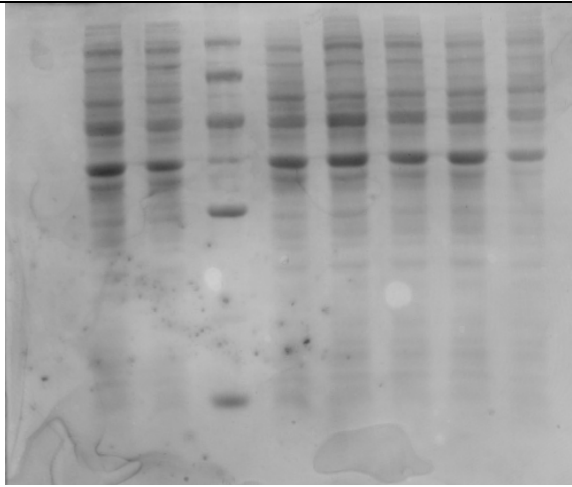


Figure 5.61: Gel 1 Run C

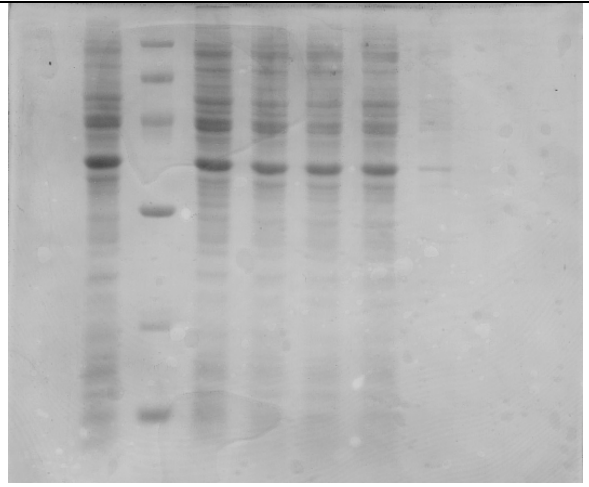


Figure 5.62: Gel 2 Run C

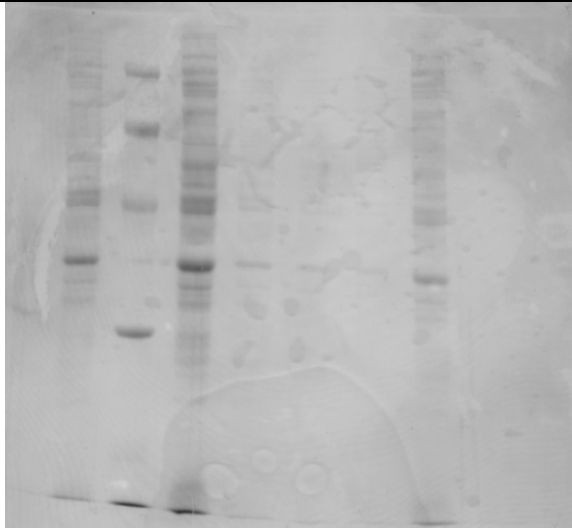


Figure 5.63: Gel 3 Run C

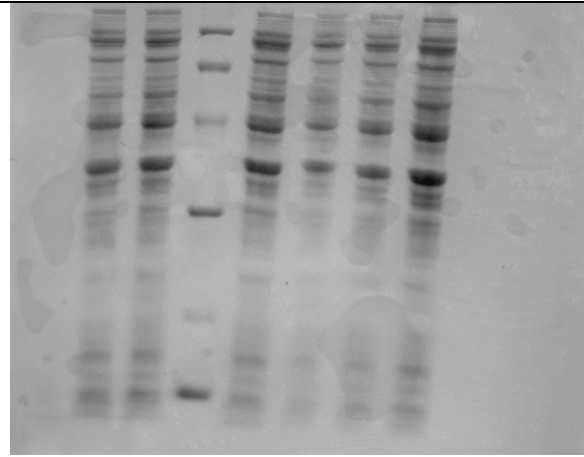


Figure 5.64: Gel 1 Run D

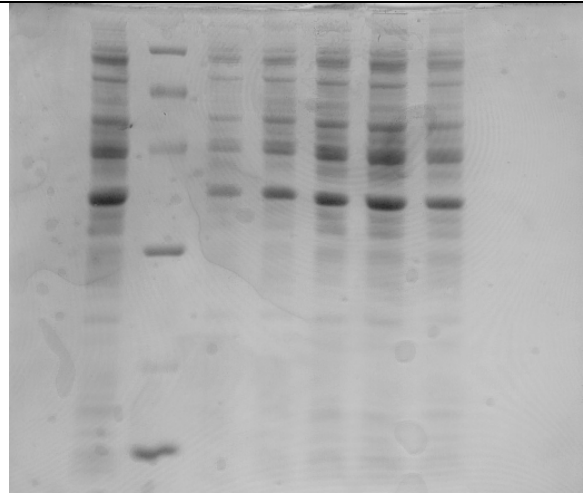


Figure 5.65: Gel 2 Run D

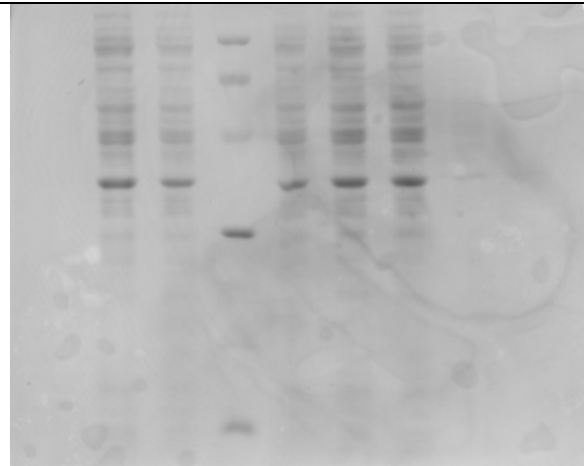


Figure 5.66: Gel 3 Run D

Table 5.8: Key for SDS PAGE figures for Temperature Control Run

		Lanes									
	GEL	1	2	3	4	5	6	7	8	9	10
Run A	Gel 1	-	9.09	std	10.24	11.44	12.53	13.52	14.50	15.08	-
	Gel 2	-	16.5	std	17.58	18.62	19.64	20.80	20.8	-	-
Run B	Gel 1	-	9.38	std	10.48	11.45	12.78	12.78 overrun	-	13.50	-
	Gel 2	-	14.33	15.47	16.67	std	17.82	19	19.98	-	-
Run C	Gel 1	-	9.46	10.46	std	11.58	12.58	13.46	14.46	15.54	-
	Gel 2	-	16.07	std	16.56	17.61	18.67	19.68	20.78	-	-
	Gel 3	-	21.97	23.13	std	24.69	25.77	26.81	27.46	-	-
Run D	Gel 1	-	5.44	7.22	std	8.60	9.74	10.71	11.71	-	-
	Gel 2	-	12.36	std	13.44	14.44	15.44	15.98	16.44	-	-
	Gel 3	-	17.54	18.54	std	19.49	20.44	21.41	22.47	-	-

* Time in Hours

5.5 Purifications

5.5.1 Introduction

Early in the fermentation experiments it was recognized that it would be necessary to have purified eYFP in order to quantify the protein production from temperature controlled fermentations. To this end several purifications were run. One such experiment involving metal ion affinity chromatography is discussed and analyzed below.

5.5.2 Ni²⁺ Purification

As the eYFP was to be expressed with a HIS6 affinity tag it followed that the first purification step should be a Ni²⁺ resin in a small column. Several purifications using procedures described in Chapter 4 were run however a larger purification run on 28 August 2006 using cells obtained in the 14 Apr 06 temperature control run will be shown as an

illustrative example of Ni²⁺ purifications run on cell samples obtained from these fermentations.

General Purification Scheme Data for 28 August 2006 Ni²⁺-NTA Affinity Purification		
Column Size	5	mLs
Amount of Cells	30.01	g
Cracking Efficiency	59	%
Lyses Device	High Pressure Homogenizer	

After cell lyses it was decided that the supernatant would be purified on the column in order to simplify the procedure and to avoid having viscosity problems frequently associated with denature/renature procedures.

Protein Concentrations by Bradford for 28 Aug 06 Ni Affinity Purification

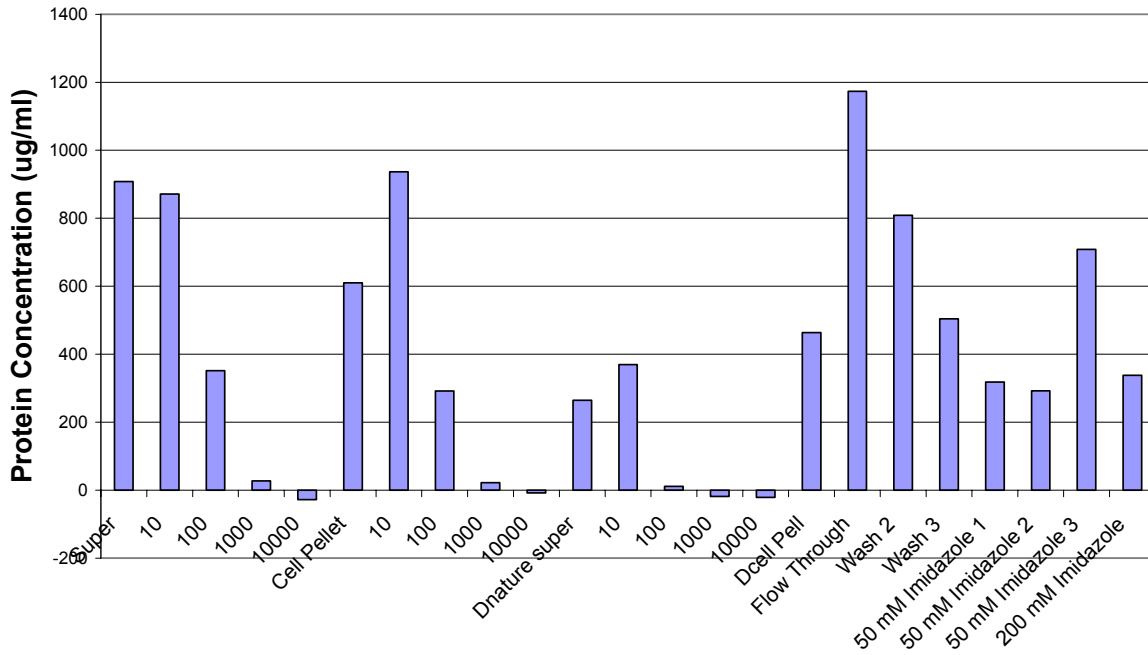


Figure 5.67: Protein Concentrations for 28 Aug 06 Purifications

Several of the protein concentrations were below the reported detectable limits of the Bradford method (Figure 5.67). Flow through and wash samples show decreasing concentrations of protein as expected since unbound protein should be easily washed off the column. The 2 column volumes of 50mM imidazole wash was evenly divided into 3 parts and showed a continuing decrease in protein concentration until near the end of the final wash where loosely bound protein was eluted from the column. The 200mM imidazole wash released all bound proteins from the column and had a protein concentration less than the final 50mM imidazole wash leading to a worrying conclusion that the eYFP may have already been eluted partly in the 50mM imidazole wash.

The SDS PAGE gel (Figure 5.68) ran afterwards lacked an identifiable band for the recombinant protein around the 30kDa marker, however there was an increasingly

concentrated band around 26 -28 kDa. While lower than expected, it was possible that this may be the protein of interest.

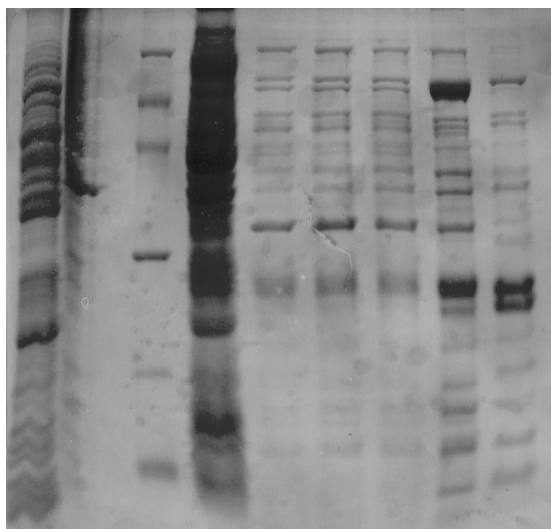


Figure 5.68: Purification Gel from 28 Aug 06 Ni²⁺ Affinity Purification (5 uL loadings)

Table 5.9: Key for 28 Aug 06 Ni²⁺ Affinity Purification Gel

Lanes									
1	2	3	4	5	6	7	8	9	10
Super	Cell Pellet	STD	Flow Through	Wash (3)	50mM Imidazole Wash (1)	50mM Imidazole Wash (3)	50mM Imidazole Wash (3)	200mM Imidazole Wash (1)	-

More troubling was the unexpected fluorescence values obtained when samples were diluted in a log fold manner (Figure 5.69) and measured using excitation wavelength of 515 nm, emission wavelength 535 nm and a cut off of 530 nm. It is expected that sample fluorescence decreases with log fold dilutions when plotted on a semi log plot or log-log plot. This unexpected result lead to several attempts to find a linear range to quantify eYFP between 1250 and 10000 fold dilutions. This range was not found and further reinforced the conclusion that problems existed with eYFP expression.

**Supernatant Fluorescence for 5 fold serial dilutions of Nickel
Affinity Purified Protein from 28 Aug 06
(ex. 515 nm em. 535 nm Cut 530 nm)**

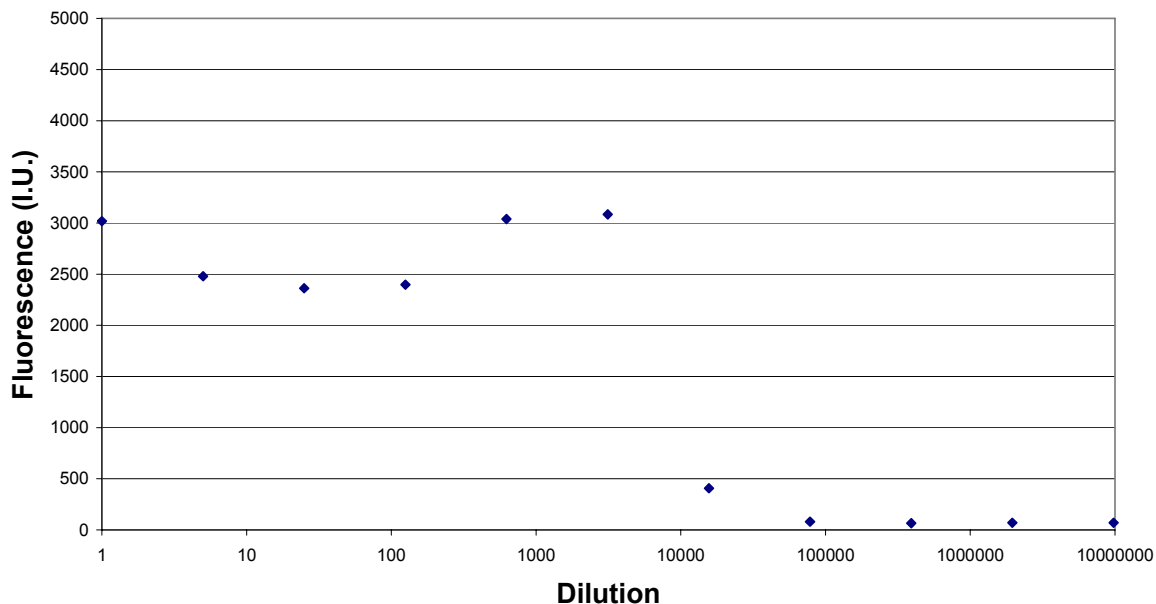


Figure 5.69: Fluorescence measurements using microwell plate reader. No linear range was found between 1250 and 12000. This was further evidence that problems existed with the eYFP expression.

5.5.3 Denature-Renature Experiments

In order to determine whether the protein was simply misfolded and in an inclusion body. It was decided to denature the protein in 8M urea and renature it by dialyzing the Urea back out. To achieve this, dialysis of a 10 mL sample was done over 24 hours with 3 1L buffer exchanges with decreasing Urea concentrations ending with 100mM Tris-HCl (pH 7.0), 100mM NaCl buffer.

Figure 5.70 shows a band around the 30 kDa molecular weight standard shown in both the cell pellet and supernatant after homogenization. eYFP falls in this band.

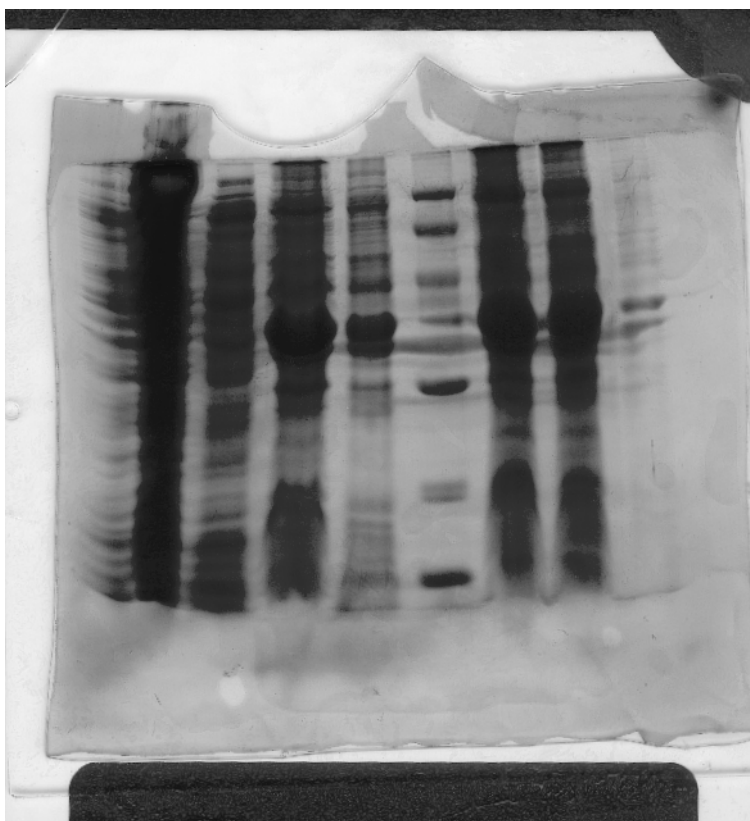


Figure 5.70: SDS PAGE gel for Denature Renature Experiment

Table 5.10: Key for Renature-Denature SDS PAGE

Denature Renature SDS PAGE Gel	
1	-
2	Supernatant After Homogenization (13 uL)
3	Supernatant After Homogenization Diluted 10X (15 uL)
4	Cell Pellet After Homogenization (16 uL)
5	Cell Pellet after Denaturation (16 uL)
6	LMW Standard
7	Dialyzed Denatured Protein (12.5 uL)
8	Dialyzed Denatured Protein (10 uL)
9	Renatured Protein (20 uL)
10	-

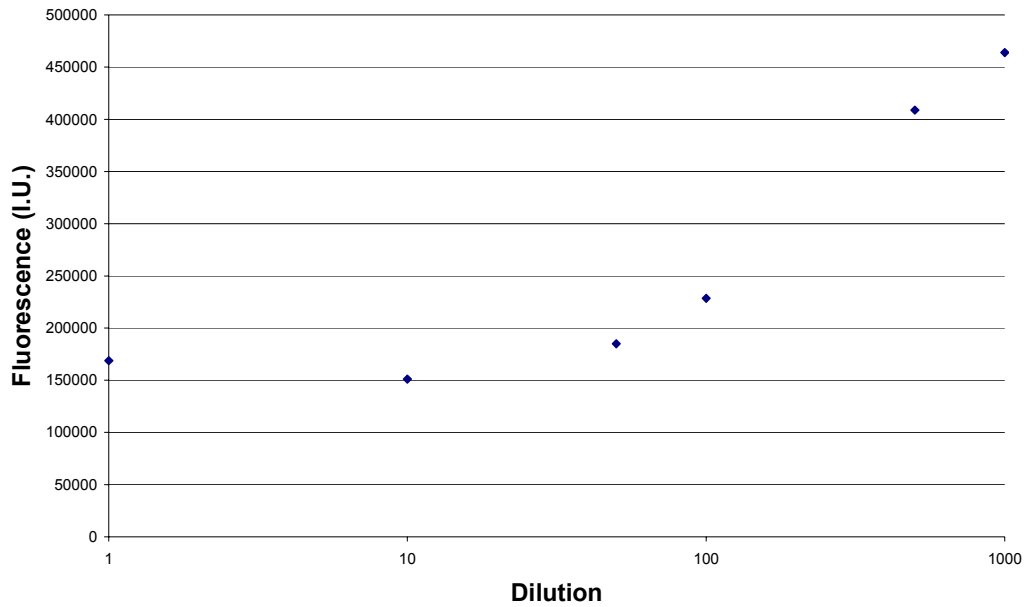
When the renatured protein is compared in concentration and fluorescence signal to the homogenized pellet it appears that fluorescence is lost slightly after renaturation (Table 5.11). From literature it is known that fluorescence indicates chromophore formation and it is expected that renaturation would cause a loss in fluorescence.

Table 5.11: Fluorescence and protein concentration of renatured protein versus homogenized protein. The homogenization pellet showed much higher fluorescence than the renatured protein indicating some fluorescence losses during renaturation. The renatured protein was more concentrated than the homogenized pellet by 300 µg/ml.

	Fluorescence (I.U.)	Protein Concentration (µg/mL)
Homogenization Pellet	206900	1230
Renatured Protein.	168200	1570

To determine more conclusively whether the protein of interest was eYFP several dilutions of the supernatant (which also had a 30 kDa band indicating soluble protein at this molecular weight) was prepared over the expected linear range of 1-1000 fold dilutions. When analyzed using a microplate however the linearly decreasing relationship expected was not seen (Figure 5.71).

Fluorescence For Undenatured Supernatant Dilutions



Protein Concentrations by Bradford Assay for Supernatant Dilutions

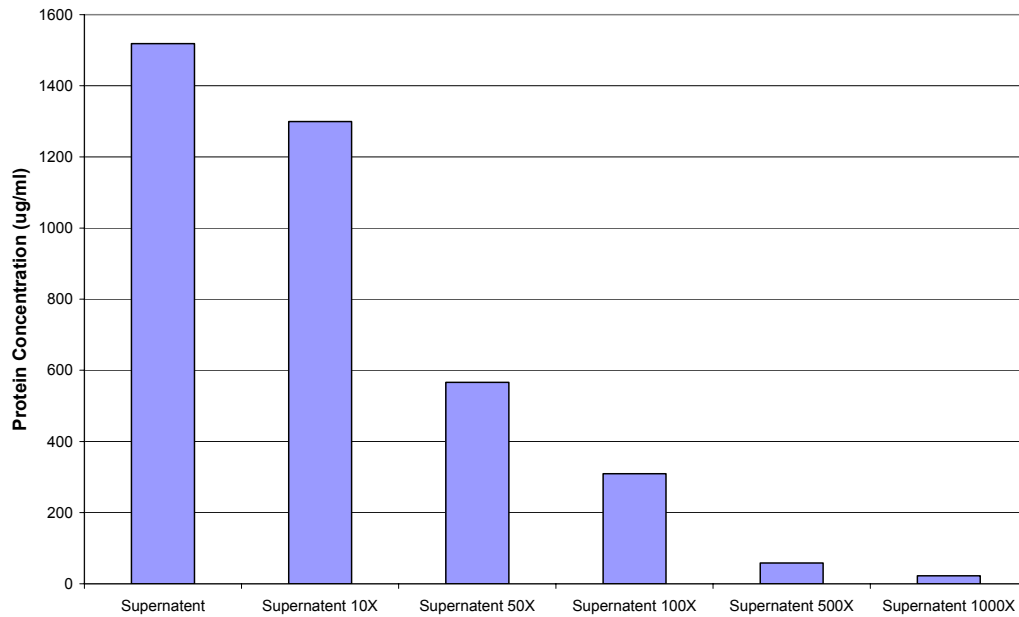


Figure 5.71 Fluorescence and protein concentrations for supernatant dilutions from Denature-Renature Experiment. The dilutions appeared to follow an exponential decrease in protein concentration but an increase in Fluorescence.

Adding to the confusion was the expected decrease in protein concentrations with each dilution. This could indicate an inner filter effect however careful review of literature (Chapter 4) reveals that this is not a problem reported with GFP or its variants in *E. coli* lysate.

5.5.4 Fluorescence Spectra Inconsistencies

The inability to repeat experiments run in literature and the discrepancies between the data from all runs lead to more generalized search for any fluorescent species in the supernatant of homogenized cell pellets. Several experiments using fluorescence spectrometers available in Engineering, Cary Eclipse (Varian Mississauga, ON), and Chemistry, QuantaMaster™ Model QM-4/2005, (Photon Technology International London, ON) lead to similar excitation and emission profiles. A scan done for excitation and emission profiles with a slit width of 1 nm gives excitation and emission values shown Figure 5.72 and expanded in 3D in Figure 5.73.

Excitation and Emission Peak of Produced Protein

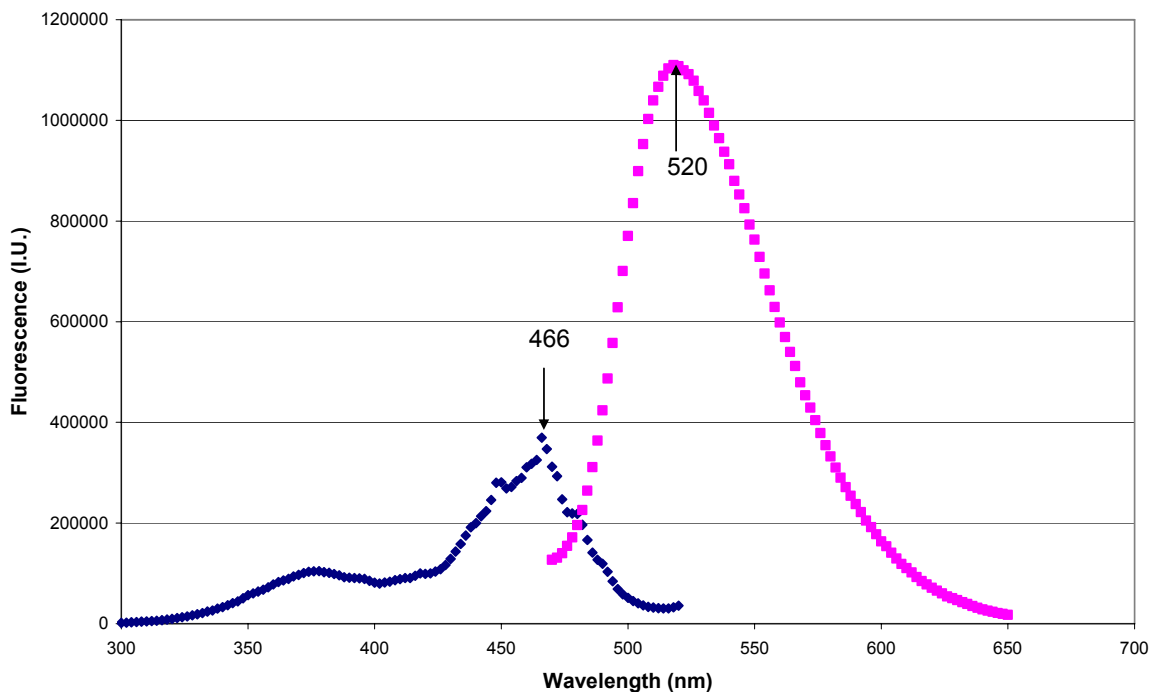


Figure 5.72: Excitation and Emission Spectra for protein produced in July 15th run Chemistry fluorescence spectrometer in 100mM Tris-HCl, 100mM NaCl (pH 7.0). The emission maxima was 520nm and the excitation maxima was 466 nm.

3D fluorescent plots of the protein show several maximas for both the emission and excitation with the peaks show in Figure 5.72. The 3D plot of fluorescence emission from produced protein showed a maxima at 524 nm for the 448 nm excitation and a smaller shoulder at 520 nm at 466nm excitation.

3D Plot of Fluorescent Emission from Produced Protein

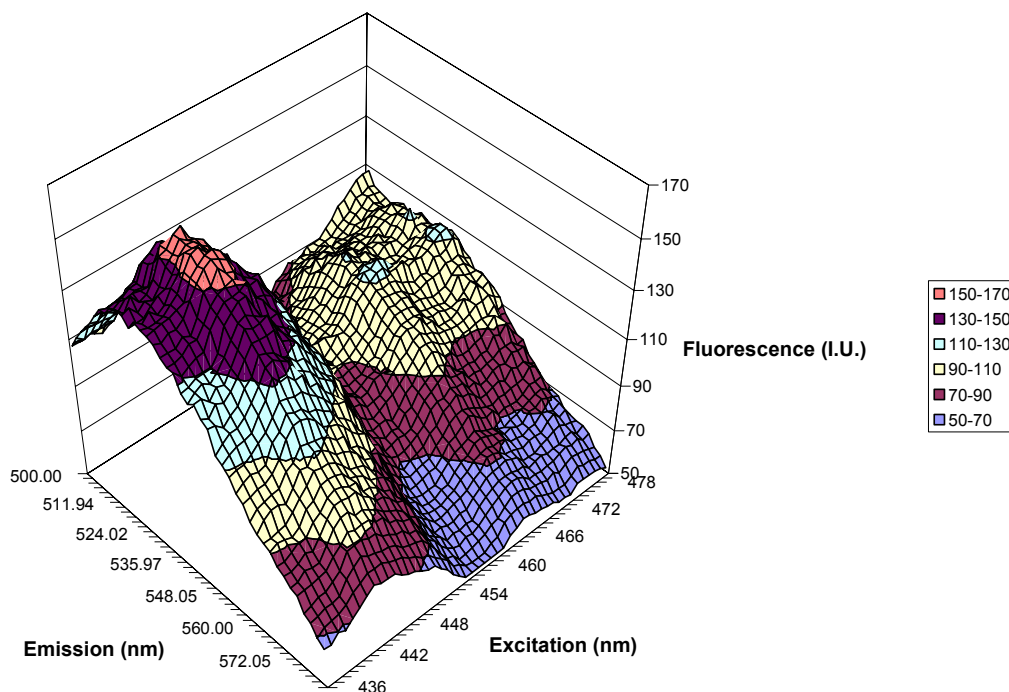


Figure 5.73: 3D Plot of Fluorescence emission for produced protein. There are several emission peaks but the maximum occurs at nearly 448 nm excitation and 524 nm emission. 100mM Tris-HCl, 100mM NaCl (pH 7.0).

The 3D plot of excitation showed several excitation peaks (Figure 5.74). The scans for these peaks were necessarily narrower than emission scans. Excitation maxima occurred at 448 nm but another peak was suggested at 468 nm. When these values were originally found, it was determined that they corresponded to no known emission and excitation maxima pairs for fluorescent proteins.

3D Plot of Fluorescent Excitation for Produced Protein

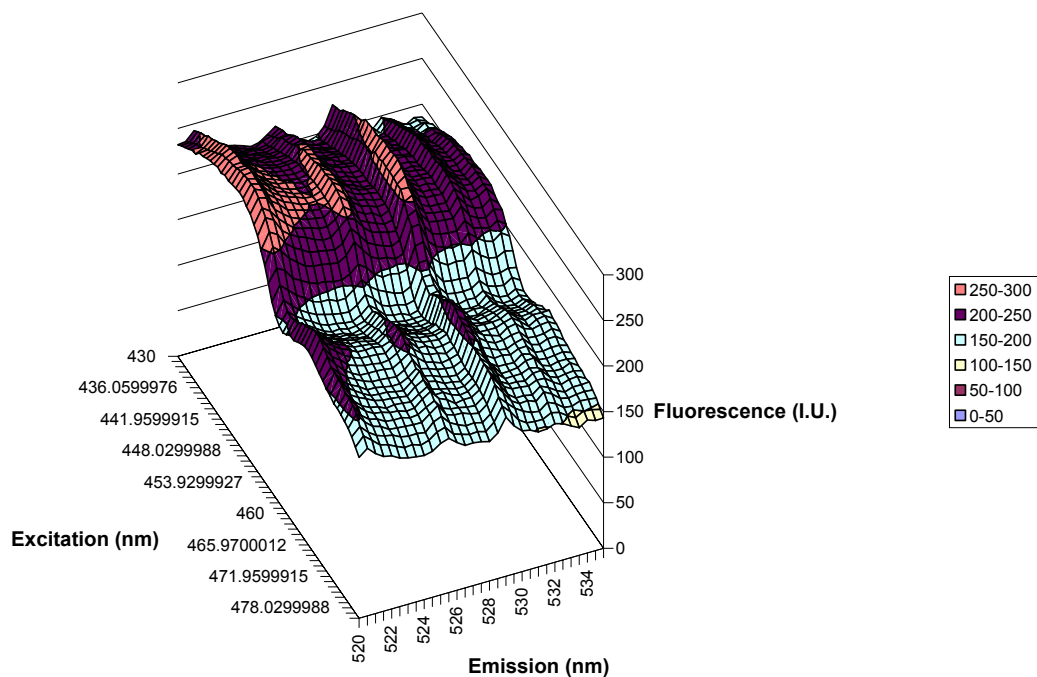


Figure 5.74: 3D Emission and Excitation Profile for Produced Protein from Engineering Fluorescence Spectrometer. 100mM Tris-HCl, 100mM NaCl (pH 7.0).

Samples run with an emission wavelength of 468 nm and an excitation wavelength of 520 nm showed a linear correlation when plotted on a log fluorescence and log dilution plot (Figure 5.76).

**Flourescence of Supernatant for homogenized final cell pellet samples from Temperature Control Runs
(ex. 515 nm, em. 535 nm, CUT 530 nm)**

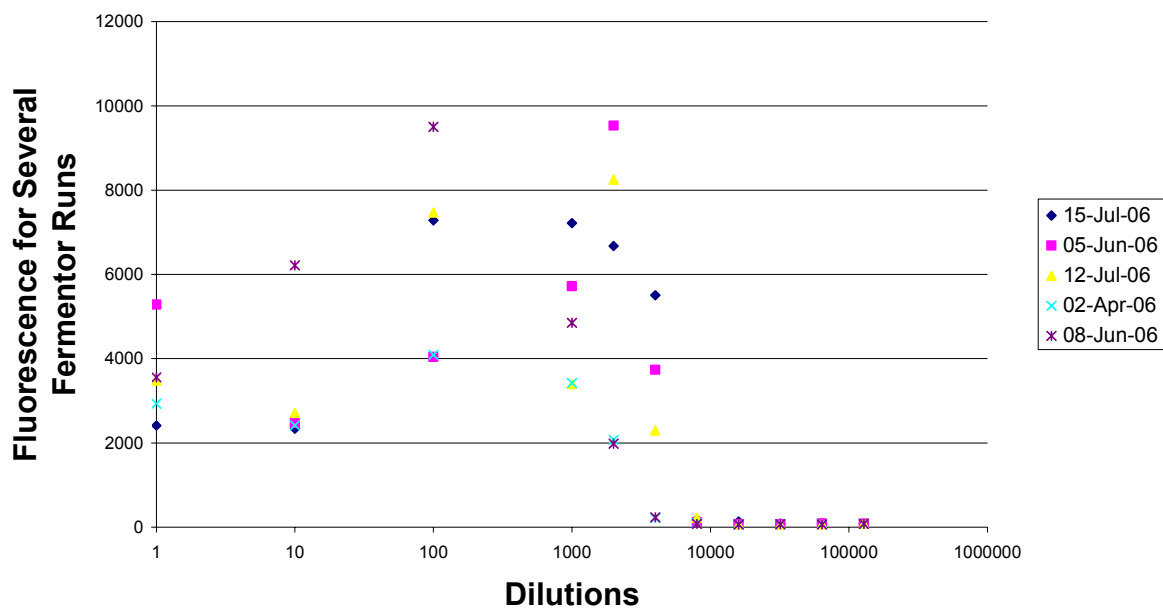


Figure 5.75: Fluorescence of supernatant for homogenized final cell pellet samples from temperature control runs. These plots do not follow the linear correlation expected when plotted on a log-log scale.

When samples from all runs are compared at 515 nm versus 468 nm values there is an obvious linear correlation (Figure 5.76). This would be expected for a potential eYFP variant however sequencing indicated that the produced protein had the correct eYFP amino acid sequence.

Fluorescence Values for Peak Emission Scan for Temperature Control Runs
(ex. 468 nm, em. 520 nm, Cut 515 nm)

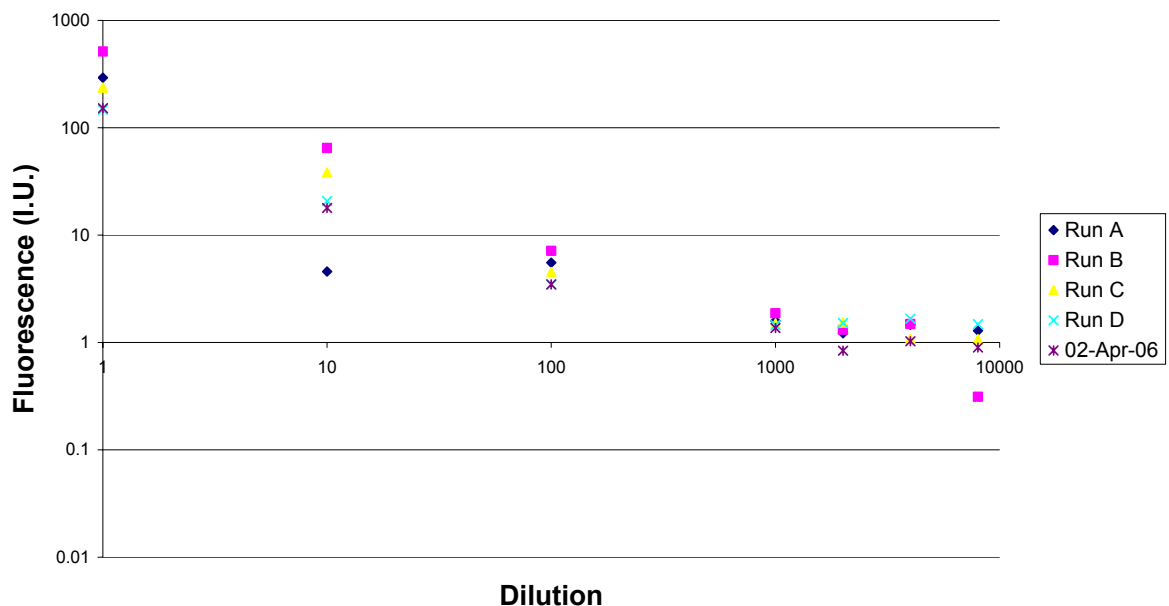


Figure 5.76: Fluorescence scan at typical eYFP values for all Temperature Control runs and one Initial Temperature Control run for eYFP and peak emission found in scan.

Excitation scans for the BL21 DE3 samples show two maxima at 468 and 448 nm (Figure 5.77). Excitation scan for fluorescence for shake flask samples show peaks at 468 and 448 nm for the shake flask samples (Figure 5.78). Peaks at 520 nm were observed for the excitations of 448 and 466 nm for the BL21 DE3 with No plasmid (Figure 5.79). There is no definite peak for the 372 nm excitation scan but given the wider shoulder than the shake flask samples it is unlikely that such a peak would be observed (Figure 5.80). Peaks at 520 nm were observed for the excitations of 448 and 466 nm for the BL21 DE3 with No plasmid. . Examination of the literature found no mention of these particular autofluorescence wavelength pairs.

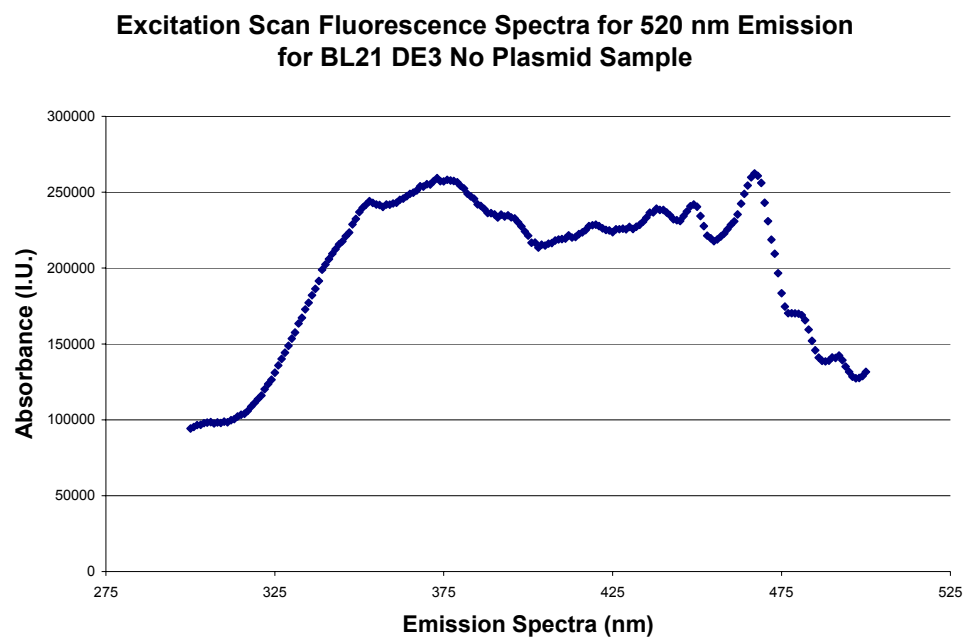


Figure 5.77: Excitation absorbance peaks for 520 nm Emission for BL21 DE3. Several peaks are observed with similarity to shake flask protein peaks. Maximum was at 468 and 448.

**Excitation Scan Fluorescence Spectra for 520 nm Emission
for 30 min Shake Flask Experiment Sample**

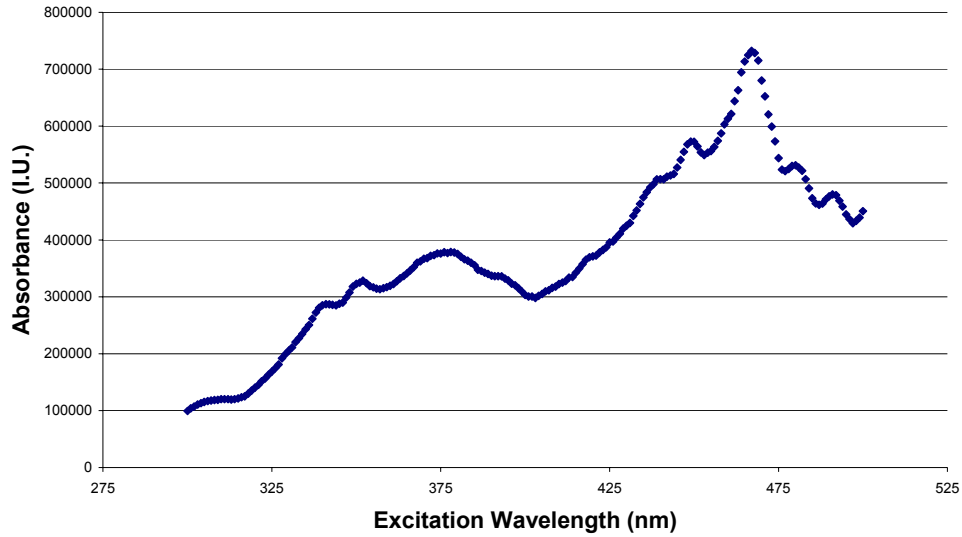


Figure 5.78: Excitation scan for fluorescence for shake flask samples. Several peaks are observed for the excitation scan with the biggest at 468 nm with a smaller peak at 448 nm.

**Fluorescence Spectra for Peak Excitation Values for BL21DE3
No Plasmid**

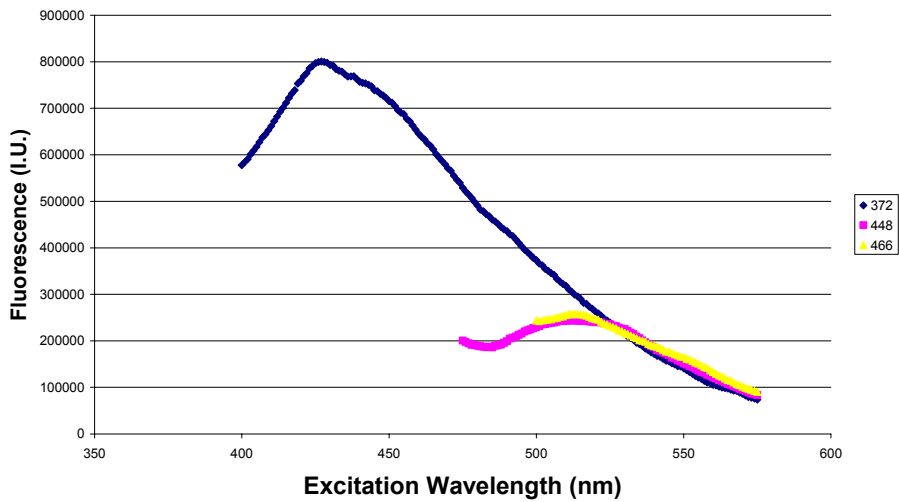


Figure 5.79: Fluorescence spectra for peak excitation value for BL21 DE3 with No Plasmid. Peaks at 520nm were observed for excitations of 448 nm and 466 nm.

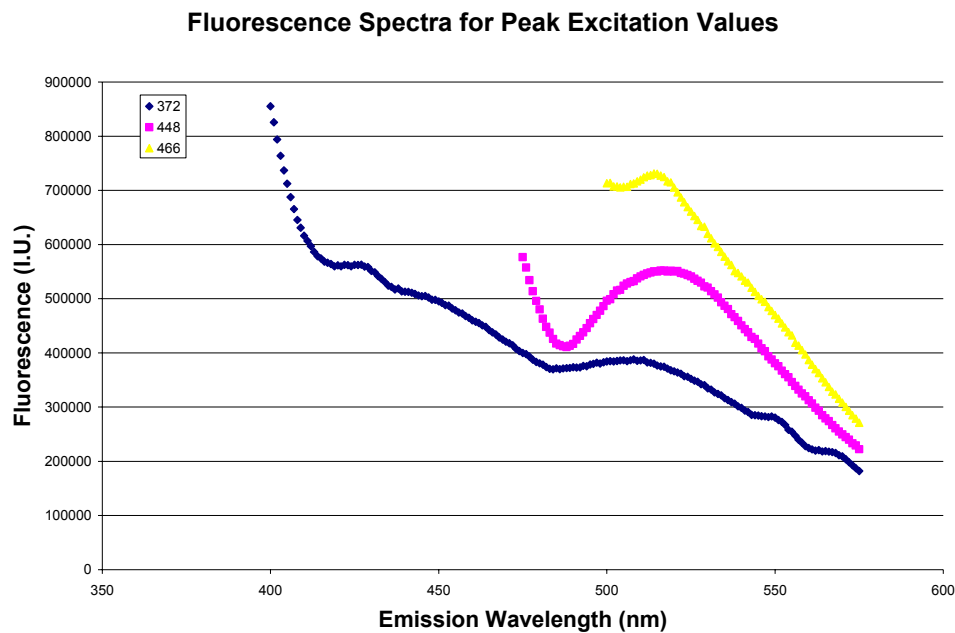


Figure 5.80: Fluorescence spectra for peak excitation value for shake flask samples. A peak at 520 nm were observed for both the 448 and 468 nm excitation values. A excitation peak at 520 nm was suggested for the 372 nm emission..

5.6 Conclusions

Temperature control is an effective means to meet oxygen demand by reducing metabolic rate and lowering specific oxygen demand. The penalty for this is slower growth and potentially slower protein production rates. That said, it is possible to achieve similar densities with better yield coefficients using temperature control, allowing cultures to be produced and maintained at a cost savings regarding consumables with potential benefit of lower acetate yields. The trade off is increased production time which may lead to higher operator costs.

Unfortunately it has been shown that eYFP production was either non-existent or at very low levels for the runs performed in the temperature control experiments. This highlights the importance of proper upstream genetic engineering and strain selection based on productivity before full production begins. The fermentor and fed-batch strategy is a means of achieving

high cell density while avoiding inhibitory levels of media components and by-products. It does not make up for poor strain selection or upstream engineering.

Had the mistake been caught earlier in the experimentation it would have been feasible to redo the genetic engineering. However, as many of the experiments had been run and given the amount of time required to run subsequent experiments, it was not feasible to begin engineering the plasmid and production mechanisms even with commercially available plasmids and having the cDNA sequence for the protein of interest. It remains unclear why our selected clone grew under selective conditions but did not over-express the recombinant protein.

5.7 Recommendations

5.7.1 Strain Selection and Initial Inoculation

It is shown that some inoculations take longer and thus are sampled more. This leads to a differing total inoculation which increases variability. Since it is rare for an inoculum culture to be sampled more than ten times it would be an easier to remove inoculum before being added to the fermentor so that each volume totals approximately forty milliliters.

Quite often the fermentor is used to boost cell densities for strains that poorly express the protein of interest. While this may work in some cases it usually leads to downstream processing which is difficult and time consuming. It is far simpler to select strains based on specific productivity and cell growth characteristics. A simple way to pick colonies which are expressing eYFP well is to image them using UV fluorescence. This may be quickly done using the UV function used to image DNA in a (BioRad Gel Doc Mississauga, ON) (Figure 5.81). Another quick method is to use a UV flashlight available in most hardware stores and choose colonies which have a high basal production of eYFP. It would be necessary to see how many platings the plasmid remained stable and protein is produced and it is recommended that experiments be set up to do this.

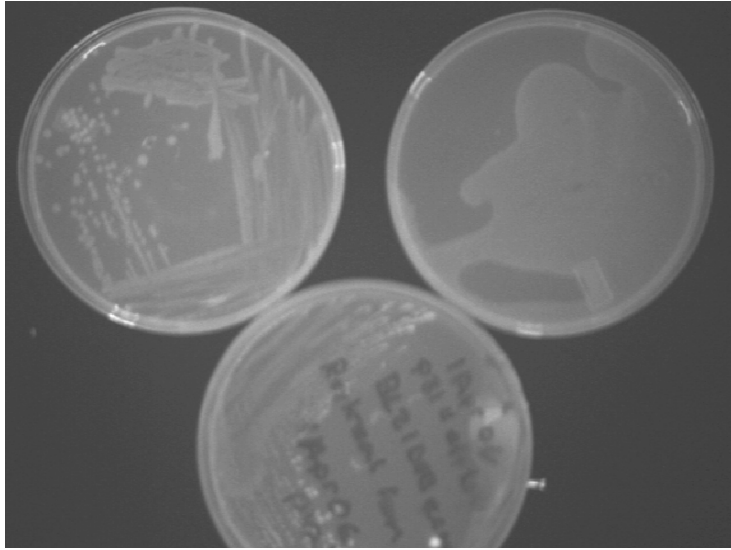


Figure 5.81: eYFP Plates imaged using UV imager.

In order to ensure better protein production it might be best to reengineer the cDNA encoding the eYFP protein to have an cut site for NCO1 for better insertion into the pRSET_B plasmid. Another option is to select a different plasmid. In both cases it is necessary to perform experiments ensuring overproduction of eYFP is stably achieved.

5.7.2 Protein Density Calculation from SDS PAGE Gels

Normalizing the gel densities and analyzing the protein responses from the SDS PAGE gels would allow a better picture into the proteome response to temperature control. Analysis with MS/MS of proteins which were significantly up or down regulated might be revealing, leading to a better temperature control approach. 2D DIGE is discussed in Chapter 4 and would be another method which may lead to a better understanding of the proteome response to temperature control.

5.7.3 Inclusion Body Formation and Protein Partitioning

Through SDS PAGE, fluorescence and protein quantification it should be possible to determine the relative amounts of protein portioned in inclusion bodies versus soluble. It has been suggested in Chapter 4 that lowering the temperature increases the soluble yield of

proteins. Exploration of whether lower temperatures also lead to slower protein formation and lower protein yields would be of benefit when choosing to use temperature as a tool to maintain dissolved oxygen concentrations.

Appendix A

Basecase Stream Reports

CHO Basecase: Stream Report

OVERALL PROCESS DATA

```
=====
Annual Operating Time      =      7879.86 h
Annual Throughput         =      14.48 kg MP
Batch Throughput          =      0.08 kg MP
Recipe Batch Time         =      240.95 h
Recipe Cycle Time         =      43.90 h
Number of Batches Per Year =      175
=====
```

MP = Main Product = Flow of tPA (in S-120)

STARTING MATERIAL REQUIREMENTS

```
=====
=====
Section      Starting      Active      Gross      Amt Needed
Name         Material      Product     Yield (%)  kg Sin/kg MP
-----
Fermentation  (none)       (none)     Unknown    0.0000
Purification Tra (none)     (none)     Unknown    0.0000
=====
```

Sin = Section Starting Material

Aout = Section Active Product

BULK RAW MATERIAL REQUIREMENTS PER SECTION

SECTIONS IN: Main Branch

Fermentation

```
-----
Raw Material          kg/Year      kg/Batch      kg/kg MP
```

Elution 3	452627.83	2586.445	31260.341
Elution 1	273062.34	1560.356	18858.809
Elution 2	314339.08	1796.223	21709.551
Media	933170.00	5332.400	64448.562
L-glutamine	766.50	4.380	52.938
Proteins	7047.25	40.270	486.712
Glucose	917.00	5.240	63.332
Biomass	1.43	0.008	0.099
tPA	10.60	0.061	0.732
Air	267848.97	1530.566	18498.752
Water	4998165.86	28560.948	345193.911
Pure_Wash	25553.17	146.018	1764.807
Section Total	7273510.03	41562.914	502338.547

Purification Train

Raw Material	kg/Year	kg/Batch	kg/kg MP

SUMMARY (Entire Process)

Raw Material	kg/Year	kg/Batch	kg/kg MP
Elution 3	452627.83	2586.445	31260.341
Elution 1	273062.34	1560.356	18858.809
Elution 2	314339.08	1796.223	21709.551
Media	933170.00	5332.400	64448.562
L-glutamine	766.50	4.380	52.938
Proteins	7047.25	40.270	486.712
Glucose	917.00	5.240	63.332
Biomass	1.43	0.008	0.099
tPA	10.60	0.061	0.732
Air	267848.97	1530.566	18498.752
Water	4998165.86	28560.948	345193.911
Pure_Wash	25553.17	146.018	1764.807
Process Total	7273510.03	41562.914	502338.547

BREAKDOWN PER RAW MATERIAL AND SECTION (kg/kg MP)

Raw Material	Fermentation	Purification Tr	Subtotal
Elution 3	31260.341	0.000	31260.341

Elution 1	18858.809	0.000	18858.809
Elution 2	21709.551	0.000	21709.551
Media	64448.562	0.000	64448.562
L-glutamine	52.938	0.000	52.938
Proteins	486.712	0.000	486.712
Glucose	63.332	0.000	63.332
Biomass	0.099	0.000	0.099
tPA	0.732	0.000	0.732
Air	18498.752	0.000	18498.752
Water	345193.911	0.000	345193.911
Pure_Wash	1764.807	0.000	1764.807

TOTAL	502338.547	0.000	502338.547
-------	------------	-------	------------

BREAKDOWN PER RAW MATERIAL AND SECTION (kg/batch)

Raw Material	Fermentation	Purification Tr	Subtotal
Elution 3	2586.445	0.000	2586.445
Elution 1	1560.356	0.000	1560.356
Elution 2	1796.223	0.000	1796.223
Media	5332.400	0.000	5332.400
L-glutamine	4.380	0.000	4.380
Proteins	40.270	0.000	40.270
Glucose	5.240	0.000	5.240
Biomass	0.008	0.000	0.008
tPA	0.061	0.000	0.061
Air	1530.566	0.000	1530.566
Water	28560.948	0.000	28560.948
Pure_Wash	146.018	0.000	146.018
TOTAL	41562.914	0.000	41562.914

BREAKDOWN PER RAW MATERIAL AND SECTION (kg/year)

Raw Material	Fermentation	Purification Tr	Subtotal
Elution 3	452627.8	0.0	452627.8
Elution 1	273062.3	0.0	273062.3
Elution 2	314339.1	0.0	314339.1
Media	933170.0	0.0	933170.0
L-glutamine	766.5	0.0	766.5
Proteins	7047.2	0.0	7047.2
Glucose	917.0	0.0	917.0
Biomass	1.4	0.0	1.4
tPA	10.6	0.0	10.6
Air	267849.0	0.0	267849.0
Water	4998165.9	0.0	4998165.9

Pure_Wash	25553.2	0.0	25553.2
TOTAL	7273510.0	0.0	7273510.0

COMPONENT BALANCE AND STREAM REPORT

STREAM NAME	S-125	S-101	S-102	S-103	S-
104					
SOURCE	INPUT	P-9	INPUT	P-1	
P-1					
DESTINATION	P-9	P-1	P-1	OUTPUT	P-
15					

STREAM PROPERTIES

ACTIVITY	U/ml	0.0	0.0	0.0	0.0
0.0					
TEMP	°C	25.0	25.0	25.0	37.0
4.0					
PRES	bar	1.0	1.0	1.0	1.0
1.0					
DENSITY	g/L	1.179	1.179	995.244	1.134
1002.802					

COMPONENT FLOWRATES (kg/Batch)

Biomass	0.0000	0.0000	0.0082	0.0000
8.3959				
Glucose	0.0000	0.0000	5.2400	0.0000
1.1009				
L-glutamine	0.0000	0.0000	4.3800	0.0000
0.0000				
Media	0.0000	0.0000	5332.4000	0.0000
5332.4000				
Nitrogen	1174.1242	1174.1242	0.0000	1179.0176
0.0000				
Oxygen	356.4414	356.4414	0.0000	357.9269
0.0000				
Proteins	0.0000	0.0000	40.2700	0.0000
40.2700				
tPA	0.0000	0.0000	0.0606	0.0000
0.1920				

```

=====
=====
TOTAL (kg/batch) 1530.5655 1530.5655 5382.3588 1536.9445
5382.3588
TOTAL (L/batch) 1297938.7434 1297938.7434 5408.0781 1355587.8507
5367.3174
=====
=====

```

```

=====
=====
STREAM NAME          S-105      S-106      S-107      S-108      S-
110
SOURCE              P-15      P-15      P-2        P-2        P-
14
DESTINATION         P-2      OUTPUT    OUTPUT     P-14
P-4
=====
=====

```

STREAM PROPERTIES

```

ACTIVITY U/ml      0.0      0.0      0.0      0.0
0.0
TEMP      °C      4.3      4.3      4.0      4.0
4.0
PRES      bar      1.0      1.0      1.0      1.0
1.0
DENSITY  g/L      1002.609 1006.139 1002.732 1002.732
1002.732

```

COMPONENT FLOWRATES (kg/Batch)

```

Biomass          0.0000      8.3959      0.0000      0.0000
0.0000
Glucose          1.0805      0.0204      1.0304      0.0501
0.0501
Media            5233.5488    98.8512    4990.7157    242.8331
242.8331
Proteins         39.5235      0.7465      37.6896      1.8339
1.8339
tPA              0.1884      0.0036      0.0316      0.1569
0.1569

```

```

=====
=====
TOTAL (kg/batch) 5274.3412 108.0176 5029.4673 244.8740
244.8740
TOTAL (L/batch) 5260.6155 107.3585 5015.7642 244.2068
244.2068
=====
=====

```

```

=====
=====
STREAM NAME          S-109          S-128          S-113          S-111          S-
112
SOURCE              INPUT          INPUT          P-4            P-4            P-
10
DESTINATION         P-4           P-4           P-10          OUTPUT
P-5
=====
=====

```

STREAM PROPERTIES

ACTIVITY	U/ml	0.0	0.0	0.0	0.0
0.0					
TEMP	°C	25.0	25.0	25.0	23.8
25.0					
PRES	bar	1.0	1.0	1.0	1.0
1.0					
DENSITY	g/L	994.704	994.704	994.704	995.181
994.704					

COMPONENT FLOWRATES (kg/Batch)

Elution 1	1560.3562	0.0000	260.0594	1300.2968
260.0594				
Glucose	0.0000	0.0000	0.0000	0.0501
0.0000				
Media	0.0000	0.0000	0.0000	242.8331
0.0000				
Proteins	0.0000	0.0000	0.0000	1.8339
0.0000				
Pure_Wash	0.0000	97.5223	0.0000	97.5223
0.0000				
tPA	0.0000	0.0000	0.1151	0.0417
0.1151				
Water	0.0000	2503.0714	0.0000	2503.0714
0.0000				

```

=====
=====
TOTAL (kg/batch)    1560.3562    2600.5937    260.1745    4145.6493
260.1745
TOTAL (L/batch)    1568.6633    2614.4389    261.5596    4165.7236
261.5596
=====
=====

```

```

=====
=====
STREAM NAME          S-114          S-118          S-126          S-117          S-
116
SOURCE              P-5           P-5           P-13           INPUT
P-6
DESTINATION         OUTPUT        P-13          P-6            P-6            P-
11
=====
=====

```

STREAM PROPERTIES

ACTIVITY	U/ml	0.0	0.0	0.0	0.0
0.0					
TEMP	°C	25.7	25.7	25.7	25.0
25.0					
PRES	bar	1.0	1.0	1.0	1.0
1.0					
DENSITY	g/L	994.442	994.442	994.443	994.704
994.704					

COMPONENT FLOWRATES (kg/Batch)

Elution 1	215.7693	44.2900	44.2900	0.0000
0.0000				
Elution 2	0.0000	0.0000	0.0000	1796.2233
359.2447				
tPA	0.0068	0.1083	0.1083	0.0000
0.0983				

```

=====
=====
TOTAL (kg/batch)    215.7761    44.3984    44.3984    1796.2233
359.3429
TOTAL (L/batch)    216.9820    44.6465    44.6465    1805.7862
361.2560
=====
=====

```

```

=====
=====
STREAM NAME          S-115          S-122          S-123          S-127          S-
124
SOURCE              P-6           P-11          P-3            P-3            P-
12
DESTINATION         OUTPUT        P-3           OUTPUT        P-12
P-8
=====
=====

```

STREAM PROPERTIES

ACTIVITY	U/ml	0.0	0.0	0.0	0.0
0.0					
TEMP	°C	25.0	25.0	25.7	25.7
25.7					
PRES	bar	1.0	1.0	1.0	1.0
1.0					
DENSITY	g/L	994.696	994.704	994.464	994.464
994.464					

COMPONENT FLOWRATES (kg/Batch)

Elution 1	44.2900	0.0000	0.0000	0.0000
0.0000				
Elution 2	1436.9787	359.2447	273.1334	86.1113
86.1113				
tPA	0.0101	0.0983	0.0155	0.0827
0.0827				

```
=====
=====
TOTAL (kg/batch)  1481.2788  359.3429  273.1489  86.1940
86.1940
TOTAL (L/batch)  1489.1766  361.2560  274.6694  86.6738
86.6738
=====
=====
```

```
=====
=====
STREAM NAME      S-119      S-130      S-120      S-121
SOURCE           INPUT      INPUT      P-8        P-8
DESTINATION      P-8        P-8        OUTPUT     OUTPUT
=====
=====
```

STREAM PROPERTIES

ACTIVITY	U/ml	0.0	0.0	0.0	0.0
TEMP	°C	25.0	25.0	25.0	25.0
PRES	bar	1.0	1.0	1.0	1.0
DENSITY	g/L	994.704	994.704	994.704	994.699

COMPONENT FLOWRATES (kg/Batch)

Elution 2	0.0000	0.0000	0.0000	86.1113
Elution 3	2586.4447	0.0000	43.1074	2543.3373
Pure_Wash	0.0000	48.4958	0.0000	48.4958
tPA	0.0000	0.0000	0.0827	0.0000
Water	0.0000	1244.7265	0.0000	1244.7265

```
=====
=====
TOTAL (kg/batch)  2586.4447  1293.2224  43.1902  3922.6710
TOTAL (L/batch)  2600.2146  1300.1073  43.4201  3943.5756
=====
```

```

=====
OVERALL COMPONENT BALANCE (kg/Batch)
=====
=====
COMPONENT                INITIAL          INPUT           OUTPUT
FINAL
=====
Biomass                   0.0000          0.0082          8.3959
0.0000
Elution 1                0.0000          1560.3562       1560.3562
0.0000
Elution 2                0.0000          1796.2233       1796.2233
0.0000
Elution 3                0.0000          2586.4447       2586.4447
0.0000
Glucose                   0.0000          5.2400          1.1009
0.0000
L-glutamine              0.0000          4.3800          0.0000
0.0000
Media                     0.0000          5332.4000       5332.4000
0.0000
Nitrogen                   7.1474          1174.1242       1179.0176
2.2541
Oxygen                    2.1698          356.4414        357.9269
0.6843
Proteins                  0.0000          40.2700         40.2700
0.0000
Pure_Wash                 0.0000          146.0181        146.0181
0.0000
tPA                       0.0000          0.0606          0.1920
0.0000
Water                     0.0000          28560.9478      28560.9478
0.0000
=====
TOTAL                      9.3173          41562.9145      41569.2934
2.9383
=====
=====

```

***E. coli* Base Case 1: Stream Report**

```

OVERALL PROCESS DATA
=====
Annual Operating Time      =          7897.58 h

```

Annual Throughput = 5.41 kg MP
 Batch Throughput = 0.03 kg MP
 Recipe Batch Time = 248.89 h
 Recipe Cycle Time = 43.46 h
 Number of Batches Per Year = 177

MP = Main Product = Flow of tPA (in S-120)

STARTING MATERIAL REQUIREMENTS

Section Name	Starting Material	Active Product	Gross Yield (%)	Amt Needed kg Sin/kg MP
Fermentation	(none)	(none)	Unknown	0.0000
Purification Tra	(none)	(none)	Unknown	0.0000

Sin = Section Starting Material
 Aout = Section Active Product

BULK RAW MATERIAL REQUIREMENTS PER SECTION

SECTIONS IN: Main Branch

Fermentation

Raw Material	kg/Year	kg/Batch	kg/kg MP
Elution 3	112782.74	637.191	20840.228
Elution 1	102059.73	576.609	18858.809
Elution 2	117487.32	663.770	21709.551
Media	849600.00	4800.000	156990.848
Air	241729.40	1365.703	44667.259
Water	1783049545.73	10073726.247	329475588.976
Pure_Wash	9550.75	53.959	1764.807
Section Total	1784482755.67	10081823.478	329740420.477

Purification Train

Raw Material	kg/Year	kg/Batch	kg/kg MP
--------------	---------	----------	----------

SUMMARY (Entire Process)

Raw Material	kg/Year	kg/Batch	kg/kg MP
Elution 3	112782.74	637.191	20840.228
Elution 1	102059.73	576.609	18858.809
Elution 2	117487.32	663.770	21709.551
Media	849600.00	4800.000	156990.848
Air	241729.40	1365.703	44667.259
Water	1783049545.73	10073726.247	329475588.976
Pure_Wash	9550.75	53.959	1764.807
Process Total	1784482755.67	10081823.478	329740420.477

BREAKDOWN PER RAW MATERIAL AND SECTION (kg/kg MP)

Raw Material	Fermentation	Purification Tr	Subtotal
Elution 3	20840.228	0.000	20840.228
Elution 1	18858.809	0.000	18858.809
Elution 2	21709.551	0.000	21709.551
Media	156990.848	0.000	156990.848
Air	44667.259	0.000	44667.259
Water	329475588.976	0.000	329475588.976
Pure_Wash	1764.807	0.000	1764.807
TOTAL	329740420.477	0.000	329740420.477

BREAKDOWN PER RAW MATERIAL AND SECTION (kg/batch)

Raw Material	Fermentation	Purification Tr	Subtotal
Elution 3	637.191	0.000	637.191
Elution 1	576.609	0.000	576.609
Elution 2	663.770	0.000	663.770
Media	4800.000	0.000	4800.000
Air	1365.703	0.000	1365.703
Water	10073726.247	0.000	10073726.247
Pure_Wash	53.959	0.000	53.959
TOTAL	10081823.478	0.000	10081823.478

BREAKDOWN PER RAW MATERIAL AND SECTION (kg/year)

Raw Material	Fermentation	Purification Tr	Subtotal
Elution 3	112782.7	0.0	112782.7
Elution 1	102059.7	0.0	102059.7
Elution 2	117487.3	0.0	117487.3
Media	849600.0	0.0	849600.0
Air	241729.4	0.0	241729.4
Water	1783049545.7	0.0	1783049545.7
Pure_Wash	9550.7	0.0	9550.7
TOTAL	1784482755.7	0.0	1784482755.7

COMPONENT BALANCE AND STREAM REPORT

STREAM NAME	S-125	S-101	S-102	S-103	S-104
SOURCE	INPUT	P-9	INPUT	P-1	
DESTINATION	P-9	P-1	P-1	OUTPUT	

STREAM PROPERTIES

ACTIVITY	U/ml	0.0	0.0	0.0	0.0
TEMP	°C	25.0	25.0	25.0	4.1
PRES	bar	1.0	1.0	1.0	1.0
DENSITY	g/L	1.179	1.179	994.704	1.268

COMPONENT FLOWRATES (kg/Batch)

Biomass	0.0000	0.0000	0.0000	0.0000
Media	0.0000	0.0000	4800.0000	0.0000
Nitrogen	1047.6550	1047.6550	0.0000	1052.0213

Oxygen	318.0478	318.0478	0.0000	319.3733
0.0000				
UnRxMedia	0.0000	0.0000	0.0000	0.0000
4160.0000				

```
=====
=====
TOTAL (kg/batch)  1365.7028  1365.7028  4800.0000  1371.3946
4800.0000
TOTAL (L/batch) 1158133.0965 1158133.0965  4825.5546 1081387.4957
4759.7342
=====
=====
```

```
=====
=====
STREAM NAME      S-132      S-131      S-133      S-105      S-
106
SOURCE           P-7        P-7        P-16       P-15       P-
15
DESTINATION      OUTPUT     P-16       P-15       P-2
OUTPUT
=====
=====
```

STREAM PROPERTIES

ACTIVITY	U/ml	0.0	0.0	0.0	0.0
0.0					
TEMP	°C	4.0	4.0	4.0	4.0
4.0					
PRES	bar	1.0	1.0	1.0	1.0
1.0					
DENSITY	g/L	1002.359	1009.165	1022.253	1002.928
1140.077					

COMPONENT FLOWRATES (kg/Batch)

Biomass	0.0000	640.0000	46.4086	45.3693
1.0393				
Cell Debris	0.0000	0.0000	385.7453	0.0000
385.7453				
Inclusion Bodie	0.0000	0.0000	207.7570	0.0000
207.7570				
tPA	0.0000	0.0000	0.0712	0.0696
0.0016				
UnRxMedia	494.2306	3665.7694	3665.7694	3583.6742
82.0952				

TOTAL (kg/batch)	494.2306	4305.7694	4305.7516	3629.1132
676.6384				
TOTAL (L/batch)	493.0675	4266.6667	4212.0215	3618.5192
593.5023				

=====

=====

STREAM NAME	S-107	S-108	S-110	S-109	S-
128					
SOURCE	P-2	P-2	P-14	INPUT	
INPUT					
DESTINATION	OUTPUT	P-14	P-4	P-4	
P-4					

=====

=====

STREAM PROPERTIES

ACTIVITY	U/ml	0.0	0.0	0.0	0.0
0.0					
TEMP	°C	4.0	4.0	4.0	25.0
25.0					
PRES	bar	1.0	1.0	1.0	1.0
1.0					
DENSITY	g/L	1002.928	1002.928	1002.928	994.704
994.704					

COMPONENT FLOWRATES (kg/Batch)

Biomass	43.2636	2.1057	2.1057	0.0000
0.0000				
Elution 1	0.0000	0.0000	0.0000	576.6087
0.0000				
Pure_Wash	0.0000	0.0000	0.0000	0.0000
36.0380				
tPA	0.0117	0.0580	0.0580	0.0000
0.0000				
UnRxMedia	3417.3476	166.3266	166.3266	0.0000
0.0000				
Water	0.0000	0.0000	0.0000	0.0000
924.9764				

=====

=====

TOTAL (kg/batch)	3460.6229	168.4903	168.4903	576.6087
961.0144				
TOTAL (L/batch)	3450.5207	167.9985	167.9985	579.6785
966.1308				

=====

=====

```

=====
=====
STREAM NAME          S-113      S-111      S-112      S-114      S-
118
SOURCE              P-4        P-4        P-10       P-5
P-5
DESTINATION         P-10      OUTPUT     P-5        OUTPUT     P-
13
=====
=====

```

STREAM PROPERTIES

```

ACTIVITY  U/ml          0.0        0.0        0.0        0.0
0.0
TEMP      °C           25.0       22.8       25.0       25.7
25.7
PRES      bar           1.0        1.0        1.0        1.0
1.0
DENSITY   g/L          994.704    995.573    994.704    994.442
994.442

```

COMPONENT FLOWRATES (kg/Batch)

```

Biomass          0.0000      2.1057      0.0000      0.0000
0.0000
Elution 1      96.1014     480.5072    96.1014     79.7347
16.3668
Pure_Wash       0.0000      36.0380     0.0000      0.0000
0.0000
tPA             0.0425      0.0154     0.0425      0.0025
0.0400
UnRxMedia       0.0000      166.3266    0.0000      0.0000
0.0000
Water           0.0000      924.9764    0.0000      0.0000
0.0000

```

```

=====
=====
TOTAL (kg/batch)  96.1440     1609.9694    96.1440     79.7372
16.4068
TOTAL (L/batch)  96.6559     1617.1288    96.6559     80.1828
16.4985
=====
=====

```

```

=====
=====
STREAM NAME          S-126      S-117      S-116      S-115      S-
122

```

SOURCE	P-13	INPUT	P-6	P-6	P-
11					
DESTINATION	P-6	P-6	P-11	OUTPUT	
P-3					

=====
 STREAM PROPERTIES

ACTIVITY	U/ml	0.0	0.0	0.0	0.0
0.0					
TEMP	°C	25.7	25.0	25.0	25.0
25.0					
PRES	bar	1.0	1.0	1.0	1.0
1.0					
DENSITY	g/L	994.443	994.704	994.704	994.696
994.704					

COMPONENT FLOWRATES (kg/Batch)

Elution 1	16.3668	0.0000	0.0000	16.3668
0.0000				
Elution 2	0.0000	663.7702	132.7540	531.0162
132.7540				
tPA	0.0400	0.0000	0.0363	0.0037
0.0363				

=====
 TOTAL (kg/batch) 16.4068 663.7702 132.7904 547.3867
 132.7904
 TOTAL (L/batch) 16.4985 667.3040 133.4973 550.3052
 133.4973
 =====

=====
 STREAM NAME S-123 S-127 S-124 S-119 S-
 130
 SOURCE P-3 P-3 P-12 INPUT
 INPUT
 DESTINATION OUTPUT P-12 P-8 P-8
 P-8
 =====

=====
 STREAM PROPERTIES

ACTIVITY	U/ml	0.0	0.0	0.0	0.0
0.0					

TEMP	°C	25.7	25.7	25.7	25.0
25.0					
PRES	bar	1.0	1.0	1.0	1.0
1.0					
DENSITY	g/L	994.464	994.464	994.464	994.704
994.704					

COMPONENT FLOWRATES (kg/Batch)

Elution 2		100.9328	31.8213	31.8213	0.0000
0.0000					
Elution 3		0.0000	0.0000	0.0000	637.1906
0.0000					
Pure_Wash		0.0000	0.0000	0.0000	0.0000
17.9210					
tPA		0.0057	0.0306	0.0306	0.0000
0.0000					
Water		0.0000	0.0000	0.0000	0.0000
459.9720					

=====

TOTAL (kg/batch)		100.9385	31.8518	31.8518	637.1906
477.8929					
TOTAL (L/batch)		101.5004	32.0292	32.0291	640.5829
480.4372					

=====

=====

STREAM NAME	S-120	S-121
SOURCE	P-8	P-8
DESTINATION	OUTPUT	OUTPUT

=====

STREAM PROPERTIES

ACTIVITY	U/ml	0.0	0.0
TEMP	°C	25.0	25.0
PRES	bar	1.0	1.0
DENSITY	g/L	994.704	994.697

COMPONENT FLOWRATES (kg/Batch)

Elution 2		0.0000	31.8213
Elution 3		71.3653	565.8252
Pure_Wash		0.0000	17.9210
tPA		0.0306	0.0000
Water		0.0000	459.9720

=====

TOTAL	(kg/batch)	71.3959	1075.5395
TOTAL	(L/batch)	71.7760	1081.2732

=====

E. coli Basecase 2: Stream Report

OVERALL PROCESS DATA

```

=====
Annual Operating Time      =      7901.46 h
Annual Throughput         =          1.18 kg MP
Batch Throughput          =          0.01 kg MP
Recipe Batch Time         =          252.76 h
Recipe Cycle Time         =          43.46 h
Number of Batches Per Year =          177
=====

```

MP = Main Product = Flow of tPA (in S-120)

STARTING MATERIAL REQUIREMENTS

```

=====
Section      Starting      Active      Gross      Amt Needed
Name         Material      Product     Yield (%)   kg Sin/kg MP
-----
Fermentation  (none)       (none)      Unknown    0.0000
Purification Tra (none)     (none)      Unknown    0.0000
=====

```

Sin = Section Starting Material
Aout = Section Active Product

BULK RAW MATERIAL REQUIREMENTS PER SECTION

SECTIONS IN: Main Branch

Fermentation

```

-----
Raw Material      kg/Year      kg/Batch      kg/kg MP
-----
Elution 3        24656.00     139.299       20840.228
Elution 1        22311.79     126.055       18858.809
Elution 2        25684.49     145.110       21709.551
Media             849600.00    4800.000      718115.535
Air               241729.40    1365.703      204319.251
Water             2080674.37   11755.222     1758668.299
Pure_Wash         2087.94      11.796        1764.807
-----

```


Section Total	3246743.99	18343.186	2744276.480
---------------	------------	-----------	-------------

Purification Train

Raw Material	kg/Year	kg/Batch	kg/kg MP
--------------	---------	----------	----------

SUMMARY (Entire Process)

Raw Material	kg/Year	kg/Batch	kg/kg MP
Elution 3	24656.00	139.299	20840.228
Elution 1	22311.79	126.055	18858.809
Elution 2	25684.49	145.110	21709.551
Media	849600.00	4800.000	718115.535
Air	241729.40	1365.703	204319.251
Water	2080674.37	11755.222	1758668.299
Pure_Wash	2087.94	11.796	1764.807
Process Total	3246743.99	18343.186	2744276.480

BREAKDOWN PER RAW MATERIAL AND SECTION (kg/kg MP)

Raw Material	Fermentation	Purification Tr	Subtotal
Elution 3	20840.228	0.000	20840.228
Elution 1	18858.809	0.000	18858.809
Elution 2	21709.551	0.000	21709.551
Media	718115.535	0.000	718115.535
Air	204319.251	0.000	204319.251
Water	1758668.299	0.000	1758668.299
Pure_Wash	1764.807	0.000	1764.807
TOTAL	2744276.480	0.000	2744276.480

BREAKDOWN PER RAW MATERIAL AND SECTION (kg/batch)

Raw Material	Fermentation	Purification Tr	Subtotal
Elution 3	139.299	0.000	139.299
Elution 1	126.055	0.000	126.055
Elution 2	145.110	0.000	145.110
Media	4800.000	0.000	4800.000

Air	1365.703	0.000	1365.703
Water	11755.222	0.000	11755.222
Pure_Wash	11.796	0.000	11.796
TOTAL	18343.186	0.000	18343.186

BREAKDOWN PER RAW MATERIAL AND SECTION (kg/year)

Raw Material	Fermentation	Purification Tr	Subtotal
Elution 3	24656.0	0.0	24656.0
Elution 1	22311.8	0.0	22311.8
Elution 2	25684.5	0.0	25684.5
Media	849600.0	0.0	849600.0
Air	241729.4	0.0	241729.4
Water	2080674.4	0.0	2080674.4
Pure_Wash	2087.9	0.0	2087.9
TOTAL	3246744.0	0.0	3246744.0

COMPONENT BALANCE AND STREAM REPORT

STREAM NAME	S-125	S-101	S-102	S-103	S-
104					
SOURCE	INPUT	P-9	INPUT	P-1	
P-1					
DESTINATION	P-9	P-1	P-1	OUTPUT	P-
17					

STREAM PROPERTIES

ACTIVITY	U/ml	0.0	0.0	0.0	0.0
0.0					
TEMP	°C	25.0	25.0	25.0	4.1
4.0					
PRES	bar	1.0	1.0	1.0	1.0
1.0					
DENSITY	g/L	1.179	1.179	994.704	1.268
1008.460					

COMPONENT FLOWRATES (kg/Batch)

Biomass	0.0000	0.0000	0.0000	0.0000
640.0000				
Media	0.0000	0.0000	4800.0000	0.0000
0.0000				
Nitrogen	1047.6550	1047.6550	0.0000	1052.0213
0.0000				
Oxygen	318.0478	318.0478	0.0000	319.3733
0.0000				
UnRxMedia	0.0000	0.0000	0.0000	0.0000
4160.0000				

```

=====
=====
TOTAL (kg/batch) 1365.7028 1365.7028 4800.0000 1371.3946
4800.0000
TOTAL (L/batch) 1158133.0965 1158133.0965 4825.5546 1081387.4957
4759.7342
=====
=====

```

```

=====
=====
STREAM NAME      S-131      S-132      S-133      S-105      S-
106
SOURCE           P-17      P-17      P-16      P-15      P-
15
DESTINATION      OUTPUT    P-16      P-15      P-2
OUTPUT
=====
=====

```

STREAM PROPERTIES

ACTIVITY	U/ml	0.0	0.0	0.0	0.0
0.0					
TEMP	°C	4.0	4.0	4.0	4.0
4.0					
PRES	bar	1.0	1.0	1.0	1.0
1.0					
DENSITY	g/L	1002.359	1045.656	1138.382	1022.332
1142.787					

COMPONENT FLOWRATES (kg/Batch)

Biomass	0.0000	640.0000	46.4086	9.9184
36.4902				
Cell Debris	0.0000	0.0000	385.7453	0.0000
385.7453				
Inclusion Bodie	0.0000	0.0000	207.7570	0.0000
207.7570				
tPA	0.0000	0.0000	0.0712	0.0152
0.0560				

UnRxMedia	4098.7008	61.2992	61.2992	13.1008
48.1984				

```
=====
=====
TOTAL (kg/batch)  4098.7008  701.2992  701.2814  23.0344
678.2469
TOTAL (L/batch)  4089.0554  670.6787  616.0336  22.5313
593.5023
=====
=====
```

```
=====
=====
STREAM NAME      S-107      S-108      S-110      S-109      S-
128
SOURCE           P-2        P-2        P-14       INPUT
INPUT
DESTINATION      OUTPUT     P-14       P-4        P-4
P-4
=====
=====
```

STREAM PROPERTIES

ACTIVITY	U/ml	0.0	0.0	0.0	0.0
0.0					
TEMP	°C	4.0	4.0	4.0	25.0
25.0					
PRES	bar	1.0	1.0	1.0	1.0
1.0					
DENSITY	g/L	1022.343	1022.104	1022.104	994.704
994.704					

COMPONENT FLOWRATES (kg/Batch)

Biomass	9.4632	0.4552	0.4552	0.0000
0.0000				
Elution 1	0.0000	0.0000	0.0000	126.0553
0.0000				
Pure_Wash	0.0000	0.0000	0.0000	0.0000
7.8785				
tPA	0.0026	0.0127	0.0127	0.0000
0.0000				
UnRxMedia	12.4995	0.6013	0.6013	0.0000
0.0000				
Water	0.0000	0.0000	0.0000	0.0000
202.2137				

```
=====
=====
```

TOTAL (kg/batch)	21.9653	1.0692	1.0692	126.0553
210.0922				
TOTAL (L/batch)	21.4852	1.0461	1.0461	126.7264
211.2107				

=====

=====

STREAM NAME	S-113	S-111	S-112	S-114	S-
118					
SOURCE	P-4	P-4	P-10	P-5	
P-5					
DESTINATION	P-10	OUTPUT	P-5	OUTPUT	P-
13					

=====

STREAM PROPERTIES

ACTIVITY U/ml	0.0	0.0	0.0	0.0
0.0				
TEMP °C	25.0	24.9	25.0	25.7
25.7				
PRES bar	1.0	1.0	1.0	1.0
1.0				
DENSITY g/L	994.704	994.805	994.704	994.442
994.442				

COMPONENT FLOWRATES (kg/Batch)

Biomass	0.0000	0.4552	0.0000	0.0000
0.0000				
Elution 1	21.0092	105.0461	21.0092	17.4312
3.5780				
Pure_Wash	0.0000	7.8785	0.0000	0.0000
0.0000				
tPA	0.0093	0.0034	0.0093	0.0005
0.0088				
UnRxMedia	0.0000	0.6013	0.0000	0.0000
0.0000				
Water	0.0000	202.2137	0.0000	0.0000
0.0000				

=====

TOTAL (kg/batch)	21.0185	316.1982	21.0185	17.4317
3.5868				
TOTAL (L/batch)	21.1304	317.8493	21.1304	17.5292
3.6068				

=====

```

=====
=====
STREAM NAME          S-126      S-117      S-116      S-115      S-
122
SOURCE              P-13      INPUT      P-6        P-6        P-
11
DESTINATION         P-6       P-6       P-11      OUTPUT
P-3
=====
=====

```

STREAM PROPERTIES

```

ACTIVITY  U/ml          0.0          0.0          0.0          0.0
0.0
TEMP      °C           25.7         25.0         25.0         25.0
25.0
PRES      bar          1.0          1.0          1.0          1.0
1.0
DENSITY   g/L          994.443     994.704     994.704     994.696
994.704

```

COMPONENT FLOWRATES (kg/Batch)

```

Elution 1          3.5780      0.0000      0.0000      3.5780
0.0000
Elution 2          0.0000     145.1101    29.0220     116.0881
29.0220
tPA              0.0088      0.0000      0.0079      0.0008
0.0079

```

```

=====
=====
TOTAL (kg/batch)    3.5868     145.1101    29.0300     119.6670
29.0300
TOTAL (L/batch)    3.6068     145.8827    29.1845     120.3050
29.1845
=====
=====

```

```

=====
=====
STREAM NAME          S-123      S-127      S-124      S-119      S-
130
SOURCE              P-3       P-3       P-12      INPUT
INPUT
DESTINATION         OUTPUT    P-12      P-8       P-8
P-8
=====
=====

```

STREAM PROPERTIES

ACTIVITY	U/ml	0.0	0.0	0.0	0.0
0.0					
TEMP	°C	25.7	25.7	25.7	25.0
25.0					
PRES	bar	1.0	1.0	1.0	1.0
1.0					
DENSITY	g/L	994.464	994.464	994.464	994.704
994.704					

COMPONENT FLOWRATES (kg/Batch)

Elution 2	22.0654	6.9566	6.9566	0.0000
0.0000				
Elution 3	0.0000	0.0000	0.0000	139.2994
0.0000				
Pure Wash	0.0000	0.0000	0.0000	0.0000
3.9178				
tPA	0.0013	0.0067	0.0067	0.0000
0.0000				
Water	0.0000	0.0000	0.0000	0.0000
100.5568				

```

=====
=====
TOTAL (kg/batch)      22.0667      6.9633      6.9633      139.2994
104.4746
TOTAL (L/batch)      22.1895      7.0021      7.0021      140.0411
105.0308
=====
=====

```

```

=====
=====
STREAM NAME          S-120      S-121
SOURCE              P-8       P-8
DESTINATION         OUTPUT    OUTPUT
=====
=====

```

STREAM PROPERTIES

ACTIVITY	U/ml	0.0	0.0
TEMP	°C	25.0	25.0
PRES	bar	1.0	1.0
DENSITY	g/L	994.704	994.697

COMPONENT FLOWRATES (kg/Batch)

Elution 2	0.0000	6.9566
Elution 3	15.6015	123.6979

Pure_Wash	0.0000	3.9178
tPA	0.0067	0.0000
Water	0.0000	100.5568

TOTAL (kg/batch)	15.6082	235.1291
TOTAL (L/batch)	15.6913	236.3826

OVERALL COMPONENT BALANCE (kg/Batch)

COMPONENT FINAL	INITIAL	INPUT	OUTPUT
Biomass 0.0000	0.0000	0.0000	46.4086
Cell Debris 0.0000	0.0000	0.0000	385.7453
Elution 1 0.0000	0.0000	126.0553	126.0553
Elution 2 0.0000	0.0000	145.1101	145.1101
Elution 3 0.0000	0.0000	139.2994	139.2994
Inclusion Bodie 0.0000	0.0000	0.0000	207.7570
Media 0.0000	0.0000	4800.0000	0.0000
Nitrogen 1.1539	5.5202	1047.6550	1052.0213
Oxygen 0.3503	1.6758	318.0478	319.3733
Pure_Wash 0.0000	0.0000	11.7963	11.7963
tPA 0.0000	0.0000	0.0000	0.0712
UnRxMedia 0.0000	0.0000	0.0000	4160.0000
Water 0.0000	0.0000	11755.2224	11755.2224
TOTAL 1.5042	7.1960	18343.1864	18348.8604

E. coli Basecase 3: Stream Report

OVERALL PROCESS DATA

```

=====
Annual Operating Time      =      7916.93 h
Annual Throughput         =           5.18 kg MP
Batch Throughput          =           0.03 kg MP
Recipe Batch Time         =          258.55 h
Recipe Cycle Time         =           43.51 h
Number of Batches Per Year =          177
=====

```

MP = Main Product = Flow of tPA (in S-120)

STARTING MATERIAL REQUIREMENTS

```

=====
=====
Section      Starting      Active      Gross      Amt Needed
Name         Material      Product     Yield (%)   kg Sin/kg MP
-----
Fermentation (none)      (none)      Unknown    0.0000
Purification Tra (none)    (none)      Unknown    0.0000
=====
=====

```

Sin = Section Starting Material
Aout = Section Active Product

BULK RAW MATERIAL REQUIREMENTS PER SECTION

```

=====
SECTIONS IN:  Main Branch

Fermentation
-----
Raw Material      kg/Year      kg/Batch      kg/kg MP
-----
Elution 3        162052.33    915.550       31260.341
Elution 1        97763.30     552.335       18858.809
Elution 2        112541.43    635.827       21709.551
Media             849600.00    4800.000      163890.181
Air               241729.40    1365.703      46630.267
Water            2888281.79   16317.976     557157.516

```

Pure_Wash	9148.69	51.687	1764.807
Section Total	4361116.92	24639.079	841271.472

Purification Train

Raw Material	kg/Year	kg/Batch	kg/kg MP
--------------	---------	----------	----------

SUMMARY (Entire Process)

Raw Material	kg/Year	kg/Batch	kg/kg MP
Elution 3	162052.33	915.550	31260.341
Elution 1	97763.30	552.335	18858.809
Elution 2	112541.43	635.827	21709.551
Media	849600.00	4800.000	163890.181
Air	241729.40	1365.703	46630.267
Water	2888281.79	16317.976	557157.516
Pure_Wash	9148.69	51.687	1764.807
Process Total	4361116.92	24639.079	841271.472

BREAKDOWN PER RAW MATERIAL AND SECTION (kg/kg MP)

Raw Material	Fermentation	Purification Tr	Subtotal
Elution 3	31260.341	0.000	31260.341
Elution 1	18858.809	0.000	18858.809
Elution 2	21709.551	0.000	21709.551
Media	163890.181	0.000	163890.181
Air	46630.267	0.000	46630.267
Water	557157.516	0.000	557157.516
Pure_Wash	1764.807	0.000	1764.807
TOTAL	841271.472	0.000	841271.472

BREAKDOWN PER RAW MATERIAL AND SECTION (kg/batch)

Raw Material	Fermentation	Purification Tr	Subtotal
Elution 3	915.550	0.000	915.550
Elution 1	552.335	0.000	552.335

Elution 2	635.827	0.000	635.827
Media	4800.000	0.000	4800.000
Air	1365.703	0.000	1365.703
Water	16317.976	0.000	16317.976
Pure_Wash	51.687	0.000	51.687

TOTAL	24639.079	0.000	24639.079
=====			

BREAKDOWN PER RAW MATERIAL AND SECTION (kg/year)

Raw Material	Fermentation	Purification Tr	Subtotal
Elution 3	162052.3	0.0	162052.3
Elution 1	97763.3	0.0	97763.3
Elution 2	112541.4	0.0	112541.4
Media	849600.0	0.0	849600.0
Air	241729.4	0.0	241729.4
Water	2888281.8	0.0	2888281.8
Pure_Wash	9148.7	0.0	9148.7

TOTAL	4361116.9	0.0	4361116.9
=====			

COMPONENT BALANCE AND STREAM REPORT

STREAM NAME	S-125	S-101	S-102	S-103	S-
104					
SOURCE	INPUT	P-9	INPUT	P-1	
P-1					
DESTINATION	P-9	P-1	P-1	OUTPUT	P-
17					

STREAM PROPERTIES

ACTIVITY	U/ml	0.0	0.0	0.0	0.0
0.0					
TEMP	°C	25.0	25.0	25.0	37.0
4.0					
PRES	bar	1.0	1.0	1.0	1.0
1.0					
DENSITY	g/L	1.179	1.179	994.704	1.134
1008.460					

COMPONENT FLOWRATES (kg/Batch)

Biomass	0.0000	0.0000	0.0000	0.0000
640.0000				
Media	0.0000	0.0000	4800.0000	0.0000
0.0000				
Nitrogen	1047.6550	1047.6550	0.0000	1052.0213
0.0000				
Oxygen	318.0478	318.0478	0.0000	319.3733
0.0000				
UnRxMedia	0.0000	0.0000	0.0000	0.0000
4160.0000				

```

=====
=====
TOTAL (kg/batch) 1365.7028 1365.7028 4800.0000 1371.3946
4800.0000
TOTAL (L/batch) 1158133.0965 1158133.0965 4825.5546 1209572.6112
4759.7342
=====
=====

```

```

=====
=====
STREAM NAME          S-131      S-132      S-133      S-105      S-
106
SOURCE              P-17      P-17      P-16      P-15      P-
15
DESTINATION         OUTPUT    P-16      P-15      P-7
OUTPUT
=====
=====

```

STREAM PROPERTIES

ACTIVITY U/ml	0.0	0.0	0.0	0.0
0.0				
TEMP °C	4.0	4.0	4.0	4.0
4.0				
PRES bar	1.0	1.0	1.0	1.0
1.0				
DENSITY g/L	1002.359	1014.561	1038.396	1003.519
1140.160				

COMPONENT FLOWRATES (kg/Batch)

Biomass	0.0000	640.0000	46.4086	44.2886
2.1200				
Cell Debris	0.0000	0.0000	385.7453	0.0000
385.7453				
Inclusion Bodie	0.0000	0.0000	207.7570	0.0000
207.7570				

tPA	0.0000	0.0000	0.0712	0.0680
0.0033				
UnRxMedia	2385.4808	1774.5192	1774.5192	1693.4573
81.0619				

```
=====
=====
TOTAL (kg/batch) 2385.4808 2414.5192 2414.5014 1737.8139
676.6875
TOTAL (L/batch) 2379.8671 2379.8671 2325.2219 1731.7196
593.5023
=====
=====
```

```
=====
=====
STREAM NAME      S-134      S-135      S-107      S-108      S-
110
SOURCE           P-7        P-7        P-2        P-2        P-
14
DESTINATION      P-2        OUTPUT    OUTPUT    P-14
P-4
=====
=====
```

STREAM PROPERTIES

ACTIVITY	U/ml	0.0	0.0	0.0	0.0
0.0					
TEMP	°C	4.0	4.0	4.0	4.0
4.0					
PRES	bar	1.0	1.0	1.0	1.0
1.0					
DENSITY	g/L	1002.357	1029.582	1002.359	1002.359
1002.359					

COMPONENT FLOWRATES (kg/Batch)

Biomass	0.0000	44.2886	0.0000	0.0000
0.0000				
tPA	0.0667	0.0013	0.0112	0.0555
0.0555				
UnRxMedia	1661.7492	31.7081	1584.6509	77.0983
77.0983				

```
=====
=====
TOTAL (kg/batch) 1661.8159 75.9980 1584.6621 77.1538
77.1538
TOTAL (L/batch) 1657.9079 73.8144 1580.9330 76.9722
76.9722
=====
=====
```

=====

STREAM NAME	S-109	S-128	S-113	S-111	S-
112					
SOURCE	INPUT	INPUT	P-4	P-4	P-
10					
DESTINATION	P-4	P-4	P-10	OUTPUT	
P-5					

STREAM PROPERTIES

ACTIVITY	U/ml	0.0	0.0	0.0	0.0
0.0					
TEMP	°C	25.0	25.0	25.0	23.9
25.0					
PRES	bar	1.0	1.0	1.0	1.0
1.0					
DENSITY	g/L	994.704	994.704	994.704	995.109
994.704					

COMPONENT FLOWRATES (kg/Batch)

Elution 1	552.3350	0.0000	92.0558	460.2792
92.0558				
Pure_Wash	0.0000	34.5209	0.0000	34.5209
0.0000				
tPA	0.0000	0.0000	0.0408	0.0148
0.0408				
UnRxMedia	0.0000	0.0000	0.0000	77.0983
0.0000				
Water	0.0000	886.0374	0.0000	886.0374
0.0000				

TOTAL (kg/batch)	552.3350	920.5583	92.0966	1457.9506
92.0966				
TOTAL (L/batch)	555.2756	925.4593	92.5869	1465.1162
92.5869				

STREAM NAME	S-114	S-118	S-126	S-117	S-
116					

SOURCE	P-5	P-5	P-13	INPUT	
P-6					
DESTINATION	OUTPUT	P-13	P-6	P-6	P-
11					

=====
 STREAM PROPERTIES

ACTIVITY	U/ml	0.0	0.0	0.0	0.0
0.0					
TEMP	°C	25.7	25.7	25.7	25.0
25.0					
PRES	bar	1.0	1.0	1.0	1.0
1.0					
DENSITY	g/L	994.442	994.442	994.443	994.704
994.704					

COMPONENT FLOWRATES (kg/Batch)

Elution 1	76.3780	15.6778	15.6778	0.0000
0.0000				
Elution 2	0.0000	0.0000	0.0000	635.8273
127.1655				
tPA	0.0024	0.0384	0.0384	0.0000
0.0348				

=====
 TOTAL (kg/batch) 76.3804 15.7161 15.7161 635.8273
 127.2002
 TOTAL (L/batch) 76.8073 15.8040 15.8040 639.2123
 127.8774
 =====

=====
 STREAM NAME S-115 S-122 S-123 S-127 S-
 124
 SOURCE P-6 P-11 P-3 P-3 P-
 12
 DESTINATION OUTPUT P-3 OUTPUT P-12
 P-8
 =====

=====
 STREAM PROPERTIES

ACTIVITY	U/ml	0.0	0.0	0.0	0.0
0.0					

TEMP	°C	25.0	25.0	25.7	25.7
25.7					
PRES	bar	1.0	1.0	1.0	1.0
1.0					
DENSITY	g/L	994.696	994.704	994.464	994.464
994.464					

COMPONENT FLOWRATES (kg/Batch)

Elution 1		15.6778	0.0000	0.0000	0.0000
0.0000					
Elution 2		508.6618	127.1655	96.6838	30.4817
30.4817					
tPA		0.0036	0.0348	0.0055	0.0293
0.0293					

```
=====
=====
TOTAL (kg/batch)    524.3432    127.2002    96.6893    30.5110
30.5110
TOTAL (L/batch)    527.1388    127.8774    97.2275    30.6808
30.6808
=====
=====
```

```
=====
=====
STREAM NAME          S-119          S-130          S-120          S-121
SOURCE               INPUT          INPUT          P-8            P-8
DESTINATION          P-8            P-8            OUTPUT         OUTPUT
=====
=====
```

STREAM PROPERTIES

ACTIVITY	U/ml	0.0	0.0	0.0	0.0
TEMP	°C	25.0	25.0	25.0	25.0
PRES	bar	1.0	1.0	1.0	1.0
DENSITY	g/L	994.704	994.704	994.704	994.699

COMPONENT FLOWRATES (kg/Batch)

Elution 2		0.0000	0.0000	0.0000	30.4817
Elution 3		915.5499	0.0000	68.3611	847.1888
Pure_Wash		0.0000	17.1666	0.0000	17.1666
tPA		0.0000	0.0000	0.0293	0.0000
Water		0.0000	440.6084	0.0000	440.6084

```
=====
=====
TOTAL (kg/batch)    915.5499    457.7749    68.3903    1335.4455
TOTAL (L/batch)    920.4242    460.2121    68.7545    1342.5626
=====
=====
```


OVERALL COMPONENT BALANCE (kg/Batch)

COMPONENT FINAL	INITIAL	INPUT	OUTPUT
Biomass 0.0000	0.0000	0.0000	46.4086
Cell Debris 0.0000	0.0000	0.0000	385.7453
Elution 1 0.0000	0.0000	552.3350	552.3350
Elution 2 0.0000	0.0000	635.8273	635.8273
Elution 3 0.0000	0.0000	915.5499	915.5499
Inclusion Bodie 0.0000	0.0000	0.0000	207.7570
Media 0.0000	0.0000	4800.0000	0.0000
Nitrogen 1.4373	5.8037	1047.6550	1052.0213
Oxygen 0.4363	1.7619	318.0478	319.3733
Pure_Wash 0.0000	0.0000	51.6875	51.6875
tPA 0.0000	0.0000	0.0000	0.0712
UnRxMedia 0.0000	0.0000	0.0000	4160.0000
Water 0.0000	0.0000	16317.9762	16317.9762
TOTAL 1.8737	7.5655	24639.0787	24644.7527

E. coli Basecase 4: Stream Report

OVERALL PROCESS DATA

```

=====
Annual Operating Time      =      7910.20 h
Annual Throughput         =      16.55 kg MP
Batch Throughput         =      0.03 kg MP
Recipe Batch Time        =      94.55 h
Recipe Cycle Time        =      13.86 h
Number of Batches Per Year =      565
=====

```

MP = Main Product = Flow of tPA (in S-120)

STARTING MATERIAL REQUIREMENTS

```

=====
Section      Starting      Active      Gross      Amt Needed
Name         Material      Product     Yield (%)   kg Sin/kg MP
-----
Fermentation (none)      (none)      Unknown    0.0000
Purification Tra (none)  (none)      Unknown    0.0000
=====

```

Sin = Section Starting Material
Aout = Section Active Product

BULK RAW MATERIAL REQUIREMENTS PER SECTION

SECTIONS IN: Main Branch

Fermentation

```

-----
Raw Material      kg/Year      kg/Batch      kg/kg MP
-----
Elution 3        517285.69    915.550       31260.341
Elution 1        312069.28    552.335       18858.809
Elution 2        359242.40    635.827       21709.551
Media             2712000.00   4800.000      163890.181
Air               138891.98    245.827       8393.448
Water             9219656.55   16317.976     557157.516
Pure_Wash         29203.44     51.687        1764.807
-----

```

Section Total	13288349.33	23519.202	803034.654
---------------	-------------	-----------	------------

Purification Train

Raw Material	kg/Year	kg/Batch	kg/kg MP
--------------	---------	----------	----------

SUMMARY (Entire Process)

Raw Material	kg/Year	kg/Batch	kg/kg MP
Elution 3	517285.69	915.550	31260.341
Elution 1	312069.28	552.335	18858.809
Elution 2	359242.40	635.827	21709.551
Media	2712000.00	4800.000	163890.181
Air	138891.98	245.827	8393.448
Water	9219656.55	16317.976	557157.516
Pure_Wash	29203.44	51.687	1764.807
Process Total	13288349.33	23519.202	803034.654

BREAKDOWN PER RAW MATERIAL AND SECTION (kg/kg MP)

Raw Material	Fermentation	Purification Tr	Subtotal
Elution 3	31260.341	0.000	31260.341
Elution 1	18858.809	0.000	18858.809
Elution 2	21709.551	0.000	21709.551
Media	163890.181	0.000	163890.181
Air	8393.448	0.000	8393.448
Water	557157.516	0.000	557157.516
Pure_Wash	1764.807	0.000	1764.807
TOTAL	803034.654	0.000	803034.654

BREAKDOWN PER RAW MATERIAL AND SECTION (kg/batch)

Raw Material	Fermentation	Purification Tr	Subtotal
Elution 3	915.550	0.000	915.550
Elution 1	552.335	0.000	552.335
Elution 2	635.827	0.000	635.827
Media	4800.000	0.000	4800.000

Air	245.827	0.000	245.827
Water	16317.976	0.000	16317.976
Pure_Wash	51.687	0.000	51.687
TOTAL	23519.202	0.000	23519.202

BREAKDOWN PER RAW MATERIAL AND SECTION (kg/year)

Raw Material	Fermentation	Purification Tr	Subtotal
Elution 3	517285.7	0.0	517285.7
Elution 1	312069.3	0.0	312069.3
Elution 2	359242.4	0.0	359242.4
Media	2712000.0	0.0	2712000.0
Air	138892.0	0.0	138892.0
Water	9219656.5	0.0	9219656.5
Pure_Wash	29203.4	0.0	29203.4
TOTAL	13288349.3	0.0	13288349.3

COMPONENT BALANCE AND STREAM REPORT

STREAM NAME	S-125	S-101	S-102	S-103	S-
104					
SOURCE	INPUT	P-9	INPUT	P-1	
P-1					
DESTINATION	P-9	P-1	P-1	OUTPUT	P-
17					

STREAM PROPERTIES

ACTIVITY	U/ml	0.0	0.0	0.0	0.0
0.0					
TEMP	°C	25.0	25.0	25.0	36.7
4.0					
PRES	bar	1.0	1.0	1.0	1.0
1.0					
DENSITY	g/L	1.179	1.179	994.704	1.135
1008.460					

COMPONENT FLOWRATES (kg/Batch)

Biomass	0.0000	0.0000	0.0000	0.0000
640.0000				
Media	0.0000	0.0000	4800.0000	0.0000
0.0000				
Nitrogen	188.5779	188.5779	0.0000	192.9442
0.0000				
Oxygen	57.2486	57.2486	0.0000	58.5741
0.0000				
UnRxMedia	0.0000	0.0000	0.0000	0.0000
4160.0000				

```

=====
=====
TOTAL (kg/batch) 245.8265 245.8265 4800.0000 251.5183
4800.0000
TOTAL (L/batch) 208463.9574 208463.9574 4825.5546 221681.0013
4759.7342
=====
=====

```

```

=====
=====
STREAM NAME      S-131      S-132      S-133      S-105      S-
106
SOURCE           P-17      P-17      P-16      P-15      P-
15
DESTINATION     OUTPUT    P-16      P-15      P-7
OUTPUT
=====
=====

```

STREAM PROPERTIES

ACTIVITY	U/ml	0.0	0.0	0.0	0.0
0.0					
TEMP	°C	4.0	4.0	4.0	4.0
4.0					
PRES	bar	1.0	1.0	1.0	1.0
1.0					
DENSITY	g/L	1002.359	1014.561	1038.396	1003.519
1140.160					

COMPONENT FLOWRATES (kg/Batch)

Biomass	0.0000	640.0000	46.4086	44.2886
2.1200				
Cell Debris	0.0000	0.0000	385.7453	0.0000
385.7453				
Inclusion Bodie	0.0000	0.0000	207.7570	0.0000
207.7570				
tPA	0.0000	0.0000	0.0712	0.0680
0.0033				

UnRxMedia	2385.4808	1774.5192	1774.5192	1693.4573
81.0619				

```
=====
=====
TOTAL (kg/batch)  2385.4808  2414.5192  2414.5014  1737.8139
676.6875
TOTAL (L/batch)  2379.8671  2379.8671  2325.2219  1731.7196
593.5023
=====
=====
```

```
=====
=====
STREAM NAME      S-134      S-135      S-107      S-108      S-
110
SOURCE           P-7        P-7        P-2        P-2        P-
14
DESTINATION      P-2        OUTPUT     OUTPUT     P-14
P-4
=====
=====
```

STREAM PROPERTIES

ACTIVITY	U/ml	0.0	0.0	0.0	0.0
0.0					
TEMP	°C	4.0	4.0	4.0	4.0
4.0					
PRES	bar	1.0	1.0	1.0	1.0
1.0					
DENSITY	g/L	1002.357	1029.582	1002.359	1002.359
1002.359					

COMPONENT FLOWRATES (kg/Batch)

Biomass	0.0000	44.2886	0.0000	0.0000
0.0000				
tPA	0.0667	0.0013	0.0112	0.0555
0.0555				
UnRxMedia	1661.7492	31.7081	1584.6509	77.0983
77.0983				

```
=====
=====
TOTAL (kg/batch)  1661.8159  75.9980  1584.6621  77.1538
77.1538
TOTAL (L/batch)  1657.9079  73.8144  1580.9330  76.9722
76.9722
=====
=====
```

```

=====
=====
STREAM NAME          S-109          S-128          S-113          S-111          S-
112
SOURCE              INPUT          INPUT          P-4            P-4            P-
10
DESTINATION         P-4            P-4            P-10          OUTPUT
P-5
=====
=====

```

STREAM PROPERTIES

ACTIVITY	U/ml	0.0	0.0	0.0	0.0
0.0					
TEMP	°C	25.0	25.0	25.0	23.9
25.0					
PRES	bar	1.0	1.0	1.0	1.0
1.0					
DENSITY	g/L	994.704	994.704	994.704	995.109
994.704					

COMPONENT FLOWRATES (kg/Batch)

Elution 1	552.3350	0.0000	92.0558	460.2792
92.0558				
Pure_Wash	0.0000	34.5209	0.0000	34.5209
0.0000				
tPA	0.0000	0.0000	0.0408	0.0148
0.0408				
UnRxMedia	0.0000	0.0000	0.0000	77.0983
0.0000				
Water	0.0000	886.0374	0.0000	886.0374
0.0000				

```

=====
=====
TOTAL (kg/batch)    552.3350    920.5583    92.0966    1457.9506
92.0966
TOTAL (L/batch)    555.2756    925.4593    92.5869    1465.1162
92.5869
=====
=====

```

```

=====
=====
STREAM NAME          S-114          S-118          S-126          S-117          S-
116
SOURCE              P-5            P-5            P-13          INPUT
P-6
=====
=====

```

DESTINATION	OUTPUT	P-13	P-6	P-6	P-11
-------------	--------	------	-----	-----	------

=====

=====

STREAM PROPERTIES

ACTIVITY	U/ml	0.0	0.0	0.0	0.0
0.0					
TEMP	°C	25.7	25.7	25.7	25.0
25.0					
PRES	bar	1.0	1.0	1.0	1.0
1.0					
DENSITY	g/L	994.442	994.442	994.443	994.704
994.704					

COMPONENT FLOWRATES (kg/Batch)

Elution 1	76.3780	15.6778	15.6778	0.0000
0.0000				
Elution 2	0.0000	0.0000	0.0000	635.8273
127.1655				
tPA	0.0024	0.0384	0.0384	0.0000
0.0348				

=====

=====

TOTAL (kg/batch)	76.3804	15.7161	15.7161	635.8273
127.2002				
TOTAL (L/batch)	76.8073	15.8040	15.8040	639.2123
127.8774				

=====

=====

=====

=====

STREAM NAME	S-115	S-122	S-123	S-127	S-124
SOURCE	P-6	P-11	P-3	P-3	P-12
DESTINATION	OUTPUT	P-3	OUTPUT	P-12	P-8

=====

=====

STREAM PROPERTIES

ACTIVITY	U/ml	0.0	0.0	0.0	0.0
0.0					
TEMP	°C	25.0	25.0	25.7	25.7
25.7					

PRES	bar	1.0	1.0	1.0	1.0
1.0					
DENSITY	g/L	994.696	994.704	994.464	994.464
994.464					

COMPONENT FLOWRATES (kg/Batch)

Elution 1		15.6778	0.0000	0.0000	0.0000
0.0000					
Elution 2		508.6618	127.1655	96.6838	30.4817
30.4817					
tPA		0.0036	0.0348	0.0055	0.0293
0.0293					

```
=====
=====
TOTAL (kg/batch)  524.3432  127.2002  96.6893  30.5110
30.5110
TOTAL (L/batch)  527.1388  127.8774  97.2275  30.6808
30.6808
=====
=====
```

```
=====
=====
STREAM NAME      S-119      S-130      S-120      S-121
SOURCE           INPUT      INPUT      P-8        P-8
DESTINATION      P-8        P-8        OUTPUT     OUTPUT
=====
=====
```

STREAM PROPERTIES

ACTIVITY	U/ml	0.0	0.0	0.0	0.0
TEMP	°C	25.0	25.0	25.0	25.0
PRES	bar	1.0	1.0	1.0	1.0
DENSITY	g/L	994.704	994.704	994.704	994.699

COMPONENT FLOWRATES (kg/Batch)

Elution 2		0.0000	0.0000	0.0000	30.4817
Elution 3		915.5499	0.0000	68.3611	847.1888
Pure_Wash		0.0000	17.1666	0.0000	17.1666
tPA		0.0000	0.0000	0.0293	0.0000
Water		0.0000	440.6084	0.0000	440.6084

```
=====
=====
TOTAL (kg/batch)  915.5499  457.7749  68.3903  1335.4455
TOTAL (L/batch)  920.4242  460.2121  68.7545  1342.5626
=====
=====
```

OVERALL COMPONENT BALANCE (kg/Batch)

COMPONENT FINAL	INITIAL	INPUT	OUTPUT
Biomass 0.0000	0.0000	0.0000	46.4086
Cell Debris 0.0000	0.0000	0.0000	385.7453
Elution 1 0.0000	0.0000	552.3350	552.3350
Elution 2 0.0000	0.0000	635.8273	635.8273
Elution 3 0.0000	0.0000	915.5499	915.5499
Inclusion Bodie 0.0000	0.0000	0.0000	207.7570
Media 0.0000	0.0000	4800.0000	0.0000
Nitrogen 1.4373	5.8037	188.5779	192.9442
Oxygen 0.4363	1.7619	57.2486	58.5741
Pure_Wash 0.0000	0.0000	51.6875	51.6875
tPA 0.0000	0.0000	0.0000	0.0712
UnRxMedia 0.0000	0.0000	0.0000	4160.0000
Water 0.0000	0.0000	16317.9762	16317.9762
TOTAL 1.8737	7.5655	23519.2024	23524.8764

E. coli Basecase 5: Stream Report

OVERALL PROCESS DATA

Annual Operating Time	=	7918.08 h
Annual Throughput	=	14.48 kg MP
Batch Throughput	=	0.02 kg MP
Recipe Batch Time	=	91.07 h
Recipe Cycle Time	=	13.18 h
Number of Batches Per Year	=	595

MP = Main Product = Flow of tPA (in S-120)

STARTING MATERIAL REQUIREMENTS

Section Name	Starting Material	Active Product	Gross Yield (%)	Amt Needed kg Sin/kg MP
Fermentation	(none)	(none)	Unknown	0.0000
Purification Tra	(none)	(none)	Unknown	0.0000

Sin = Section Starting Material

Aout = Section Active Product

BULK RAW MATERIAL REQUIREMENTS PER SECTION

SECTIONS IN: Main Branch

Fermentation

Raw Material	kg/Year	kg/Batch	kg/kg MP
Elution 3	452598.28	760.669	31260.341
Elution 1	273044.51	458.898	18858.809
Elution 2	314318.56	528.266	21709.551
Media	2372860.00	3988.000	163890.181
Air	121523.31	204.241	8393.448
Water	8292622.93	13937.181	572760.076
Pure_Wash	25551.50	42.944	1764.807

Section Total	11852519.07	19920.200	818637.214
---------------	-------------	-----------	------------

Purification Train

Raw Material	kg/Year	kg/Batch	kg/kg MP
--------------	---------	----------	----------

SUMMARY (Entire Process)

Raw Material	kg/Year	kg/Batch	kg/kg MP
Elution 3	452598.28	760.669	31260.341
Elution 1	273044.51	458.898	18858.809
Elution 2	314318.56	528.266	21709.551
Media	2372860.00	3988.000	163890.181
Air	121523.31	204.241	8393.448
Water	8292622.93	13937.181	572760.076
Pure_Wash	25551.50	42.944	1764.807
Process Total	11852519.07	19920.200	818637.214

BREAKDOWN PER RAW MATERIAL AND SECTION (kg/kg MP)

Raw Material	Fermentation	Purification Tr	Subtotal
Elution 3	31260.341	0.000	31260.341
Elution 1	18858.809	0.000	18858.809
Elution 2	21709.551	0.000	21709.551
Media	163890.181	0.000	163890.181
Air	8393.448	0.000	8393.448
Water	572760.076	0.000	572760.076
Pure_Wash	1764.807	0.000	1764.807
TOTAL	818637.214	0.000	818637.214

BREAKDOWN PER RAW MATERIAL AND SECTION (kg/batch)

Raw Material	Fermentation	Purification Tr	Subtotal
Elution 3	760.669	0.000	760.669
Elution 1	458.898	0.000	458.898
Elution 2	528.266	0.000	528.266
Media	3988.000	0.000	3988.000

Air	204.241	0.000	204.241
Water	13937.181	0.000	13937.181
Pure_Wash	42.944	0.000	42.944
TOTAL	19920.200	0.000	19920.200

BREAKDOWN PER RAW MATERIAL AND SECTION (kg/year)

Raw Material	Fermentation	Purification Tr	Subtotal
Elution 3	452598.3	0.0	452598.3
Elution 1	273044.5	0.0	273044.5
Elution 2	314318.6	0.0	314318.6
Media	2372860.0	0.0	2372860.0
Air	121523.3	0.0	121523.3
Water	8292622.9	0.0	8292622.9
Pure_Wash	25551.5	0.0	25551.5
TOTAL	11852519.1	0.0	11852519.1

COMPONENT BALANCE AND STREAM REPORT

STREAM NAME	S-125	S-101	S-102	S-103	S-
104					
SOURCE	INPUT	P-9	INPUT	P-1	
P-1					
DESTINATION	P-9	P-1	P-1	OUTPUT	P-
17					

STREAM PROPERTIES

ACTIVITY	U/ml	0.0	0.0	0.0	0.0
0.0					
TEMP	°C	25.0	25.0	25.0	36.7
4.0					
PRES	bar	1.0	1.0	1.0	1.0
1.0					
DENSITY	g/L	1.179	1.179	994.704	1.135
1008.460					

COMPONENT FLOWRATES (kg/Batch)

Biomass	0.0000	0.0000	0.0000	0.0000
531.7333				
Media	0.0000	0.0000	3988.0000	0.0000
0.0000				
Nitrogen	156.6768	156.6768	0.0000	160.3045
0.0000				
Oxygen	47.5640	47.5640	0.0000	48.6653
0.0000				
UnRxMedia	0.0000	0.0000	0.0000	0.0000
3456.2667				

```

=====
=====
TOTAL (kg/batch) 204.2409 204.2409 3988.0000 208.9698
3988.0000
TOTAL (L/batch) 173198.8046 173198.8046 4009.2316 184179.9653
3954.5458
=====
=====

```

```

=====
=====
STREAM NAME      S-131      S-132      S-133      S-105      S-
106
SOURCE           P-17      P-17      P-16      P-15      P-
15
DESTINATION      OUTPUT    P-16      P-15      P-7
OUTPUT
=====
=====

```

STREAM PROPERTIES

ACTIVITY U/ml	0.0	0.0	0.0	0.0
0.0				
TEMP °C	4.0	4.0	4.0	4.0
4.0				
PRES bar	1.0	1.0	1.0	1.0
1.0				
DENSITY g/L	1002.359	1014.561	1038.396	1003.519
1140.160				

COMPONENT FLOWRATES (kg/Batch)

Biomass	0.0000	531.7333	38.5578	36.7965
1.7614				
Cell Debris	0.0000	0.0000	320.4901	0.0000
320.4901				
Inclusion Bodie	0.0000	0.0000	172.6114	0.0000
172.6114				
tPA	0.0000	0.0000	0.0592	0.0565
0.0027				

UnRxMedia	1981.9370	1474.3297	1474.3297	1406.9808
67.3489				

```
=====
=====
TOTAL (kg/batch)  1981.9370  2006.0630  2006.0483  1443.8337
562.2145
TOTAL (L/batch)  1977.2729  1977.2729  1931.8719  1438.7704
493.1015
=====
=====
```

```
=====
=====
STREAM NAME      S-134      S-135      S-107      S-108      S-
110
SOURCE           P-7        P-7        P-2        P-2        P-
14
DESTINATION      P-2        OUTPUT     OUTPUT     P-14
P-4
=====
=====
```

STREAM PROPERTIES

ACTIVITY	U/ml	0.0	0.0	0.0	0.0
0.0					
TEMP	°C	4.0	4.0	4.0	4.0
4.0					
PRES	bar	1.0	1.0	1.0	1.0
1.0					
DENSITY	g/L	1002.357	1029.581	1002.359	1002.359
1002.359					

COMPONENT FLOWRATES (kg/Batch)

Biomass	0.0000	36.7965	0.0000	0.0000
0.0000				
tPA	0.0554	0.0011	0.0093	0.0461
0.0461				
UnRxMedia	1380.6367	26.3441	1316.5808	64.0558
64.0558				

```
=====
=====
TOTAL (kg/batch)  1380.6921  63.1417  1316.5901  64.1020
64.1020
TOTAL (L/batch)  1377.4456  61.3275  1313.4918  63.9511
63.9511
=====
=====
```

```

=====
=====
STREAM NAME          S-109          S-128          S-113          S-111          S-
112
SOURCE              INPUT          INPUT          P-4            P-4            P-
10
DESTINATION         P-4           P-4           P-10          OUTPUT
P-5
=====
=====

```

STREAM PROPERTIES

ACTIVITY	U/ml	0.0	0.0	0.0	0.0
0.0					
TEMP	°C	25.0	25.0	25.0	23.9
25.0					
PRES	bar	1.0	1.0	1.0	1.0
1.0					
DENSITY	g/L	994.704	994.704	994.704	995.109
994.704					

COMPONENT FLOWRATES (kg/Batch)

Elution 1	458.8983	0.0000	76.4831	382.4153
76.4831				
Pure_Wash	0.0000	28.6811	0.0000	28.6811
0.0000				
tPA	0.0000	0.0000	0.0339	0.0123
0.0339				
UnRxMedia	0.0000	0.0000	0.0000	64.0558
0.0000				
Water	0.0000	736.1494	0.0000	736.1494
0.0000				

```

=====
=====
TOTAL (kg/batch)    458.8983    764.8306    76.5169    1211.3139
76.5169
TOTAL (L/batch)    461.3414    768.9024    76.9243    1217.2674
76.9243
=====
=====

```

```

=====
=====
STREAM NAME          S-114          S-118          S-126          S-117          S-
116
SOURCE              P-5           P-5           P-13          INPUT
P-6
=====
=====

```


DESTINATION	OUTPUT	P-13	P-6	P-6	P-
11					

STREAM PROPERTIES

ACTIVITY	U/ml	0.0	0.0	0.0	0.0
0.0					
TEMP	°C	25.7	25.7	25.7	25.0
25.0					
PRES	bar	1.0	1.0	1.0	1.0
1.0					
DENSITY	g/L	994.442	994.442	994.443	994.704
994.704					

COMPONENT FLOWRATES (kg/Batch)

Elution 1	63.4574	13.0256	13.0256	0.0000
0.0000				
Elution 2	0.0000	0.0000	0.0000	528.2665
105.6533				
tPA	0.0020	0.0319	0.0319	0.0000
0.0289				

TOTAL (kg/batch)	63.4594	13.0575	13.0575	528.2665
105.6822				
TOTAL (L/batch)	63.8141	13.1305	13.1305	531.0789
106.2448				

STREAM NAME	S-115	S-122	S-123	S-127	S-
124					
SOURCE	P-6	P-11	P-3	P-3	P-
12					
DESTINATION	OUTPUT	P-3	OUTPUT	P-12	
P-8					

STREAM PROPERTIES

ACTIVITY	U/ml	0.0	0.0	0.0	0.0
0.0					
TEMP	°C	25.0	25.0	25.7	25.7
25.7					

PRES	bar	1.0	1.0	1.0	1.0
1.0					
DENSITY	g/L	994.696	994.704	994.464	994.464
994.464					

COMPONENT FLOWRATES (kg/Batch)

Elution 1		13.0256	0.0000	0.0000	0.0000
0.0000					
Elution 2		422.6132	105.6533	80.3281	25.3252
25.3252					
tPA		0.0030	0.0289	0.0046	0.0243
0.0243					

```
=====
=====
TOTAL (kg/batch)  435.6418  105.6822  80.3327  25.3495
25.3495
TOTAL (L/batch)  437.9645  106.2448  80.7799  25.4906
25.4906
=====
=====
```

```
=====
=====
STREAM NAME      S-119      S-130      S-120      S-121
SOURCE           INPUT      INPUT      P-8        P-8
DESTINATION      P-8        P-8        OUTPUT     OUTPUT
=====
=====
```

STREAM PROPERTIES

ACTIVITY	U/ml	0.0	0.0	0.0	0.0
TEMP	°C	25.0	25.0	25.0	25.0
PRES	bar	1.0	1.0	1.0	1.0
DENSITY	g/L	994.704	994.704	994.704	994.699

COMPONENT FLOWRATES (kg/Batch)

Elution 2		0.0000	0.0000	0.0000	25.3252
Elution 3		760.6694	0.0000	56.7966	703.8727
Pure_Wash		0.0000	14.2626	0.0000	14.2626
tPA		0.0000	0.0000	0.0243	0.0000
Water		0.0000	366.0721	0.0000	366.0721

```
=====
=====
TOTAL (kg/batch)  760.6694  380.3347  56.8210  1109.5326
TOTAL (L/batch)  764.7191  382.3595  57.1235  1115.4458
=====
=====
```

OVERALL COMPONENT BALANCE (kg/Batch)

COMPONENT FINAL	INITIAL	INPUT	OUTPUT
Biomass 0.0000	0.0000	0.0000	38.5578
Cell Debris 0.0000	0.0000	0.0000	320.4901
Elution 1 0.0000	0.0000	458.8983	458.8983
Elution 2 0.0000	0.0000	528.2665	528.2665
Elution 3 0.0000	0.0000	760.6694	760.6694
Inclusion Bodies 0.0000	0.0000	0.0000	172.6114
Media 0.0000	0.0000	3988.0000	0.0000
Nitrogen 1.1942	4.8219	156.6768	160.3045
Oxygen 0.3625	1.4638	47.5640	48.6653
Pure_Wash 0.0000	0.0000	42.9437	42.9437
tPA 0.0000	0.0000	0.0000	0.0592
UnRxMedia 0.0000	0.0000	0.0000	3456.2667
Water 0.0000	0.0000	13937.1814	13937.1814
TOTAL 1.5567	6.2857	19920.2001	19924.9143

Appendix B

Fermentator Supplementary Material

Table B.1: Final Weights for Shake Flask Run.

Flask	Tare Weight (g)	Weight (g)	Final Weight (g)
1	7.59	7.66	0.07
2	7.6	7.69	0.09
3	7.57	7.66	0.09
4	7.59	7.71	0.12
5	7.61	7.68	0.07
6	7.59	7.71	0.12
7A	7.56	7.65	0.09
7B	7.58	7.71	0.13
8A	7.6	7.67	0.07
8B	7.58	7.64	0.06
9A	7.58	7.67	0.09
9B	7.6	7.68	0.08
22A	7.59	7.67	0.08
22B	7.59	7.65	0.06
22C	7.59	7.66	0.07
22D	7.61	7.71	0.1
37A	7.56	7.64	0.08
37B	7.58	7.7	0.12
37C	7.59	7.64	0.05
37D	7.55	7.64	0.09

	22 Controls		37 Controls
Average	0.0775	Average	0.085
Variance	0.000292	Variance	0.000833
Std.			
Dev.	0.017078	Std. Dev.	0.028868

Bibliography

- Agerkvist I, Enfors S-O. 1990. Characterization of *E. coli* cell disintegrates from a bead mill and high pressure homogenizers. *Biotechnology and Bioengineering* 36(11):1083-1089.
- Akesson M, Hangander P, Axelsson JP. 2001. Avoiding Acetate Accumulation in *Escherichia coli* Cultures Using Feedback Control of Glucose Feeding. *Biotechnology and Bioengineering* 73(3):223-230.
- Baneyx F, Mujacic M. 2004. Recombinant protein folding and misfolding in *Escherichia coli*. *Nature Biotechnology* 22(11):1399-1409.
- Barnicki SD, Sirrola JJ. 2003. Process Synthesis Overview. *Computers and Chemical Engineering* 28:441-446.
- Bezaire J. 2005. Development and Validation of an in-situ, Multi-parameter, Optical Probe for Real-time Fermentation Monitoring. Waterloo, Ontario: University of Waterloo. 225 p.
- Cabanne C, Noubhani AM, Dieryck W, Santarelli X. 2004. Evaluation of three expanded bed adsorption anion exchange matrices with the aid of recombinant enhanced green fluorescent protein overexpressed in *Escherichia coli*. *Journal of Chromatography B*. 808:91-97.
- Calik P, Yilgor P, Ayhan P, Demir AS. 2004. Oxygen transfer effects on recombinant benzaldehyde lyase production. *Chemical Engineering Science* 59:5075-5083.
- Chen Y, Krol J, Sterkin V, Fan W, Yan X, Huang W, Cino J, Julien C. 1999. New process control strategy used in a rapamycin fermentation. *Process Biochemistry* 34:383-389.
- Clark KJR, Chaplin FWR, Harcum SW. 2004. Temperature Effects on Product-Quality-Related Enzymes in Batch CHO Cell Cultures Producing Recombinant tPA. *Biotechnology Progress* 20(6):1888-1892.
- Clontech. 1999. Clontech Plasmid Map and eYFP information.
- Clontech, editor. 2001. Living Colors Users Manual. Mountain View, CA: Clontech. 47 p.
- de Mare L, Velut S, Lendung E, Cimander C, Norrman B, Karlsson EN, Holst E, Hagander P. 2005. A cultivation technique for *E. coli* fed-batch cultivations operating close to

- the maximum oxygen transfer capacity of the reactor. *Biotechnology Letters* 27:983-990.
- Deschamps JR, Miller CE, Ward KB. 1995. Rapid Purification of Recombinant Green Fluorescent Protein Using the Hydrophobic Properties of an HPLC Size-Exclusion Column. *Protein Expression and Purification* 6:555-558.
- Felber LM, Cloutier SM, Kundig C, Kishi T, Brossard V, Jichlinksi P, Leisinger H-J, Deperthes D. 2004. Evaluation of the CFP-substrate-YFP system for protease studies: advantages and limitations. *Bio Techniques* 36(5):878-885.
- Forman SM, DeBernardez ER, Feldberg RS, Swartz RW. 1990. Crossflow Filtration for the Separation of Inclusion Bodies from Soluble Proteins in Recombinant *Escherichia coli* Cell Lysate. *Journal of Membrane Science* 48:263-279.
- Gadgil M, Kapur V, Hu W-S. 2005. Transcriptional Response of *Escherichia coli* to Temperature Shift. *Biotechnology Progress* 21:689-699.
- Gadgil M, Kapur V, Hu W. 2005. Transcriptional Response of *Escherichia coli* to Temperature Shift. *Biotechnology Progress* 21:689-699.
- Ghose S, Mc Nerney TM, Hubbard B. 2002. pH Transitions in Ion-Exchange Systems: Role in the Development of a Cation-Exchange Process for a Recombinant Protein. *Biotechnology Progress* 18:530-537.
- Griesbeck O, Baird GS, Campbell RE, Zacharias DA, Tsien RY. 2001. Reducing the Environmental Sensitivity of Yellow Fluorescent Protein. *The Journal of Biological Chemistry* 276(31):29188-29194.
- Groep ME, Gregory ME, Kershenbaum LS, Bogle IDL. 2000. Performance Modeling and Simulation of Biochemical Process Sequences with Interacting Unit Operations. *Biotechnology and Bioengineering* 67(3):300-310.
- Haddadin Fa, Harcum SW. 2005. Transcriptome Profiles For High-Cell-Density Recombinant and Wild-Type *Escherichia coli*. *Biotechnology and Bioengineering* 90(2):127-153.
- Hedhammar M, Graslund T, Hober S. 2005. Protein Engineering Strategies for Selective Protein Purification. *Chemical Engineering and Technology* 28(11):1315-1325.

- Heim R, Prasher D, Tsein RY. 1994. Wavelength mutations and posttranslational autooxidation of green fluorescent protein. *Proceedings of the National Academy of Science USA* 91:12501-12504.
- Hendrick V, Winepenninckx P, Abdelkafi C, Vandeputte O, Cherlet M, Marique T, Renemann G, Loa A, Kretzmer G, Werenne J. 2001. Increased productivity of recombinant tissular plasminogen activator (t-PA) by butyrate and shift of temperature: a cell cycle phases analysis. *Cytotechnology* 36:71-83.
- Intelligen I. 2006.
- Invitrogen. 2001. pRSET A,B, and C For high-level expression of recombinant proteins in *E. coli*. Invitrogen. p 1-27.
- Jayaraman S, Haggie P, Wachter R, Remington SJ, Verkman AS. 2000. Mechanism and Cellular Applications of a Green Fluorescent Protein-based Halide Sensor. *The Journal of Biological Chemistry* 275(9):6047-6050.
- Johansson HJ, Jagersten C, Shiloach J. 1996. Large scale recovery and purification of periplasmic recombinant protein from *E. coli* using expanded bed adsorption chromatography followed by new ion exchange media. *Journal of Biotechnology* 48:9-14.
- Kim Y-H, Han KY, Lee K, Lee J. 2005. Proteome response of *Escherichia coli* fed-batch culture to temperature downshift. *Applied Microbiological Biotechnology* 68:786-793.
- Kipriyanov S, Moldenhauer G, Little M. 1997. High level production of soluble small-chain antibodies in small-scale *Escherichia coli* cultures. *Journal of Immunology Methods* 200:69-77.
- Lee FWF, Elias CB, Todd P, Kompala DS. 1998. Engineering Chinese hamster ovary (CHO) cells to achieve an inverse growth - associated production of a foreign protein, B-galactosidase. *Cytotechnology* 28:73-80.
- Lee GH, Cooney D, Middelberg APJ, Choe WS. 2006a. The economics of inclusion body processing. *Bioprocess and Biosystems Engineering* 29:73-90.

- Lee GH, Cooney D, Middelberg APJ, Choe WS. 2006b. The economics of inclusion body processing. *Bioprocess and Biosystems Engineering* 29(2):73-90.
- Lee H-J, Im H. 2003. Purification of recombinant plasminogen activator inhibitor-1 in the active conformation by refolding from inclusion bodies. *Protein Expression and Purification* 31:99-107.
- Lin AA, Kimura R, Miller WM. 1993. Production of tPA in Recombinant CHO Cells Under Oxygen-Limited Conditions. *Biotechnology and Bioengineering* 42:339-350.
- Ling Y, Wong HH, Thomas CJ, Williams DRG, Middleburg APJ. 1997. Pilot-scale extraction of PHB from recombinant *E. coli* by homogenization and centrifugation. *Bioseparation* 7:9-15.
- Lloyd DR, Leelavatcharamas V, Emery AN, Al-Rubeai M. 1998. The role of the cell cycle in determining gene expression and productivity in CHO cells. *Cytotechnology* 30:49-57.
- Makino Y, Amada K, Taguchi H, Yoshida M. 1997. Chaperonin-mediated Folding of Green Fluorescent Protein. *The Journal of Biological Chemistry* 272(19):12468-12474.
- Manosroi J, Tayapiwatana C, Gotz F, Werner RG, Manosroi A. 2001. Secretion of Active Recombinant Human Tissue Plasminogen Activator Derivatives in *Escherichia coli*. *Applied and Environmental Microbiology* 67(6):2657-2664.
- Marks D. 2003. Equipment design considerations for large scale cell culture. *Cytotechnology* 42:21-23.
- Middelberg APJ. 2002. Preparative protein refolding. *Trends in Biotechnology* 20(10):427-443.
- Middelberg APJ. 1995. Process Scale Disruption of Microorganisms. *Biotechnology Advances* 13(3):491-551.
- Middelberg APJ, O'Neill BK, Bogle IDL. 1991. A Novel Technique for the Measurement of Disruption in High-Pressure Homogenization: Studies on *E. coli* Containing Recombinant Inclusion Bodies. *Biotechnology and Bioengineering* 38:363-370.
- Miller SA, editor. 1973. *Liquid-Solid Systems*. 5th ed. Montreal: McGraw-Hill Book Company.

- Mustafa MA, Washbrook J, Lim AC, Zhou Y, Titchener-Hooker NJ, Morton P, Berezenko S, Farid SS. 2004. A Software Tool to Assist Business-Process Decision-Making in the Biopharmaceutical Industry. *Biotechnology Progress* 20:1096-1102.
- Nagai T, Ibata K, Park ES, Kubota M, Mikoshiba K, Miyawaki A. 1999. A variant of yellow fluorescent protein with fast and efficient maturation for cell-biological applications. *Nature Biotechnology* 20:87-90.
- Obukowicz MG, Gustafson ME, Junger KD, Leimgruber RM, Wittwer AJ, Wun T-C, Warren TG, Bishop BF, Mathis KJ, McPherson DT and others. 1990. Secretion of Active Kringle-2-Serine Protease in *Escherichia coli*. *Biochemistry* 29(41):9737-9745.
- Phadtare S, Inouye M. 2004. Genome-Wide Transcriptional Analysis of the Cold Shock Response in Wild-Type and Cold-Sensitive Quadruple-csp-Deletion Strains of *Escherichia coli*. *Journal of Bacteriology* 186(20):7007-7014.
- Phue J-N, Noronha SB, Hattacharyya R, Wolfe AJ, Shiloach J. 2005. Glucose Metabolism at High Density Growth of *E. coli* B and *E. coli* K: Differences in Metabolic Pathways Are Responsible for Efficient Glucose Utilization in *E. coli* B as Determined by Microarrays and Northern Blot Analyses. *Biotechnology and Bioengineering* 90(7):805-820.
- Prasher D, Eckenrode VK, Ward WW, Prendergast FG, Cormier MJ. 1992. Primary structure of the *Aequorea victoria* green-fluorescent protein. *Gene* 111:229-233.
- Putnam C. 1999. Protein Calculator. La Jolla, CA: The Scripps Research Institute.
- Qiu J, Swartz JR, Georgiou G. 1998. Expression of Active Human Tissue-Type Plasminogen Activator in *Escherichia coli*. *Applied and Environmental Microbiology* 64(12):4891-4896.
- Reid BG, Flynn GC. 1997. Chromophore Formation in Green Fluorescent Protein. *Biochemistry* 36:6786-6791.
- Rosenow MA, Huffman HA, Phail ME, Wachter R. 2004. The Crystal Structure of the Y66L Variant of Green Fluorescent Protein Supports a Cyclization-Oxidation-Dehydration Mechanism for Chromophore Maturation. *Biochemistry* 43:4464-4472.

- Rouf SA. 1999. Evaluation of Process Simulators for an Integrated Bioprocess Design [Ph. D.]. Waterloo: University of Waterloo. 337 p.
- Rouf SA, Chisti Y, Moo-Young M. 1996. Tissue-Type Plasminogen Activator: Characteristics, Applications and Production Technology. *Biotechnology Advances* 14(3):239-266.
- Rouf SA, Moo-Young M, Scharer JM, Douglas PL. 2000. Single versus multiple bioreactor scale-up economics for high value products. *Biochemical Engineering Journal* 6:25-31.
- Saito Y, Ishii Y, Sasaki H, Hayashi M, Fujimura T, Imai Y, Nakamura S, Suzuki S, Notani J, asada T and others. 1994. Production and Characterization of a Novel Tissue-Type Plasminogen Activator Derivative in *Escherichia coli*. *Biotechnology Progress* 10:472-279.
- Schaffner J, Winter J, Rudolph R, Schwarz E. 2001. Cosecretion of Chaperones and Low-Molecular-Size Medium Additives Increases the Yield of Recombinant Disulfide-Bridged Proteins. *Applied and Environmental Microbiology* 67(9):3994-4000.
- Senger RS, Karim MN. 2003. Effect of Shear Stress on Intrinsic CHO Culture State and Glycosylation of Recombinant Tissue-Type Plasminogen Activator Protein. *Biotechnology Progress* 19:1199-1209.
- Shanklin T, Roper K, Yengeswaran PK, Marten MR. 2001. Selection of Bioprocess Simulation Software for Industrial Applications. *Biotechnology and Bioengineering* 72(4):483-489.
- Shepard SR, Boyd GA, Schrimsher JL. 2001. Routine manufacture of recombinant proteins using expanded bed adsorption chromatography. *Bioseparation* 10:51-56.
- Shiloach J, Fass R. 2005. Growing *E. coli* to high cell density - A historical perspective on method development. *Biotechnology Advances* 23:345-357.
- Siddiqi SF, Titchener-Hooker NJ, Shamiou PA. 1996. Simulation of Particle Size Distribution Changes Occuring During High-Pressure Disruption of Bakers' Yeast. *Biotechnology and Bioengineering* 50:145-150.

- Sterbacek Z, Votruba J. 1993. An expert system applied to the control of an industrial-scale bioreactor. *The Chemical Engineering Journal* 51:B35-B42.
- Svennson M, Silfversparre G, Haggstrom L, Enfors S-O. 2005. Control of endotoxin release in *Escherichia coli* fed-batch cultures. *Bioprocess and Biosystems* 27:289-292.
- Takagi M, Hia HC, Jang JH, Yoshida T. 2001a. Effects of High Concentrations of Energy Sources and Metabolites on Suspension Culture of Chinese Hamster Ovary Cells Producing Tissue Plasminogen Activator. *Journal of Bioscience and Bioengineering* 91(5):515-521.
- Takagi M, Moriyama T, Yoshida T. 2001b. Effects of Shifts Up and Down in Osmotic Pressure on Production of Tissue Plasminogen Activator by Chinese Hamster Ovary Cells in Suspension. *Journal of Bioscience and Bioengineering* 91(5):509-514.
- van Hee P, Hoeben MA, van der Lans RGJM, van der Wielen LAM. 2006. Strategy for Selection of Methods for Separation of Bioparticles From Particle Mixtures. *Biotechnology and Bioengineering* 94(4):689-709.
- Vasquez-Alvarez E, Pinto JM. 2004. Efficient MILP formulations for the optimal synthesis of chromatographic protein purification processes. *Journal of Biotechnology* 110:295-311.
- Vlakh EG, Platonova GA, Vlasov GP, Kasper C, Tappe A, Kretzmer G, Tennikova TB. 2003. In vitro comparison of complementary interactions between synthetic linear/branched oligo/poly-L-lysines and tissue plasminogen activator by means of high performance monolithic-disk affinity chromatography. *Journal of Chromatography A*. 992:109-119.
- Waldenstrom M, Holmgren E, Attersand A, Kalderen C, Lowenaldler B, Raden B, Hansson L, Pohl G. 1991. Synthesis and secretion of a fibrinolytically active tissue-type plasminogen activator variant in *Escherichia coli*. *Gene* 99:243-248.
- Wang Z, Shah JV, Chen Z, Sun C-H, Berns MW. 2004. Fluorescence correlation spectroscopy investigation of a GFP mutant-enhanced cyan fluorescent protein and its tubulin fusion in living cells with two-photon excitation. *Journal of Biomedical Optics* 9(2):395-403.

- Wheelwright SM. 1989. The design of downstream processes for large-scale protein purification. *Journal of Biotechnology* 11:89-102.
- Wurm FM. 2004. Production of recombinant protein therapeutics in cultivated mammalian cells. *Nature Biotechnology* 22(11):1393-1398.
- Xiao C, Huang Z, Li W, Hu X, Qu W, Gao L, Liu G. 1999. High density and scale-up cultivation of recombinant CHO cell line and hybridomas with porous microcarrier Cytopore. *Cytotechnology* 30:143-147.
- Xie D-M, Liu D-H, Zhu H-L, Liu Y-Q, Zhang J-A. 2002. Model-based optimization of temperature and feed control strategies for glycerol production by fed-batch culture of osmophilic yeast *Candida krusei*. *Biochemical Engineering Journal* 11:111-121.
- Xu H-M, Zhang G-Y, Ji X-D, Cao L, Shu L, Hua Z-C. 2005. Expression of soluble, biologically active recombinant human endostatin in *Escherichia coli*. *Protein Expression and Purification* 41(2):252-258.
- Yun Z, Takagi M, Yoshida T. 2001. Effect of Antioxidants on the Apoptosis of CHO Cells and Production of Tissue Plasminogen Activator in Suspension Culture. *Journal of Bioscience and Bioengineering* 91(6):581-585.
- Zanette D, Dundon W, Soffientini A, Sottani C, Marinelli F, Akesson A, Sarubbi E. 1998. Human IL-1 receptor antagonist from *Escherichia coli*: Large-scale microbial growth and protein purification. *Journal of Biotechnology* 64:187-196.
- Zhang L, Patel HN, Lappe JW, Wachter R. 2006. Reaction Progress of Chromophore Biogenesis in Green Fluorescent Protein. *Journal of the American Chemical Society* 128:4766-4772.
- Zheng M, Du G, Guo W, Chen J. 2001. A temperature-shift strategy in batch microbial transglutaminase fermentation. *Process Biochemistry* 36:525-530.
- Zhou YH, Titchener-Hooker NJ. 1999a. Simulation and Optimization of an Integrated Bioprocess: a case study. *Journal of Chemical Technology and Biotechnology* 74:289-292.
- Zhou YH, Titchener-Hooker NJ. 1999b. Visualizing Integrated Bioprocess Designs Through "Windows of Operation". *Biotechnology and Bioengineering* 65(5):550-557.